UAB
Universitat Autònoma de Barcelona

Characterization of HIV-1 Elite Controller Envelope Glycoproteins and Incorporation as Candidate Antigens in a Virus-Like Particle Vaccine Platform

Anna Pons-Grífols

Characterization of HIV-1 Elite Controller Envelope Glycoproteins and Incorporation as Candidate Antigens in a Virus-Like Particle Vaccine Platform

Anna Pons-Grífols

Doctoral Thesis 2025

PhD programme in Advanced Immunology
Department of Cellular Biology, Physiology and Immunology
Universitat Autònoma de Barcelona

Characterization of HIV-1 Elite Controller Envelope Glycoproteins and Incorporation as Candidate Antigens in a Virus-Like Particle Vaccine Platform

Thesis presented by Anna Pons-Grífols to qualify for the PhD degree in Advanced Immunology by the *Universitat Autònoma de Barcelona.*

The presented work has been performed in the Cell Virology and Immunology (VIC) group, at IrsiCaixa, directed by Dr Julià Blanco Arbués and Dr Benjamin Trinité and tutored by Dr Julià Blanco Arbués.

Anna Pons Grífols
PhD candidate

Julià Blanco Arbués, PhD
Thesis director & tutor

Benjamin Trinité, PhD
Thesis director

Badalona, June 30th, 2025

This work was supported by the PI20/00093 and PI23/01269 and PI20CIII/000008 projects, integrated in the National R + D + I and funded by the Instituto de Salud Carlos III and the European Regional Development Fund. This work has also been sponsored partly by Grífols.

The author of this thesis has been supported by a predoctoral grant from Generalitat de Catalunya and Fons Social Europeu (2022 FI_B 00698).

Unrelated to this work, Dr. Julià Blanco Arbués is founder and shareholder of the spin-off AlbaJuna Therapeutics S.L and reports institutional grants from HIPRA and MSD. The author of this thesis declares no conflicts of interest.

The printing of this thesis was fully funded by Fundació Privada Institut de Recerca sobre Immunopatologies-Caixa IrsiCaixa.

Cover design and layout: Elisa Jara Basterrechea
Images and graphs were created using Biorender, Inkscape or GraphPad Prism.

El Dr. Julià Blanco Arbués, investigador de la Fundació Institut d'Investigació en Ciències de la Salut Germans Trias i Pujol (IGTP) i professor de la Universitat de Vic-Universitat Central de Catalunya, i el Dr. Benjamin Trinité, investigador de la Fundació Privada Institut de Recerca sobre Immunopatologies-Caixa IrsiCaixa,

certifiquen

que el treball experimental i la redacció de la memòria de la Tesi Doctoral titulada ***"Characterization of HIV-1 Elite Controller Envelope Glycoproteins and Incorporation as Candidate Antigens in a Virus-Like Particle Vaccine Platform"*** han estat realitzats per l'Anna Pons Grífols sota la seva direcció, i que

consideren

que és apte per a ser presentat i optar al grau de Doctora en Immunologia Avançada per la Universitat Autònoma de Barcelona.

I per a que quedi constància, signen aquest document a Badalona,
el 30 de juny de 2025.

Dr. Julià Blanco Arbués

Dr. Benjamin Trinité

TABLE OF CONTENTS

SUMMARY

Vaccines have proved to be pivotal in the fight against emergent pathogens. SARS-CoV-2 vaccine's accelerated development benefited from decades of research into HIV as well as in other fields. Despite all these advances, modest to no success has been achieved in an effective HIV vaccine development so far. Compared to SARS-CoV-2, developing an HIV vaccine has proven uniquely difficult due to the virus's high mutation rate, its ability to evade the immune system, and a lack of natural protective immunity in infected individuals. Consequently, there is a need for the development of new immunogens and strategies that can induce broad neutralizing antibody response along with protective CD4+ and CD8+ T-cell responses. Specifically, the study of rare cases of people living with HIV (PLWH) who can naturally control HIV replication and disease progression could provide insights into viral control mechanisms. Among controllers, elite controllers (EC) maintain low viral loads and stable CD4+ T-cell counts for long periods in the absence of antiretroviral treatment. This control is still not fully understood but it could require an interplay of genetic, immunological and viral factors. Notably, some ECs exhibit viruses with defective envelope glycoproteins (Env) that might have contributed to the development of this phenotype.

The hypothesis of this work was that Env sequences isolated from HIV-infected ECs, present specific properties that could be beneficial for the balance of viral pathogenesis and immune responses, including the elicitation of broadly neutralizing antibodies. Additionally, their expression on the surface of a viral-like particle (VLP)-based platform vaccine, optimized to display high antigenic density, would improve their immunogenicity in vaccine strategies.

To test this, we functionally characterized a large collection of EC Env clones and, in parallel, we selected representative Env molecules with the best surface and antigenicity expression to be incorporated in a VLP platform. Selection was based on the exposure and detection of neutralizing epitopes. Functional characterization confirmed previous results, highlighting that ECs presented less fusogenic Envs compared to progressors and viremic controllers. This analysis was complemented with the longitudinal characterization of humoral response in 79 EC plasma samples of the ECRIS cohort to understand the contribution of neutralization capacity to EC phenotype. ECs that

maintain control for a long period of time (persistent controllers, PC) were compared with those who lose it eventually (transient controllers, TC). While their neutralizing capacities were heterogenous, no differences were observed between them during their control periods. Notably, PC showed a dominance of HLA-B protective alleles over non-protective, while TC harbored no main protective ones. This confirms a variable interplay between virological, immunological and genetic factors in this phenotype.

To further understand control mechanisms, we characterized the case of an EC that lost control 32 years after diagnosis. A comprehensive virological and immunological study was performed on available longitudinal samples. We assessed reservoir evolution and dynamics of viral quasispecies, functionality of Env clones and autologous neutralizing capacity. This extensive sampling identified evident changes in sequence evolution and function during control period. These fluctuations were also reflected in the immune response analyzed, suggesting a highly dynamic virological and immunological scenario during the control period instead of a steady-state one in this case.

In parallel, candidate antigens selected among different most common recent ancestors (MRCA) of EC Env sequences were characterized and incorporated in a VLP platform through fusion-protein strategies to obtain particles capable of displaying high antigenic density. As this strategy met technical challenges, alternatives strategies were used. Both standard VLP production and preliminary immunogenicity assays were performed. Antigens formulated into a nucleic acid vaccine strategy and delivered *in vivo* by DNA electroporation in two doses showed immunogenicity but did not elicit neutralizing antibodies. Further refinement of VLP production, a higher number of immunization doses and the use of different vaccination regimens will be required to improve its global efficiency.

Overall, the study of control mechanisms in extreme phenotypes, as well as the role of Env, proves of high potential and interest to inform the development of new therapeutic strategies that could contribute to HIV cure and vaccine development.

RESUM

Les vacunes han demostrat ser fonamentals en la lluita contra patògens emergents. El desenvolupament accelerat d'una vacuna contra el SARS-CoV-2 es va beneficiar de dècades de recerca sobre el VIH i altres àmbits. Tot i aquests avenços, fins ara només s'ha aconseguit un èxit modest, o cap, en el desenvolupament d'una vacuna efectiva contra el VIH. Comparat amb el SARS-CoV-2, desenvolupar una vacuna contra el VIH s'ha demostrat especialment difícil a causa de l'alta taxa de mutació del virus, la seva capacitat d'evadir el sistema immunitari i la manca d'una immunitat protectora natural en les persones infectades. En conseqüència, cal desenvolupar nous immunògens i estratègies que puguin induir una resposta d'anticossos neutralitzants de gran amplitud, juntament amb respostes cel·lulars protectores tant CD4+ com CD8+.

En particular, l'estudi de casos poc freqüents de persones que viuen amb el VIH que poden controlar naturalment la replicació del virus i la progressió de la malaltia podria proporcionar indicis sobre els mecanismes de control viral. Entre aquests controladors, destaquen els "controladors d'elit" (EC) que mantenen càrregues virals baixes i nivells estables de limfòcits CD4+ durant períodes prolongats en absència de tractament antiretroviral. Els mecanismes d'aquest control encara no estan completament definits, però podrien requerir una interacció de factors genètics, immunològics i virals. Cal destacar que alguns EC presenten virus amb glicoproteïnes d'embolcall (Env) defectuoses que podrien haver contribuït al desenvolupament d'aquest fenotip.

La hipòtesi d'aquest treball és que les seqüències d'Env aïllades de persones EC infectades amb el VIH presenten propietats específiques que podrien ser beneficioses per a l'equilibri entre la patogènesi viral i les respostes immunitàries, inclosa la inducció d'anticossos àmpliament neutralitzants. A més, la seva expressió a la superfície d'una plataforma de vacuna basada en partícules similars a virus (VLP), optimitzada per mostrar alta densitat antigènica, milloraria la seva immunogenicitat en estratègies vacunals.

Per avaluar aquestes hipòtesis, es va caracteritzar funcionalment una àmplia col·lecció de clons d'Env de EC i, en paral·lel, es van seleccionar molècules representatives d'Env amb la millor expressió superficial i antigenicitat per ser incorporades a una plataforma VLP. La selecció es va basar en l'exposició i detecció d'epítops neutralitzants. La

caracterització funcional va confirmar resultats previs, posant en relleu que els EC presentaven Envs menys funcionals en comparació amb progressors i controladors vírics. Aquesta anàlisi es va complementar amb la caracterització longitudinal de la resposta humoral en 79 mostres de plasma d'EC de la cohort ECRIS per entendre la contribució de la capacitat de la neutralització al fenotip EC. Els EC que mantenen el control durant períodes prolongats (controladors persistents, PC) es van comparar amb aquells que el perden eventualment (controladors transitoris, TC). Tot i que les seves capacitats neutralitzants eren heterogènies, no es van observar diferències entre ells durant els períodes de control. És destacable que els PC mostraven una dominància d'al·lels protectors HLA-B respecte als no protectors, mentre que els TC no presentaven cap dels principals al·lels protectors. Això confirma una interacció variable entre factors virològics, immunològics i genètics en aquest fenotip.

Per entendre millor els mecanismes de control, es va caracteritzar el cas d'un EC que va perdre el control 32 anys després del diagnòstic. Es va dur a terme un estudi virològic i immunològic complet sobre les mostres longitudinals disponibles. Es va avaluar l'evolució del reservori i la dinàmica de les quasiespècies virals, la funcionalitat dels clons d'Env i la capacitat de neutralització autòloga. Aquestes anàlisis exhaustives van identificar canvis evidents en l'evolució i la funció de seqüències virals durant el període de control. Aquestes fluctuacions també es van reflectir en la resposta immune analitzada, suggerint un escenari virològic i immunològic altament dinàmic durant el període de control, i no un comportament estàtic, en el cas estudiat.

En paral·lel, es van caracteritzar antígens candidats seleccionats entre els diferents ancestres recents més comuns (MRCA) de seqüències Env d'EC i es van incorporar a una plataforma VLP mitjançant estratègies de proteïna de fusió per obtenir partícules capaces de mostrar alta densitat antigènica. Donat que aquesta estratègia va presentar reptes tècnics, es van emprar estratègies alternatives. Es va dur a terme tant la producció estàndard de VLP com assaigs preliminars d'immunogenicitat. Els antígens formulats en una estratègia vacunal basada en àcids nucleics i administrats *in vivo* per electroporació de DNA en dues dosis van mostrar immunogenicitat, però no van induir anticossos neutralitzants. Serà necessari refinar la producció de VLP, augmentar el nombre de dosis d'immunització i emprar diferents règims vacunals per millorar-ne l'eficiència global.

En conjunt, l'estudi dels mecanismes de control en fenotips extrems, així com el paper d'Env, mostra un gran potencial i interès per informar el desenvolupament de noves estratègies terapèutiques que puguin contribuir a la curació del VIH i al desenvolupament de vacunes.

LIST OF ABBREVIATIONS

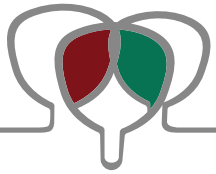

aa	Amino acid
Ab	Antibody
ADCC	Antibody Dependent Cell Cytotoxicity
ADCP	Antibody dependent cellular phagocytosis
AIDS	Acquired Immunodeficiency Syndrome
AMP	Antibody mediated prevention
APC	Antigen Presenting Cell
ART	Antiretroviral Therapy
ATI	Analytical treatment interruption
bNAb	Broadly Neutralizing Antibody
BSA	Bovine Serum Albumin
CD4bs	CD4 Binding Site
CO_2	Carbon Dioxide
CoRIS	Spanish AIDS Research Network cohort
CRF	Circulating Recombinant Form
CT	Cytoplasmic Tail
CTL	Cytolytic T Lymphocyte
D10	DMEM with 10% FBS
DC	Dendritic Cell
DEAE	Diethylaminoethyl-Dextran
dH2O	Distilled Water

DMEM	Dulbecco's Modified Eagle Medium
DMSO	Dimethyl Sulfoxide
DNA	Deoxyribonucleic Acid
dsDNA	Double Stranded DNA
EC	Elite Controller
ECRIS	EC CoRIS Cohort
ED	Ectodomain
EDTA	Ethylenediaminetetraacetic Acid
EEC	Exceptional Elite Controller
ELISA	Enzyme-Linked Immunosorbent Assay
Env	Envelope Glycoprotein
ER	Endoplasmic reticulum
EV	Extracellular Vesicle
FBS	Foetal Bovine Serum
Fc	Crystallisable Fragment
FeLV	Feline Leukemia Virus
GALT	Gut-associated lymphoid tissue
h	Hour
HBV	Hepatitis B Virus
HCV	Hepatitis C Virus
HEK293	Human Embryonic Kidney 293
HIV	Human Immunodeficiency Virus
HLA	Human Leukocyte Antigen
HPV	Human papiloma virus
IBiS	Instituto de Biomedicina de Sevilla
ID50	Half maximal inhibitory dose
IDU	Intravenous drug use
IFN	Interferon
Ig	Immunoglobulin

Img	Image
ISCIII	Instituto de Salud Carlos III
LB	Lysogeny broth
LoC	Loss of Control
LTNP	Long term non-progressor
LTR	Long Terminal repeats
mDC	Myeloid dendritic cells
MHC	Major Histocompatibility Complex
MHC-I	Major Histocompatibility Complex Class I
MHC-II	Major Histocompatibility Complex Class II
MRCA	Most Recent Common Ancestor
MuLV	Murine Leukemia Virus
NAb	Neutralizing Antibody
NK	Natural Killer Cells
nNAb	Non-neutralizing Antibody
°C	Celsius Degrees
p	p-value
PBMC	Peripheral blood mononuclear cells
PBS	Phosphate Buffer Saline
PC	Persistent Controllers
PLWH	People living with HIV
PrEP	Pre-exposure Prophylaxis
PROG	Progressor
PRR	Pattern Recognition Receptors
PTC	Post-treatment Controller
PV	Pellet volume
r	Spearman correlation coeficient
RIS	Spanish AIDS Research Network (Red de investigación en SIDA)
RNA	Ribonucleic acid

RP	Rapid Progressor
RT	Reverse Transcriptase
SARS-CoV-2	Severe Acute Respiratory Syndrome Coronavirus
SD	Standard deviation
SEM	Standard error of the mean
SIV	Simian Immunodeficiency Virus
SN	Supernatant
SOSIP	Soluble stabilized gp40 I559P
SP	Signal Peptide
SPF	Specific Pathogen Free
STED	Stimulated Emission Depletion Microscopy
TC	Transient Controllers
TCID50	Half maximal Tissue Culture Infective Dose
TEM	Transmission Electron Microscopy
TLR	Toll-like receptors
TM	Transmembrane
UNAIDS	Joint United Nations Program on HIV/AIDS
VC	Viremic Controller
VL	Viral Load
VLP	Virus-Like Particle
WB	Western Blot
x g	Relative Centrifugal Force

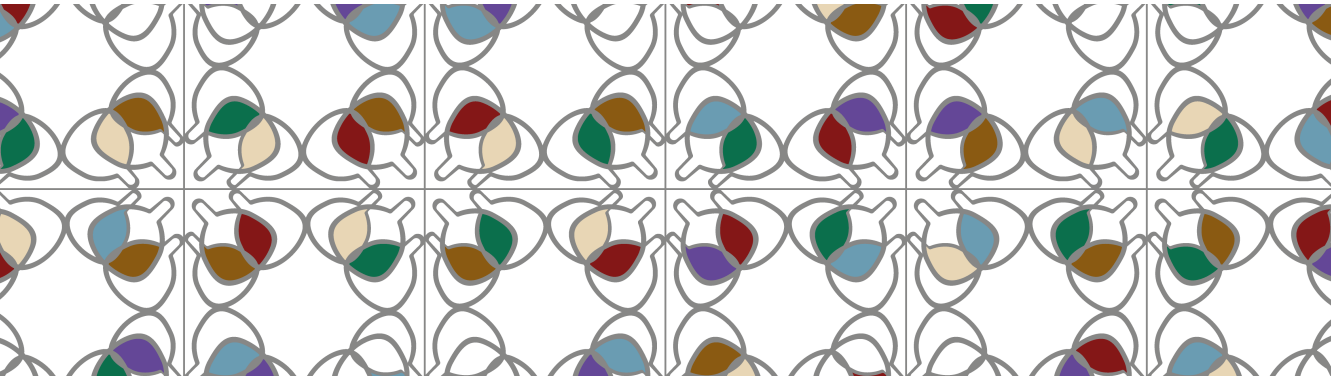

INTRODUCTION

1. The Human Immunodeficiency Virus (HIV)

HIV is a blood-borne virus (Family Retroviridae, Subfamily Orthoretrovirinae, Genus Lentivirus) (Coffin et al. 2021) that attacks the immune system by infecting and destroying mainly CD4+ T cells (Barré-Sinoussi et al. 1983). If untreated, HIV infection can lead to acquired immunodeficiency syndrome (AIDS), increasing the risk of developing opportunistic infections, which are normally fatal. In 2023, 39.9 million people were living with HIV (PLWH), and although great efforts have been made in terms of treatment and healthcare, there is still no vaccine or functional cure available yet, making it a major global health issue. Thanks to advances in prevention strategies and antiretroviral treatments (ART), new HIV infections have been reduced by 60% since the 90s (Joint United Nations Programme on HIV/AIDS (UNAIDS) 2024) and made people living with HIV (PLWH) life expectancy similar to the non-infected population (Wandeler, Johnson, and Egger 2016). Despite this great success, approximately 1.3 million people were newly infected in 2023 (Joint United Nations Programme on HIV/AIDS (UNAIDS) 2024).

Disparities in access to treatment in developing countries remain one of the major challenges. Moreover, recent political events in the United Stated remind us of the fragile state of the research and prevention effort threatening the international objectives of the UNAIDS 95-95-95: 95% of PLWH should know their status, 95% of those diagnosed should receive sustained ART, and 95% of those treated should achieve viral suppression (Joint United Nations Programme on HIV/AIDS (UNAIDS) 2024).

As a result, HIV remains a chronic, uncurable infectious disease with several challenges in the scientific, medical, and social fields.

1.1. HIV types, subtypes and distribution

HIV can be subdivided into HIV-1 and HIV-2 types. Although they can both lead to AIDS development, HIV-1 is more prevalent and pathogenic than HIV-2 and

has a higher replicative capacity (Reeves and Doms 2002; Popper et al. 1999). This manuscript will focus on HIV-1.

HIV-1 strains are classified into M, N, O, and P groups and circulating recombinant forms (CRFs). Group M accounts for 'major' as its increased pathogenicity accounts for more of 90% of HIV infections globally. Group M diversified in different clades or subtypes unevenly distributed across the globe. While central Africa houses most variants with no prevalent clade, subtype A is predominant in Eastern Europe, Central Asia and East Africa, subtype B is the predominant strain in Western Europe, America and Australia, and subtype C is present in Southern Africa and India. CRFs are predominant in southeast Asia (Gartner et al. 2020) (Figure 1).

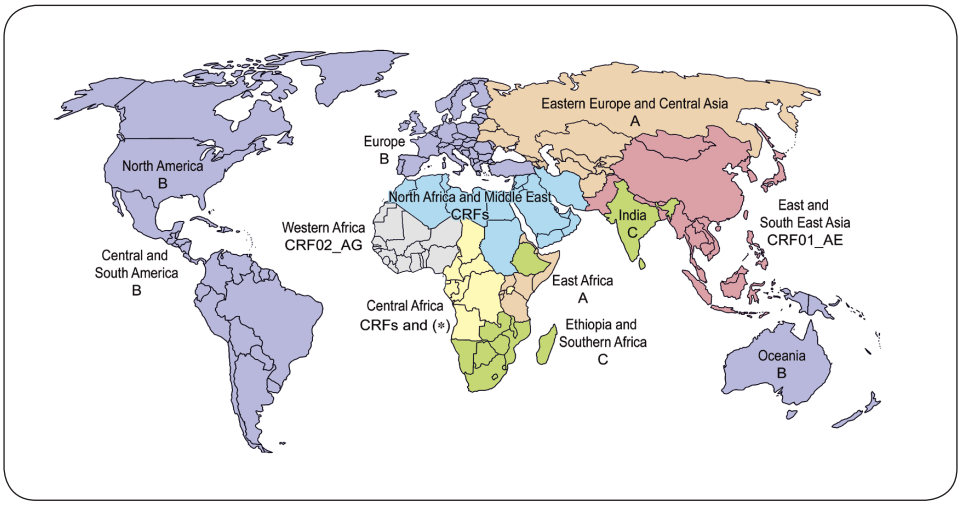

Figure 1. Global distribution map of HIV-1 M Clades. Each predominant clade in a geographic area is represented by one colour. CRF: circulating recombinant form. Areas with no predominant clade and high heterogeneity are marked with a (*). Adapted from (Gartner et al. 2020).

1.2. Virus Genome and Structure

The mature HIV-1 virion is formed by a lipid envelope containing both the genetic material and viral structural proteins. To establish a productive infection, the RNA genome is reverse transcribed to DNA and integrated into the host genome.

The HIV-1 genome consists of two 9.75 kb single-stranded RNAs, that contains a total of 9 genes with overlapping sequences (Figure 2). They can be classified into 3 major groups whether they code for structural, accessory and regulatory proteins.

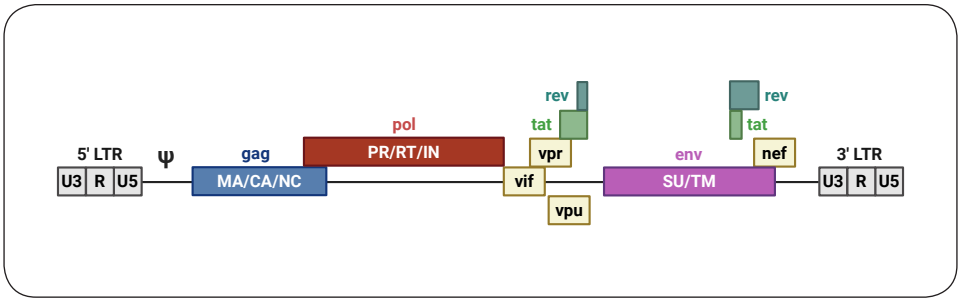

Figure 2. Schematic representation of the HIV genome. Adapted from the Biorender 'HIV-1 genome' template.

Three genes code for structural proteins, namely i) the group-specific antigen protein (Gag), a polyprotein that will be processed to yield matrix/MA, capsid/CA and nucleocapsid/NC and other small proteins; ii) the polymerase protein (Pol) containing all the viral enzymes (protease/PR, reverse transcriptase/RT and integrase/IN); and iii) the envelope glycoprotein (Env) the sole external viral protein in the virion (Frankel and Young 1998).

Six genes smaller genes code for accessory and regulatory proteins (Nef, Rev, Tat, Vif, Vpr and Vpu) which are responsible for a plethora of functions that block cellular restriction factors and promote HIV genome transcription, allowing for the completion of the HIV replication life cycle). Like other retroviral genomes, it is flanked by two long-terminal-repeats (LTR) sequences involved in its integration and transcription (Figure 2).

1.3. HIV-1 life cycle

HIV-1 main targets are immune cells, primarily CD4+ T helper cells (Dalgleish et al. 1984; Klatzmann et al. 1984) and to a lesser extent macrophages/microglia cells (Koenig et al. 1986) and dendritic cells. HIV-1 enters these cells via the binding of the viral Env to the CD4 receptor and a co-receptor, CCR5 or CXCR4, at the cell surface. Most primary HIV isolates use CCR5 as a coreceptor (named R5 viruses) and at a late stage of the infection the virus can evolve to use CXCR4 (named X4 or syncytial viruses) (Schuitemaker et al. 1992; Van't Wout et al. 1994) which are usually more pathogenic and associated with a more rapid progression toward AIDS (Connor et al. 1997).

Env is displayed on the surface of the virus and is structured as a trimer of three gp160 precursor molecules. Each gp160 is formed by two subunits that are non-covalently attached: gp120 and gp41 (Robey et al. 1985) . Gp120 or SU, is responsible for targeting the host receptors while gp41 contains the fusion apparatus necessary for viral entry (Chan et al. 1997) (Figure 2). Upon contact between gp120 and the CD4 receptor, a series of conformational changes allow the binding of the coreceptor

(Figure 3) and finally, the fusion process can take place via the gp41 subunit and its fusion peptide, allowing the release of the HIV-1 capsid containing the genome and viral enzymes into the cytoplasm of the target cell (Chen 2019).

The HIV capsid helps protect the viral genome from cellular detection and degradation, while allowing the entrance, through small pores, of the deoxynucleotides triphosphate (dNTPs), necessary for the reverse transcription of the RNA genome to DNA (Muller et al. 2022; Jacques et al. 2016). The reverse transcriptase (RT) enzyme that mediates this process is a low fidelity enzyme with a lack of proofreading activity (Abram et al. 2010). This leads to a high rate of mutations which explains the great genetic diversity observed within individuals and the quick viral evolution under immunological and/or therapeutic pressure.

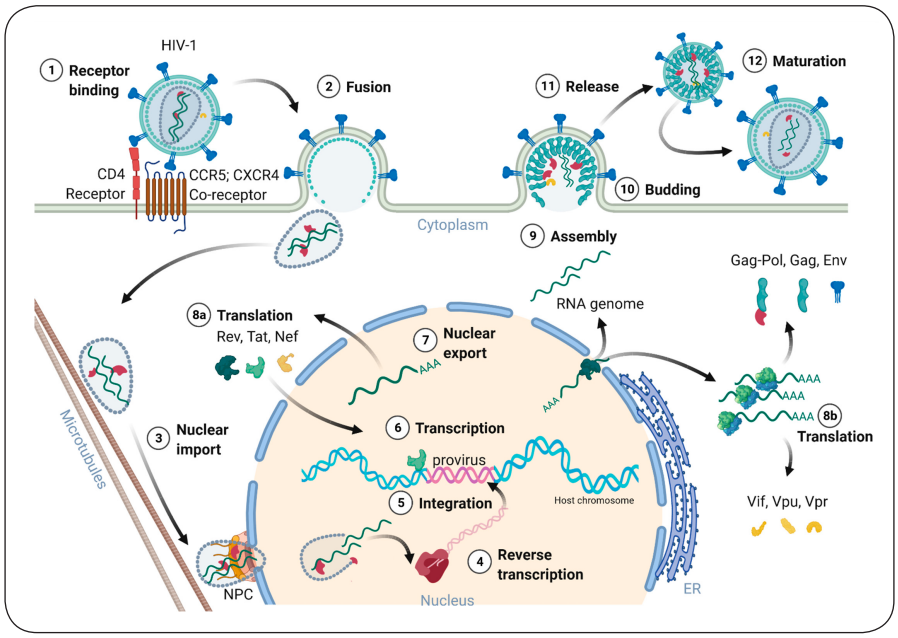

Figure 3. Schematic representation of HIV-1 life cycle. Image from (van Heuvel et al. 2022).

The viral capsid is transported through microtubules towards the nucleus where it enters through the nuclear pore (Zila et al. 2021). After entering the nucleus, and once the reverse transcription is completed, the viral capsid disassembles to release the viral dsDNA genome (Burdick et al. 2020; Müller et al. 2021). Here, viral integrase proteins will mediate the integration of the viral dsDNA into the host genome, preferably into highly transcriptionally active areas. However, at this stage, the proviral DNA can potentially remain latent for years establishing a viral reservoir until stimuli driven reactivation. If the cell is activated, it will start producing new viral proteins and pack them into virions. In the early stage of the virus transcription, the early accessory

proteins Rev, Tat and Nef are produced and start to regulate the host cell for optimal viral replication. Notably, Tat greatly enhances the transcription rate of the provirus while Rev allows for the export of partially spliced and unspliced viral RNAs from the nucleus to the cytoplasm. This leads to the translation of the structural proteins (Gag, Pol, Env) which will generate new viral particles. Env is expressed as a gp160 precursor inside the endoplasmic reticulum (ER) and along the secretory pathway where it undergoes post-translational modifications such as glycosylation and cleavage into gp120 and gp41 subunits. Once ready, produced proteins will assemble at the cell membrane and bud as immature HIV-1 particles. Following virus budding, the Gagpol polyprotein undergoes auto processing leading to the cleavage of Gag-derived structural elements and the final viral maturation necessary for viral infectivity. Mature viral HIV-1 particles have a size of approximately 120nm (Figure 3, Top right).

1.3.1. Envelope Glycoproteins

The Env glycoprotein plays a central role in viral infection, as it determines the virus's ability to bind to and fuse with the host cell membrane. These processes are driven by conformational changes in the glycoprotein, which not only mediate cell entry but also contribute significantly to the virus' pathogenesis. Therefore, a comprehensive study of the Env glycoprotein spanning from its genome to its functional involvement in viral entry and immune evasion is critical. Identifying points of viral vulnerability might help develop targeted therapeutic strategies.

a. Env Structure and function

Each Env is formed by a trimer of gp160 precursor molecules. Each molecule is cleaved by the cellular protease Furin (Hallenberger et al. 1992) to yield the subunits gp120 and gp41, which intervene in different viral entry steps (Figure 4). Situated at the N-terminal of the protein we find the Signal Peptide (SP), a structure of around 30 aminoacids (aa) necessary for Env trafficking to the ER where it undergoes modifications such as glycan addition and is exported to the cell surface. SP is cleaved during Env protein maturation and will not be present in the final protein. Changes in SP can greatly impact virus sensitivity to neutralizing antibodies, changing virus susceptibility by altering glycan composition (Upadhyay et al. 2020; Owji et al. 2018) (Figure 4).

Gp120 is the most exposed viral surface antigen and contains the domains that will allow for its binding to CD4 and CCR5/CXRC4 receptors and coreceptors, respectively (Figure 4). Its sequence contains five conserved areas (C) and five variable (V) loops that can vary in length and glycosylation therefore affecting immune detection and response (Olvera et al. 2021; Curlin et al. 2010). The gp120 region from C2 to V5 (C2V5) is commonly used to study viral diversity. This region is necessary for the binding to CD4 so it is exposed to the immune system. As a result, it often mutates and impacts immune escape, viral transmission, and neutralizing responses (McCaffrey et al. 2004;

Friedrich et al. 2021). Compared to other regions of gp160 that are more conserved, the study of this region allows a more precise analysis of diversity between subgroups (Yuan, Li, and Zhang 2013).

Gp41, contains both an extracellular or ectodomain (ED) and a cytoplasmic tail (CT), linked by a transmembrane (TM) sequence (Figure 4). While the ED exposes the fusion peptide upon binding to the target cell, the CT determines several steps in the viral cycle ranging from endocytosis to incorporation into virions (Postler and Desrosiers 2013). Of note, lentiviruses CT tend to be particularly large (~200aa) (Hunter and Swanstrom 1990), and mutations, deletions or truncations in this area can affect Env incorporation and infectivity.

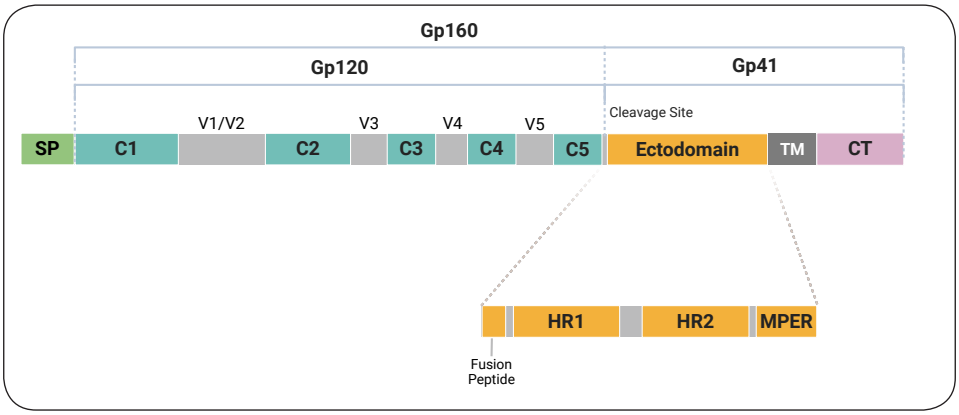

Figure 4. Schematic representation of Env genome structure. The immature protein is labeled as gp160, and their cleaved subunits as gp120 and gp41. Specific domains of each subunit are labelled with their specific names or constant regions (C) and variable regions (V).SP: Signal Peptide, TM: transmembrane domain, CT: Cytoplasmic Tail. Adapted from (Steckbeck, Kuhlmann, and Montelaro 2013) with Biorender.com.

b. Env in Immune Evasion

Being the only protein on the surface of viral particles and directly exposed to the immune system, Env is the sole viral target for antibody recognition and virus neutralization. As a result, HIV-1 has developed strategies to avoid immune recognition by humoral immunity. They are sophisticated mechanisms based on mutating, covering or hiding the vulnerability epitopes of this viral protein (Lewis et al. 2015).

By having a high mutation rate, especially in the Env sequence, the virus can escape any viral immunity that could have been mounted against previous Env. Even if this high mutation rate is beneficial for the virus, it can, in some cases, be detrimental for viral fitness and lead to defective viruses. To further impede immune system recognition, Env is incorporated in the viral membrane at a low density of 8-14 Env trimers (Zhu et al. 2006) for each virion. These are low levels compared to other enveloped viruses like murine leukemia viruses (MuLV) and simian immunodeficiency virus (SIV), which

present approximately 100 and 70 spikes at their surfaces, respectively (Sougrat et al. 2007).

The virus can cover or hide vulnerability sites through a glycan shield and conformational masking (Lewis et al. 2015; Pancera et al. 2014). The glycan shield is a structure composed of sugars that cover the Env surface and hide conserved epitopes targeted by NAbs. Alterations in this shield have been shown to impact on viral binding, infectivity and neutralization capacity (Wei et al. 2003). Interestingly however, there are some glycan-dependent bNAbs that rely on potential N-glycosilation sites and the trimer structure (Y. Z. Cohen et al. 2015). Importantly, viral mutation can also affect the positioning of glycosylation sites (Hargett et al. 2019).

Finally, it is well established that Env undergoes conformational changes during viral entry, and that these rearrangements can expose otherwise hidden vulnerable structures. At the same time, the exposure of non-relevant epitopes during conformational changes upon Env-CD4 interaction, can drive the generation of non-neutralizing antibodies (nNAbs) (Richard et al. 2024), diverting the immune response towards non-immunodominant regions. The rest of the time, Env transitions mostly through three conformations: open, closed or intermediate (Zhao et al. 2022) (Figure 5). The differential exposure of epitopes as the trimer opens defines the neutralization capacity of the antibodies and establishes viral tiers (Montefiori et al. 2018). Tier 1 viruses transition between the open and intermediate Env conformation. Tier 2 and 3 viruses present mostly a closed conformation and as a result have less epitope accessibility, restricting neutralization. Most circulating strains have a tier 2 neutralization phenotype, making them mostly the focus of vaccine research and antibody development.

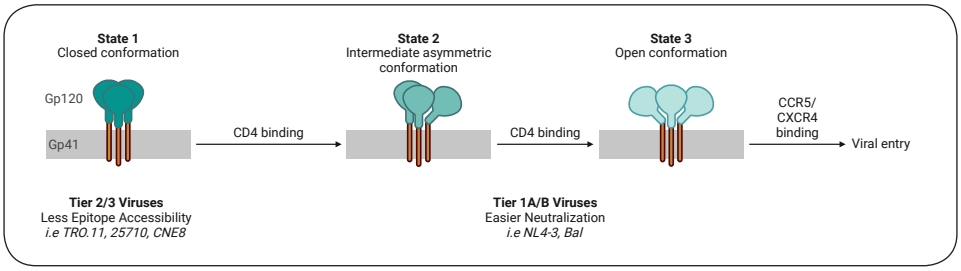

Figure 5. HIV-1 Env conformational states and related viral tiers. Adapted from a Biorender template based on Alsahafi et al. 2019; and Montefiori et al. 2018.

1.4. Pathogenesis of HIV-1 infection

Once HIV-1 enters target cells and establishes infection, its complex interactions with the host's immune responses determine HIV-1 pathogenesis, leading to clinical progression and increased vulnerability to opportunistic infections (Sabin and Lundgren 2013). HIV-1 infection can be divided into three main phases: i) acute ii) chronic and iii) AIDS, that can be defined by the progression of the viral load (VL) and the CD4+ T-cell count measured in the plasma (Figure 6). Indeed, the hallmark of AIDS is the progressive depletion of the CD4+ T-cell compartment (McCune 2001).

Acute infection is defined as the early stage within 2-4 weeks after infection, where HIV-1 multiplies rapidly in CD4+ T cells located in secondary lymphoid organs and gut-associated lymphoid tissue (GALT) and seeds the viral reservoir (Alcamí and Coiras 2011; Centlivre et al. 2007). During this phase, a significant depletion of the CD4+ T-cell compartment occurs. Although CD4+ T cells can succumb from the direct cytopathic effect of the virus, notably because of virus budding and syncytia formation, a majority of the eliminated cells are not in fact productively infected (Matrajt et al. 2014). This so called "bystander" T-cell death is a consequence of the pre-integration detection of viral DNA products of reverse transcription and the activation of programmed cell death via pyroptosis and apoptosis (Yin et al. 2020; Monroe et al. 2014). These pathways are mostly deleterious and contribute to the general inflammatory state (C. Zhang et al. 2021; Doitsh et al. 2013).

Acute HIV infection is accompanied by a cytokine storm which triggers Flu-like symptoms in the host (Pastor et al. 2017). While the mounting of the immune response is key to early protection against the virus, systemic inflammation may also drive HIV pathogenesis and provide a favorable environment for the seeding of the HIV reservoir (Catalfamo, Le Saout, and Lane 2012).

Thanks to cytotoxic CD8+ T cells and HIV-1 specific antibodies, viremia will eventually be controlled to a relatively stable level named viral setpoint (Ndhlovu et al. 2015). A partial recovery of the CD4+ T-cell count is also observed. However, from this point on, HIV infection will enter a chronic phase which can extend for prolonged periods of time (Figure 6, middle). Even if plasma viremia is reduced, the high virus variability avoids total immune control. The high number of infected cells and persistent viral replication in some organs leads to a chronic phase of systemic inflammation, immune activation and exhaustion along with the progressive depletion and dysfunction of CD4+ T cells (Doitsh et al. 2013; Catalfamo, Le Saout, and Lane 2012; C. Zhang et al. 2021). If untreated, the CD4+ T-cell depletion and immune dysfunction will lead to AIDS and the appearance of opportunistic infections and malignancies (Deeks et al. 2015) (Figure 6, right).

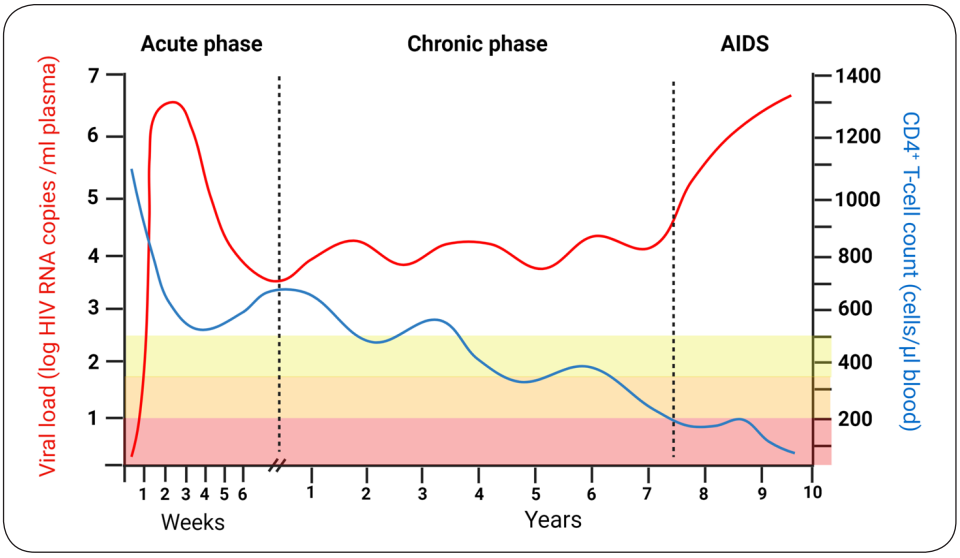

Figure 6. Clinical HIV-1 pathogenesis representation. Viral load is shown as RNA copies/mL (red), and CD4+ T-cell count in cells/µL (blue). Peripheral CD4+ T-cell counts are normally over 500cells/µL. Levels below this amount are represented with three colours according to their associated risk. Thresholds at 500 cells/µL (yellow) and 350 cells/µL (orange) are normally definitory of disease progression. Values below 200 cells/µL are associated with an increased risk of opportunistic infections and AIDS. Image extracted from (Bayón-Gil, 2024).

1.4.1. Immune responses

The immune system will influence the course of infection, acting both as a host for HIV-1 and the main fighting mechanism. Its response is articulated by the innate and adaptive immune systems, that will initiate and coordinate the response to contain and eliminate the virus via cellular and humoral mechanisms.

a. Innate immune response

Innate immunity is the first barrier upon infection, which allows an early defense during the acute phase until more specific immune responses have developed. It is composed of different types of cells, such as macrophages, dendritic cells (DC) and natural killer (NK) cells (Murphy and Weaver 2017).

Macrophages and dendritic cells will be the first to detect HIV-1 through pattern recognition receptors (PRR) like Toll-like receptors (TLR), RIG-I-like receptors or Lectins like Siglec (Yin et al. 2020; Perez-Zsolt et al. 2021). As a result, these antigen presenting cells (APC) will get activated and start secreting proinflammatory cytokines and chemokines that will help recruit other immune cells to the infection site, as well as drive the production of antiviral proteins such as type I interferons (IFN) (Utay

and Douek 2016). While activated macrophages will stay onsite maintaining the inflammatory state and cell recruitment, activated DC will bind to HIV-1 virions and migrate to the lymph nodes. There they will present viral antigens through the MHC-II molecules to lymphocytes, initiating a specific adaptive immune response. This transport to secondary lymphoid organs is also used by the virus to access areas enriched in CD4+ T cells, their main target cell, and contributes to viral spreading (Perez-Zsolt et al. 2021).

NK cells will help with the clearance of HIV-1 infected cells. They can recognize them via the downregulation of HLA-I molecules by the infected cells, or by the detection of viral antigens through antibody-dependent cell toxicity (ADCC) mechanisms (Flórez-Álvarez, Hernandez, and Zapata 2018). Additionally, they contribute to the production of proinflammatory and antiviral proteins such as cytokines and chemokines, helping modulate the adaptive immune response (Murphy and Weaver 2017).

b. Adaptive Immune Response

The adaptive immunity is elicited later in the acute phase and allows the transition to a chronic phase. This highly specific response is orchestrated by the CD4+ T cells, and acts through humoral and cellular branches to tackle the virus. The humoral immune response will allow the production of HIV-1 specific antibodies by B-cells, and the cellular, the activation of cytotoxic CD8+ T cells to kill infected cells and block viral replication.

i. Humoral response

Following infection, B cells will start producing antibodies against the pathogen by undergoing several processes like somatic hypermutation and isotype switching to enhance antibody efficacy. Depending on their neutralization capacity and breadth, antibodies can be classified in non-neutralizing (nNAb), neutralizing (NAb), and broadly neutralizing antibodies (bNAbs). Although nNAb showed to play a role in viral clearance (Horwitz et al. 2017), NAb and specifically bNAbs are the focus of vaccine research (Burton and Hangartner 2016; Haynes et al. 2022).

Neutralizing Antibodies

While some neutralizing antibodies can be elicited in the months following acute HIV infection, they are highly specific of the infecting strains. In contrast, bNAbs, can recognize multiple divergent HIV strains but are elicited in only 1% of PLWH several years after infection. Indeed, they result from a complex and long selection antigenic process (Simek et al. 2009). bNAbs have become a key focus of the research both for the development of monoclonal antibodies and to inform vaccine strategy.

bNAbs target conserved epitopes on the viral envelope, thus overcoming viral evasion mechanisms and its high mutation rate, making them more effective against

a broader range of variants. The screening of large cohorts of PLWH has allowed the identification and isolation of several bNAbs that exhibit broad neutralization against different viral regions (Figure 7). They predominately target highly conserved epitope clusters such as the V3 loop in the glycan shield, the V1/V2 apex on gp120, the CD4 binding site (CD4bs), the gp120/gp41 interface, the FP and the MPER region of gp41.

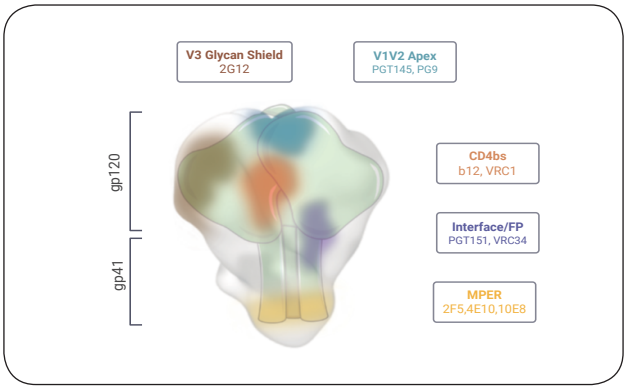

Figure 7. Schematic HIV-Env map with the main vulnerability domains. Some examples of broadly neutralizing antibodies (bNAbs) are included under each region. Adapted from (Tarrés-Freixas et al. 2024; West et al. 2014).

Although they have proved to be useful in HIV treatment and prevention as bNAb infusions (Mascola et al. 2000; Lynch et al. 2015), they face important limitations such as a short half-life, and high production costs which limit their accessibility. To address these limitations, vaccine research is focusing on strategies to produce bNAbs through vaccination, eliminating the need of repeated antibody infusions. Some of these strategies are prime-boost vaccination approaches with engineered immunogens (P. Zhang et al. 2021).

Fc-mediated functions (ADCC, ADCP)

In parallel to their role in virus neutralization, antibodies can guide immune cells to target and destroy infected cells. Antibodies can bind viral proteins, notably Env, at the surface of infected cells. The most stable antibodies covering the infected cells can then recognized via their Fc region by NK cells and macrophages (Forthal and Finzi 2018). This leads to two effector mechanisms: antibody dependent cellular cytotoxicity (ADCC) mediated by NK cells via the release of perforin and granzymes, and antibody dependent cellular phagocytosis (ADCP), mediated by macrophages.

ii. Cellular response

Cellular immunity is central to controlling HIV infection, with CD4+ and CD8+ T cells as key components. These T cells recognize viral antigens presented via major histocompatibility complex (MHC) molecules: CD4+ T cells through MHC class II and CD8+ T cells through MHC class I. Upon antigen recognition, CD4+ T cells become activated and coordinate the adaptive immune response, primarily through the secretion of cytokines that stimulate various immune cells. This activation is crucial for helping CD8+ T cells fully differentiate into cytotoxic T lymphocytes (CTLs), which then eliminate infected cells using mechanisms such as apoptosis and the release of perforin and granzymes—like NK cells. CD8+ T cells are determinant in the establishment of a low viral setpoint after acute infection significantly impacting the size and persistence of the viral reservoir (Ananworanich et al. 2016). The depletion of this cell subset in SIV-infected macaques has proven to dramatically increase plasma viremia and impair immune response (Cartwright et al. 2016; Jin et al. 1999). This could be reverted after repopulating CD8+ T cells, highlighting their role in maintaining viral suppression (Cartwright et al. 2016).

However, as HIV preferentially targets CD4+ T cells, their activation can also increase the pool of susceptible host cells. This promotes viral replication and contributes to faster disease progression. As CD4+ T cells are depleted over time, the immune system becomes progressively compromised, leading to increased vulnerability to opportunistic infections (McCune 2001). This CD4+ T-cell loss can also lead to an impairment of the CD8+ T-cell response, which relies on cytokine signaling for their activation. Additionally, the chronic immune activation caused by HIV replication can lead to cell exhaustion, reducing the capacity to kill and eliminate infected cells efficiently (Khaitan and Unutmaz 2011).

1.5. Natural Control of HIV Infection

Natural control of HIV infection has been observed in some subgroups of PLWH. Such viral control may result from genetic, virological and/or immunological factors (Thèze et al. 2010) (Figure 8). The interaction of these factors can be observed in extreme phenotypes. Although several terms have been used in the past for PLWH controlling the infection (Gurdasani et al. 2014), they have been grouped under the LTNP category for their shared characteristics.

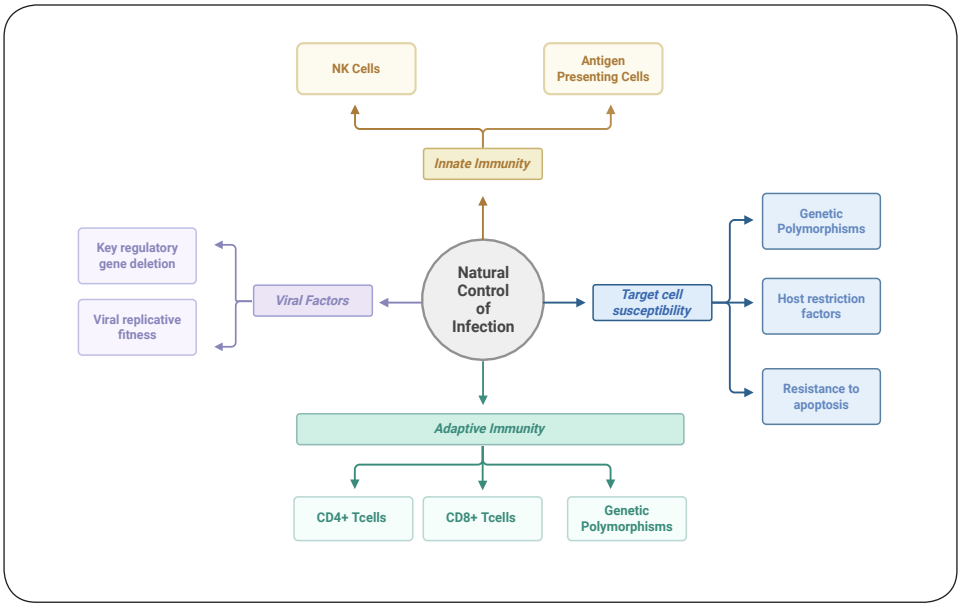

Figure 8. Factors leading to natural control of infection include genetic, virological and immunological factors. Adapted from (Romero Martín, 2022).

LTNP are a small percentage of the PLWH population (1-5%) (Okulicz et al. 2009) able to control disease progression to different extents. They are characterized by low VL, stable CD4+ T-cell counts (>500cells/μL) and being asymptomatic for more than 10 years in absence of ART. Depending on their specific VL they can be subclassified as non-controllers, viremic controllers (VC), and elite controllers (EC) (Casado et al. 2010) (Table 1). Additionally to these phenotypes, clinical trial studies revealed that control can be achieved in some individuals after treatment interruption (ATI), known as posttreatment controllers (PTC) (Sáez-Cirión et al. 2013; Climent et al. 2022; Etemad et al. 2023), pediatric cohorts (Garcia-Broncano et al. 2019; Hartana et al. 2022) and people on long-term ART (Lian et al. 2023).

Table 1. Definitions and characteristics summary of clinical non-progressor groups.

LTNP Phenotypes	Acronym	Definition	Asymptomatic Infection	VL (HIV-1 RNA copies/ mL)
Elite Controllers	EC	Low to undetectable levels in plasma by commercially available assay	+ 10 years	<50
Viremic Controllers	VC	Viral replication off ART to low HIV-1 levels	+10 years	50-2000
Post Treatment Controllers	PTC	Controllers after analytical treatment interruption (ATI)	-	<400

The study of HIV infection control in extreme phenotypes has led to the understanding of the underlying mechanisms that might have led to this control. These are of great relevance as they could provide novel therapeutic strategies that involve permanent virological control without ART, turning EC the closest opportunity of a functional HIV cure.

2. Elite Controllers

EC are a unique phenotype of PLWH who can control infection in absence of ART. These individuals maintain undetectable VL in plasma and lack disease progression for extended periods, mainly over 10 years (Lambotte et al. 2005) (Figure 9). A rare subset, the Exceptional Elite Controllers (EEC), show sustained viral suppression for periods beyond 20 years. Analysis of EEC reported cases, highlight that additional characteristics that could differentiate EEC from EC include low immune system stimulation, undetectable reservoirs and less reactive HIV-specific cellular and humoral responses (María Salgado et al. 2024).

Different genetic, immunological and viral determinants have been associated with this clinical phenotype and made them widely studied as a model for a functional HIV-1 cure (O'Connell, Bailey, and Blankson 2009).

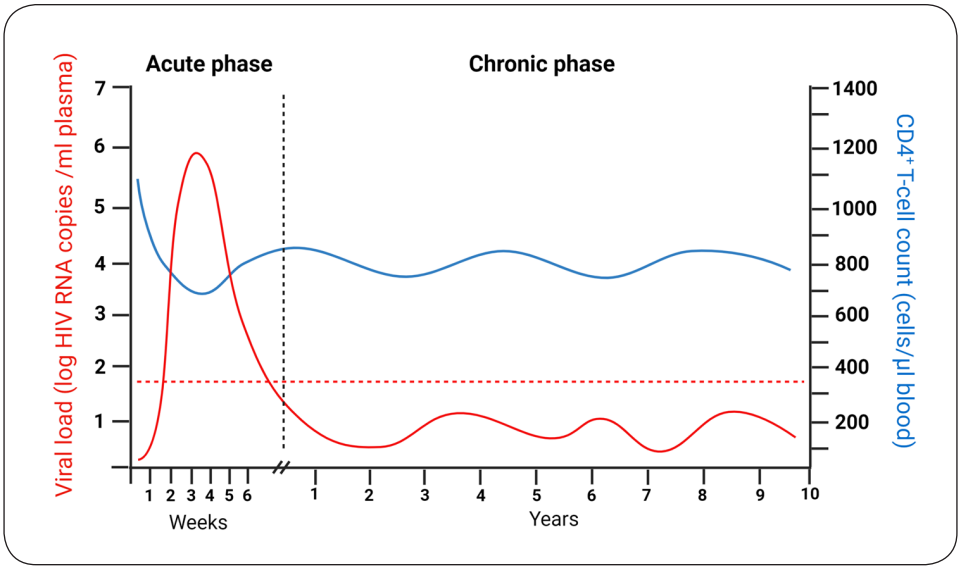

Figure 9. Schematic representation of HIV-1 infection pathogenesis in Elite Controllers. Vertical dotted line (black) separates the acute from the chronic infection phase. Viral loads as HIV RNA copies/mL are marked in red. Horizontal dotted line (red) marks the limit of detection of standard clinical assays (>50 copies/mL). CD4+ T-cell counts as cells/µL are marked in blue. Image from (Bayón-Gil 2024).

2.1. Factors associated with Natural HIV Control

In this section, we will focus on the biological mechanisms that allow individuals to be protected against a pathogen, and in the case of EC, suppress viral replication and control disease progression without ART.

2.1.1. Clinical Progression

If untreated, most HIV infection cases will eventually progress towards a state of immunodeficiency within 10 to 15 years (Sabin and Lundgren 2013), however, the progression rate differs between each individual (Cao et al. 1995) . The progression rate is defined as the time from HIV infection to AIDS in absence of ART and can be clinically characterized by CD4+ T-cell counts and viral load levels (VL). Hence, we can identify a progression spectrum from the rapid progressors on one side, and long term non-progressors (LTNP) or controllers in the other (Figure 10).

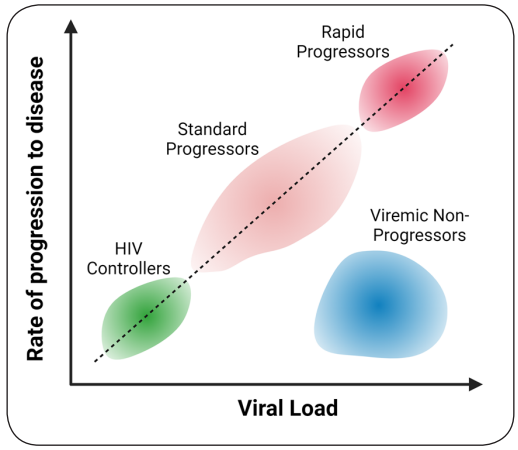

Figure 10. Main HIV-1 phenotypes according to disease progression rate and viral load setpoint. Image from (Bayón-Gil, 2024).

Progressors are those PLWH who, in absence of treatment, clinically progress towards AIDS. According to the progression rate, PLWH can be classified as rapid progressors, standard, or slow progressors. If classified according to viral dating, they are classified as old progressors, if their sequences are contemporary to LTNPs, or modern progressors if they are from recent circulating strains (Pérez-Yanes et al. 2022) (Figure 11). These have implications at the functional level, as sequences from modern progressors present a higher replication and viral evolution, probably due to immune pressure in an ART context (Pérez-Yanes et al. 2022).

LTNP, in contrast, do not progress towards AIDS if untreated. They are examples of natural HIV control, and their characterization is important to better understand the protective immune responses and help develop better vaccines and therapies.

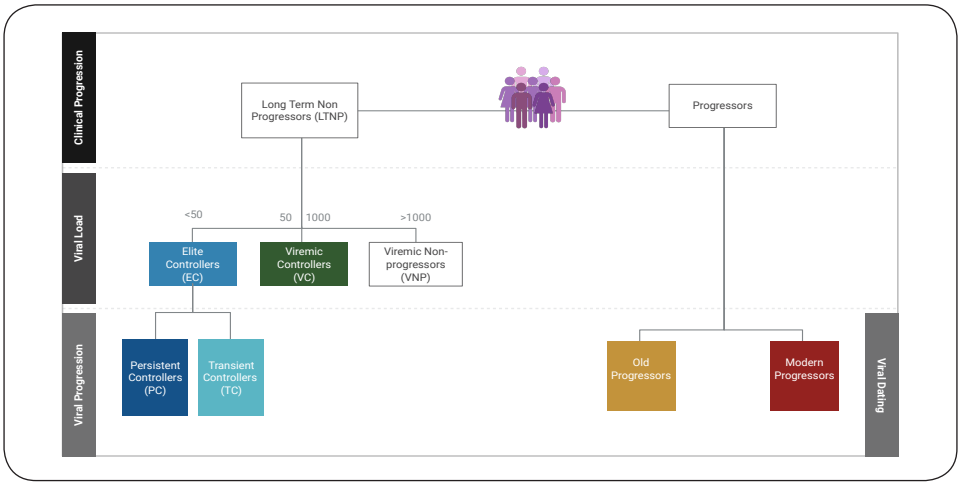

Figure 11. Schematic representation of the main HIV-1 phenotypes described in the literature, according to clinical progression, viral HIV-1 loads, viral progression and viral dating. Viral load values represent HIV RNA copies/mL of plasma. Created with Biorender.com.

2.1.2. Genetic factors

As in other conditions, genetic factors such as mutations or certain alleles can influence HIV-1 acquisition, susceptibility and clinical progression (McLaren and Fellay 2021). One key determinant is CCR5, as polymorphisms in this co-receptor affect HIV attachment and entry, leading to slower disease progression or resistance to infection (Ioannidis et al. 2001). When it comes to the immune response, specific HLA alleles can confer advantages or disadvantages against specific pathogens, but also to cancer and autoimmune diseases. In the case of HIV-1, favorable HLA alleles allow a better presentation of viral peptides to the immune system, leading to more effective control (McLaren and Fellay 2021). Both these genetic determinants were shown to be enriched in LTNP cohorts helping maintain viral suppression in absence of ART (Magierowska et al. 1999).

a. CCR5 Polymorphisms

Viral entry depends on the CCR5 co-receptor. Polymorphisms in the CCR5 receptor, such as CCR5Δ32 deletion, have been associated with reduced risk of HIV infection compared to CCR5 homozygotes (Y. Huang et al. 1996; Dean et al. 1996) . While it has been observed that a high proportion of LTNP carry CCR5 polymorphisms (Stewart et al. 1997; Rodríguez-Da Silva et al. 2017) their presence is not a guarantee of viral control (Smoleń-Dzirba et al. 2017).

In 2007, a PLWH suffering from leukemia received an allogeneic bone marrow

transplant from a homozygous CCR5Δ32 donor and as a result, was cured from both the leukemia and HIV/AIDS. The so-called Berlin patient was the first PLWH cured from HIV infection (Gupta et al. 2020). The same strategy was repeated successfully with four more PLWH (Gupta et al. 2020; Hütter et al. 2009). However, cases like the Geneva patient, showed that while the use CCR5Δ32 donor provide a clear advantage, it might not be strictly necessary to achieve remission if the host immune cells are fully eliminated before ART interruption (Sáez-Cirión et al. 2024).

b. HLA function and structure

The HLA or human major histocompatibility complex (MHC) encodes for molecules that present antigens to T cells enabling the adaptive immune response and elimination of infected cells (Klasse et al. 2020; Cohen et al. 1999). MHC can be from two classes, either Class I or Class II depending on their expression and cells they present to. Class I MHC molecules are expressed on all nucleated cells, therefore recognizing endogenous antigen and presenting them to CD8+ T cells (Murphy and Weaver 2017). They are considered classical if encoded by HLA-A, HLA-B or HLA-C genes and non-classical if coded by HLA-E, HLA-F, or HLA-G. Class II MHC molecules are expressed only on B cells, antigen presenting cells (APC), macrophages, and some T lymphocytes. They mostly present exogenous proteins, that have been endocytosed, degraded and transported to the cell surface. HLA downregulation is used by the virus to evade immune detection, allowing the persistence of infected cells (Klasse et al. 2020; G. B. Cohen et al. 1999).

Importantly, there is a high degree of HLA polymorphism which influences individual capacity to bind and present specific antigens. This is believed to be an evolutionary mechanism intended to optimize the immune response against specific pathogens relevant to a specific population (Prugnolle et al. 2005). However, this means that individuals HLA can confer both advantages and disadvantages depending on the pathogens. As the genes encoding the HLA are polymorphic, a specific nomenclature has been established to differentiate them. This naming contains their HLA gene and an asterisk followed by up to four numbers that correspond to their allele group and antigen specificity (Figure 12).

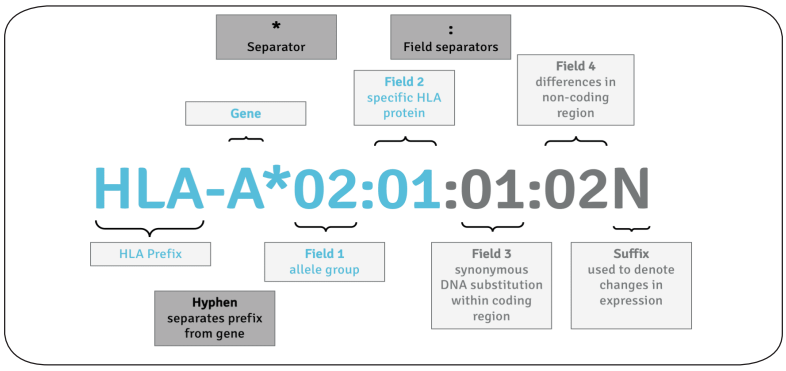

Figure 12. HLA Nomenclature. Source: www.hlaprotein.com

In HIV-1, alleles such as HLA-B*57, B58, B27 and polymorphisms in HLA-C such as rs9264942 appear in high proportion in EC cohorts and have been associated with increased control in both cohort and genome-wide association studies (Migueles et al. 2000; International HIV Controllers Study et al. 2010). The differential expression of some alleles, however, has been linked to rapid disease progression for their role modulating immune responses like NK activity (Li et al. 2022; Apps et al. 2013; Ramsuran et al. 2018). This highlights that viral control depends on the interplay between more factors beneath genetic ones.

2.1.3. Immunological factors

HIV control can depend as well on several immunological features. As seen in clinical progression, both innate and adaptive immunity play a role in the establishment of setpoint viremia and neutralization and control the virus, respectively. In the case of ECs, present some enhanced functions that might account for the exceptional control during longer periods.

As a first barrier, innate immunity and specifically APC and NK cells will act in the viral recognition and elimination. Although limited data is available, ECs present a higher proportion of plasmacytoid dendritic cells (Barblu et al. 2012), major IFN-I producers, along with myeloid dendritic cells (mDC) with enhanced antigen-presenting properties (Huang et al. 2010). Additionally, EC have shown that the presence of specific NK cell receptors along with protective HLA class I alleles (Martin et al. 2007; 2002) or a higher cell subtype presence like NKG2C+ memory-like NK cells and γδ T cells (Climent et al. 2022) have been associated with an increased control of viral replication. Moreover, their expression helps modulate the adaptive immune response but its direct contribution in viral control has frequently been overlooked (Sugawara, Reeves, and Jost 2022) .

In terms of cellular adaptive immunity, it is well established that CD8+ T cells

play a major role in controller phenotypes. CD8+ T cells in ECs exhibit enhanced cytotoxicity against infected cells (Migueles et al. 2008) and a high polyfunctionality, especially in the presence of favorable HLA alleles like B*57 and B*27 (McLaren and Fellay 2021).

In contrast, while the primary objective of an HIV sterilizing vaccine is to elicit bNAbs, the role of natural humoral immunity in controllers is unclear. Compared to non-controllers with higher viral loads, lower HIV-1-specific antibody titers are normally elicited in these controllers, probably due to low circulating antigen levels (Casado et al. 2020). While neutralizing response seems to be lower in controllers versus viremic individuals (Sajadi et al. 2011), studies about antibody functionality present opposite results. Some suggested that EC may have increased ADCC compared to viremic individuals (Madhavi et al. 2017; Lambotte et al. 2009), while others report a lack of ADCC antibodies or ADCC mediator cells (Smalls-Mantey et al. 2012; Isitman et al. 2016). More recent studies supported the latter, establishing that while these antibodies might be reduced, they actually present a higher polyfunctionality that might account for this effect (Ackerman et al. 2016). In any case, further research is needed to clarify the potential role of ADCC antibodies in HIV-1 control.

In summary, strategies promoting the innate and adaptive response through Ab development and increase of specific cell subsets could help bring PLWH closer to long-term HIV remission.

2.1.4. Viral Factors

The effect of viral factors on the control of viral replication and clinical progressions has not been studied as widely as for host or immunologic factors.

The study of different cohorts and non-progressor clusters have identified defective viruses with reduced replication capacity (Cao et al. 1995; Rhodes et al. 2000; Zaunders, Dyer, and Churchill 2011; Pérez-Yanes et al. 2022; Casado et al. 2013). These defective viruses can arise from deletions or mutations in different genes such as Nef (Rhodes et al. 2000) and Env (Casado et al. 2013; Pérez-Yanes et al. 2022), and have been greatly collected and explained in (Valenzuela-Fernández et al. 2022)

Specifically, EC viruses have been described to present poor fusogenicity and infectivity of the viral Env (Pérez-Yanes et al. 2022), poor binding to CD4 receptor (Casado et al. 2018) and a higher exposure of epitopes targeted by neutralizing antibodies (Lian et al. 2021). These defects, along with other host factors, might have helped a better immune system recognition and targeting of the virus at early stages.

In addition to these defective viruses, EC present differential chromosomal integration of intact and defective proviruses, in heterochromatin and euchromatin regions, respectively (Lian et al. 2021). This preferential site integration might resemble the block and lock strategy used against the latently infected reservoir that stands as the main barrier to HIV cure.

2.2. Reservoir Size and composition

The reservoir is one of the critical factors that keeps HIV-1 from being completely cured. Even with ART and undetectable levels of circulating viruses, viral reservoirs remain as latent centers within immune cells, allowing rebound if treatment is discontinued (Palmer et al. 2011).

HIV reservoirs are mainly present in blood (peripheral blood mononuclear cells, PBMCs) and in lymphoid tissues, such as lymph nodes and GALT, where the virus can evade the immune response (Veazey and Lackner 1998). Within these reservoirs, HIV can exist in either intact or defective forms, that will also influence where the viral genetic material (proviral DNA) is integrated into host cell's DNA. Intact proviruses have the potential to produce infectious viruses if reactivated, tending to integrate in transcriptionally active regions. In contrast, defective proviruses that carry mutations or deletions that prevent them from producing functional viruses, are often found in heterochromatic regions. Even if integrated in areas with low transcription activity, defective viruses can still contribute to viral genetic persistence.

Although early treatment has been observed to restrict reservoirs, it does not completely prevent its formation or lead to its eradication (Luzuriaga et al. 2015). In the case of natural control of infection, such as in EC, immune selection pressure might have led to smaller and less transcriptionally active reservoirs (Jiang et al. 2020). Nevertheless, replication competent viruses have been retrieved from EC reservoirs (Jiang et al. 2020), suggesting that latency is not a permanent or irreversible state but a dynamic process.

To better understand the role of the viral reservoir in natural control and its translation to functional cure strategies, further characterization is needed in terms of composition, quantification, genomic location, intactness and evolution (Gasca-Capote et al. 2024).

2.3. Elite Controllers as a model of functional cure

Due to undetectable VL, stable CD4+ T-cell levels, low reservoir for long periods of time in absence of ART, EC have been considered a model for the functional cure of HIV-1. They are, however, a heterogenous and dynamic phenotype resulting in different clinical outcomes, including a proportion of EC that loses HIV-1 control over time (Gasca-Capote and Ruiz-Mateos 2024). Mechanisms responsible for control and loss of spontaneous viral control in these individuals are still not fully understood, but their characterization provides important insights into vaccine strategies and immunological therapies.

2.4. Loss of virological control

Historically, controlling phenotypes have been grouped under a single definition. However, the loss of virological and/or immunological control in a proportion of EC raised concerns about whether this phenotype remained a relevant model for functional cure.

As a consensus, virological control is considered if during a year period, at least 3 consecutive measurements of plasma viremia are <50 copies/mL (Yang et al. 2017). Occasional blips (short-term increases of VL >50 copies/mL) can be observed but they are temporary and do not necessarily indicate clinical progression. They are normally viruses arising from the reservoir, not from new viral replication. In contrast, loss of viral control (LoC) has been stablished if ≥3 consecutive viremia measurements are ≥50 copies/mL or if one is already ≥1,000 RNA copies/mL (Yang et al. 2017). Finally, the loss of immunological control is considered when CD4+ T-cell counts get below 350 cells/μL (Noel et al. 2015).

Although several factors have been identified as risk factors for the loss of virological control, the characterization of these individuals is still relevant to fully understand the complexity of the phenotype. Beyond control mechanisms, risk factors for the loss of control can also be classified into viral and host factors (Table 2). Viral factors include viral blips (Yang et al. 2017; Chereau, Madec, Sabin, Obel, Ruiz-Mateos, Chrysos, et al. 2017), coinfections (Leon et al. 2016a; Madec et al. 2013), HIV-1 superinfections (Clerc et al. 2010; Caetano et al. 2019; Braibant et al. 2010) and change of tropism (Rosás-Umbert et al. 2019). Host factors are more complex, involving clinical, epidemiological and demographic variables, such as gender and age. However, decline of HIV-specific CD8+ T-cell response (Pernas et al. 2018; Collins et al. 2021), elevated systemic inflammation (Pernas et al. 2018; El-Far et al. 2016) and other host genetic factors have been identified as possible contributors.

Understanding the mechanisms behind loss of control may help refine models for the study of permanent HIV remission. Additionally, it can help understand how viral remission can be achieved in these individuals, aid in biomarker identification for individuals at risk of loss of control, support participant monitoring during ATI trials and refining correlates of protection (Casado et al. 2010). As a result, longitudinal studies have been comparing EC who maintain virological control with those who eventually lose it in absence of ART (Pernas et al. 2013; Casado et al. 2007; Pernas et al. 2012) establishing two phenotypes: persistent and transient controllers.

Table 2. Summary of Viral and Host Factor associated with the loss of virological control in EC individuals

VIRAL FACTORS		**Reference**
Viral Blips		(Yang et al. 2017; Chereau, Madec, Sabin, Obel, Ruiz-Mateos, Van Der Valk, et al. 2017)
Superinfections		(Clerc et al. 2010; Caetano et al. 2019; Braibant et al. 2010)
HOST FACTORS		
Clinical	Nadir	(Leon et al. 2016a; Madec et al. 2013)
	Coinfections (HCV, HBV)	(Leon et al. 2016a; Madec et al. 2013)
Epidemiological	Risk factor for HIV acquisition	(Leon et al. 2016a; Madec et al. 2013)
	Seroconversion year	(Leon et al. 2016a; Madec et al. 2013)
Demographic	Gender	(Leon et al. 2016; Madec et al. 2013)
	Age	(Leon et al. 2016; Madec et al. 2013)
HIV-specific T cell response		(Pernas et al. 2018; Gasca-Capote and Ruiz-Mateos 2024)
Pro-inflammatory milieu		(Pernas et al. 2018; El-Far et al. 2016)

2.4.1. Persistent Controllers and Transient Controllers

Persistent Controllers (PC) have been defined by those EC that maintain virological control over time and for the moment the best functional cure model. Transient controllers (TC) are those EC that although having controlled the virus for prolonged periods, they lose control overtime (Gasca-Capote and Ruiz-Mateos 2024). Both phenotypes present differences at metabolomic, proteomic, T-cell, and NK response level (Table 3). While the study of control mechanisms in ECs has already been used as vaccine strategies targeting T-cell response and bNAb elicitation, this further classification might allow to better define a functional cure model and to identify permanent HIV remission associated biomarkers.

Table 3. Phenotypic differences between PC and TC at a genomic, biomarker, immunological and virological level. (*Continued*)

		Persistent Controllers	Transient Controllers
Genomic (Casado et al. 2020b; Gasca-Capote et al. 2024)	**HLA**	HLA-B*57 and HLA-B*27,especially overrepresented.	Reduced frequency of protective ones.
Biomarkers (Rodríguez-Gallego et al. 2019)	**Proteomic Profile**	Less proinflammatory profile. Greater levels of extracellular vesicle-associated cytokines (Poveda et al. 2023).	Increased expression of proteins related to transendothelial migration, coagulation, and inflammation mechanisms.
	Metabolomic Profile (Tarancon-Diez et al. 2019)	Less mitocondrial damage and oxidative stress.	Deregulated mitochondrial function, higher oxidative stress,increased immunological activation.
	miRNA	-	Expression of miRNA like hsa-miR-376a-3p and hsa-miR- 199a-3p, associated to loss (Masip et al. 2021).

Table 3. Phenotypic differences between PC and TC at a genomic,biomarker, immunological and virological level.(*Continued*)

		Persistent Controllers	Transient Controllers
Immunological	**Polifunctionality** (Gasca-Capote and Ruiz-Mateos 2024)	Highly polyfunctional HIV-1-specific T-cell response, especially in CD8+ T cells .	Reduced and less polyfunctional HIV-specific T-cell response.
	CD4/CD8 (Collins et al. 2021)	Associated with several disturbances in CD4 and CD8 T cell homeostasis (Benito et al. 2024).	Lower and drastic decrease of HIV-specific T-cell responses (lower CD4/CD8 ratio) prior loss of control (Mendoza et al. 2012).
	NK	Memory-like populations coexpressing NKG2C and NKG2A in durable control (Sánchez-Gaona et al. 2024)	Limited data available regarding the role of NK.
	DC	Increased number of myeloid dendritic cells (mDCs)and plasmacytoid dendritic cells (pDCs) (Dominguez-Molina et al. 2018).	Limited data available regarding the role of DC.
Virological	**Proviruses** (Gasca-Capote et al. 2024)	Absence or low proportion of intact proviruses. Preferentially integrated in centromeric satellite DNA or zinc finger genes.	Greater proportion of intact proviruses. Mostly integrated into genic regions.
	Others	More prone to spontaneously clear HCV (Dominguez-Molina et al. 2020)	

3. HIV Vaccines

Forty years of medical and basic research have contributed to great progress in the treatment and prevention of HIV/AIDS, albeit, with no successful result on a definitive cure. Recently, pre-exposure prophylaxis (PrEP) has proven to be a new successful weapon for HIV prevention and the release of a new class of capsid-targeted drug, Lenacapavir, offers new perspective on long-acting treatment (Jogiraju et al. 2025a). Despite this undeniable success, the virus is still circulating and certain regions of the world such as eastern Europe are even seeing an increase in transmission. In general, access to treatment is still highly inequal across the world and relies heavily on international aid. Recent political events demonstrate how fragile and reversible the current situation is. In this context, and although the development of an HIV vaccine has remained elusive, it still appears as a necessary game changer to achieve global HIV eradication (Jogiraju et al. 2025a). HIV vaccines can be separated in preventive and therapeutic vaccines depending on their main goal (Tarrés-Freixas et al. 2024). The objective of preventive vaccines is to develop a broad and durable sterilizing humoral immunity that can block infection all together. Therapeutic vaccines, on the other hand, aim to boost the immune response, helping viral control and potentially improving the clearance of latently infected cells for example in combination with latency reactivating agents.

Passive immunization with bNAbs has demonstrated effectiveness in preventing infection in animal models (Escolano, Dosenovic, and Nussenzweig 2017). Moreover, the Antibody mediated protection (AMP) trials have demonstrated proof of concept protection efficacy of a VRCO1 antibody-based vaccine against a small subset of VRCO1 sensitive infecting virus (Corey et al. 2021; Gautam et al. 2016). However, its widespread use is limited by their low half-life, and high costs related to their administration and manufacturing, making global accessibility challenging. Although AMP has limitations, it is an interesting tool in the fight against HIV, which would benefit to be administered along other long-term strategies such as active immunization. With this, an antigen is administered through a vaccine platform to stimulate the body to generate antibodies and involve other immune system responses like ADCC (Rahman et al. 2023). Antigen candidates or immunogens for HIV vaccination can be categorized into those that would induce cellular responses and those that would elicit protective humoral responses. They are both necessary to effectively target HIV and provide durable protection.

3.1. Envelope Antigens

The Env protein is the only viral protein at the surface of the virus, and it is necessary and sufficient to mediate the viral entry. It is the only target of effective NAbs, and as a result, the main immunogen candidate for HIV vaccine development (Burton and Hangartner 2016).

Immunizations with unmodified Env proteins generate an insufficient protective response, mainly due to viral escape mechanisms. As mentioned earlier, Env is a highly variable and unstable protein, with a low incorporation density at the viral surface. This, added to the presence of a glycan shield, makes the virus able to avoid immune responses and therefore lead to low bNAb production.

An efficient vaccine would need to provide a potent, broad and long-lasting immune response, with neutralizing effects through generation of bNAbs. Env trimers alone cannot induce bNAbs which require a long Ab affinity maturation process to be able to neutralize. As a result, engineered immunogens have been designed to optimize immune priming and speed up this process.

3.1.1. Germline Targetting

Natural bNAb-producing B cells require multiple rounds of somatic hypermutation and affinity maturation in germinal centers to develop their broad neutralizing capabilities (Kwong and Mascola 2012). Therefore, to achieve the induction of bNAbs by vaccination, researchers proposed a strategy called germline-targeting (Saunders et al. 2019). It is based on reverse vaccinology, and it aims to stimulate specific precursor B cells previously identified as the origin of specific bNAb-producing B cells. These precursors cannot be elicited directly with complete Env immunogens; hence, the strategy consists in a sequential immunization utilizing Env derived immunogens with increasing complexity.

The process can be separated into two main steps, priming and boosting, which ensure the activation of the right B cells and the shaping of their immune response towards areas of interest (McGuire 2019). Priming is the first and most critical step (Figure 13). In this phase, a germline-targeting immunogen is used to activate the rare naïve B cells that have the potential to develop into a bNAb-producing cells. Once activated, these B cells undergo sequential boosting with carefully designed immunogens. Each booster is intended to progressively guide the B cells through somatic hypermutation and affinity maturation toward the desired antibody profile (Haynes et al. 2022). This boosting process incorporates shepherding and polishing steps, in which immunogens are designed not only to promote maturation but also to redirect the immune response away from non-neutralizing or off-target pathways (Saunders et al. 2019).

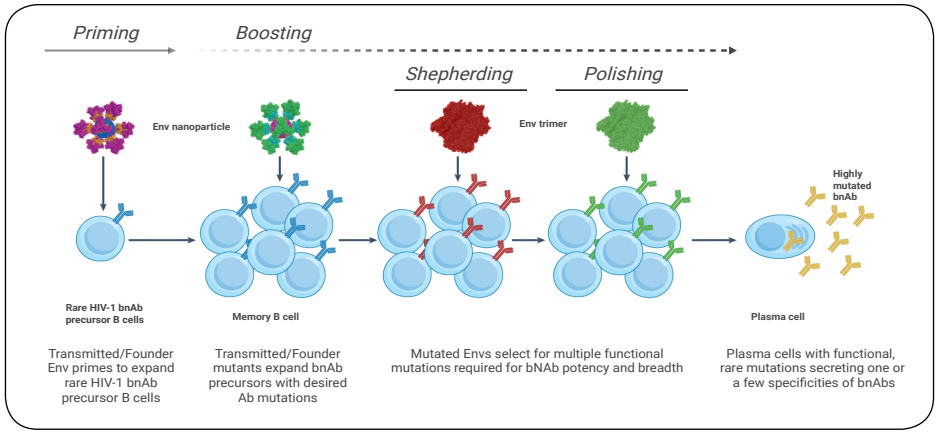

Figure 13. Schematic representation of the Germline targeting strategy. Adapted from (Haynes et al. 2022; Haynes 2021) with Biorender.com.

As a result, engineered immunogens need to present specific characteristics in each step of the process. Priming immunogens need to have a high affinity for germline receptors (BCRs), so they are often simplified versions of the epitope to ensure attachment. Additionally, they tend to present minimal glycan shields, to ensure rare precursors will access the epitope without interference. Finally, to maximize B-cell activation, they are often presented in scaffolded structures or multivalent platforms such as nanoparticles (Brinkkemper and Sliepen 2019; Sliepen et al. 2015; Kanekiyo et al. 2019; Tokatlian et al. 2018). This virus-mimicking arrangement helps focus the immune response on the target epitope while avoiding irrelevant but immunodominant areas.

In contrast, boosting immunogens will need to be progressively more complex to refine the epitope exposed versions and shape antibody response. Formats such as SOSIP trimers are commonly used to increase immunogen resemblance to the native viral structure (Pugach et al. 2015; Sanders et al. 2013). As B cells mature, more glycosylated immunogens are also reintroduced to train them to recognize fully glycosylated forms of circulating viruses. During shepherding and polishing, techniques like immunofocusing and epitope masking can also be used to limit irrelevant regions and better guide B cells towards the desired Ab profile.

3.1.2. Envelope Engineering

The first attempts had limited success even if Env was tested in multiple forms. While these initial immunogens were unable to induce broadly protective responses, more advances have been developed in the past years: from the selection of optimal immunogens to stabilization of the antigen (Sanders et al. 2013) to different administration platforms and combinations of vaccination regime strategies

(Hosseinipour et al. 2021; Tokatlian et al. 2018; Tarrés-Freixas et al. 2023). Engineered immunogens include:

- Linear epitope-based vaccines (peptide immunogens) consisting of simple primary or secondary amino acid structures. These were tested against the membrane-proximal region (MPER) in gp41 and the V3 loop in gp120, and the fusion peptide in gp41 (Wang et al. 2024).
- Epitope scaffolds: constituted of a specific Env epitope mounted on a heterologous scaffold protein to ensure proper conformational presentation.
- Different gp120 based immunogens containing the full monomer or specific elements of gp120: core protein or outer domain (OD) only (Caniels et al. 2025).
- Trimeric proteins, which include different attempts to mimic the full Env trimer ectodomain notably using uncleaved gp140 (gp120 + gp41 ectodomain lacking the furin site) or native like stabilized SOSIP Env trimers which maintain a prefusion conformation (Sanders et al. 2013).

While some of these strategies, notably epitope scaffolds, Env OD and native like trimers are showing encouraging results for the induction of bNAbs, delivery as (easier to produce) soluble monomers or trimers do not properly elicit BCR crosslinking and B-cell activation. In fact, the only successful subunit-based vaccines (against hepatitis B and human papillomavirus) are based on self-assembling Virus-like nanoparticles presenting multiple copies of the immunogens (Wheeler et al. 2009; Ho, Jeevan-Raj, and Netter 2020). Therefore, there is a parallel effort to explore different approaches to allow multimeric immunogen presentation.

3.1.3. Multimeric presentation

Delivery strategies range from soluble proteins, multivalent platforms or nucleic acids and have proved to be safe and effective for immunogen delivery. However, the presentation of immunogens in multimeric platforms has been a strategy to increase the magnitude and quality of the immune response against these antigens (Thalhauser and Breunig 2020). Multiple animal studies have shown an improved Ab response, with over a 10-fold increase in NAb titers compared to soluble proteins in the RSV field (Marcandalli et al. 2019). These multimeric platforms would allow an increased antigen valency (Kato et al. 2020), better BCR cross-linking and an improved trafficking, uptake and presentation (Brinkkemper and Sliepen 2019; Tokatlian et al. 2019), as well as the display of mosaic immunogens contributing to Ab breadth (Kanekiyo et al. 2019). In the case of HIV, however, poor display of non-native Env might have led to lower NAb increases.

Platforms can be based on synthetic protein clusters or lipidic nanoparticles such as VLPs (Gao, Wijewardhana, and Mann 2018). As synthetic protein clusters, there are ferritin nanoparticles or eOD-GT8 which allow the incorporation of 8 or 60 trimers respectively (Sliepen et al. 2015; Kato et al. 2020).

a. HIV-1 based virus-like particles (VLP)

Virus-like particles (VLP) are used as a vaccine platform that has been proven effective and safe against multiple viruses such as hepatitis B virus (HBV) or the human papilloma virus (HPV) (Lua et al. 2014). They are produced with structural or capsid viral proteins, thus resembling native viruses without being replicative or infectious due to their lack of infectious genetic material and regulatory proteins. Their particle size and surface immunogen display contribute to high immunogenicity, enabling efficient recognition and internalization by APCs. By mimicking viral particles, they facilitate targeted trafficking to lymph nodes, promoting B and T cell stimulation.

In the case of HIV, the fact that HIV Gag is enough to produce VLPs (Gheysen et al. 1989; Cervera et al. 2013) has been used to incorporate proteins on their surface and act as vaccine preparations (Visciano et al. 2011; Tarrés-Freixas et al. 2023). Their production was classically focused on the co-transfection of Env with Gag. Due to the escape nature of the native Env, this leads to low exposure at the surface. As a result, both immunogen modifications and new VLP production strategies like the use of fusion proteins have been envisioned and developed with good results (Tarrés-Freixas et al. 2023). As an advantage, both strategies could also be delivered as nucleic acid vaccines (DNA or mRNA) (Tarrés-Freixas et al. 2024), enabling their flexible use in heterologous vaccination regimens and improving scalability, stability, and cost-effectiveness in their production.

i. Env/Gag Co-expression

The Env/Gag co-expression or co-transfection is a widely used method to produce VLPs that mimic HIV-1 without being infectious (Beltran-Pavez et al. 2021). It is based on the co-transfection of gag and env constructs either in DNA or mRNA format into a producing cell line. Several cell lines like HEK293, CHO and Expi293F have shown to be suitable, each with its advantages and limitations. Once inside the cell, the produced Gag proteins will self-assemble into budding particles (VLPs), incorporating the Env proteins that will be produced and expressed in the cellular membrane (Figure 14,left). This VLPs can be collected from the culture medium and purified for vaccine use. Some examples of this strategy as mRNA vaccines, showed they are capable of neutralizing antibodies elicitation that reduce SHIV infection in macaques (Zhang et al. 2021). This method however faces some limitations as natural Env incorporation is inefficient and results in low density Env exposure.

ii. Env-Gag Fusion Protein

Several strategies have been developed to enhance density at the surface, such as the generation of fusion proteins encoding for a range of antigen sizes from MPER of HIV-1, to RSV-F of RSV (Tarrés-Freixas et al. 2023; Trinité et al. 2024; Ortiz et al. 2023; Barajas et al. 2024).Now we addressed the generation of full-Env VLPs.

Fusion protein constructs, compared to cotransfection strategies, do not rely on the transfection of two separate plasmids as Env and Gag are delivered as a single construct, fused through an HIV-1 transmembrane domain (Env-Gag) (Figure 14, right). This method was expected to reduce the low Env incorporation to the cellular membrane. Env-Gag proteins are expected to have an impact on Env incorporation, as well as an effect on immune presentation and antibody responses. This fusion could facilitate the formation of VLPs, which would also mimick the HIV native structure and would target both cellular and humoral immunity (Tarrés-Freixas et al. 2023). Theoretically, after protein production in the ER and migration to the cell membrane, the new budding VLPs should contain as many immunogens on the surface as Gag molecules are contained in the VLP.

In addition, this construct might increase Env stability and enhance antigen presentation of Env as the addition of Gag would need the truncation of the Env CT, improving both Env availability and targeting by the immune system. Nevertheless, it could also disrupt Env trafficking and affect glycosylation and folding. Both these factors could alter epitope exposition by making Env more accessible to immune responses and to the development of nNAbs.

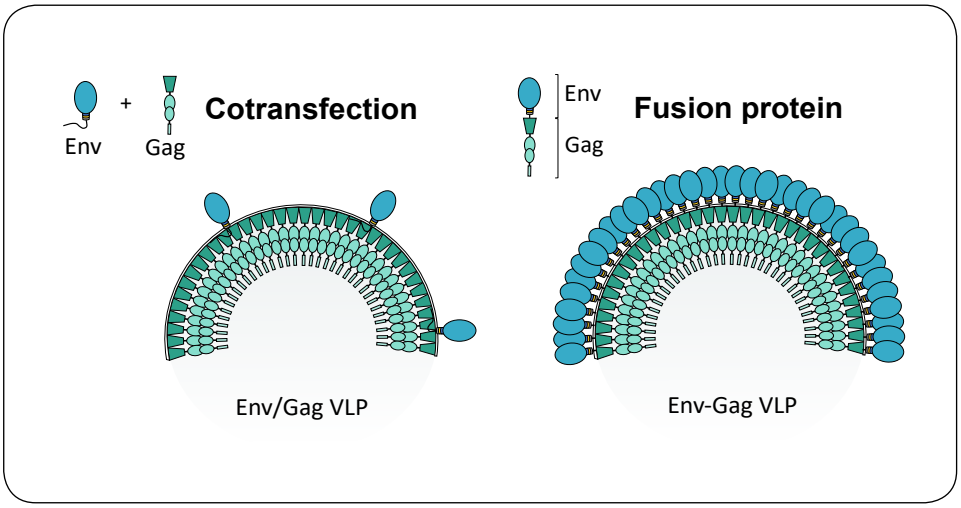

Figure 14. VLP production strategies: Cotransfection and Fusion protein. Cotransfection with unmodified HIV Gag and Env would allow low density to escape immune surveillance. The fusion protein could help achieve high density of Env at the surface. Adapted from the original by Dr. Benjamin Trinité.

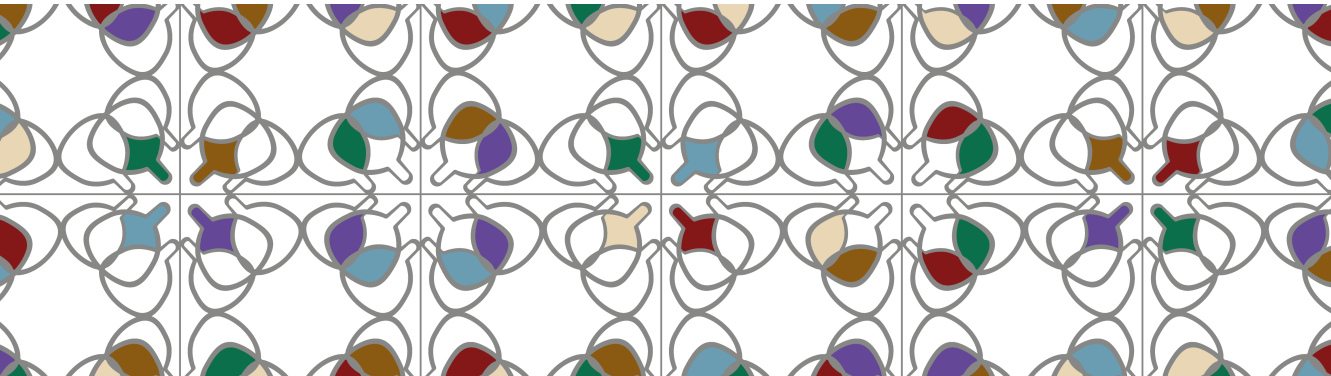

HYPOTHESIS AND OBJECTIVES

Hypothesis

HIV-1 has several strategies to evade the immune system recognition and induction of protective responses. These have hampered so far, the development of effective protective vaccines. However, some individuals, Elite Controllers (EC), can naturally control HIV-1 replication in absence of ART. While specific mechanisms explaining this control are still not well understood and multifactorial, it has been shown to be linked to specific Env functional properties in some cases.

As the EC phenotype is rare, several of our previous studies (Pérez-Yanes et al. 2022; Casado et al. 2018; 2013) had a limited sample size. To further understand the Env contribution to this phenotype, we expanded this analysis to samples from the largest EC Spanish cohort (ECRIS) and hypothesized that EC Envs properties can be directly or indirectly associated to viral control. Specifically, decreased functionality might allow an easier tackling by the immune system therefore generating lower immune damage and potentially better immune responses, including neutralizing ones.

To address the vaccine challenge of eliciting protective responses, we hypothesized that the use of Env sequences isolated from HIV ECs as immunogens, could be beneficial for the elicitation of bNAb responses, due to their lower affinity for CD4 and lower fusogenicity.

Additionally, to further improve antigen delivery and presentation, the candidate antigen will be incorporated into a VLP platform by fusing it with Gag. This fusion protein strategy proved to be efficient in previous works by our group (Tarrés-Freixas et al. 2023; Ortiz et al. 2023; Barajas et al. 2024; Trinité et al. 2024).

Objectives

The main objective was the characterization, selection and optimization of an HIV-1 EC Envelope (Env) derived immunogen and its implementation in a VLP-based vaccine candidate optimized to display high antigenic density. The following specific objectives were then formulated:

1. EC Cohort Characterization. Expand characterization of the role of Env and its associated neutralizing responses in the ECRIS Cohort.

1.1. Functional characterization of the Env and comparation between controlling and non-controlling clinical phenotypes.

1.2. Characterization of neutralizing responses and their contribution to the natural control of infection.

2. Antigenicity and immunogenicity analysis of Env sequences from EC

2.1. EC Envelope Selection. Selection of representative Envs from the EC with the best surface and antigenicity expression.

2.2. Production of candidate Env–expressing VLPs. Incorporation of the candidate antigens in a Viral-Like-Particle platform (VLP) following a strategy to obtain VLPs capable of displaying high antigenic density.

2.3. Analysis of Env immunogenicity in an animal model. Analysis of neutralization responses.

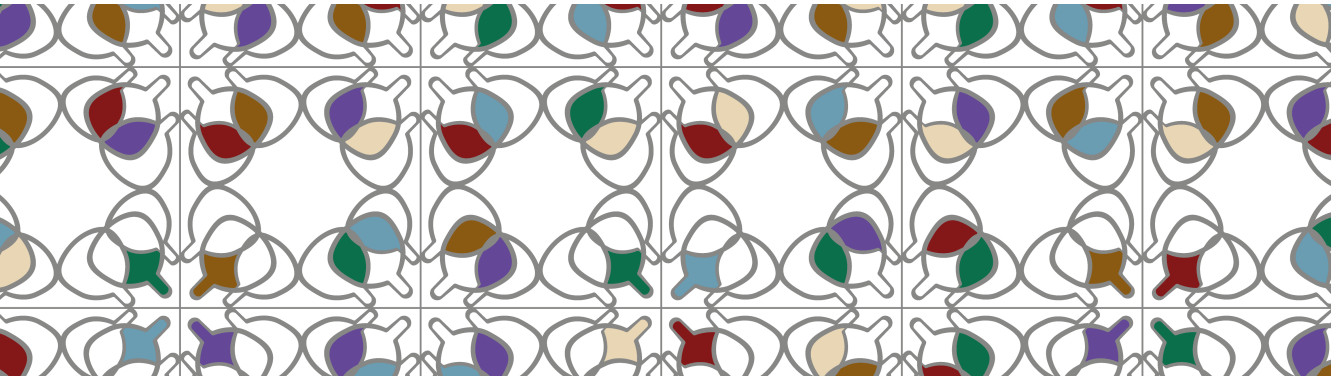

MATERIALS AND METHODS

1. Study participant samples and animal procedures

1.1. Ethical Statement

Study participant samples were obtained from the HIV controllers (ECRIS cohort) of Spanish AIDS Research Network cohort (CoRIS). The ECRIS cohort incorporates individuals from the long-term non-progressor (LTNPs) cohort, CoRIS cohort, and different hospitals. They are all contained in the Biobank HIV Hospital Gregorio Marañón (HGM). This cohort is formed by participants who gave written informed consent for genetic analysis studies and were registered as sample collection in the Spanish National Registry of Biobanks for Biomedical Research with number C.0004030. Consent was approved by the Ethical and Investigation Committees of the Centro Sanitario Sandoval (Madrid, Spain). All samples were encoded and de-identified in these centers. All clinical investigations were conducted according to the principles indicated in the Declaration of Helsinki. The studies were approved by the Comité de Ética de la Investigación y de Bienestar Animal of the Instituto de Salud Carlos III (ISCIII) under no. CEI PI 05_2010-v3 and CEI PI 09-2013. All animal procedures were evaluated and approved by the Ethical Committee on Animal Experimentation (CEEA) of the Germans Trias i Pujol Research Institute (IGTP), and the Ministry of Territory and Sustainability of the Generalitat de Catalunya.

2. Viral Envelopes

A total of 70 viral Env clones were obtained from samples of different origins collected in the HIV HGM BioBank integrated into the Spanish AIDS Research Network (RIS-RETIC, ISCIII). Upon obtention and reception, samples were processed following current procedures and frozen. Sample identification numbers (ID) and characteristics are summarized in Table 4. All clones were HIV-1 subtype B and belonged to ECs, LTNP-Viremic Controllers (VC) and standard progressors contemporary to LTNPs. In the case of ECs that lost control (TC), only Envs

isolated during the control period are displayed. Envs isolated during the viremic period (n=5) are further included and explained in Table 11 in the results section. Of the current cohort, four Envs had to be discarded for identification mistakes from the Biobank, a fifth one for the presence of a stop codon, and a sixth one which was duplicated from already published data. As a result, from the 70 Envs, only 59 will be displayed in the functional analysis (Figure 15, Figure 16). According to their phenotypical groups, displayed Env clones can be traced back to 20 EC individuals, one VC and 14 Progressors. EC individuals were represented by 39 clones, VC by one clone and progressors by 19 clones (Figure 16).

Table 4. Epidemiological, clinical, and host characteristics of the viral Envs. Envs isolated from the same individual are associated with brackets. Only Envs isolated during the control period are included. LTNP : Long-term non progressor. EC: elite controller. #N/A: Not available. (*Continued*)

Clinical group	Sub-group	Env Code	ID Code	Sex	Viral load at sampling (copies/mL)	Diagnostic time	Sampling time	HLA-B (Type: Subtype)	Viral Dating (B Ancestor Los Alamos)
LTNP	EC	1	MVS-048	F	<20	1986	2017	B51/B57	1983
		2	MVS-048	F	<20	1986	2017	B51/B57	1983
		3	MVS-033	M	<39	1987	2008	B07/B57	1983
		4	MVS-033	M	<39	1987	2008	B07/B57	1983
		5	MVS-035	M	<37	1988	2013	B15/B-	1989
		6	MVS-035	M	<37	1988	2013	B15/B-	1989
		7	MVS-065	M	<20	1986	2013	#N/A	1986
		8	MVS-065	M	<20	1986	2013	#N/A	1987
		9	MVS-064	F	<50	1985	2012	#N/A	2003
		10	MVS-064	F	<50	1985	2012	#N/A	2003
		11	MVS-072	F	<20	1994	2013	B49/B51	1985
		12	MVS-072	F	<20	1994	2013	B49/B51	1985
		13	MVS-072	F	<50	1994	2009	B49/B51	1983
		18	MVS-001	F	<37	1989	2015	B57:01/B14:02	1984
		19	MVS-001	F	<37	1989	2015	B57:01/B14:02	1984
		20	MVS-001	F	<50	1989	2004	B57:01/B14:02	1983
		21	MVS-051	M	<19	1988	2013	B35/B57	1991
		22	MVS-071	M	<50	2003	2005	B14/B35	1993
		23	MVS-071	M	<50	2003	2005	B14/B35	1995
		24	MVS-071	M	<50	2003	2013	B14/B35	1995

Table 4. Epidemiological, clinical, and host characteristics of the viral Envs. Envs isolated from the same individual are associated with brackets. Only Envs isolated during the control period are included. LTNP :Long-term non progressor. EC: elite controller. #N/A: Not available. *This individual is heterozygous for CCR5Δ32 *(Continued)*.

Clinical group	Sub-group	Env Code	ID Code	Sex	Viral load at sampling (copies/mL)	Diagnostic time	Sampling time	HLA-B (Type: Subtype)	Viral Dating (B Ancestor Los Alamos)
		25	MVS-031	M	<20	1984	2007	B27/B49	1991
		26	MVS-031	M	<20	1984	2007	B27/B49	1991
		27	MVS-083	M	<37	2004	2016	#N/A	2012
		29	MVS-020	M	<19	1990	2007	B14/B51	1985
		30	MVS-020	M	<19	1990	2007	B14/B51	1988
		31	MVS-090	M	<50	1989	2004	B40/B57	1988
		32	LTNP2	M	<50	1987	2003	B44:02/B56:01	1983
		33	LTNP2	M	<50	1987	2003	B44:02/B56:01	1983
		34	MVS-092	M	<50	1986	2004	B07/B52	1998
		35	MVS-093	M	<50	1992	2005	B44:02/B57:01	1998
		36*	MVS-088	F	<50	1986	2009	B39:01/B44:02	1991
		37*	MVS-088	F	403	1986	2017	B39:01/B44:02	1990
		39*	MVS-088	F	403	1986	2017	B39:01/B44:02	1989
		40*	MVS-088	F	134	1986	2018	B39:01/B44:02	1990
		45	MVS-040	F	<37	1992	2013	B39:01/B57:01	1984
		46	MVS-040	F	<37	1992	2013	B39:01/B57:01	1991
		47	MVS-019	M	<50	1985	2004	B15/B44	1988
		48	MVS-087	M	<37	1988	2011	B27/B35	1988
		49	MVS-087	M	<37	1988	2011	B27/B35	1988
	Viremic	50	MVS-099	M	#N/A	1986	2005	B13:02/B40:01	2004
Progressor	Old	52	AM89-AS6	M	#N/A	1989	1989	#N/A	2002
		53	AM89-AS6	M	#N/A	1989	1989	#N/A	2010
		54	AM93-I3-93	M	87000	1993	1993	B40:02/B44:02	1997
		55	AM93-I5-93	F	10000	1993	1993	#N/A	1986
		56	AM93-I9-93	M	51000	1992	1993	#N/A	1988
		57	AM-93-I10-93	F	89000	1993	1993	B15:01/B49:01	1988
		58	AM93-I12-93	M	61000	1992	1993	B45:01/B49:01	2001
		59	AM93-I12-93	M	61000	1992	1993	B45:01/B49:01	1983

Table 4. Epidemiological, clinical, and host characteristics of the viral Envs. Envs isolated from the same individual are associated with brackets. Only Envs isolated during the control period are included. LTNP : Long-term non progressor. EC: elite controller. #N/A: Not available.

Clinical group	Sub-group	Env Code	ID Code	Sex	Viral load at sampling (copies/mL)	Diagnostic time	Sampling time	HLA-B (Type: Subtype)	Viral Dating (B Ancestor Los Alamos)
		60	AM93-I13-93	M	77000	1988	1993	B18:01/B45:01	2005
		61	AM94-I15-94	F	39000	1988	1994	#N/A	1993
		62	AM93-I24-93C	M	#N/A	1990	1993	#N/A	1993
		63	AM93-I24-93C	M	#N/A	1990	1993	#N/A	2006
		64	AB99-23	#N/A	#N/A	#N/A	1999	#N/A	2006
		65	AB99-23	#N/A	#N/A	#N/A	1999	#N/A	2015
		66	AG93-IV1-94	M	#N/A	1992	1994	#N/A	1999
		67	AG93-IV1-94	M	#N/A	1992	1994	#N/A	1983
		68	AG93-IV10-94	F	#N/A	1991	1994	B40:02/B44:02	1983
		69	AG93-IV13-94	M	#N/A	1992	1994	B07:02/B14:02	1983
		70	AB99-12-33-18	#N/A	#N/A	#N/A	1999	B15:01/B44:03	1983

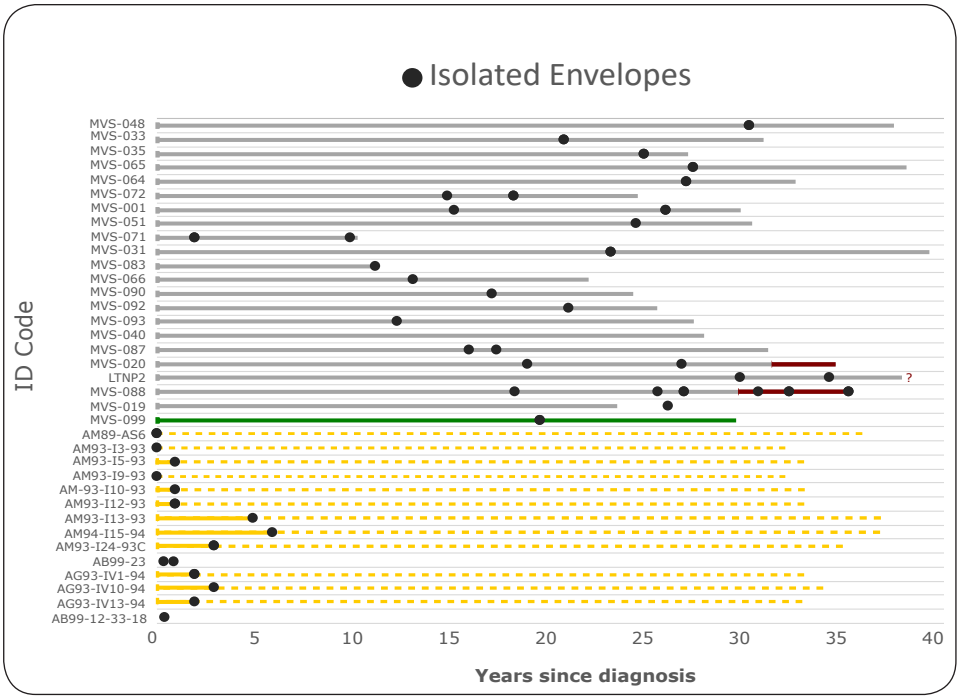

Figure 15. Timeline of isolated Env clones per individual (ID Code). Env clones are displayed as black dots. Horizontal lines display longitudinally available follow-up (years), while color represents phenotypical groups: EC (grey), VC (green), Progressors (Yellow). Discontinuous line represents unknown follow-up endpoint. No line is represented when clinical follow-up and diagnosis time are not available. Loss of control periods are marked in red. ?: Loss of control date is unknown.

Functional data from these Envs was pooled with an previous analysis to include samples from the largest Spanish EC cohort (ECRIS) (n=55) reaching to a total of 98 Env clones for an extended comparison among the following groups: EC (n=53), LTNP-VC (n=15), and Old Progressors (n=30) (Figure 16). Sample ID and characteristics of this extended data is published and available (Casado et al. 2018; Pérez-Yanes et al. 2022).

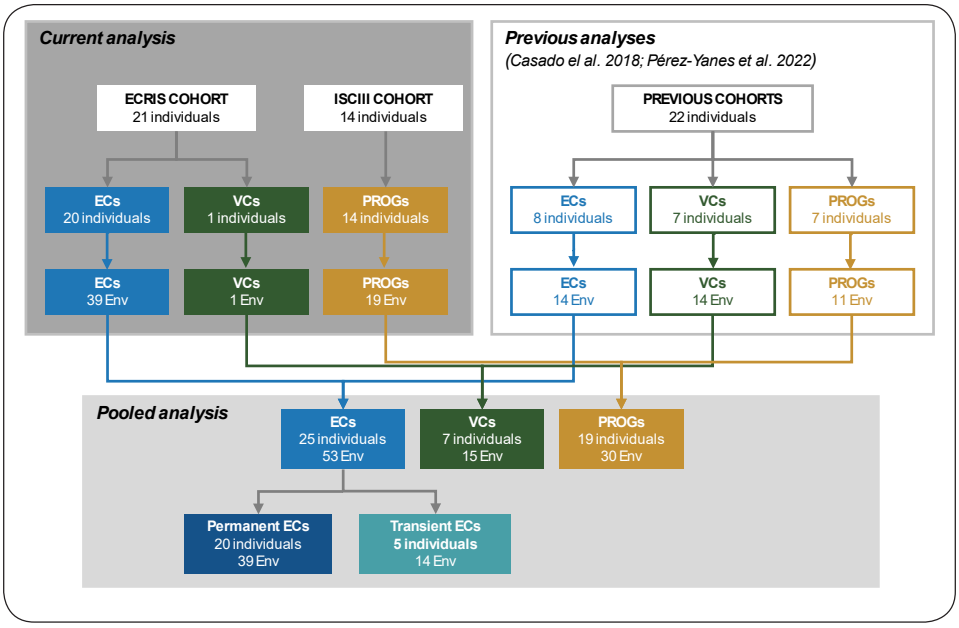

Figure 16. Flow chart of the cohort study analysis. Total individuals' discrepancies in the pooled cohort accounts for the study of independent Env from the same individuals in both current and previous analyses. ECRIS: EC CoRIS Cohort. ISCIII: Instituto de Salud Carlos III. EC: Elite Controller; VC: Viremic Controller; PROG: Progressors contemporary to the EC. Although they can be named Old progressors, we just kept progressors to simplify naming along the manuscript. Nevertheless, identifying color (yellow) has been maintained as in Figure 10 and (Pérez-Yanes et al. 2022).

2.1. Generation of Env expressing plasmids

The generation of Env expressing plasmids and their phylogenetic analysis was performed at ISCIII by the team of Dra. María Pernas and Dra. Concepción Casado.

2.1.1. Isolation, amplification, cloning, and sequencing.

For the generation of Env expressing plasmids Env genes were amplified at limiting dilution by nested PCR from proviral DNA. The products, designated primary thereafter, were cloned into the pcDNA3.1D/V5-His's Topo expression vector (Invitrogen). Expression plasmids were amplified into Mix & Go! DH5α cells (Zymopure), and clones were sequenced to check for the correct insertion of the Env gene.

2.1.2. Phylogenetic analysis

Evolutionary history of Env sequences was inferred using the Neighbor-Joining method. The percentage of trees on which the associated taxa clustered together with values above 90% is displayed next to the branches. Evolutionary distances were calculated using the Poisson correction method and are expressed in terms of the number of amino acid substitutions per site. All evolutionary analyses were conducted in MEGA X (Kumar et al. 2018).

Reference sequences HXB2 and S61 (89ES061) of HIV-1 (http://www.hiv.lanl.gov) were used as external reference group to establish the tree root. The C2V5 region of the Env gene was analyzed to track viral evolution instead of full Env sequences. This region additionally contains key glycosylation sites that influence immune escape and viral replication.

2.2. HIV-1 Env Pseudoviruses

HIV-1 Env pseudoviruses were produced by cotransfecting Expi293F cells, a HEK293 derived cell line adapted to grow in suspension, with a pSG3ΔEnv backbone and Env-coding plasmids of interest in a 1:2 psG3:Env ratio. Transfection was done using ExpiFectamine293 Transfection kit (ThermoFisher Scientific) following manufacturer's instructions and incubated at 37°C, 8% CO_2 with continuous orbital shaking at 125rpm. Enhancers 1 and 2 were added to the transfected cells 18 h post-transfection. Pseudoviruses were harvested 48 h post-transfection, clarified by centrifugation at 400 × g for 5 min and filtered with a syringed-plugged Millex-GP 0.45μm filter unit (Merck & Co.). Pseudoviruses were aliquoted and kept at −80°C until use.

Before neutralization assays, pseudoviruses were titrated by incubation at 37°C with 10,000 TZM-bl cells for 48 h, at a starting 1:10 dilution and serial 1:5 dilutions. Then, cells were incubated for 2 min in a shaker with BriteLite plus Reporter Gene Assay System (Perkin Elmer). Bioluminescence was analyzed by luminometry with an Ensight Multimode Plate Reader (Perkin Elmer).

2.3. Functional assays

We have previously described the poor fusogenicity of the viral Envs isolated from a small group of ECs (Casado et al. 2018; Pérez-Yanes et al. 2022). In this work, we expanded our functional data to include 59 samples from both the largest Spanish EC cohort (ECRIS) and ISCIII cohort and performed a new pooled analysis with previous data to a total of 98 Env clones belonging to ECs, LTNP-Viremic Controllers (LTNP-VC) and Old Standard Progressors (Figure 16). Newly analyzed samples contained 39 EC Env, one VC Env that were functionally compared to 19 Old standard Progressors

infected at the same period.

Full-length Envs were first amplified and inserted into a pcDNA3.1 expression plasmid. Then, transiently expressed in HEK293T cells to further evaluate Env expression, antigenicity, fusogenicity and infectivity. Env expression and antigenicity were analyzed by flow cytometry; fusogenicity and infectivity by a TZM-bl cell-based assay (Figure 17). Envs isolated during the viremic periods of an EC individual that lost control (n=5), were removed from this analysis to not confound EC fusogenicity interpretations and will be displayed separately in a following section. Before neutralization assays, pseudoviruses were titrated by incubation at 37°C with 10,000 TZM-bl cells for 48 h, at a starting 1:10 dilution and serial 1:5 dilutions. Then, cells were incubated for 2 min in a shaker with BriteLite plus Reporter Gene Assay System (Perkin Elmer). Bioluminescence was analyzed by luminometry with an Ensight Multimode Plate Reader (Perkin Elmer).

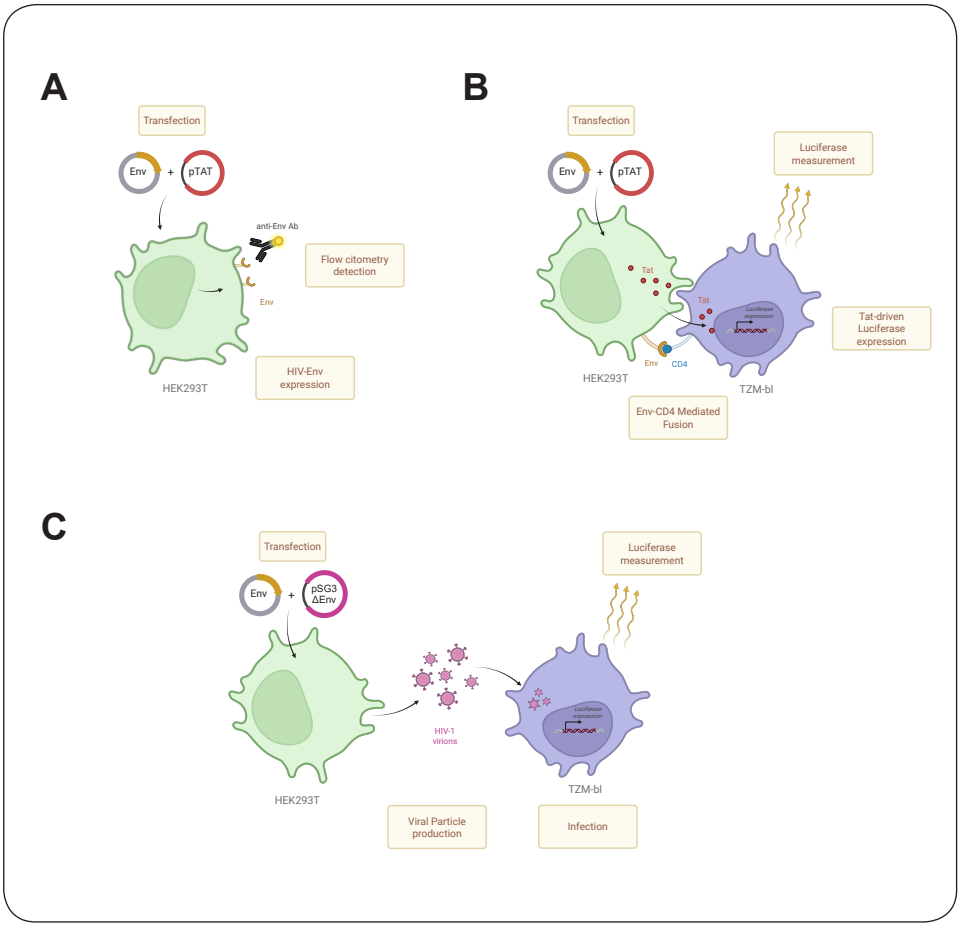

Figure 17. Experimental technique outlines for the analysis of Env expression, Env-mediated cell-to-cell fusion and viral infectivity. (A) Env expression: HEK293T cells were cotransfected with primary or reference full-length viral env and a ptat Δenv HIV-1 expression plasmid. Cell-surface Env expression was analyzed by flow cytometry using a combination of specific anti-Env antibodies. (B) Env-mediated fusion activity: HEK293T cells were cotransfected with a primary or reference Envs and a ptat HIV-1 expression plasmid. After, they were cocultured with TZM-bl cells to enable synapsis formation via Env/CD4-mediated binding. Fusion activity was measured through luciferase measurement, driven by tat-regulation of luciferase gene expression. (C) Env-mediated viral infection: TZM-bl cells were infected with serial dilutions of viral particles obtained from transfected HEK293T carrying the different primary or reference HIV-1 Envs and a pSG3Δenv plasmid. After 48 h, infectivity capacity in TZM-bl cells was analyzed by a luciferase assay. Adapted from Pérez-Yanes et al. 2022 in Biorender.

2.3.1. Transfection

HEK293T cells were seeded at 1mL 0.2M/mL in 24-well plates one day before transfection in D10 medium. Cells were then transfected with 1ug DNA at a 2:1 ptat:Env ratio with X-tremeGENE 9 transfection reagent (#06365809001; Sigma Aldrich) following manufacturer's instructions and incubated at 37°C, 5% CO_2 for 24h. Next day, cells were harvested and counted after being detached with Versene (15040066; ThermoFisher Scientific) to perform the following expression and functional assays.

2.3.2. Expression

To test Env expression, 1 × 10^5 Env/Tat co-transfected HEK-293T cells were incubated with combinations of anti-Env monoclonal antibodies: either 2G12 and IgGb12 or PG9 and PGT145 at 1μg/mL for 1h at 4°C. After primary staining, cells were washed with staining buffer and incubated with an APC Goat Fab2 antihuman IgG (109-136-098, Jackson Immunoresearch) at a 1/500 dilution for 1h at 4°C (Figure 17A).

This antibody combination was chosen to analyze Env expression by targeting two conserved regions of Env (CD4bs and V1/V2 loops) and covering different functional and structural aspects. b12+2G12 combination targets CD4bs and the glycan shield, providing information on Env accessibility (open/closed conformation) and glycosylation masking. PG9+PGT145 targets V1/V2 and V3 loops. These trimer-specific regions will detect properly folded and functional Envs.

Stained cells were acquired on a BD FACSCelesta™ Cell Analyzer (BD, USA) with FACSDiva™ Software version 8.0.1.1 (BD) and analyzed with FlowJo™ v10.6.1 Software (BD).

2.3.3. Fusogenicity

To test fusogenic activity, 1 × 10^4 Env/Tat co-transfected or control Tat-transfected HEK-293T cells were mixed (ratio 1:1) in 96-well Optical Bottom Plates with CD4+CXCR4+CCR5+ TZM-bl reporter cells for 6h at 37°C (Figure 17B). Luciferase activity resulting from Tat mediated transactivation was measured using the EnSight Multimode Plate Reader and BriteLite Plus Luciferase reagent (PerkinElmer, USA). Fusogenicity values from individual Envs were normalized to BaL-Env- mediated fusion.

The assay provides an indirect but quantitative measure of fusion events (Cunyat et al., 2012). NL4-3 and BaL-Env expression plasmids were used as positive controls for Env staining and as reference value for fusion activity (BaL=100%), as similarly reported (Curriu et al., 2012; Cabrera-Rodriguez et al., 2019).

2.3.4. Infectivity

To assess the infectivity of amplified Envs, Env bearing pseudoviruses were tested on TZM-bl cells. Pseudoviruses were produced as mentioned earlier and plated them with 1×10^5 TZM-bl cells in the presence of 18 μg/mL DEAE-dextran hydrochloride (Sigma) (Figure 17C). After 48 h of incubation at 37°C, luciferase activity was measured using Brite-Lite (PerkinElmer) and detected with a Fluoroskan Accent (Labsystems). Uninfected TZM-bl cells served as a negative control. The $TCID_{50}$ (Median Tissue Culture Infectious Dose) was calculated using the Montefiori template and normalized to viral concentrations.

3. Plasma Samples

A total of 72 EC plasma samples from different origins were obtained from the HIV HGM BioBank integrated in the Spanish AIDS Research Network (RIS-RETIC, ISCIII) and Centro Sanitario Sandoval (Madrid, Spain). Upon obtention and reception, samples were processed following current procedures and frozen. A comprehensive timeline was designed to illustrate analyzed plasma samples and longitudinal clinical data in reference to years from diagnosis for each participant (Figure 18). Periods of viral control loss are also displayed. Sample identification numbers (ID) and characteristics are summarized in Table 5.

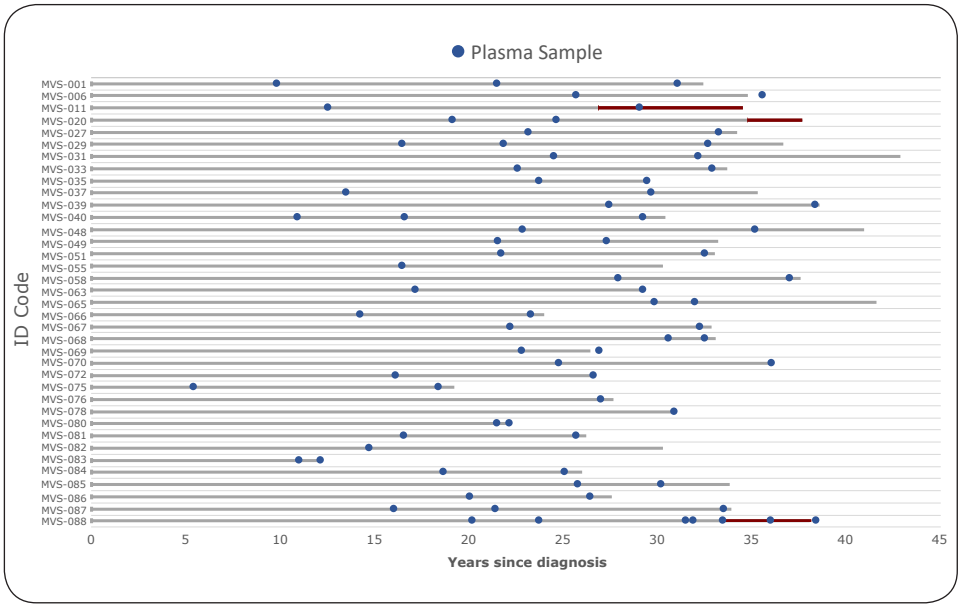

Figure 18. Timeline of analyzed plasma samples per EC individual (ID Code). Horizontal grey line displays available follow-up, with analyzed plasma samples displayed as blue dots. Loss of control periods are marked in red.

Table 5. Epidemiological, clinical, and host characteristics of the Plasma Samples. Samples from the same individual are associated with brackets.PC: Persistent controller, TC: transient controller. #N/A: Not available. (*Continued*)

Progression Group	ID Code	Sex	Diagnostic time	Sampling Time	Sample ID	Viral Load at Sampling (copies/mL)	CD4 T-cell Counts (cells/μL)	HLA B (Type: Subtype)	Time to Loss of Control (Years)
PC	MVS-001	F	1989	1998	MVS-001-V2	<500	728	B57:01/B14:02	
	MVS-001	F	1989	2009	MVS-001-V17	<50	1066	B57:01/B14:02	
	MVS-001	F	1989	2018	MVS-001-V25	#N/D	#N/D	B57:01/B14:02	
	MVS-006	M	1986	2010	MVS-006-V3	19	1380	B15/B57	
	MVS-006	M	1986	2019	MVS-006-V5	#N/D	#N/D	B15/B57	
	MVS-027	F	1987	2009	MVS-027-V4	50	630	B14/B27	
	MVS-027	F	1987	2018	MVS-027-V7	#N/D	#N/D	B14/B27	
	MVS-029	M	1988	2003	MVS-029-V2	<50	800	B27:05/B58:01	
	MVS-029	M	1988	2008	MVS-029-V9	<50	515	B27:05/B58:01	
	MVS-029	M	1988	2018	MVS-029-V18	<37	720	B27:05/B58:01	
	MVS-031	M	1984	2007	MVS-031-V1	20	802	B27/B49	
	MVS-031	M	1984	2014	MVS-031-V8	#N/D	#N/D	B27/B49	
	MVS-033	M	1987	2008	MVS-033-V3	39	717	B07/B57	
	MVS-033	M	1987	2018	MVS-033-V5	19	968	B07/B57	
	MVS-035	M	1988	2010	MVS-035-V1	50	639	B15/B-	
	MVS-035	M	1988	2015	MVS-035-V4	#N/D	#N/D	B15/B-	
	MVS-037	F	1991	2004	MVS-037-V1	20	1392	B13/B44	
	MVS-037	F	1991	2019	MVS-037-V4	#N/D	#N/D	B13/B44	
	MVS-039	M	1983	2008	MVS-039-V2	#N/D	#N/D	B51/B57	
	MVS-039	M	1983	2018	MVS-039-V5	#N/D	#N/D	B51/B57	
	MVS-040	F	1992	2002	MVS-040-V1	60	654	B39:01/B57:01	
	MVS-040	F	1992	2008	MVS-040-V8	#N/D	#N/D	B39:01/B57:01	
	MVS-040	F	1992	2019	MVS-040-V19	<37	#N/D	B39:01/B57:01	
	MVS-048	F	1986	2007	MVS-048-V2	#N/D	#N/D	B51/B57	
	MVS-048	F	1986	2019	MVS-048-V5	#N/D	#N/D	B51/B57	
	MVS-049	F	1987	2007	MVS-049-V2	#N/D	#N/D	B13/B57	
	MVS-049	F	1987	2013	MVS-049-V4	20	1359	B13/B57	
	MVS-051	M	1988	2008	MVS-051-V2	39	912	B35/B57	
	MVS-051	M	1988	2018	MVS-051-V4	#N/D	#N/D	B35/B57	
	MVS-055	F	1989	2004	MVS-055-V4	50	1217	B57/B1	

Table 5. Epidemiological, clinical, and host characteristics of the Plasma Samples. Samples from the same individual are associated with brackets.PC:Persistent controller, TC: transient controller. #N/A: Not available. (*Continued*)

Progression Group	ID Code	Sex	Diagnostic time	Sampling Time	Sample ID	Viral Load at Sampling (copies/mL)	CD4 T-cell Counts (cells/μL)	HLA B (Type: Subtype)	Time to Loss of Control (Years)
	MVS-065	M	1986	2013	MVS-065-V1	20	1074	B14:02P/ B41:01P	
	MVS-065	M	1986	2015	MVS-065-V2	20	999	B14:02P/ B41:01P	
	MVS-066	F	1996	2010	MVS-066-V1	50	738	B35:01P/ B40:02P	
	MVS-066	F	1996	2018	MVS-066-V2	#N/D	#N/D	B35:01P/ B40:02P	
	MVS-067	F	1988	2009	MVS-067-V1	#N/D	#N/D	B39/B57	
	MVS-067	F	1988	2018	MVS-067-V4	#N/D	#N/D	B39/B57	
	MVS-068	M	1989	2017	MVS-068-V2	#N/D	#N/D	B15/B44	
	MVS-068	M	1989	2019	MVS-068-V3	#N/D	#N/D	B15/B44	
	MVS-069	M	1994	2015	MVS-069-V2	#N/D	#N/D	B51/B57	
	MVS-069	M	1994	2019	MVS-069-V3	#N/D	#N/D	B51/B57	
	MVS-070	F	1985	2008	MVS-070-V2	#N/D	#N/D	B51/B57	
	MVS-070	F	1985	2019	MVS-070-V3	#N/D	#N/D	B51/B57	
	MVS-072	F	1994	2009	MVS-072-V1	50	754	B49/B51	
	MVS-072	F	1994	2019	MVS-072-V3	#N/D	#N/D	B49/B51	
	MVS-075	F	1999	2004	MVS-075-V1	<50	1354	B27:05/B44:02	
	MVS-075	F	1999	2016	MVS-075-V6	37	1071	B27:05/B44:02	
	MVS-076	F	1984	2009	MVS-076-V1	50	1083	B57negative	
	MVS-078	F	1988	2017	MVS-078-V1	50	1083	B07:02P/ B57:01P	
	MVS-080	M	1984	2004	MVS-080-V1	50	974	B39/B57	
	MVS-080	M	1984	2005	MVS-080-V2	50	503	B39/B57	
	MVS-081	M	1996	2011	MVS-081-V1	20	860	B27/B38	
	MVS-081	M	1996	2019	MVS-081-V3	#N/D	#N/D	B27/B38	
	MVS-082	F	1996	2004	MVS-082-V1	50	1160	B27/B78	
	MVS-083	M	2004	2004	MVS-083-V1	67	568	B48:01P/ B51:01P	
	MVS-083	M	2004	2016	MVS-083-V2	37	420	B48:01P/ B51:01P	

Table 5. Epidemiological, clinical, and host characteristics of the Plasma Samples. Samples from the same individual are associated with brackets.PC: persistent controller, TC: transient controller. #N/A: Not available. (*Continued*)

Progression Group	ID Code	Sex	Diagnostic time	Sampling Time	Sample ID	Viral Load at Sampling (copies/ mL)	CD4 T-cell Counts (cells/ µL)	HLA B (Type: Subtype)	Time to Loss of Control (Years)
	MVS-084	F	1995	2012	MVS-084-V1	20	1220	B14:01P/ B57:03P	
	MVS-084	F	1995	2018	MVS-084-V3	#N/D	#N/D	B14:01P/ B57:03P	
	MVS-085	M	1985	2009	MVS-085-V2	#N/D	#N/D	B38/B57	
	MVS-085	M	1985	2013	MVS-085-V3	#N/D	#N/D	B38/B57	
	MVS-086	F	1989	2008	MVS-086-V2	#N/D	#N/D	B27/B52	
	MVS-086	F	1989	2014	MVS-086-V4	#N/D	#N/D	B27/B52	
	MVS-087	M	1988	2003	MVS-087-V2	<50	842	B27/B35	
	MVS-087	M	1988	2008	MVS-087-V9	104	756	B27/B35	
	MVS-087	M	1988	2019	MVS-087-V20	#N/D	#N/D	B27/B35	
TC	MVS-011	F	1992	2004	MVS-011-V1	#N/D	#N/D	B7/B55	-12,9
	MVS-011	F	1992	2019	MVS-011-V7	#N/D	#N/D	B7/B55	2,5
	MVS-020	M	1990	2007	MVS-020-V3	#N/D	#N/D	B14/B51	-14,28
	MVS-020	M	1990	2012	MVS-020-V7	19	1065	B14/B51	-9,16
	MVS-088	F	1986	2004	MVS-088-V1	51	894	B39:01/B44:02	-11,2
	MVS-088	F	1986	2008	MVS-088-V4	69	1175	B39:01/B44:02	-7,9
	MVS-088	F	1986	2015	MVS-088-V17	<37	#N/D	B39:01/B44:02	-0,7
	MVS-088	F	1986	2015	MVS-088-V18	<37	1149	B39:01/B44:02	-0,3
	MVS-088	F	1986	2017	MVS-088-V19	403	#N/D	B39:01/B44:02	1,1
	MVS-088	F	1986	2019	MVS-088-V26	311	816	B39:01/B44:02	3,5
	MVS-088	F	1986	2021	MVS-088-V30	4370	480	B39:01/B44:02	5,7

These 79 plasma samples belonged to a total of 37 individuals, 32 PC and 3 TC. The PC group was sex-balanced, with 17 individuals each, while the TC are 2 females and 1 male (Table 6).

Table 6. Clinical Phenotypes of Elite Controllers

EC Subgroup	Acronym	Participants	Females	Males
Persistent Controller	PC	35	17	17
Transient Controller	TC	3	2	1

3.1. Humoral Response

3.1.1. Neutralization assay

The neutralizing capacity of plasma from the EC LTNP cohort was analyzed via an in vitro pseudovirus neutralization assay. To assess the generation of neutralizing antibodies upon HIV-1 infection, we used a previously described pseudovirus-based neutralization assay (Pradenas et al. 2021). Briefly, in Nunc 96-well cell culture plates (Thermo Fisher Scientific), 4,000 TCID50 of a luciferase-reporter HIV-based pseudovirus bearing individual Env Isolates were preincubated with three-fold serial dilutions (1/60 - 1/14,580) of the heat-inactivated (56°C for 30 minutes) plasma samples, for 1h at 37°C. Then $1x10^4$ TZM-bl cells treated with DEAE-Dextran (Sigma-Aldrich) were added. Results were read after 48 h using the EnSight Multimode Plate Reader and BriteLite Plus Luciferase reagent (PerkinElmer, USA). The values were normalized, and the ID50 (reciprocal dilution inhibiting 50% of the infection) was calculated by plotting and fitting all duplicate neutralization values and the log of plasma samples dilution to a 4-parameters equation in Prism 10.0 (GraphPad Software, USA). This assay has been previously validated with a replicative viral inhibition assay (Trinité et al. 2021).

Neutralization assays were also used to test evaluate sensitivity of different pseudoviruses to the panel of different NAb shown in Table 7.

Table 7. bNAbs used in the neutralization assay.

Target		Name
CD4bs		B12
		N6
		3BNC117
Glycan specific	Mannose	2G12
	V3	pG9
	V2	10_1074
Trimer		PGT145
MPER		4E10
		10E8

3.1.2. Binding assay

Expi293F cells were transfected with each of the Env plasmid isolated from the case and the control Env NL4-3 and TRO.11. Transfection was performed in absence of Enhancer treatment to limit Env cytopathicity. Two days after transfection Expi cells were stained with individual plasmas pre-diluted 1/1000 or a control 2G12 + b12 bNAb cocktail for 30 min at 4°C in PBS. After 3 buffer washes, cells were stained with a secondary anti-human IgG AlexaFluor 647 labeled antibody (109-136-098, Jackson Immunoresearch) for 30 min at 4°C in PBS. After three buffer washes, stained cells were acquired on a BD FACSCelesta™ Cell Analyzer (BD, USA) with FACSDiva™ Software version 8.0.1.1 (BD) and analyzed with FlowJo™ v10.6.1 Software (BD).

4. HIV-1 based virus-like Particles

HIV-1 Gag VLPs were designed to display different Env candidates at their surface with the objective of inducing a potent immune response. Several strategies can be used for VLP production. The most common strategy, leading to classical VLPs, is the cotransfection of plasmids coding separately for the Env of interest and HIV-1 Gag. Expression of Gag in the cytoplasm leads to VLP budding at the surface of the cells and release into the supernatant. While this method is simple, the incorporation of Env molecule into the VLP is very limited. Our team developed an alternative strategy based on the expression of fusion protein incorporating both the antigen of interest and Gag. This strategy has successfully been used in several works (Tarrés-Freixas et al. 2023;

Ortiz et al. 2023; Barajas et al. 2024; Trinité et al. 2024). With this second strategy, VLPs are produced intracellularly along the secretory pathway and are not efficiently released in the supernatant. Therefore, in this case, VLP production requires additional steps of extraction and purification detailed below. On the other hand, classical VLP obtained by cotransfection were analyzed directly into the culture supernatants.

4.1. Immunogen Design

The hypothetical most recent common ancestor (MRCA) EC Env sequences 409, 440, 535 and the B41 constructs were generated with the GeneArt service (ThermoFisher Scientific, Waltham, MA, USA) and inserted into a pcDNA3.1 vector. To focus the analyses on the immunogenicity and function of the extracellular domain of Env, the corresponding ectopic domain sequences were introduced into a 535 structure background, thus maintaining the signal peptide (SP), transmembrane domain (TM) and cytoplasmic tail (CT) from construct 535 (Figure 19). The resulting constructs were named with the STC535 suffix: 409STC535,440STC535,B41STC535. For simplicity, generated constructs will be referred to their MRCA Node (409, 440, 535, B41) and original names (B41) over the manuscript.

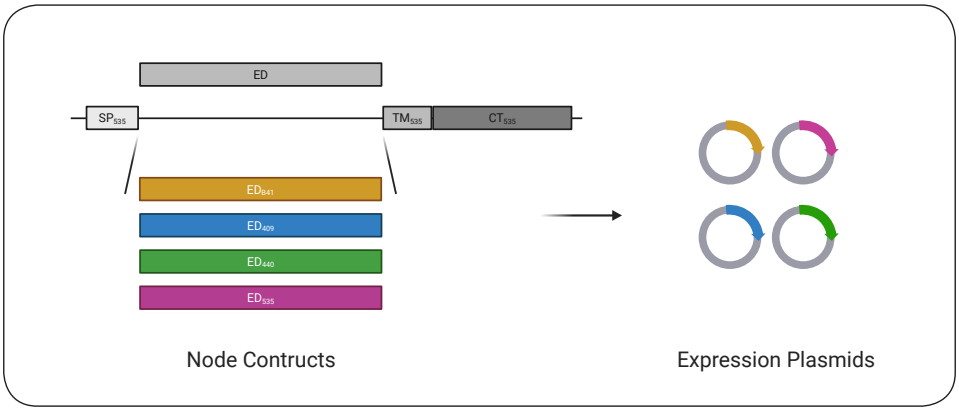

Figure 19. Schematic representation of the generation of MRCA env expressing plasmids. MRCA expression plasmids were designed by replacing the extracellular domain (ED, gp120 and gp41) of node 535 Env sequence and replacing it by the ED of nodes 409 and 440 as well as the reference Env B41. This allowed to restrict the analysis of antigenicity related to the ED of each MRCA node. SP: signal peptide, ED: extracellular domains, gp120 and gp41 ectodomain, TM: Transmembrane domain, CT: cytoplasmic tail.

To test our Gag fusion protein strategy, an Env-Gag (409-Gag) construct, the 535 CT domain was replaced by the GagHXB2 sequence. Env-Gag fusion constructs were inserted into a pcDNA3.4 topo vector (Figure 20). All constructs included various restriction enzyme sites to facilitate the cloning of different immunogens and the use

of different vectors. A KpnI restriction site (GGTACC) was added at the 5' end of the gene of interest, immediately followed by a Kozak sequence (GCCACC) and the start codon (ATG). A BamHI restriction site (GGATCC) was included within the GS-linker sequence between the transmembrane domain and GagHXB2. Finally, a pair of stop codons and a XhoI restriction site (TGATGACTCGAG) were included at the 3' end. Synthesized plasmids were resuspended in 50µL of nuclease-free H2O (AM9906, ThermoFisher Scientific) and transformed upon arrival. Remanent plasmid DNA was kept at -20°C for future use.

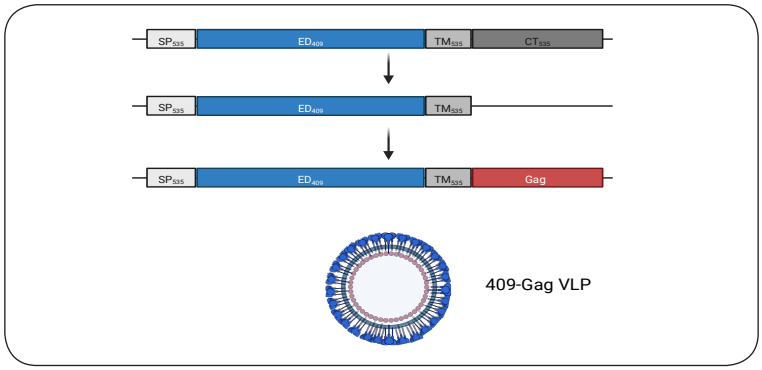

Figure 20. Fusion protein design. The 409 MRCA expressing sequence was modified to include Gag of HIV-1 next to the transmembrane domain. SP : signal peptide, ED: extracellular domains, gp120 and gp41 ectodomain, TM: transmembrane domain, CT: cytoplasmic tail.

4.1.1. Modifications

Different construct variants were designed and generated to optimize immunogen expression and VLP formation. These were synthesized via GeneArt synthesis platform (ThermoFisher Scientific). The three main modifications we did focused on the SP, TM and CT of the Env (Figure 4).

First, SP and TM modifications avoid antigen retention inside the host cell. Sp535 was replaced by the H5 sequence, and arginine in position 696 was substituted by an alanine (R696A, R>A)(Long et al. 2011). Both SP exchanges and TM modifications have shown to affect antigen translocation and therefore modify exposure and antigenicity (Upadhyay et al. 2024; Tarrés-Freixas et al. 2023). Finally, to increase Env incorporation into classical VLPs (cotransfection), we generated an additional construct where the last 110 amino acids of the CT were truncated (Figure 21).

Figure 21. Generation of a CT truncated 409 construct to enhance Env incorporation. SP: Signal Peptide, ED: Ectodomain,TM: transmembrane domain, CT: Cytoplasmic Tail.

4.1.2. Transformation and cryopreservation

To generate large quantities of the construct plasmids, designed DNA plasmids were amplified into *Mix & Go*! Competent DH5α cells (Zymopure) according to the manufacturers' protocol. Briefly, 1μL of plasmid DNA was added to Mix&Go tube pre-thawed on ice, mixed gently for some seconds, and incubated on ice for 10 minutes. After, 200 μL of SOC medium (15544034, ThermoFisher Scientific) was added to the cells and incubated for 30 minutes (min) at 37°C and with continuous shaking at 225 revolutions per minute (rpm).

Transformed bacteria were diluted 1/50 in SOC medium, spread in prewarmed culture plates and incubated at 37°C O/N. Culture plates used were Lysogeny Broth (LB) agar plates containing 100 micrograms/milliliter (μg/mL) ampicillin (ThermoFisher Scientific). Next day, grown well isolated colonies were picked and seeded into 13mL culture tubes (Sarstedt, Nümbrecht, Germany) with 6mL LB + 100 μg/mL ampicillin (ThermoFisher Scientific) for O/N culture at 37°C and 225rpm. For a high plasmid generation, 1mL of this preinoculum was transferred after a few hours to 200 mL of LB in a 500mL Erlenmeyer flask for O/N culture. Once grown, 0.5 mL of the medium were mixed with 0.5mL of a 30% glycerol solution for long-term conservation glycerol stock at −80 °C. The rest of the culture was used for plasmid extraction.

4.1.3. DNA purification

For plasmid DNA extraction of small cultures, a NucleoSpin Mini kit (Macherey-Nagel) was used, while for bigger cultures, a Zymopure II Plasmid Maxiprep kit (Zymopure).
Briefly, bacterial cultures were centrifuged at 3,000 relative centrifugal forces (× g) for 15 min and the supernatant was discarded. The pellet was then processed according to manufacturers' instructions. Extracted DNA was quantified in the eluted fraction by absorbance determination at 260 nm using a Nanodrop One (ThermoFisher Scientific).

4.2. VLP Production and purification

4.2.1. Culture Transfection and harvest

VLPs were produced in Expi293F cells cultured either in Erlenmeyer flasks or 6 well plates in Expi293F medium and under continuous orbital shaking (125 rpm) at 37°C and 8% CO_2 conditions. Cells were transfected with the construct of interest using ExpiFectamine293 Transfection kit (ThermoFisher Scientific) following manufacturer's instructions. Enhancers 1 and 2 were added (unless mentioned otherwise) to the transfected cells 18h post-transfection. Culture was harvested 48h post-transfection and pellet and supernatant (SN) separated by centrifugation for VLP purification and characterization. Classical VLP were analyzed in the SN while Env-Gag fusion based VLP were analyzed in both SN and cell pellet.

4.2.2. Cell Lysis and VLP extraction (Env-Gag fusion based VLP only)

In the case of the fusion protein strategy, transfected cell pellet underwent a VLP extraction protocol. To characterize and localize protein production before and after VLP extraction, both SN and pellet from transfected cells were analyzed. The method for intracellular VLP recovery and extraction was adapted from (Kee et al. 2010; Gaik, Pujar, and Titchener-Hooker 2008). Briefly, pellet was resuspended in 1 pellet volume (PV) of detergent free lysis buffer (on ice, followed by an optional manual homogenization with a tissue grinder on ice (Table 8) (CS1, KIMBLE). After disruption of the cells, 2PV of lysis buffer containing 0.2% Triton X-100 were added. Samples were kept in a spinning orbital at 4°C for 4 h to allow the release of VLPs.

Table 8. Lysis Buffer composition (before addition of 0.2% Triton X-100).

Lysis Buffer Composition	Provider
Phosphate buffer pH 7.4	Gibco
2 mM EDTA	ThermoFisher Scientific
2 mM EGTA	Merck
Protease Inhibitor Complete™ ULTRA Tablets EDTA-free	Merck

Samples were spinned for 15min x 3000g to remove debris and contaminants, and SN were processed as follows. In order to reduce detergent content, SN was added to a tube containing 0,1g Amberlite XAD-4 beads (Merck) and incubated 2h at 4°C in a spinning orbital. Processed SN was then filtered with a 70μM strainer (Greiner bio-one) to remove the beads.

4.2.3. Purification

In order to further purify extracted VLPs, SN underwent ultracentrifugation for 2h at 29,000 x g and 4°C on a double cushion sucrose solution (30%/70% sucrose PBS). VLP were harvested in the 30%-70% interphase. Ultracentrifuge used was a Sorvall WX 100 series with a TH-641 rotor (ThermoFisher Scientific). Sucrose was removed from the sample by dialysis with Spectra-Por Float-A-Lyzer G2 (Merck) following the manufacturer's recommendation against 1× PBS.

4.3. Characterization

VLP production and antigenicity was characterized in the supernatants or following extraction in the case of Env-Gag fusion based VLP. Flow cytometry was also used to characterize the Env antigenicity at the surface of the transfected producer cells.

4.3.1. Flow cytometry

Flow cytometry was used to characterize the antigenicity of both MRCA and individual isolates at the surface of producer cells. Freshly harvested transfected producer cells were counted, and 1 x 10^6 cells were seeded into a 96 well plate. Cells were washed with PBS, centrifuged, and stained with 100uL of the following bNAbs for 1h at 4°C (Table 9). Anti-Env bNAbs were prepared in staining buffer (PBS+10% foetal bovine serum (FBS; ThermoFisher Scientific). After staining, cells were washed with staining buffer and incubated with an APC Goat Fab2 antihuman IgG13 (109-136-098, Jackson Immunoresearch) at 1/500 for 1h at 4°C. Finally, cells were washed with PBS and run in a BD FACSCelesta™ Flow Cytometer (BD, Franklin Lakes, NJ, USA). Data analysis was performed with FlowJo v10.8.1 (Tree Star, Ashland, OR, USA).

Table 9. bNAb Antibody Staining Panel

Target	Name	Epitope	Reference	Work. dil.	Provider
CD4bs	b12	Conformational	AB011	1 µg/mL	Polymun
	2G12	N-linked glycans (295, 332, 386, 392 & 448)	AB002	1 µg/mL	Polymun
V1V2 loops	PG9	Quaternary trimer dependent (Glycans N156 and N160)	AB015	1 µg/mL	Polymun
	PGT145	Quaternary trimer dependent (Glycan N160)	ARP-12703	1 µg/mL	NIH
MPER	2F5	ELDKWA	AB001	4 µg/mL	Polymun
	10E8	NWFDITNWLWYIK	ARP-12294	2 µg/mL	NIH

4.3.2. Western Blot

To assess the composition of different VLP particles, Western Blot (WB) were performed. Briefly, SN or lyzed cell pellet proteins were run in NuPAGE Bis-Tris 4%–12% acrylamide gels (NP0321; Thermo Fisher Scientific) with BlueStar pre-stained protein ladder as a molecular weight marker (523005; NIPPON Genetics). Proteins were blotted onto polyvinylidene fluoride (PVDF) membrane (Ref. 1704156; Bio-Rad) using the Trans-Blot Turbo Transfer System (Ref. 1704150; Bio-Rad), and membranes were blocked with EveryBlot Blocking Buffer (12010020; Bio-Rad). Primary antibodies used were 2F5 (Table 9), p17+p24+p55 Gag (Rabbit polyclonal, ab63917, Abcam), and gp120 (Goat polyclonal biotinylated, ab53937, Abcam).

Secondary antibodies used were HRP-Affinipure Goat anti-human IgG, HRP-Affinipure Donkey anti-rabbit, and a HRP Affinipure Donkey Anti-Goat IgG (Table 10).

Table 10. Table of Secondary antibodies used.

Antibody	Reference	Work dilution	Provider
HRP-Affinipure Goat anti-human IgG	109-036-098	1/10000	Jackson immunoResearch
HRP-AffiniPure Donkey anti-rabbit IgG	711-036-152	1/10000	Jackson immunoResearch
HRP Affinipure Donkey Anti-Goat IgG	705-035-147	1/10000	Thermo Fisher Scientific

Membranes were developed with SuperSignal West Femto Maximum Sensitivity Substrate (Ref. 34094; Thermo Fisher Scientific) according to the manufacturer's instructions. Images were acquired with ChemiDOC MP Imaging System (12003154; Bio-Rad) and processed and merged with ImageLab 6.0.1 software (Bio-Rad).

4.3.3. Microscopy

To visualize how the observed protein production translated to VLP synthesis and Env incorporation, we used Transmission Electron Microscopy (TEM), and Confocal and STED Microscopy.

a. Transmission Electron Microscopy (TEM)

To visualize VLP production, VLP-producing cells were analyzed by TEM. Briefly, Expi293F cells were transiently transfected with the construct of interest following the previously mentioned protocols. Then, 2ml of each culture of interest was centrifuged at progressively decreasing speeds (420g,300g,300g) for 5 min each, after which SN was discarded and resuspended with 500 µL Versene before proceeding. After the last centrifugation, SN was discarded, and sample was fixed by resuspension with 2mL glutaraldehyde 2.5% in 0.1M PBS at 4°C. Once fixed, samples were kept at 4°C and sent refrigerated following the biological samples delivery protocol to the Microscopy Service at Universitat Autònoma de Barcelona (UAB). Upon reception, pellets were embedded in epon resin and polymerized at 60°C for 48h. Sections of 70 nm in thickness were obtained with a Leica EM UC6 microtome (Wetzlar), stained with 2% uranyl acetate and Reynold's solution (0.2% sodium citrate and 0.2% lead nitrate). Ultrafine cuts were mounted onto copper 200 mesh grids. Samples were analyzed using a JEM-1400 transmission electron microscope (Jeol Ltd., Akishima, Japan) and images taken at 120 kV.

b. Confocal and STED Microscopy

To visualize antigen incorporation and display at the VLP surface, purified VLPs were stained for confocal microscopy.

A 10 µL aliquot of ultracentrifuge-purified particles were adhered on round 13mm No. 1.5 poly-Lysine coated coverslips (631-0150, VWR) and set onto a 24-well plate for further processing (Figure 22). Coverslips were then fixed with 3% PFA/PBS for 15 min at RT, followed by blocking with 2% BSA/PBS for 15 min at RT. Staining was performed with a b12 Ab (AB011, Polymun) at 2ng/µL in 2% BSA/PBS for 1h at RT. No permeabilization was needed since Env is a surface staining. Samples were then washed in PBS 3x 5 min at RT and stained with 1:500 anti-human Fab AB STAR RED secondary antibody (STRED,abberior). Wash cycles were repeated, and stained coverslips were fixed with 3% PFA/PBS for 5 min at RT and washed again in PBS 1x5 min. Stained coverslips were mounted onto microscope glass slides with SlowFade Diamond mounting media (S36967, ThermoFisher Scientific) and sealed with Twinsil (#13001000, Picodent, Wipperfürth, Germany). Fixed samples were then imaged using an Abberior STEDYCON confocal microscope and analyzed with the Stedycon and ImageJ/Fiji software.

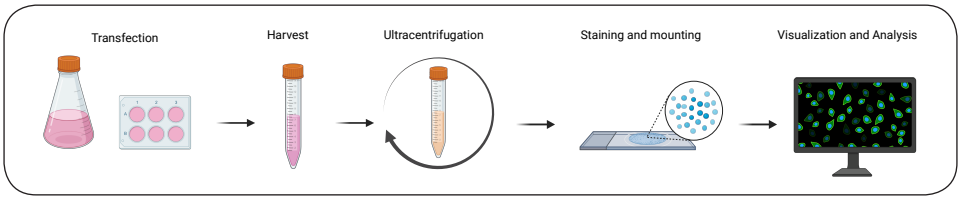

Figure 22. **Schematic protocol for Confocal Microscopy sample preparation.**

5. Animal procedures

In this project, a BALB/c mouse strain was used as the animal model for the characterization of VLP-induced immune responses. The BALB/c strain is one of the most widely used inbred strains in immunology and infectious disease research. They present a Th2-biased response, meaning this strain is an exceptional responder to immunization (Hiroyuki Watanabe 2004).

5.1. Ethics statement and animal welfare

All animal experiments performed in this project were evaluated and approved by the Ethical Committee on Animal Experimentation (CEEA) of the Germans Trias i Pujol Research Institute (IGTP), and the Ministry of Territory and Sustainability of the Generalitat de Catalunya. All work was performed at the Centre for Comparative

Medicine and Bioimage (CMCiB), with all procedures are in accordance with the 3R principle and prioritize animal welfare. PREPARE and ARRIVE Guidelines were followed for experiment planning and reporting (Kilkenny et al. 2010; Smith et al. 2017).

BALB/c mice were purchased at the age of 5 weeks (Envigo) and acclimated for at least 7 days before experiment initiation. Animals were housed at the Specific-Pathogen Free (SPF) facility for the whole duration of the experiment and were fed ad libitum. Temperature and humidity were kept at a constant range (21-22 °C, 30-40% humidity), with 12h light/dark cycles with progressive light change. Animals were housed by sex in groups of 2-5 animals/cage with environmental enrichment; cages were cleaned twice a week. All procedures were performed cautiously, and animals underwent peri¬odic veterinary inspection.

5.2. Immunization

There is evidence suggesting that HIV-1 Gag may not form VLPs optimally in murine cells (Mariani et al. 2000). As a result, to evaluate construct immunogenicity prior to the development of more sophisticated delivery strategies such as mRNA synthesis, we immunized BALB/c mice to compare 409 and B41 constructs as protein as well as check the impact of the CT truncation. Candidate constructs 409 and 409trunc were evaluated along with B41 and an empty pcDNA3.1 vector as controls (Figure 23A). A total of 28 BALB/c mice (n=8 per group, n=4 per control) were divided in sex-balanced groups and immunized with two doses of DNA, electroporated intramuscularly and separated by a 3-week interval between each dose (Figure 23B).

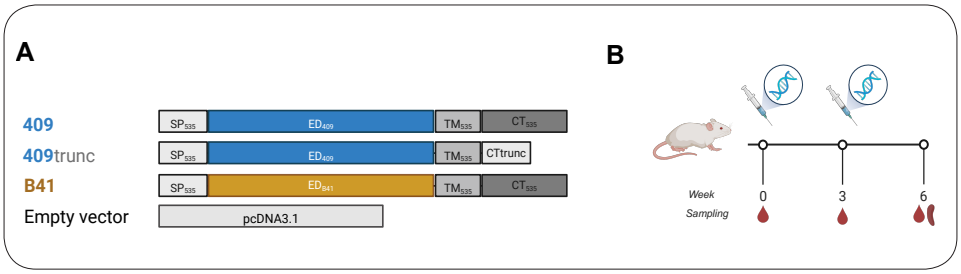

Figure 23. Schematic representation of the immunization strategy and sample collection. A) DNA candidate constructs for DNA immunization. SP: Signal Peptide, ED: extracellular domains of gp120 and gp41, TM: transmembrane domain, CT: Cytoplasmic Tail, Trunc: truncated. B) BALB/c mice were immunized with a total of 2 doses of DNA via intramuscular electroporation with a 3-week interval between doses. Blood samples were collected prior to each immunization and at endpoint along with spleens.

5.3. In vivo DNA electroporation

DNA delivery through electroporation allows the internalization of the DNA inside the target cells by the destabilization of their plasma membrane. This strategy is applied at the injection site and allows a better uptake of plasmidic DNA.

Immunization in mice was performed by in vivo electroporation at the posterior hind leg following a 20μg intramuscular DNA injection. Before the procedure, mice were anesthetized with 5% isoflurane (Baxter) at 1 L/min using the Veterinary Anesthesia Workstation (Minerve Equipement Veterinaire) and maintained during the procedure with 3% isoflurane. Immediately after DNA inoculation, the muscle was electroporated at the site of injection with a NEPA21 in vivo electroporator (NepaGene) using variable gap tweezers with 2 round-shaped SS Plate Electrodes (Sonidel). The electroporation protocol was optimized in-house for maximal expression and consisted of 8 positive pulses of 60 Volts (V) and 20 milliseconds (ms) separated by a 1s interval.

5.4. Sample collection and processing

Blood samples were collected prior to each immunization via facial vein puncture with a 25G needle (Novico Medica, Barcelona, Spain). Approximately 100μL of blood per animal were collected in a 1.5mL tube (Sarstedt). At the end of the 6-week follow-up, all animals were euthanized and blood samples and spleens from each animal were taken for ex vivo immune analysis. Euthanasia was performed under deep isoflurane anesthesia by whole blood extraction via intracardiac puncture followed by cervical dislocation as a confirmatory method.

After coagulation, serum was recovered from whole blood by centrifugation for 10 min at 4000×g. Serum was heat inactivated for 30 min at 56°C, centrifuged at 10,000xg for 5 min to pellet any debris, and frozen at -80°C until analysis. Spleens were processed upon collection and splenocytes frozen at -80°C until analysis.

6. Analysis of vaccine-induced immune responses

Vaccine-induced immune responses were characterized by a TZM-bl based neutralization assay and a binding assay.

6.1. In vitro pseudovirus neutralization assay

The neutralizing capacity of vaccine-induced antibodies against the different vaccine candidates, was analyzed via an in vitro pseudovirus neutralization assay in endpoint plasma samples.

Sera samples from vaccinated and unvaccinated mice were heat inactivated for 30 min at 56°C and prediluted 1:60 in D10. Then 100µL of each sample were transferred to a Nunc 96-well cell culture plate (Thermo Fisher Scientific) and incubated with 50µL of each pseudovirus at a concentration of 4,000 50% Tissue Culture Infective Dose (TCID50)/mL for 45-95 min at 37°C and 5%CO_2. Meanwhile, TZM-bl cells were detached with Versenne, counted, and prepared at 0,1x10^6 cells /mL with D10 and a 1:133 dilution of DEAE-Dextran (Sigma-Aldrich). Then, 100µL of TZM-bl cell preparation were added to the plate and incubated for 48h at 37°C and 5% CO_2. Results were read using the EnSight Multimode Plate Reader and BriteLite Plus Luciferase reagent (PerkinElmer, USA). The values were normalized, and the ID50 (reciprocal dilution inhibiting 50% of the infection) was calculated by plotting and fitting all duplicate neutralization values and the log of plasma samples dilution to a 4-parameters equation in Prism 10.0 (GraphPad Software, USA). This assay has been previously validated with a replicative viral inhibition assay (Trinité et al. 2021).

6.2. Total anti-Env mouse IgG binding assay

Expi293F cells were transfected with a 409STC535_IRES_GFP construct (which expresses both 409STC535 Env and cytosolic GFP) in absence of enhancer treatment. Two days later, cells were washed and incubated with 1/50 PBS dilutions of each animal endpoint sera for 1 hour at 4°C. After 3 washes in PBS, cells were then stained with anti-mouse IgG secondary antibody labeled with AF647 (115-605-071, Jackson Immunoresearch) for 30 min at 4°C. After 3 washes in PBS, cells were acquired on a BD FACSCelesta™ Cell Analyzer (BD, USA) with FACSDiva™ Software version 8.0.1.1 (BD) and analyzed with FlowJo™ v10.6.1 Software (BD). AF647 fluorescence of gated GFP bright cells was calculated for each serum.

7. Statistical analysis

Statistical analyses were performed using Prism 10.0 (GraphPad Software Inc.) and R v4.1.1. A p-value equal or inferior to 0.05 was considered significant for all analyses. Comparisons between groups were calculated with Kruskal-Wallis and Mann-Witney tests. A two-sided Fisher's exact test was used to compare protective alleles between cluster groups. Multiple comparisons were adjusted using the Benjamini and Hochberg method (FDR). Correlations were calculated with a Non-parametric Spearman Test. Simple linear regressions were also calculated for the same data. A Log-normal Welch t-test was used to compare constructs Geomeans in microscopy data.

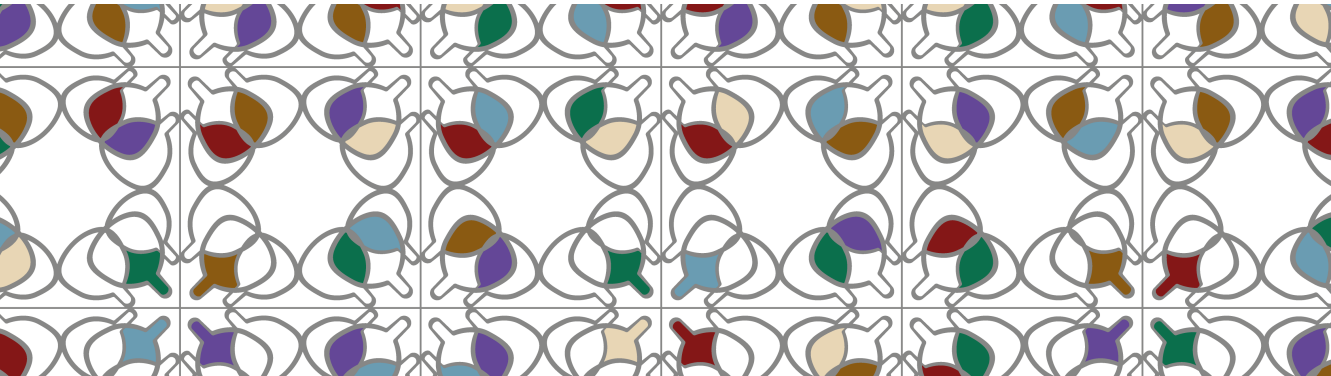

RESULTS

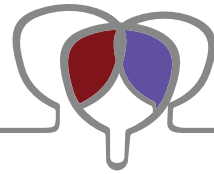

1. Functional characterization of HIV-1 Envs from a LTNP Cohort

In this first section, we expanded the characterization of the ECRIS Cohort with the analysis of 70 Envs. All this information is not only relevant in understanding early HIV events, but to additionally analyze the impact of Env in these clinical progression phenotypes. As a result, sequences were analyzed genetically and phenotypically, to further understand their functionality and genome impact on clinical progression of three different HIV-1 phenotypical groups: EC, VC and Progressors.

1.1. Cohort description and Env collection

Participant characteristics are summarized in Table 4. PBMC samples available from the biobank corresponded to a total of 35 individuals, 20 elite controllers, one viremic controller and 14 contemporary progressor individuals. Most of them were male (70%) and infected during the early HIV pandemic (mean+/-SD diagnostic date was 1989+/-5 for ECs, and 1991+/-2 for Progressors).

From these participants, a total of 70 Env sequences were amplified and cloned in expression vectors (see Figure 15 for sample distribution). All Envs were characterized, however, only 59 were included in the final analysis due to exclusion criteria regarding the sample or the time-point relevance. Briefly, sample exclusion was due to errors in the clinical data provided (n=4), presence of stop codons (n=1), or as duplicates of already published data (n=1). Related to time-point relevance, EC samples obtained during viremic periods or during loss of control were not included in the analysis (n=5).

1.2. Phenotypic analysis

1.2.1. Env expression

From these Env clones, we first analyzed potential expression differences by comparing the different clinical groups. Surface expression level was measured on transfected HEK293T cells (Figure 17), using two different bNAb antibody combinations (b12+2G12 and PG9+PGT145)(Figure 24A).

Envs obtained from ECs (n=39) presented no significant differences in expression compared to those from Progressors (n=19) (Figure 24B). VC Env clone (n=1) was excluded from direct comparison due to the limited sample size.

These results are in line with previous studies in which Env expression differences were limited to the comparison of EC with more evolved Env isolated from recently infected individuals (Pérez-Yanes et al. 2022; Valenzuela-Fernández et al. 2022; Cabrera-Rodríguez et al. 2019). These data suggest that Env role in viral load regulation and clinical pathogenesis is not completely dependent on its expression but, probably, also its functionality.

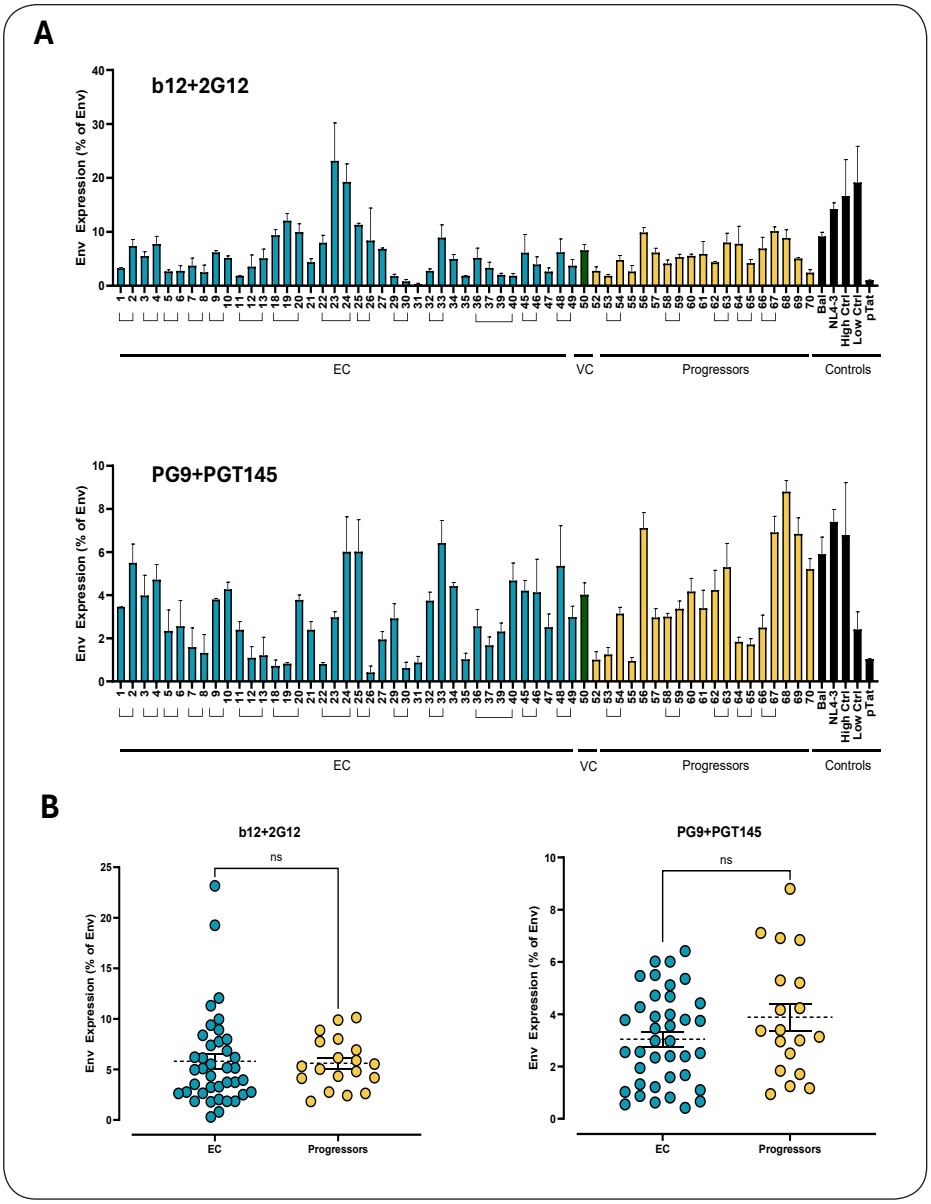

Figure 24. Env protein expression (% of Envelope) of different HIV-1 Env clones isolated from LTNP-EC (n=39,blue), VC (n=1, green) and non-controller progressor individuals (n=19, yellow). Values show the Mean+SEM of each group. Each bar or dot is the Mean of three to four independent experiments depending on the envelope. Envs isolated from the same individual are associated with brackets. A) Expression was evaluated by flow cytometry using combinations of specific anti-Env antibodies. Reference HIV-1 viral strains, a low and a high fusogenic Env, and pTat were used as controls (black). B) Comparation of Env protein Expression between EC and progressor individuals. A Mann-Whitney non-parametric statistical test was used to compare both groups. ns: statistically non-significant.

1.2.2. Fusogenicity

Following Env expression, the next key process in HIV infection is the interaction with the CD4 receptor leading to membrane fusion. A lower fusogenic activity by EC Envs has been associated with their control phenotype (Casado et al. 2018; Pérez-Yanes et al. 2022). To expand these observations, we measure Env fusogenic activity in the newly isolated EC Env. We quantified fusogenicity in co-cultures of Env/Tat cotransfected HEK293T with TZM-bl cells by measuring Tat-mediated luciferase expression. All fusogenicity values are reported relative to BaL Env which was used as reference along with additional controls in all the experiments. Differences in clone fusogenicity were analyzed between individuals and phenotypic groups (Figure 25A). EC Envs showed a trend for lower fusogenicity compared to progressors (median values: 0.38 and 0.91 relative to Bal, respectively), but no statistical significance was reached.

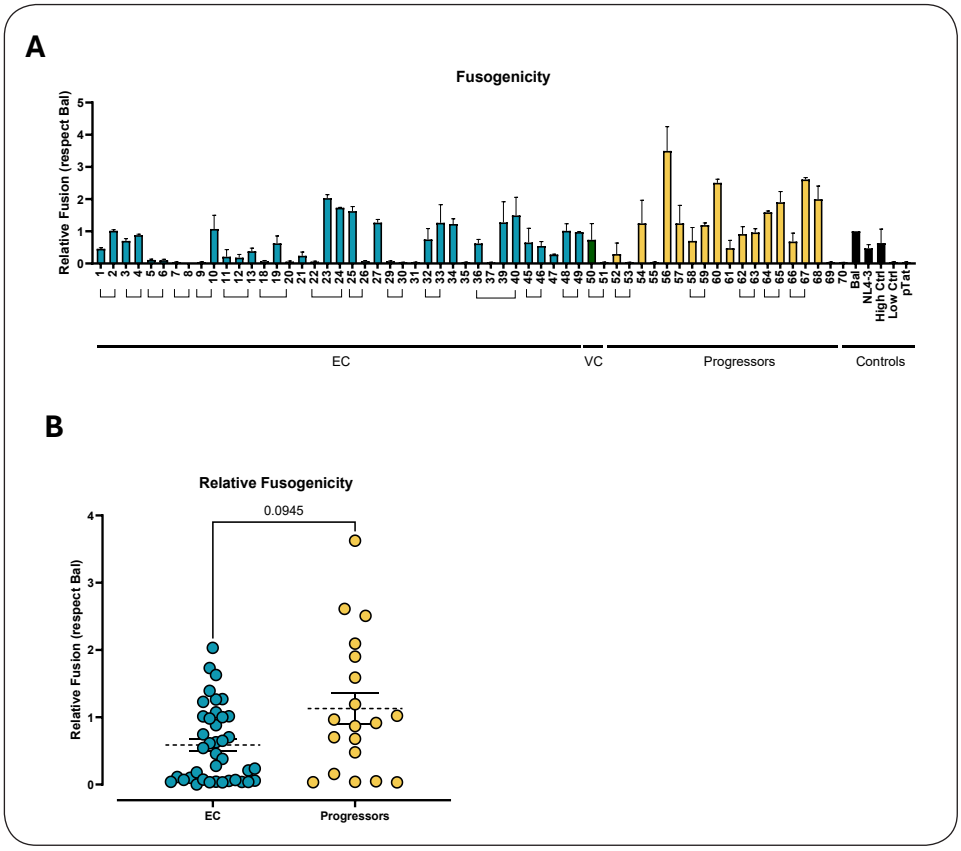

Figure 25. Fusogenic capacity analysis of HIV-1 Envs from the ECRIS cohort. A) Relative Fusogenic activity of the different HIV-1 Env clones isolated from LTNP-EC (n=39, blue), VC (n=2, green) and non-controller progressor individuals (n=19, yellow). Controls (black) included reference HIV-1 viral strains BaL and NL4-3 Env, low and high fusogenic Envs, and a no Env condition (ptat). Envs isolated from the same individual are associated with brackets. Fusion activity is calculated relative to Bal. Each bar shows the Mean+SEM of three to four independent experiments depending on the envelope. B) Comparation of Env protein fusogenicity between EC and progressor individuals. Fusion activity was calculated relative to BaL. Values show the Mean+SEM of each group. Each dot is the Mean of three to four independent experiments depending on the envelope. A Mann-Whitney non-parametric statistical test was used to compare both groups. P-value is considered significant if <0.05.

1.2.3. Correlation between viral Env characteristics

The high mutational rate of HIV-1 allows the production of highly heterogenous clones that differ in viral fitness to maintain replication and transmission under high immune pressure. As a result, there is a high intra-individual diversity of viruses with differential Env expression and functionality. While the reduction of Env exposure at the viral surface is used as one of the main evasion mechanisms, sometimes the

expression of highly fusogenic Envs might counteract this purpose.

We compared Env expression and fusogenicity from different phenotypic groups to observe if there was a correlation between these 2 functions, and more importantly, if differences were observed between phenotypical groups (Figure 26). Significative positive correlations (r=0.5222, r=0.590) were found using both antibody combinations (p<0.001) when all Env were analyzed.

These correlations were maintained inside phenotypical groups, with progressors showing a higher fusogenicity for the same expression percentage compared to EC, which can be visualized in their slope for b12+2G12 detection, in linear regression analysis. Slope (95%CI) were 0.07 (0.04-0.10) for ECs and 0.31 (0.17-0.45) for Progressors, p<0.0001. No slope differences were observed with PG9+PGT145, although differences in y-axis intercept values were observed (p=0.038), being higher for progressors.

To conclude, while fusogenicity and expression are correlated and show differential correlations between EC and VC, a lower Env fusogenicity is not always associated with a low Env expression.

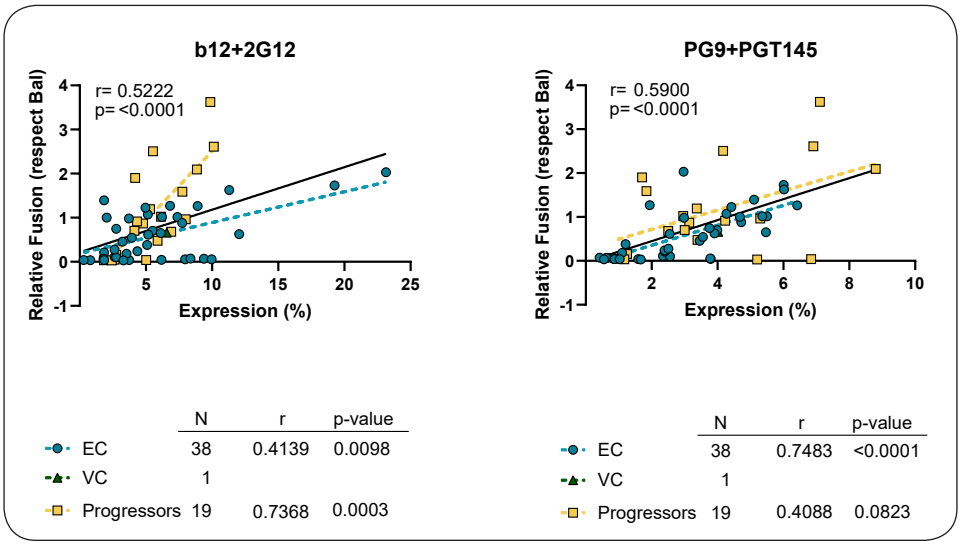

Figure 26. Correlation of Env protein expression with fusion capacity in the current cohort containing EC, VC and Progressors. Spearman nonparametric correlation. Correlations were calculated with a Non-parametric Spearman Test, with r and p values for all Envs shown on the top left, and for all subgroups shown under each graph. Simple linear regression for all Envs is represented as a black line, or a color dotted line if corresponding to a subgroup. Circles shown are the Mean + SEM of three independent experiments. N: sample number. r: Pearson correlation coefficient ranges from -1 to +1, being 0 no relation. P-value is considered significant if <0.05.

2. Functional Characterization of HIV-Envs from a Pool Cohort

Both expression and fusogenicity data generated in this work with the large collection of Env isolated from ECs and Progressor individuals were consistent with previous reports using a lower number of samples detecting lower functionality in ECs. However, as this significance was still probably limited by sample size, we explored the possibility of having a full picture of the relationship of Env function and AIDS progression in early years of the HIV pandemic in Spain, by pooling data from the newly isolated Env (n=59) with those previously analyzed (n=39) (Casado et al. 2018; Pérez-Yanes et al. 2022) (Figure 16). To ensure reproducibility of the fusogenicity analysis conducted overtime across different laboratories and researchers, internal controls and duplicated Envs were compared. Internal controls across three experimental settings demonstrated high technical consistency with minimal variation, supporting the reliability of the data and validating the pooled analysis of fusogenicity data (Figure 27). In contrast, expression data were neither pooled nor compared due to additional methodological variables over time, including changes in cytometry instrumentation and the use of an additional anti-Env antibody combination not previously analyzed.

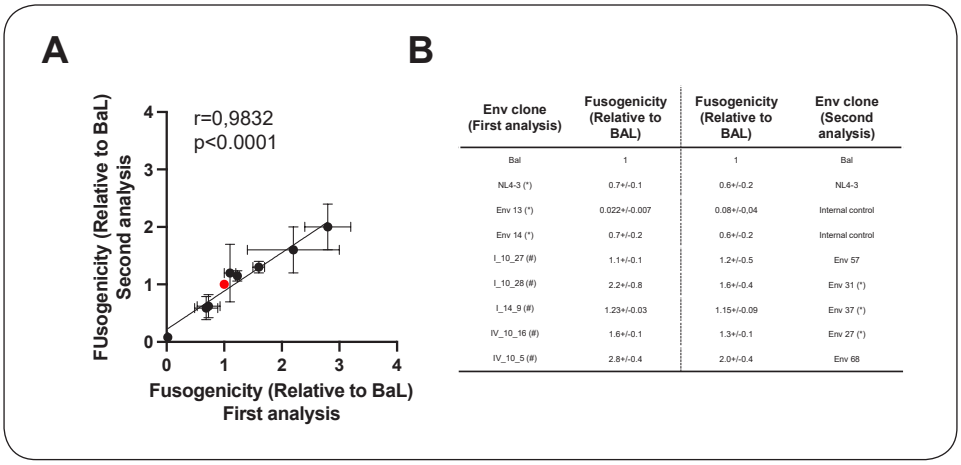

Env clone (First analysis)	Fusogenicity (Relative to BAL)	Fusogenicity (Relative to BAL)	Env clone (Second analysis)
Bal	1	1	Bal
NL4-3 (*)	0.7+/-0.1	0.6+/-0.2	NL4-3
Env 13 (*)	0.022+/-0.007	0.08+/-0,04	Internal control
Env 14 (*)	0.7+/-0.2	0.6+/-0.2	Internal control
I_10_27 (#)	1.1+/-0.1	1.2+/-0.5	Env 57
I_10_28 (#)	2.2+/-0.8	1.6+/-0.4	Env 31 (*)
I_14_9 (#)	1.23+/-0.03	1.15+/-0.09	Env 37 (*)
IV_10_16 (#)	1.6+/-0.1	1.3+/-0.1	Env 27 (*)
IV_10_5 (#)	2.8+/-0.4	2.0+/-0.4	Env 68

Figure 27. Correlation for the reproducibility of the fusogenicity assay. A) Fusogenic capacity relative to BaL (red dot) from Env clones that were analyzed at different times and by different investigators was compared. Values show the Mean±SD of three to four replicates for experiment B) Summary table with Fusogenicity values indicating the clones analyzed and the corresponding references *Pérez-Yanes et al. 2022, #Casado et al. 2018. r: Pearson correlation coefficient ranges from -1 to +1, being 0 no relation. P-value is considered significant if <0.05.

2.1. Genotypic and phylogenetic analysis

To further support the validity of a pooled analysis to investigate the HIV-1 Env role in virological control and progression, we also explored the sequence landscape in a phylogenetical tree containing the pooled cohort of the 59 analyzed sequences plus the 29 sequences published in previous works (Pérez-Yanes et al. 2022; Casado et al. 2018) (Figure 28A).

Envs from previous analyses (empty symbols) could be found evenly distributed along the tree with those from the current analysis (solid symbols). Therefore, correspondence of functional and genotypical data between analyses, suggested that a pooled cohort might be representative of the different phenotypical groups and therefore its analysis could provide relevant conclusions.

In addition to genotypically validating the pooled analysis, the phylogenetic analysis of the viral Env gene sequences (C2V5 region) revealed associations between the different progression groups. Most EC clustered in a group containing 32 sequences, along with four VC and three progressor sequences. Outside of this cluster, we could find 22 EC, 11 VC and 27 Old progressor sequences ($p<0.0001$) (Figure 28B). Interestingly, this big cluster group dominated by ECs, contained all the individuals infected by low replicating viruses that allowed to link the function of Env to the non-progressor phenotype (Casado et al. 2013).

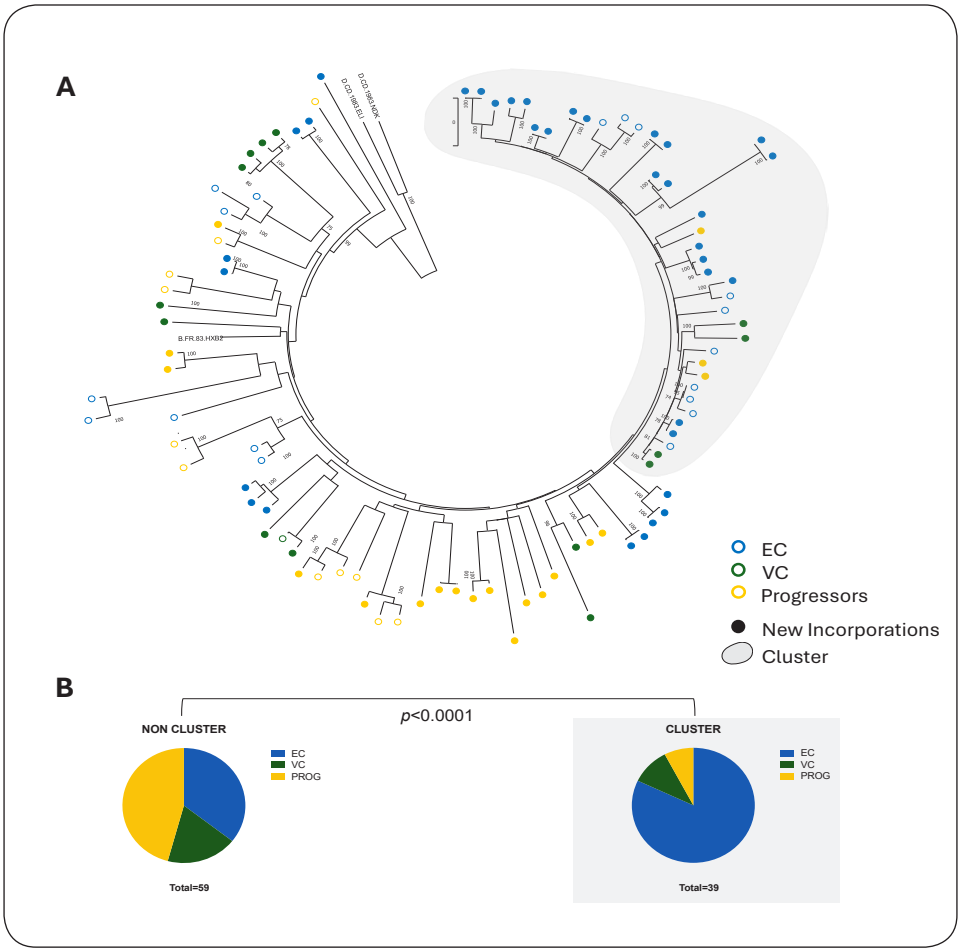

Figure 28. Phylogenetic analysis of the analyzed pool cohort. A) Phylogenetical tree of the pooled cohort. New Envelopes analyzed in this work are marked with a filled symbol. The cluster containing the majority of EC Envs is shaded. Two subtype D sequences (D.C.D) were added to root the tree. HXB2 was added for subtype B reference. EC: Blue, VC: Green, Old: Yellow. The evolutionary history was inferred by using the Maximum Likelihood method and General Time Reversible model (Nei and Kumar 2000). The tree with the highest log likelihood (-33089,30) is shown. The percentage of trees in which the associated taxa clustered together (>70%) is shown next to the branches. Initial tree(s) for the heuristic search were obtained automatically by applying Neighbor-Join and BioNJ algorithms to a matrix of pairwise distances estimated using the Maximum Composite Likelihood (MCL) approach and then selecting the topology with superior log likelihood value. A discrete Gamma distribution was used to model evolutionary rate differences among sites (5 categories (+G, parameter = 0,4775)). The rate variation model allowed for some sites to be evolutionarily invariable ([+I], 18,60% sites). The tree is drawn to scale, with branch lengths measured in the number of substitutions per site. This analysis involved 102 nucleotide sequences. Codon positions included were 1st+2nd+3rd+Noncoding. All positions with less than 95% site coverage were eliminated. There were a total of 2469 positions in the final dataset. Evolutionary analyses were conducted in MEGA X (Kumar et al. 2018). B) Cluster and No Cluster clinical subgroups. P-value is considered significant if <0.05.

To evaluate the potential genetic and functional differences between EC Env sequences located in the cluster (n=32) or outside (n=22), we performed a comprehensive comparative analysis of both subgroups EC Env sequences. First, we explored the impact of protective HLAs and sex (Figure 29A).

While the inclusion of protective alleles remains a topic of discussion and any analysis might be limited by the specific allele selection, in this work we focused on HLA-B B*57, B*27, B*13:02 and B14*:02 as protective alleles (McLaren and Fellay 2021), acknowledging that others like HLA-B*52 (Carrington and Walker 2012) may be protective as well but were not as prevalent in our cohort. The cluster contained 16 participants while the no cluster group contained 10 participants. While individuals enclosed in the cluster showed higher number of HLA-B associated with viral control (62.5%) compared to those outside the cluster (30%) (Figure 29A), there was no statistical significance (p=0.22). Additionally, no differences could be found in terms of sex, where males were more present in both groups (75 and 80%, respectively) (Figure 29B).

In addition, we analyzed Env genetic distance to the ancestor and its functionality in terms of fusogenicity and expression. The cluster of sequences containing low replicating viruses showed to have a significantly shorter genetic distance to the subtype B ancestor for both C2V5 region and gp160 (p=<0.001, p=0.0009 respectively). This suggests EC Env sequences in the cluster were less evolved than the ones we find outside (Figure 29C). In terms of functionality, no differences were found between Env groups differences in fusogenic capacity (p=0.306), nor expression by PG9+PT145 (p=0.217) detection (Figure 29D). Expression by b12+2G12 detection, however, may suggest a trend towards a lower Env expression (p=0.086) in the cluster group.

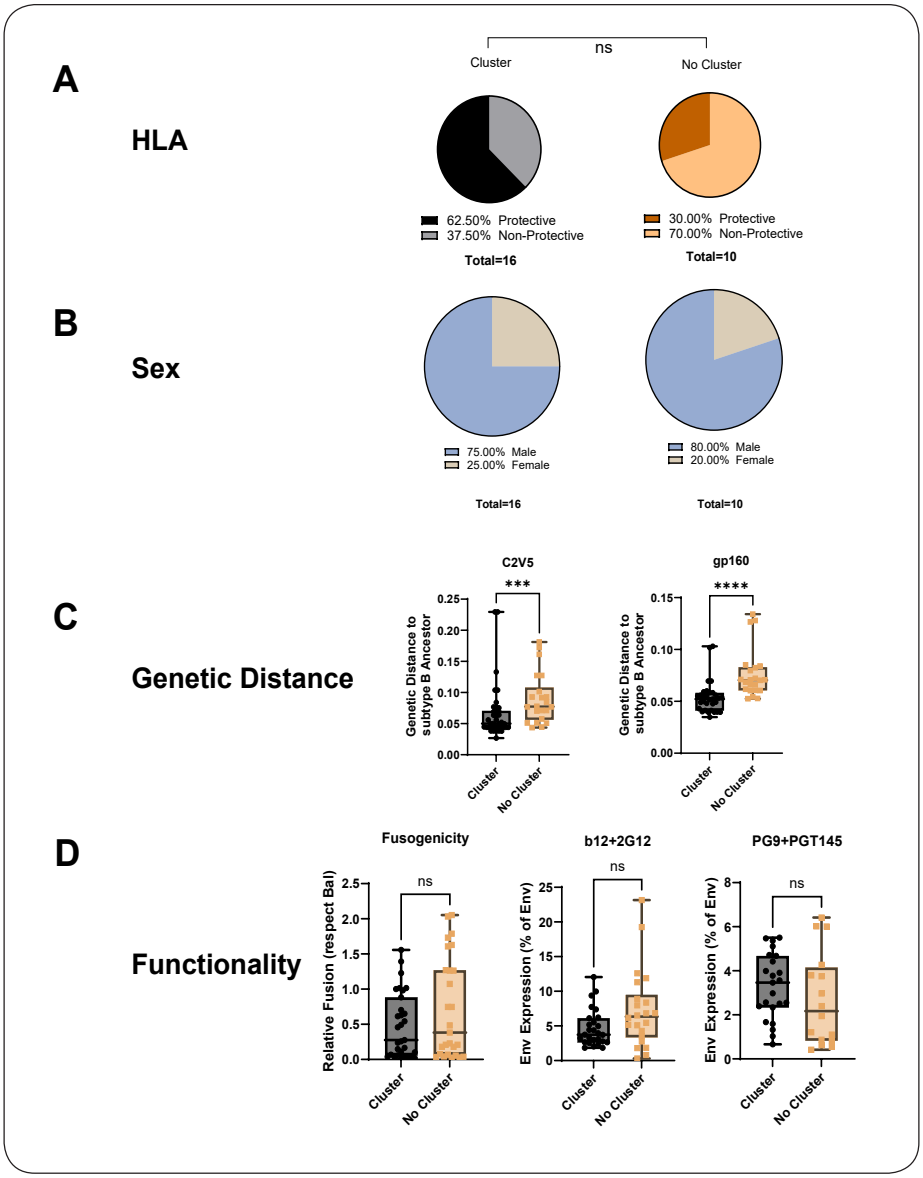

Figure 29. Analysis and characterization of EC Env subclustering. Sequences contained in the biggest EC cluster were compared to those outside the cluster. Cluster contained previously analyzed sequences (mBio) of a cluster of individuals infected by the same virus. A two-sided Fisher's exact test or a Mann-Whitney non-parametric statistical test were used to compare groups in A and C-D respectively. ns: no significance. *P < 0.05, ***P < 0.001. ****P < 0.0001. A) Prevalence of Protective HLA-B alleles B) Sex of participant regarding Cluster. C) Envelope distance to the Subtype B Ancestor (Los Alamos) for C2V5 region and gp160. D) Fusogenic activity of the isolated Env clones relative to Bal as 100% of infection and Env Expression evaluated by flow cytometry using combinations of specific anti-Env antibodies. Values show the Mean and Min Max of individual values. Individual values are the Mean of three to four independent experiments.

2.1.1. Genetic Distance

Finally, we performed the pooled analysis of 98 Env sequences that we have characterized genotypically and phenotypically. First, we compared the genetic distance of C2V5 region and the full gp160 sequence among ECs, VCs and progressors in the pooled tree (Figure 28). As expected, we observed that ECs maintain a lower genetic distance to the subtype B ancestor compared to progressors through analysis of more conserved and variable regions (Figure 30). A lower genetic distance from the ancestor suggests less viral replication, and therefore a reduced evolution and possibility of mutations to arise. In contrast, although a clear trend was observed when ECs were compared to VCs, the higher distance of VCs did not reach statistical significance (p= 0.06 for C2V5 and p=0.07 for gp160).

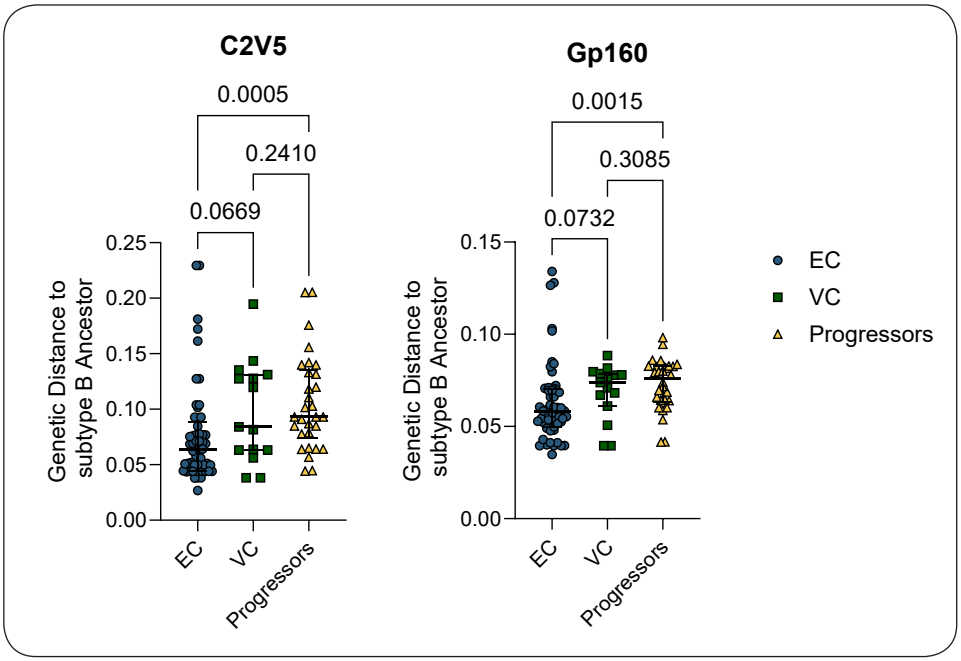

Figure 30. Genetic distance to subtype B ancestor according to phenotypical group and Env region. Horizontal bars show the mean and min to max values. A Kruskal-Wallis test with FDR Method was used to correct for multiple comparisons. Horizontal bars show median with interquartile range.EC: Elite Controllers, VC: Viremic Controllers.

To further investigate whether phenotypic differences between ECs showing a persistent control (PC) or a transient control (TC) was reflected in Env evolution variations, we also assessed their genetic distance to the subtype B ancestor. Therefore, ECs were split into two subgroups (PC, n=44 Envs and TC, n=14 Envs) and were compared to VC and Progressor individuals (Figure 31). No differences were observed between EC

subgroups when the C2V5 region was analyzed. In this analysis, PC maintained similar trends when compared with other groups as shown for the whole EC (Figure 30). In contrast, PC displayed a lower genetic distance in full-length gp160 analysis compared to all the rest of controller and progressor phenotypes (p= 0.015, 0.015 and 0.0002 respectively) (Figure 31).

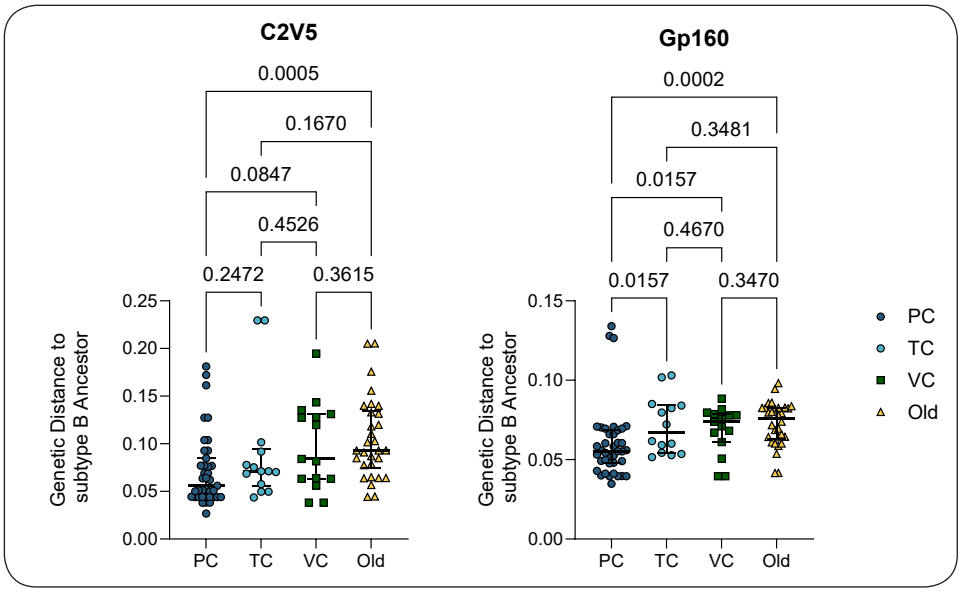

Figure 31. Genetic distance to subtype B ancestor according to phenotypical subgroup and Env region. EC were divided in PC and TC. Horizontal bars show the median with interquartile range Each dot is the mean of three to four independent experiments depending on the envelope. A Kruskal-Wallis test with FDR Method was used to correct formultiple comparisons. Horizontal bars show median with interquartile range. PC: Persistent Controllers,TC: Transient Controllers, VC: Viremic Controllers.

2.2. Phenotypic analysis

2.2.1. Fusogenicity

A similar analysis was performed for functional Env data. Fusogenicity analysis from the pooled Env collection, revealed significantly lower median EC Env fusogenicity values than those of the progressors (n=35) (Figure 32). No statistical differences in fusogenicity were found between EC and VC Envs. Interestingly, despite the impaired fusogenicity observed in ECs, a relevant fraction of their Envs (12/51) were fully functional (defined as a relative fusogenicity value >1), showing higher fusogenicity than the reference BaL Env.

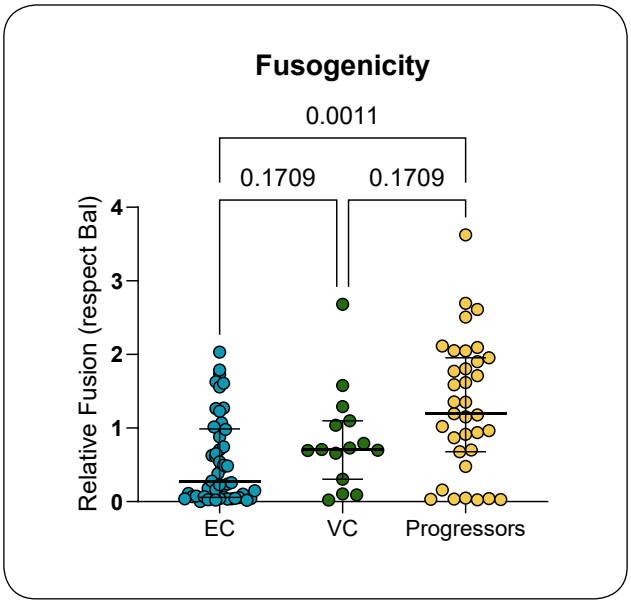

Figure 32. Fusogenic capacity comparative of HIV-1 Envs between EC, VC and progressors from the pooled ECRIS cohort (n=98). Relative fusion Env activity is calculated respect Bal as a 100% of infection. Horizontal bars show the Median with interquartile range. Each dot is the mean of three to four independent experiments depending on the envelope. Statistical differences were identified using a Kruskal-Wallis test with multiple comparison test (*P < 0.05, **P < 0.005).

Additionally, no significant differences (0.7605) were detected in fusogenic capacity between PC and TC (Figure 33). Whether this restricted Env evolution is a cause or consequence of their distinct virological and immunological background will need to be further evaluated.

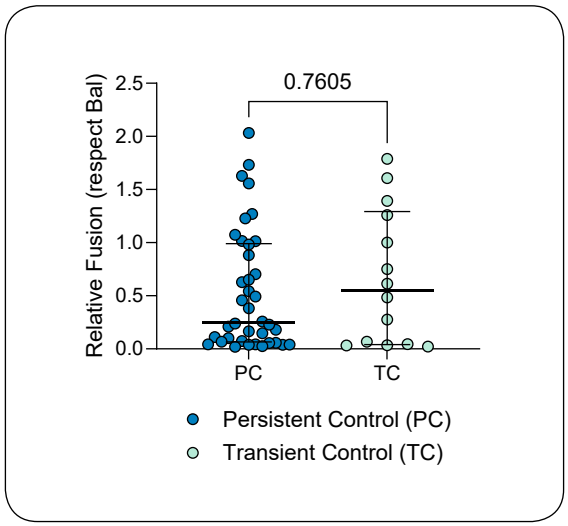

Figure 33. Relative Env fusogenic capacity in PC and TC. Horizontal bars show the Median with interquartile range. Each dot is the mean of three to four independent experiments depending on the envelope. PC: Persistent Controllers, TC: Transient Controllers. P-value is considered significant if <0.05.

To conclude, HIV-1 EC Env fusogenicity was lower than progressor Envs, but similar to VC Envs. Notably, fully functional Envs were identified in some EC individuals, suggesting that additional factors, beyond poor Env function, are involved in the natural control of infection.

2.3. Correlation between viral Env characteristics in the Pool Cohort

A correlation between genotypical and functional data was done to observe if the increase of genetic distance was related to an increase in functionality, and specifically, if a lower genetic distance could account for a lower Env functionality in EC Envs. While we found a positive but not significant correlation with Env expression for the two antibody combinations (p=0.06 for b12+2G12;p=0.25 for PGT145), correlation in progressor Envs was significant for b12+2G12 expression (p=0.02) (Figure 34A,B). A significant positive correlation was observed between fusogenicity and genetic distance to the subtype B ancestor (p=0.0018) (Figure 34C). In general, we can observe that less evolved sequences (less genetic distance to the ancestor) tend to be less functional as seen in expression and fusogenicity. These results are in accordance with previous cohort characterizations (Pérez-Yanes et al. 2022).

Positive correlations were observed for Env expression and fusogenicity, only with statistical significance in the latter (p=0.018) and Env expression as detected by

b12+2G12 in progressors (p=0.02) (Figure 34). This data suggests that viral evolution in progressor individuals correlates with expression, while an increase in function takes place in a global sense.

The confirmation that more evolved Envs presented an increased functionality raised more questions around this increase in PC and TC, as well as the possible role of HLAs. Since the presence of protective HLA could confer better viral control through CTL and NK cells, we investigated whether less fusogenic and therefore less functional Env were differentially observed in individuals presenting protective or non-protective alleles (Figure 35). Protective alleles included in this analysis were HLA-B*27, B*57, B*13:02 and B*14:02 (McLaren and Fellay 2021). No significative differences were found between HLAs in fusogenic capacity (p=0.8939). Similarly, no differences were observed in Env fusogenicity when ECs were disaggregated by sex (p=0.3919,Figure 35).

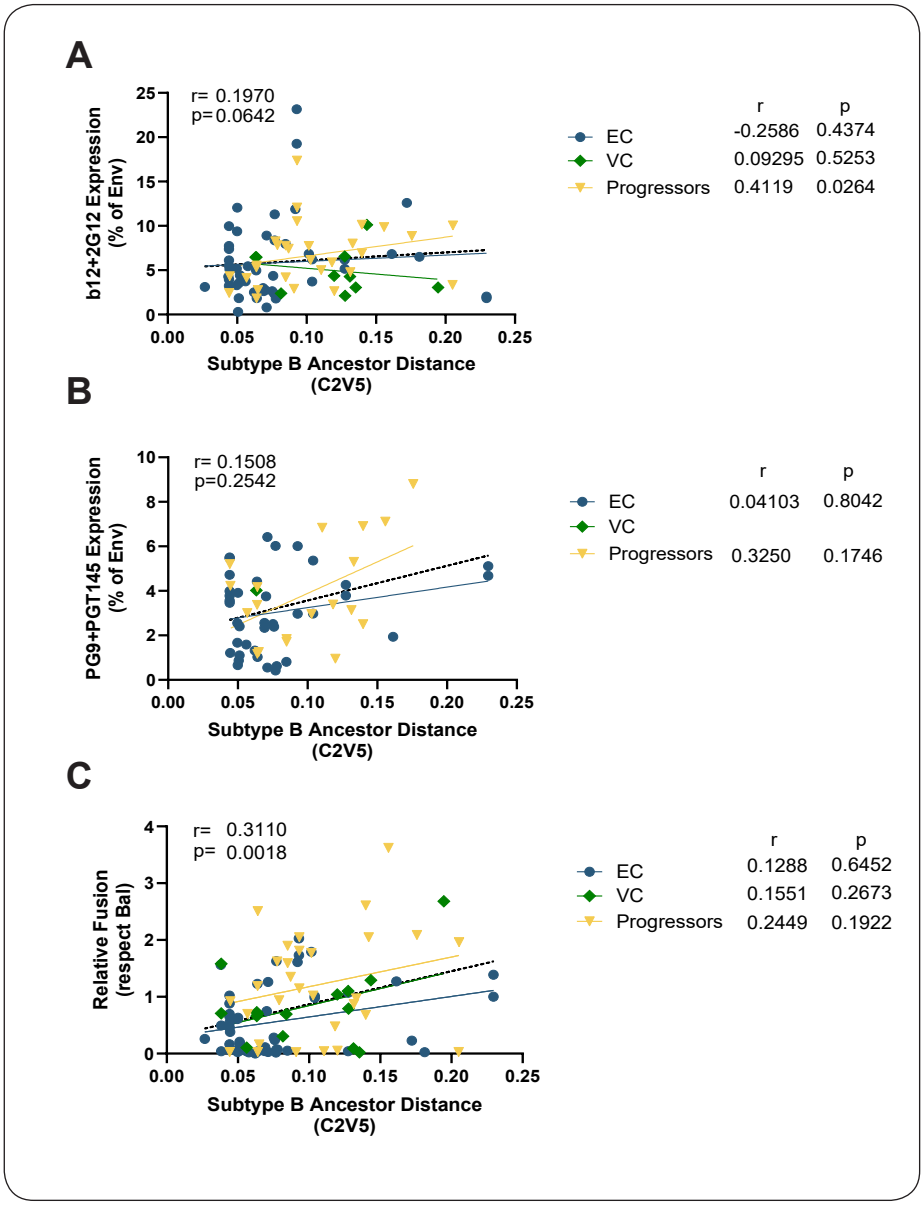

Figure 34. Correlation of Env expression and fusion with the nucleotide genetic distance to subtype B ancestor (C2V5, Los Alamos). Correlations were calculated with a Non-parametric Spearman Test, with r and p values for all Envs shown on the top left, and all subgroups shown on the right. Simple linear regression for all Envs is represented as a dotted black line or with the color corresponding to each subgroup. Circles shown are the Mean + SEM of three independent experiments. For b12+2G12 expression and fusogenicity, pool cohort values are shown. PG9+PGT145 shows only available values on the current analysis cohort. A) b12+2G12 Expression B) PG9+PGT145 Expression C) Relative Fusion to Bal. r: Pearson correlation coefficient ranges from -1 to +1, being 0 no relation. P-value is considered significant if <0.05.

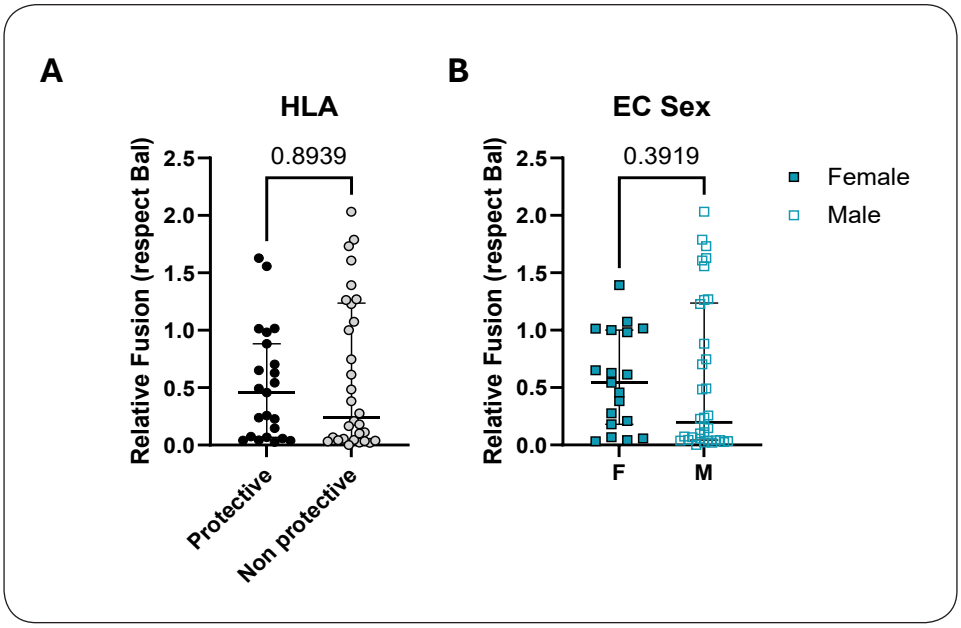

Figure 35. **Relative EC Env fusogenic capacity of the pool cohort depending on A) sex or B) the presence of protective non-protective HLA alleles.** Horizontal bars show the median with interquartile range. Each dot is the mean of three to four independent experiments depending on the envelope. A Mann-Whitney non-parametric statistical test was used to compare both groups. P-value is considered significant if <0.05.

3. Characterization of Humoral response in EC Cohort

The second objective in the study was to characterize neutralizing responses and their contribution to the natural control of infection in the ECRIS Cohort. While cellular immunity, and specifically CD8+ T cells have been related to this control, a proportion of controller individuals frequently develop potent polyfunctional antibody responses that also contribute to viral control either via neutralization or ADCC. To fully describe the neutralizing response, besides analyzing reference strains (NL4-3, TRO.11), the use of autologous viruses can provide a more accurate picture. However, no autologous viruses or individual Env clones were available for all individuals. Therefore, we determined several most common recent ancestor (MRCA) sequences which we used as surrogates of autologous neutralization. Briefly, available ECRIS cohort sequences were phylogenetically analyzed to define the MRCA of these sequences, which we hypothesized would recapitulate individual Env characteristics. These MRCA sequences were included in a large screening of neutralizing activity using 74 longitudinal plasma samples corresponding to 37 EC individuals available from the ECRIS cohort (Figure 18, Table 4).

3.1. Definition of MRCA sequences from EC

A complete set of Env sequences available when plasma samples were obtained was analyzed to identify their MRCA. At that time (2020) only a limited number of Env sequences from EC were available and corresponded to previously reported studies (Pérez-Yanes et al. 2022; Casado et al. 2018). The phylogenetic analysis of the isolated Env sequences displayed a distribution based on viral progression. Most EC Envs clustered together with some LTNP and progressor sequences contemporary to the ECs (Old progressors), while most recent infections (modern) showed higher sequence diversity and distance (Figure 36). A detailed analysis of the EC cluster allowed the identification of three main nodes (409,440,535) in the phylogenetic tree. An MRCA sequence was determined for each of these nodes as we hypothesized that they could recapitulate individual Env characteristics. Interestingly, node 409 included Env sequences reported in the first EC cluster identified (Casado et al. 2013), showing low CD4 binding and fusogenicity (Casado et al. 2018). MRCA 440 and 535 included a wider range of EC sequences that also contained sequences from VC and standard progressors.

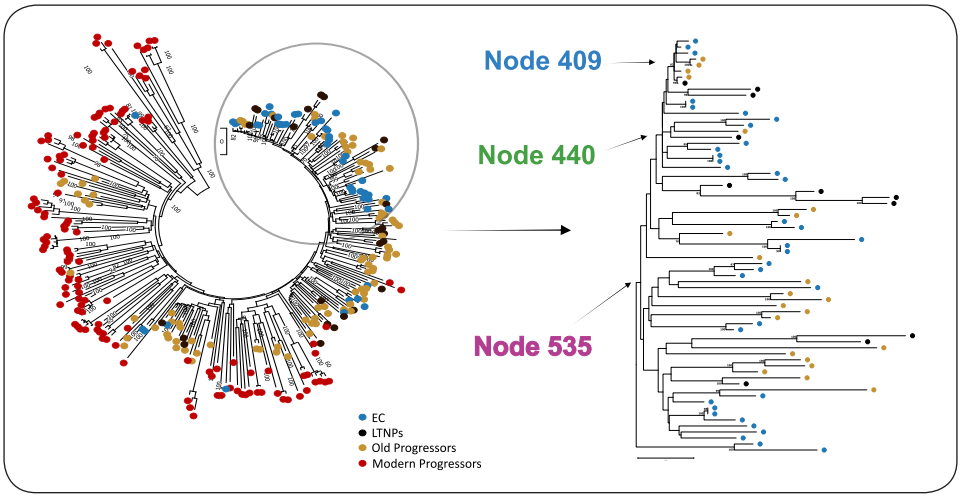

Figure 36. Phylogenetical Tree of analyzed samples. Circled area containing most EC sequences is shown on the right. Three main MRCA Nodes were identified: 409,440,535.

Once these MRCA nodes were established, we analyzed the sequences and generated them by gene synthesis as described in the Material and Methods section (6.5.1a Design and Generation of Immunogen Candidates). Regarding the analysis of sequences, a full analysis is illustrated in Figure 37. The three sequences showed similar length, with one additional residue Threonine 396 residue in node 535. Several amino acid changes were observed among sequences, the most relevant ones affecting glycosylation sites,

node 535 showed 29 potential N-glycosylation sites, while node 440 and 409 showed 28 and 27 sites, respectively. Compared to 535 sequence, node 440 loses a glycosylated asparagine at position 339 (HXB2 numbering), and node 409 has an additional mutation losing asparagine 386 (HXB2 numbering).

Figure 37. MRCA Sequence nucleotide sequence alignment along HXB2 reference. Key Env regions are circled with the corresponding color in the upper schematic Env structure.

3.2. *Functional characterization of MRCA Node Env*

Since MRCA sequences are theoretical sequences, they had to be synthesized through gene synthesis with codon optimization. To ensure their functionality and neutralization sensitivity, we performed an infectivity and neutralization assay.

To analyze both their infectivity and neutralization capacity different pseudoviruses containing MRCA 409, 440, 535 Envs and reference sequences (B41, FCVE1, NL4-3 and TRO.11) were generated by cotransfecting Env-expression plasmids and the defective HIV backbone plasmid pSG3 (Figure 19).

3.2.1. Infectivity

Their infectivity was tested via a TZM-bl based assay (Figure 17C). MRCA pseudoviruses confirmed to be functional, showing differential infectivity levels compared to the reference Env B41 (a codon optimized sequence). The results showed lower infectivity of the 409 node sequence, with intermediate values for 440 and the highest functionality observed for the 535 sequence. These data suggest that MRCA sequences recapitulate the previously reported poor fusogenicity observed in Env clones associated to the node 409 (Casado et al. 2018).

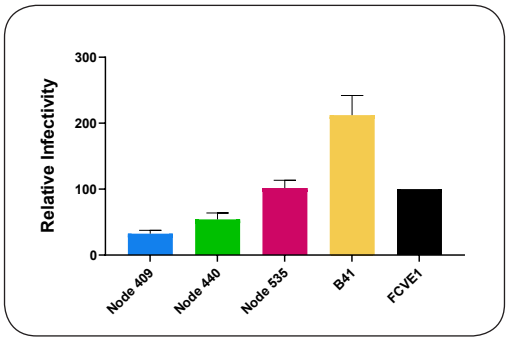

Figure 38. Infectivity of the different codon optimized MRCA sequences pseudoviruses. FCVE1 pseudovirus was included as a reference. The infectivity values were normalized according to the RC of the control virus FCVE1 (value = 100). Bars represent standard deviation from two experiments with three replicates per experiment.

3.2.2. Neutralization sensitivity

Once confirmed the functionality of the synthetic sequences, pseudoviruses were tested for neutralization sensitivity against an extended panel of bNAbs (Table 9). Two reference Env NL4.3 and TRO.11 were also tested. While NL4-3 is a Tier 1 virus with open conformation, TRO.11 is a Tier 2 virus and shows more resistance to neutralization by plasma samples (Seaman et al. 2010).

Notably, some differences in neutralization sensitivity were observed. Consistent with the different degrees of glycosylation, 2G12 failed to neutralize 409 pseudoviruses, while recovered activity against 440 and 535. 409 was also more resistant to PG9, but highly sensitive to PGT145, a trimer specific antibody, suggesting that all MRCA Env are in a closed form. The last glycan-dependent antibody tested, 10-1074, potently neutralized 409 and 535 pseudoviruses, while lost some potency against 440. No major homogeneous trends were observed for the 3 anti CD4bs antibodies tested (b12, N6 and 3BNC117). In contrast, the two anti-MPER antibodies tested showed stronger neutralization capacity against 409 pseudoviruses, suggesting better accessibility of this region in this MRCA (Figure 39).

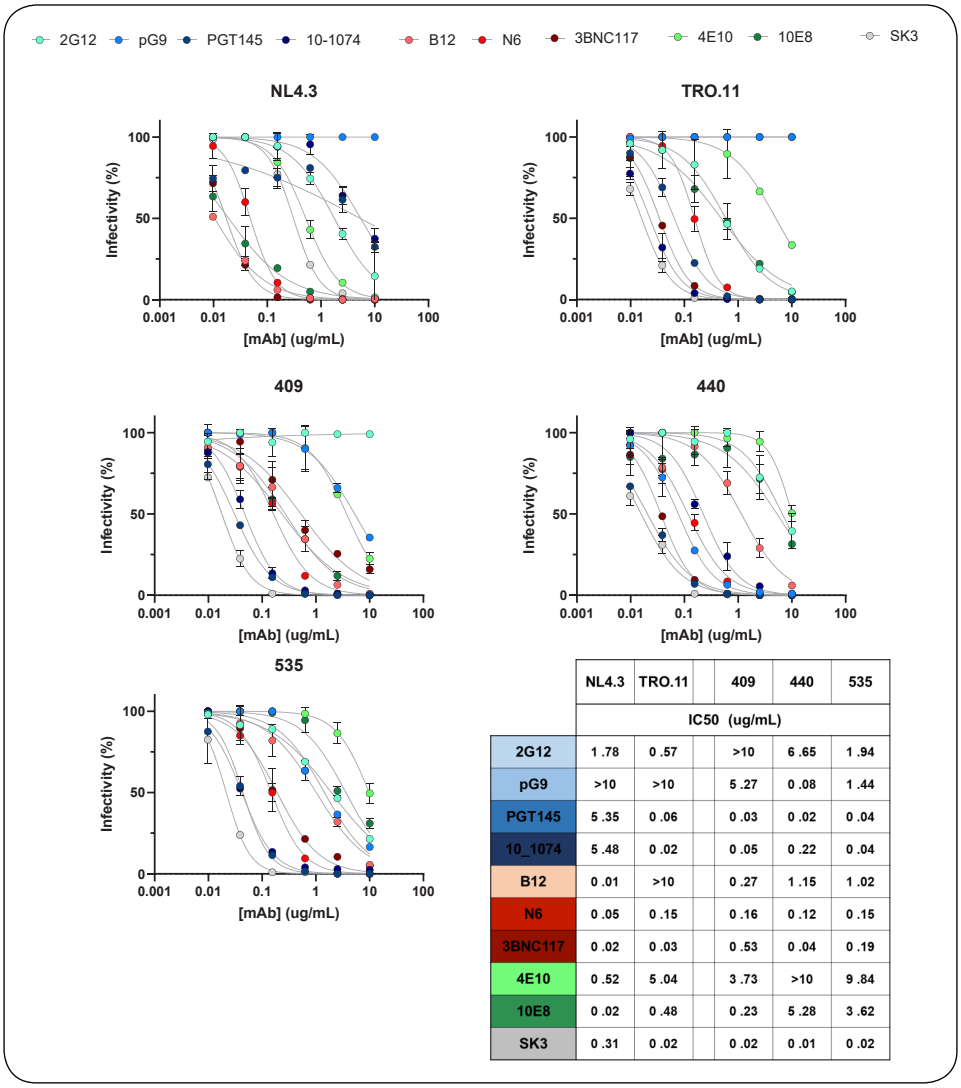

	NL4.3	TRO.11		409	440	535
	IC50 (ug/mL)					
2G12	1.78	0.57		>10	6.65	1.94
pG9	>10	>10		5.27	0.08	1.44
PGT145	5.35	0.06		0.03	0.02	0.04
10_1074	5.48	0.02		0.05	0.22	0.04
B12	0.01	>10		0.27	1.15	1.02
N6	0.05	0.15		0.16	0.12	0.15
3BNC117	0.02	0.03		0.53	0.04	0.19
4E10	0.52	5.04		3.73	>10	9.84
10E8	0.02	0.48		0.23	5.28	3.62
SK3	0.31	0.02		0.02	0.01	0.02

Figure 39. Sensitivity of reference strains and MRCA pseudoviruses against the indicated bNAbs. Values are shown as IC50 (µg/mL). The SK3 antibody (grey symbols) is an anti CD4 antibody used as positive control of neutralization.

3.3. *Analysis of plasma neutralizing activity in ECs*

Once the collection of pseudoviruses were characterized, we analyzed the neutralizing activity of plasma samples from EC individuals obtained from the ECRIS cohort. Of the total of 79 plasma samples analyzed, most individuals had at least two follow-up samples. Four individuals had three follow-up samples. Only four individuals had one plasma sample available (Figure 18).

Neutralization capacity of the plasma at different timepoints was analyzed against Tier 1 and Tier 2 viruses (Montefiori et al. 2018) (NL4-3 and TRO.11, respectively), and the three MRCA pseudoviruses (409, 440, 535). Although longitudinal samples were analyzed, we first explored the last available sample from each participant (n=36), ordered by NL4-3 neutralization and EC subgroup (PC and TC) (Figure 40). Only samples during the control period of TC were included, as a result, last available samples prior to loss of control (LoC) are shown. Plasmas analyzed were sampled a median of 25.4 (11.3-35.7) years after diagnosis.

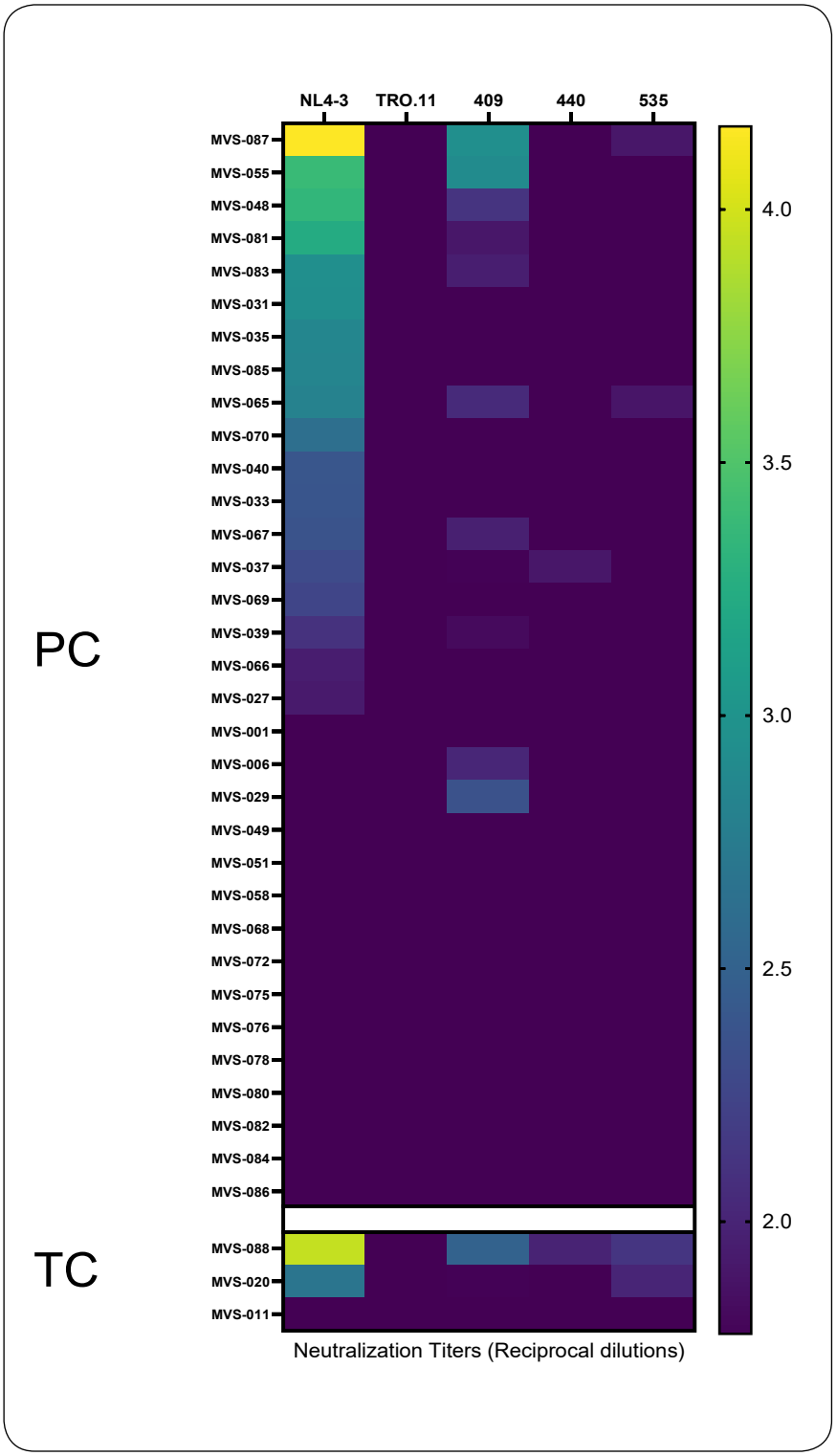
NL4-3
TRO.11
409
440
535
MVS-087
MVS-055
MVS-048
MVS-081
MVS-083
MVS-031
MVS-035
MVS-085
MVS-065
MVS-070
MVS-040
MVS-033
MVS-067
MVS-037
MVS-069
MVS-039
MVS-066
MVS-027
MVS-001
MVS-006
MVS-029
MVS-049
MVS-051
MVS-058
MVS-068
MVS-072
MVS-075
MVS-076
MVS-078
MVS-080
MVS-082
MVS-084
MVS-086
MVS-088
MVS-020
MVS-011
PC
TC
4.0
3.5
3.0
2.5
2.0
Neutralization Titers (Reciprocal dilutions)

Figure 40. Neutralization titer Heatmap (reciprocal dilution) of HIV-1 EEC plasma samples against reference strains (NL4-3 and TRO.11), and 409, 440 and 535 MRCA sequences*. Only the last plasma sample from each participant is displayed (n=32) and ordered according to NL4-3 neutralization and EC subgroup: persistent (PC) or transient controller (TC). The limit of quantification is <60. *Node sequences from an EC cluster in a phylogenetic tree containing EC Env nucleotide sequences from Spanish samples.

Out of the 36 EC plasma samples, 20 (56%) showed detectable neutralization against NL4-3, but none against TRO.11. Regarding the different MRCA, only 12 (33%) ECs showed detectable neutralization against 409, 2 (6%) against 440, and 4 (11%) against 535. The higher neutralization against 409 MRCA might be due to its origin in a cluster of low replicating viruses, probably with some Env defects and a higher exposure of some epitopes.

Interestingly, the individual with the highest neutralization response (MVS-087) has later been identified as losing immunological control at the time of sampling. Unfortunately, no further follow-up is available to observe if these changes in immune and neutralization titers could have been indicators of a later virological LoC. Regarding the TC, we could observe heterogenous neutralization levels that might reflect specific virological and immunological changes at each sampling time and individual prior LoC: MVS-088 -0,3 years; MVS-020 -9 years and MVS-011 -12,9 years.

3.3.1. Neutralization in Persistent and Transient Controllers

The majority of studies focused on EC are cross-sectional and missing potential longitudinal evolution. This is due to the small number of EC and lack of immunogical and virological data available longitudinally. As our plasma cohort gathered 37 EC individuals with longitudinal follow-up, we analyzed the evolution of neutralizing activity and disaggregated all collected data into their PC and TC classifications to assess possible differences in terms of sex, HLA-B alleles and neutralization capacity during the control period.

This analysis contained a total of 37 individuals, 35 PC (92%) and 3 TC (8%). No differences were observed in terms of sex and distribution of HLA protection alleles. Of the PC, 17 were female and 17 male, while TC were 2 females and 1 male.

To assess any differences in neutralizing capacity during the control period between PC and TC, we analyzed the first and last plasma sample available from each individual. Low to no changes in neutralization titers against NL4-3, TRO.11 and the three MRCA were observed between PC and TC in the analyzed plasma cohort. Time difference between samples has to be taken into account for an accurate interpretation (Figure 18). There is a mean time difference of 6.98 years between the first and last samples (min 1.07-max 19.75), with 9 individuals with a sample difference over 10 years, and 22 under 10 years. Both big- and small-time differences only picture a moment during follow-up and might not represent virological changes that have happened during the follow-up. Globally however, it showed that neutralization levels were maintained

overtime, with some exceptions in both PC and TC individuals. Interestingly, MVS-087 presented a 100-fold increase in neutralizing capacity against NL4-3 and more than a 10-fold against 409. There was a 17-year difference between each sample and during that time, two envelopes could be isolated from PBMCs.

In TC, MVS-020, presented a 10-fold increase against NL4-3 in a sample 9.16 years prior LoC, with undetectable VL and with a 5 year difference with the first one. Overall, while neutralizing capacities in EC might be heterogenous, could also be a great tool to better understand undergoing changes at a virological, immunological and reservoir level that could predict LoC in these individuals and allow the implementation of therapeutic strategies.

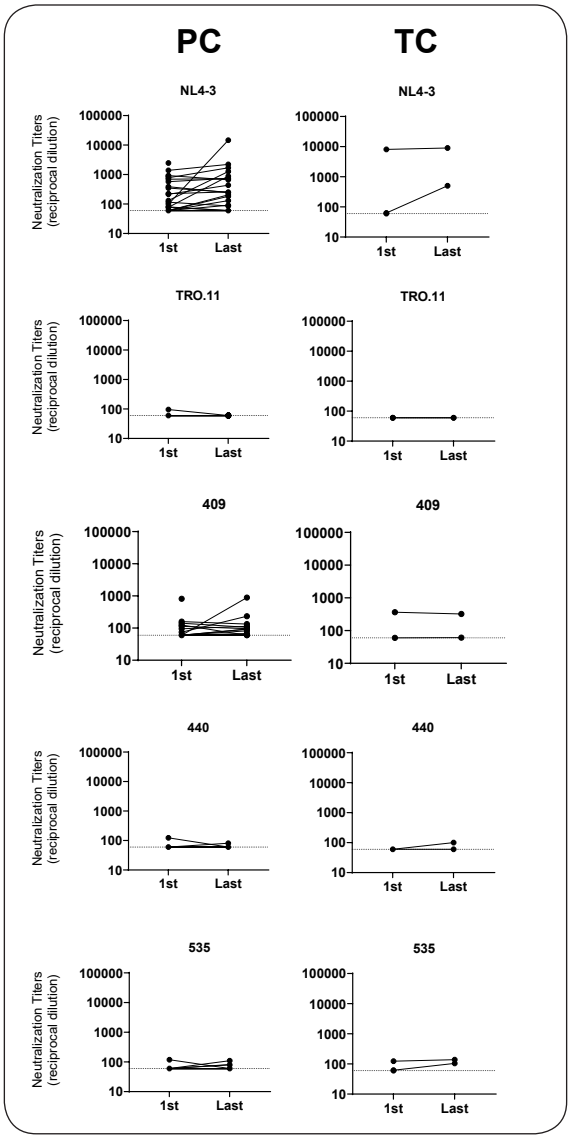

Figure 41. Neutralization titer changes between the control period between PC and TC. First and last plasma samples available from each individual are plotted. The horizontal dotted line marks the limit of quantification (<60).

Secondly, we analyzed the proportion of protective and non-protective HLA alleles in our EC cohort. Of the PC, 26 presented protective HLA-B alleles (76%) and 8 non-protective (24%). All TC (n=3) presented non-protective HLA-B alleles (Figure 42A). Finally, we wanted to see if this presence of protective alleles correlated with an improved neutralizing capacity and we could not observe significant differences (Figure 42B,C).

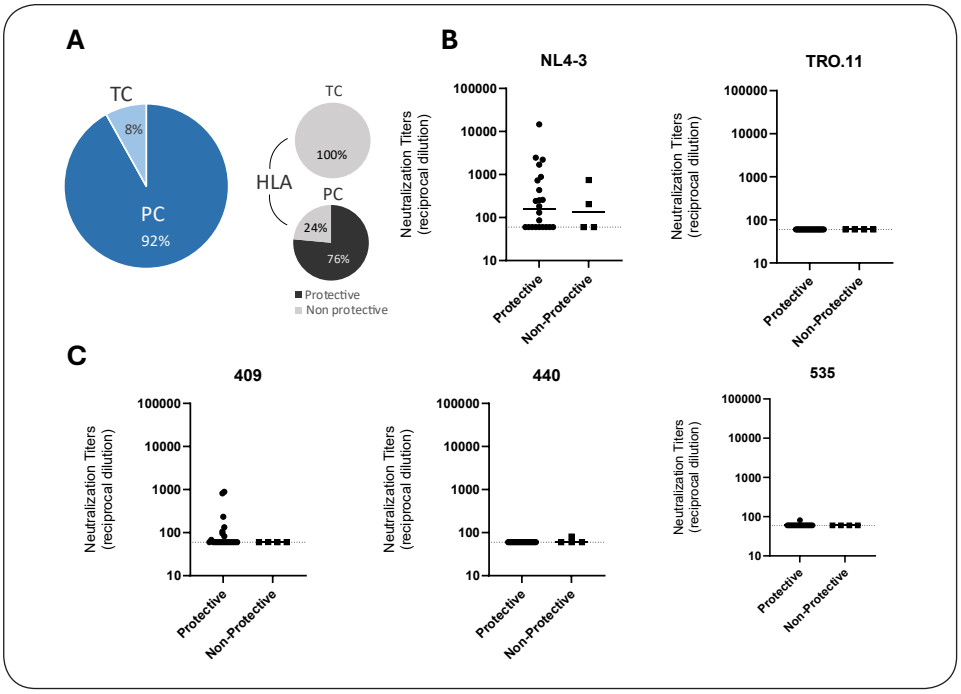

Figure 42. Prevalence of Protective HLA alleles on the plasma samples cohort and effect on neutralization titers. A) Pie Charts illustrating the PC/TC and protective/nonprotective allele distribution in the sample cohort.B) Neutralization Titers against Reference HIV-1 strains. C) Neutralization Titers against three MRCA.

4. Characterization of the Loss of control in an Exceptional Elite Controller case

The longitudinal follow-up of the cohort of Elite Controllers has allowed the identification of the case of an EEC that lost virological control 32 years after her HIV diagnosis. The characterization of loss of control cases is important to further understand mechanisms involved in control and loss of control, which could allow for the development of new therapies as well as the identification of biomarkers that could predict the loss of control in other controllers. In this case, we performed a detailed, longitudinal characterization of the HIV-1 reservoir, viral evolution, humoral and immune (B- and T-cell) response in this previous EEC (Frances et al. 2025). Viral evolution, functionality and humoral response are going to be discussed in this manuscript.

4.1. Clinical and Data

The case focuses on a woman born in 1965 (MVS-088) who was diagnosed with HIV in 1986 (19 years old) and was clinically followed since 1990 in Centro Sandoval in Madrid. A comprehensive virological and immunological study was performed on available longitudinal samples (n=35) between 19 and 37 years after diagnosis (2004-2021) (Figure 43). She presented a protective genetic background with heterozygous CCR5Δ32 and HLA-C (rs9264942), but no protective HLA-B (B39:01/B44:02).

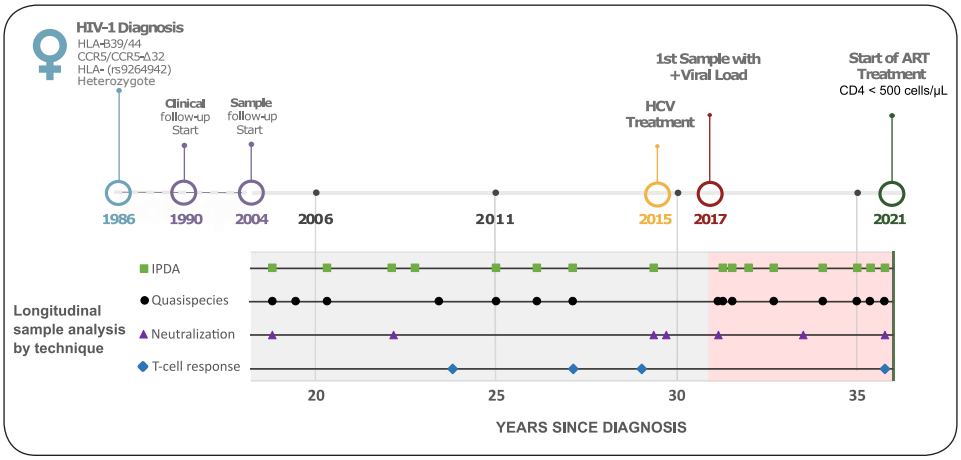

Figure 43. Timeline of EEC MVS-088 with major events and performed analysis. Each analyzed sample appears as a dot next to the corresponding technique. HCV: Hepatitis C Virus, ART: Antiretroviral treatment, IPDA: Intact Proviral DNA Assay.

During her follow-up she maintained stable CD4+ and CD8+ T-cell counts around a 1000 cells/μL and undetectable VL for 31 years since diagnosis, except for four transient episodes (blips) with ≤150 copies/mL (Figure 44, black). In December 2016, the EEC lost viral control and saw a progressive decrease in the CD4+ T-cell counts and a reversion of the CD4/CD8 ratio (Figure 44). For this reason, she started ART in October 2021 (Figure 43).

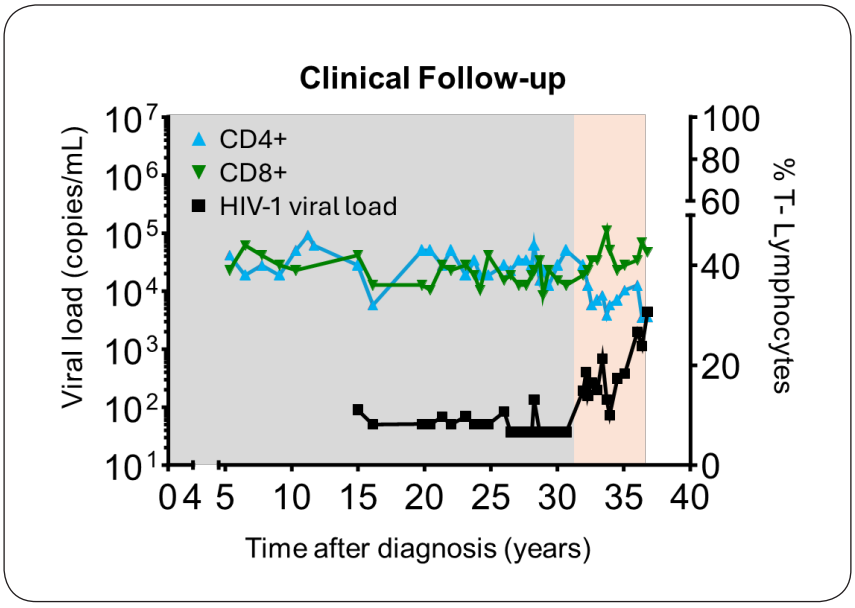

Figure 44. Clinical Follow-up of viral loads and T-cell counts. Viral loads are expressed in HIV-1 RNA copies/mL and appear as black squares. CD4+ and CD8+T cells are expressed in % and appear as blue and green triangles, respectively. Light grey box indicates EEC period and the orange the loss of control period during follow-up.

4.1.1. Molecular

To further understand mechanisms that led to this LoC we focused on viral Env and plasma samples. On Env, we analyzed evolution and dynamics of viral quasispecies; infective capacity and fusogenicity of isolated clones. For plasma, we assessed its autologous neutralizing capacity.

4.1.2. Genotypic and phylogenetic analysis

Viral envelopes, isolated during the follow-up period, and their associated sample characteristics are summarized in Table 11. Some full Envs first isolated during the control period (grey) were also present during the LoC (orange).

Table 11. Characteristics of isolated MVS-088 viral Envelopes. Envelopes isolated during viral control analysis are marked in bold and grey. Envelopes isolated during the LoC period are highlighted in orange. Although firstly isolated during the control period, Env39 and 40 were also found in samples during the loss of control.#N/A: not available.(*)Viral dating is extrapolating beyond the available data, showing therefore a future date, meaning the sequence has too much evolved from the reference ancestral ones.

Clinical group	Sub-group	Env Code	ID Code	Viral load at sampling (copies/mL)	Sampling time	Viral dating
LTNP	EC	**36**	MVS-088	<50	2009	1984
		37	MVS-088	403	2017	1984
		38	MVS-088	4370	2021	#N/A
		39	MVS-088	403	2017	2028*
		40	MVS-088	134	2018	2028*
		41	MVS-088	403	2017	#N/A
		42	MVS-088	4370	2021	#N/A
		43	MVS-088	4370	2021	#N/A
		44	MVS-088	134	2018	#N/A

Phylogenetic analyses of the C2V5 region of isolated Env sequences showed the presence of a single subtype variant B. Env sequences isolated during the control period remained homogeneous and close to the ancestral virus with limited divergence (Figure 45A). This divergence, however, was increased during the loss of control period. Genetic distances to the MRCA were assessed and showed more evolved Envs during the loss of control period (Figure 45B).

4.1.3. Functional analysis

To further evaluate if Env evolution correlated with an increase in functionality, we analyzed their fusogenic capacity and infectivity. Previous studies of HIV-1 cohorts observed that EC Env are defective in some cases (Valenzuela-Fernández et al. 2022; Lassen et al. 2009), and that their poor fusogenicity and reduced expression of the viral

envelope glycoprotein (Pérez-Yanes et al. 2022; Casado et al. 2018) might account for the development of a controller phenotype. As a result, Envs isolated after the loss of control were expected to present a higher functionality and have substantially evolved to escape the immune response.

a. Fusogenicity

We analyzed the fusogenic capacity of the different full length Env clones that could be isolated during the control and loss of control periods (Figure 45C). Reference HIV-1 viral strains, high and low fusogenic envelopes and TZM-bl cells were used as controls. Envelope sequence diversity increased 10 years prior loss of control (Figure 45A) and was associated with increased functionality (Figure 45C).

b. Infectivity

Infective capacity of the isolated Envs was analyzed via a TZM-bl based assay. Env infectivity increased along fusogenicity and genetic distance, with the highest level in env44, isolated during the loss of control period (Figure 45D).

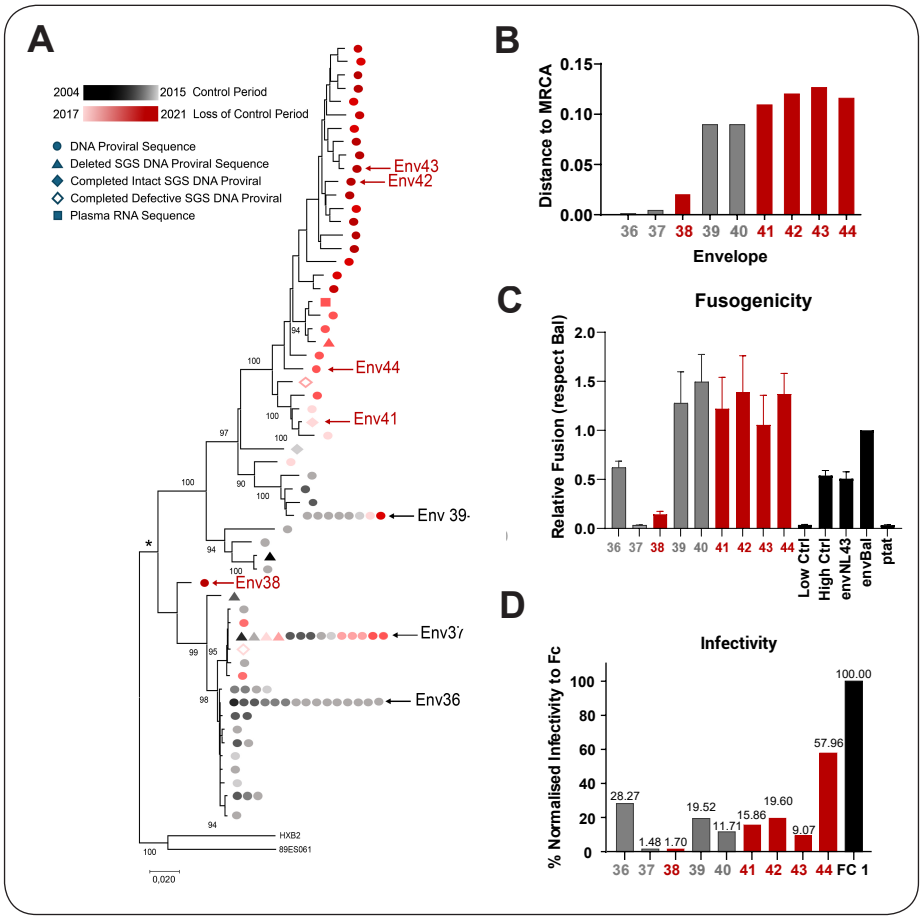

Figure 45. Genotypic and Phenotypic characterization of isolated HIV-1 EEC Env Clones isolated during the control (grey) or loss of control period (red). A) Phylogenetic Tree of the isolated Env sequences. Their MRCA is marked by *. The evolutionary history was inferred using the Neighbor-Joining method and evolutionary distances calculated using the Poisson correction method. The % of trees where the associated taxa clustered with values >90% is displayed next to the branches. B) Envelope distance to the MRCA. C) Fusogenic activity of the isolated Env clones relative to Bal as 100% of infection. Reference HIV-1 viral strains, a low and a high fusogenic Env, and ptat were used as controls (white). Values show the Mean +/- SEM of four independent experiments (n=4). D) Infectivity of pseudoviruses bearing the isolated EEC Env or the reference Env FC 1. Envelopes are displayed by distance to the MRCA.

4.1.4. Correlation between viral Env characteristics

In all Env clones analyzed (n=9), genetic distance positively correlated with functionality defined by both infectivity and fusogenicity (Figure 46), but with no statistical significance (p=0.1497, p=0.6034).

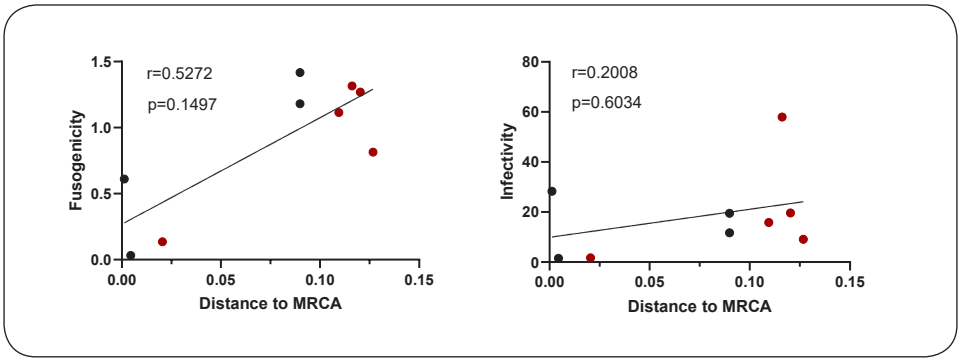

Figure 46. Correlation of Genetic Distance to MRCA and functionality and expression assays. Envs isolated during the control period (black) and loss of control period (red). r=Peason correlation coefficient ranges from -1 to +1, being 0 no relation. p value is considered significative if <0.05.

4.1.5. Risk factors for loss of control

a. Envelope evolution and change of viral tropism

Extensive sampling during the control period identified evident fluctuations in viral populations with signs of quasispecies evolution (estimated by Env divergence and sequence diversity) (Figure 47). Remarkably, as noted in the phylogenetic analysis, Env evolution started to increase during the control period, around ten years prior to the loss of control and then remained stable until viral replication was detectable in plasma.

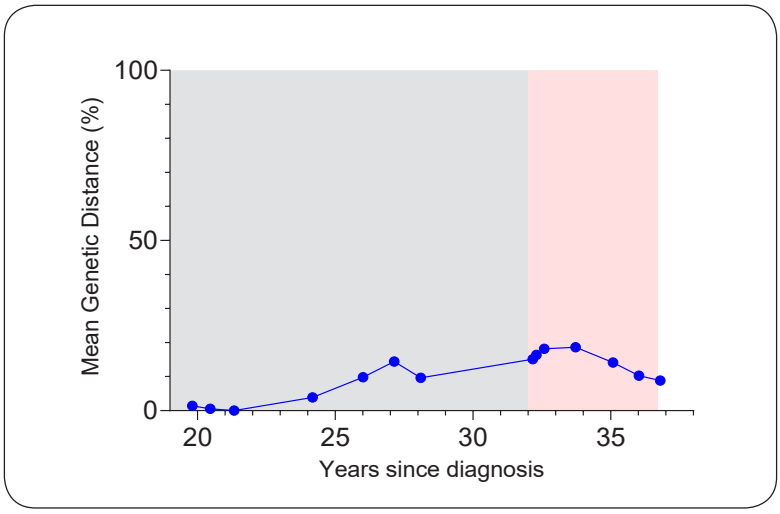

Figure 47. Evolution of Env sequences within MVS-088 according to genetic distance. Light grey box indicates EEC period.

Changes in viral tropism have been associated to viral escape in some individuals (Rosás-Umbert et al. 2019). In this case, tropism for all isolated Envs was predicted via PSSM. All isolated Envs were R5 until 2018, where CXCR4 genotypes were detected for the first time. Interestingly, isolated Envs (env40 and env44) were R5. It is common to isolate envelopes with different tropisms within the same sample. Further samples during the loss of control period (env42 and env 43) had an X4 phenotype. As this change of tropism is only a prediction, phenotype should be further determined experimentally (Garrido et al. 2008).

Table 12. Tropism Prediction of MVS-088 Envs. * In this sample X4 sequences could be already detected.

Env clone	Sampling Time	Time to loss of control (years)	Tropism
36	2009	-6.9	R5
37	2017	1.1	R5
39	2017	1.1	R5
41	2017	1,1	R5
40	2018	2.7	R5
44	2018	2.7	R5*
38	2021	5.7	R5
42	2021	5.7	X4
43	2021	5.7	X4

It is interesting that even with the presence of X4 sequences from 2018, it was not until 2021 that viral control was finally lost. Being an CCR5Δ32 heterozygote, one would expect this change of tropism to lead to a faster disease progression (Connor et al. 1997), suggesting the involvement of multiple factors in the virological control in this case.

b. Superinfection

The hypothesis of a superinfection was discarded by phylogenetical analysis, where all Env sequences from MVS-088 were represented along multiple nucleotide sequences from other individuals. All sequences from the case were clustered together with a 100% value (Figure 48). In the case of superinfection, and therefore different viruses, these would not have clustered together and would be spread across the tree. It could

be argued that with only one plasma sequence available the superinfection possibility cannot be completely ruled out, but it would be a relative unlikely case. In addition, the evolution of the emerging virus could be traced back before the loss of control.

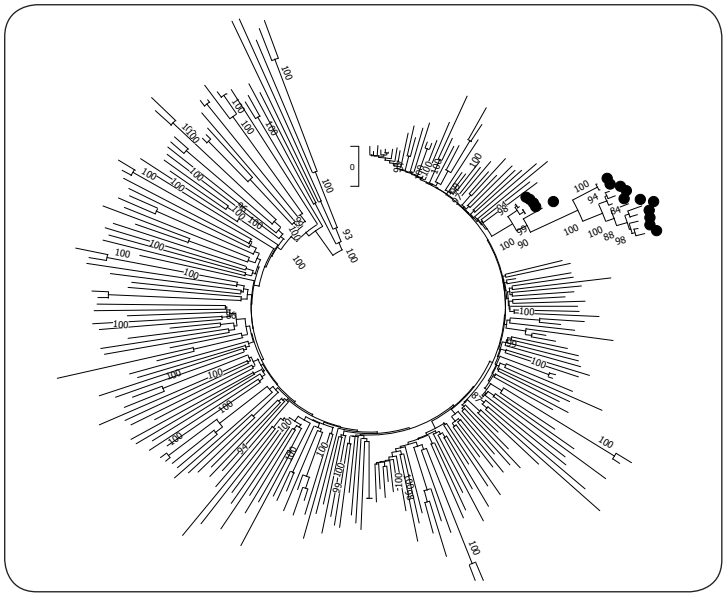

Figure 48. Phylogenetic Tree of EEC MVS-088 samples along other subtype B sequences. The evolutionary history was inferred using the Neighbor-Joining method. The percentage of replicate trees in which the associated taxa clustered together in the bootstrap test with value upper 80% (500 replicates) are shown next to the branches. The evolutionary distances were computed using the Maximum Composite Likelihood method and are in the units of the number of base substitutions per site. This analysis involved 251 nucleotide sequences. Codon positions included were 1st+2nd+3rd+Noncoding. All positions with less than 95% site coverage were eliminated. There were a total of 2383 positions in the final dataset. Evolutionary analyses were conducted in MEGA X.

4.2. Longitudinal analysis of autologous neutralization in plasma samples

In some PLWH, the presence of neutralizing antibodies might have helped in viral control. To assess the titers and role of neutralizing antibodies in MVS-088, we analyzed longitudinal plasma samples from 18 to 36 years since diagnosis (covering both control and loss of control periods) for the presence of neutralizing antibodies (Figure 18).

A total of 7 plasma samples were available, four of them collected during the control period (between 18 and 30 years of HIV diagnosis) and three of them collected during the viremic period prior to ART start (32-36 years after HIV diagnosis).

4.2.1. Neutralization

Neutralization capacity was analyzed against two reference strains with different neutralizing capacities (NL4-3 and TRO.11, Tier 1 and Tier 2 viruses), the previously described MRCA Nodes 409, 440 and 535 and autologous viruses. (Figure 49).

Longitudinal plasma samples showed high and stable neutralization titers against NL4-3, but no neutralization against TRO.11. While all plasma samples showed autologous neutralization against Env isolated during the control period (Envs 36,37,39,40), low to no neutralization titers were observed against Envs isolated after loss of control (Envs 38,41,42,43,44). Envelopes emerging after loss of control were resistant to neutralizing antibodies present in samples from the control period. Autologous neutralization against dominant ancestral Env36 was observed in all samples analyzed (before and after loss of control). Neutralization of MRCA sequences appeared to recapitulate autologous neutralization against Env isolated during the control period.

To summarize, neutralization of contemporaneous viruses is observed during the EEC period and reduced after the loss of EEC status. High neutralization titers and viral evolution during elite control period could be signs of ongoing replication related to the loss of exceptional control.

Longitudinal analysis of neutralization of the different autologous Env, show in general flat profiles, However, low levels of neutralization could be detected prior to loss of control against env39 and env42. Although env39 was detected prior to loss of control, env42 could only be isolated in the viremic period. Finally, a small increase in neutralization of env44 could be noticed in latter timepoints, suggesting continuous evolution of B-cell responses (Figure 49, Figure 50).

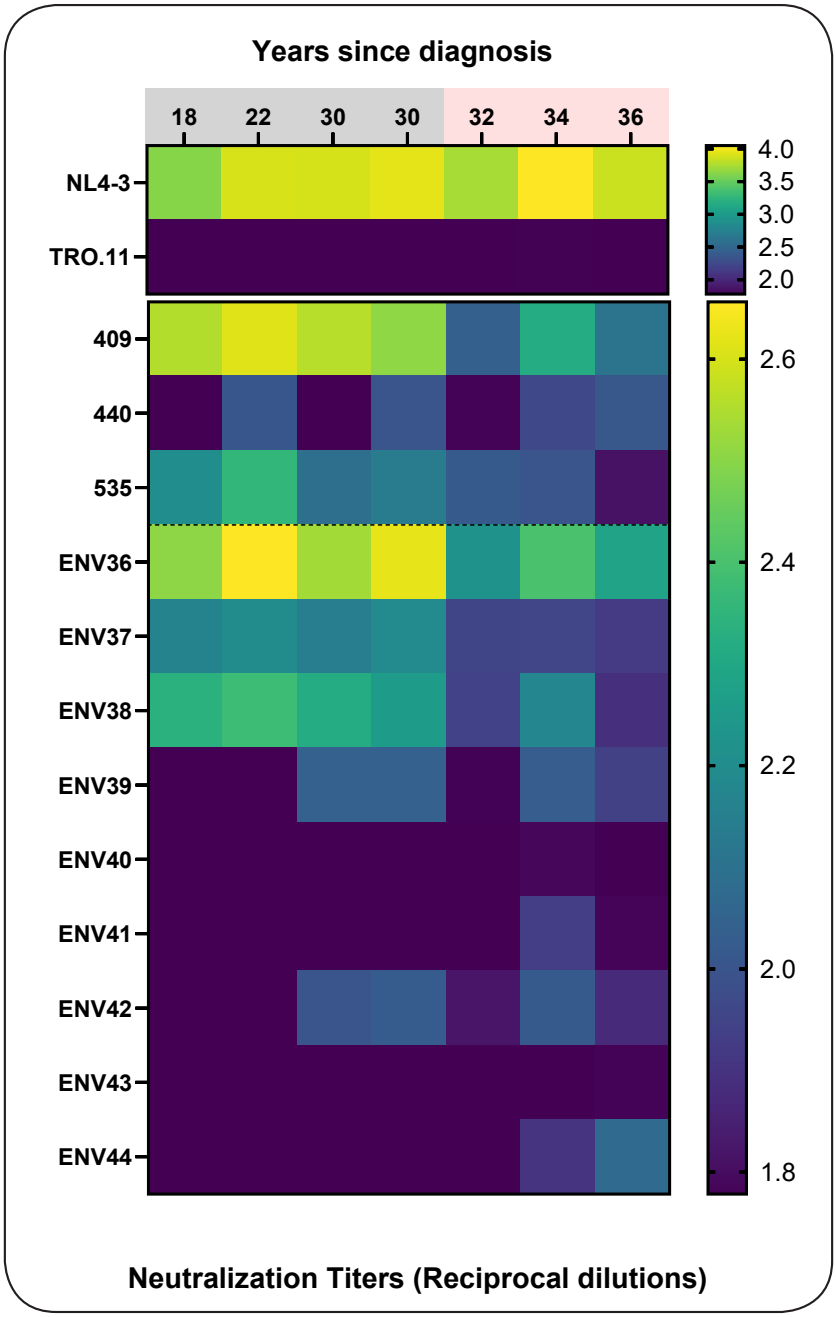

Figure 49. HIV-1 EEC plasma sample neutralization titers heatmap (reciprocal dilution) against reference strains (NL4-3 and TRO.11), MRCA nodes⋆ and autologous Env pseudoviruses (Env 36-44). Plasma samples and autologous Envs from before (grey) and after loss of control (red) were analyzed. The limit of quantification is <60. ⋆Nodes from a phylogenetic tree containing EC Env nucleotide sequences from Spanish samples.

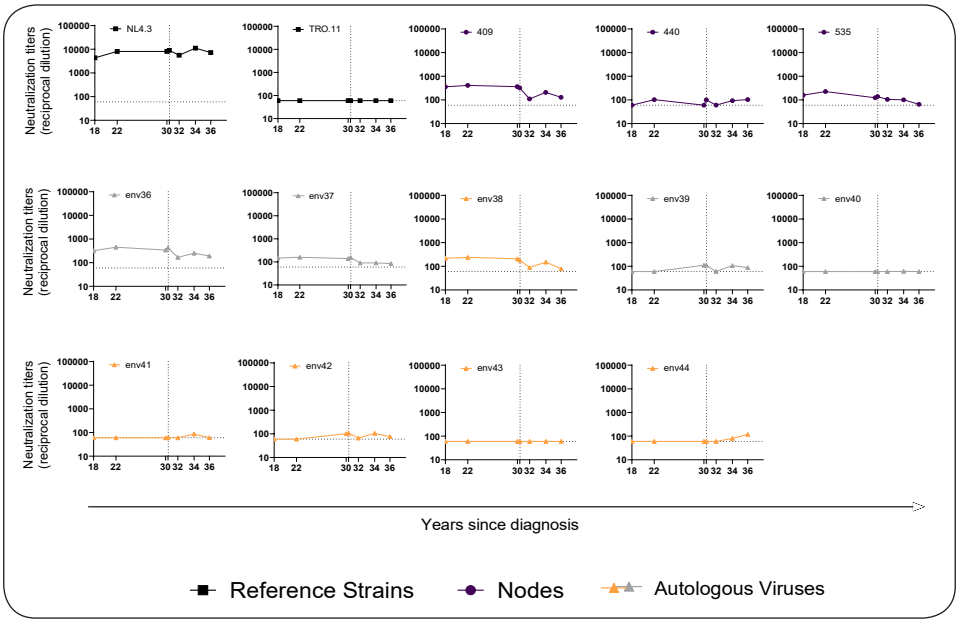

Figure 50. Longitudinal visualization of the neutralization capacity of available plasma samples. Neutralization capacity was tested against reference HIV-1 (NL4-3, TRO.11), MRCA nodes* and autologous Env pseudoviruses (env 36-44). Autologous Envs isolated before (grey) and during the loss of control (orange) were analyzed. Env39 and 40 were also found in samples during the loss of control. The horizontal dotted line marks the limit of quantification (<60). The vertical dotted line separated the control from the loss of control period. *Nodes from a phylogenetic tree containing EC Env nucleotide sequences from Spanish samples.

4.2.2. Binding assay

Neutralizing antibodies are a small fraction of total antibody responses. Non-neutralizing antibodies may mediate Fc-related immune functions such as ADCC. As a first approach to evaluate Env-binding antibodies, we performed a flow-cytometry-based binding assay using available plasma samples and including autologous envelopes transiently expressed in Expi293F cells. Binding results showed redundant profiles compared to neutralization of the Tier 1 virus NL4-3 (Figure 50). Binding antibodies were detectable for all Env tested (NL4-3, TRO.11, MRCA and autologous sequences) and seemed to be a measure total anti-Env antibody titers, providing however reduced information on its specificity (Figure 51). Differences in the magnitude of signal detected among Env were directly related to the expression level as measured by the b12 antibody.

The longitudinal analysis (Figure 51) only showed a relevant increase from the first to the second sample and a peak in the first sample collected in the viremic period.

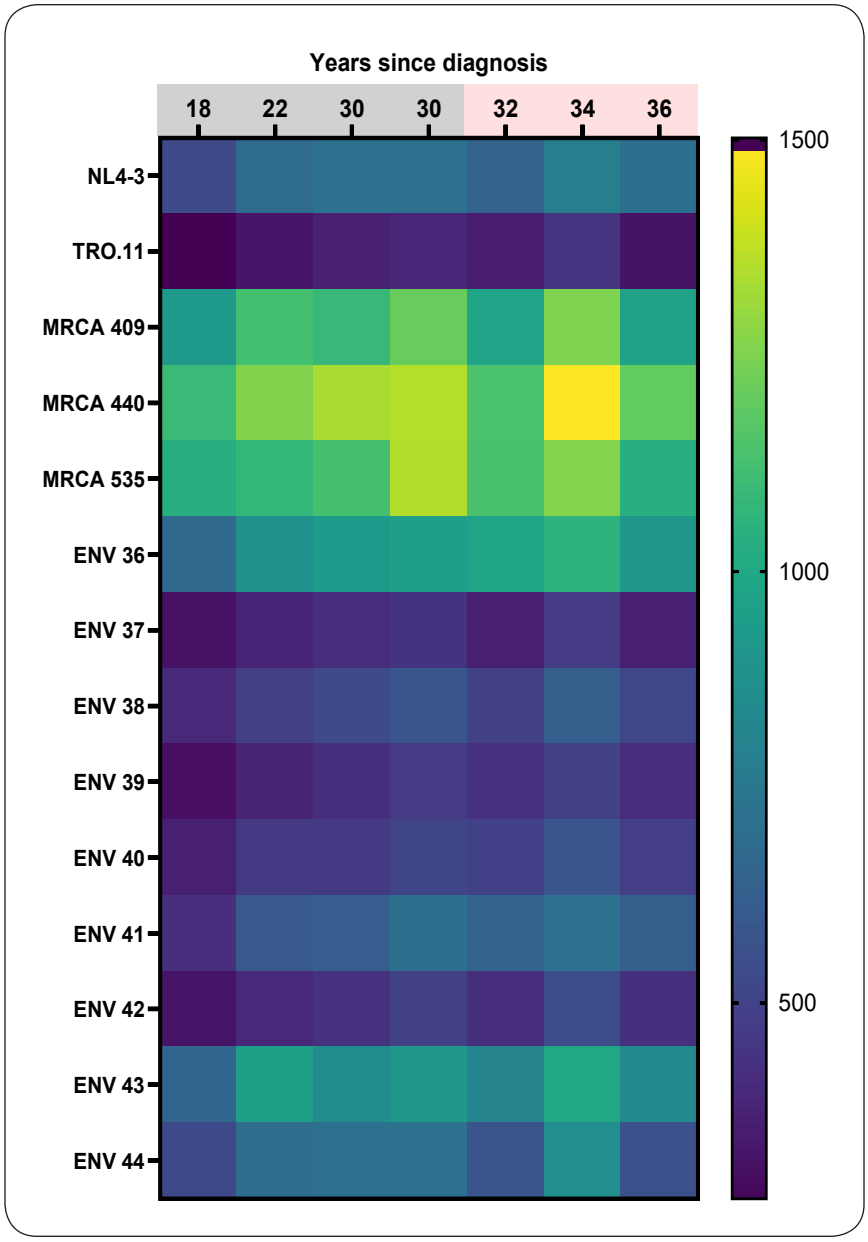

Figure 51. Binding activity heatmap of the different plasma samples against reference, MRCA and autologous pseudoviruses. Plasma samples and autologous Envs from before (grey) and after loss of control (red) were analyzed. Values are shown as the GeoMean.

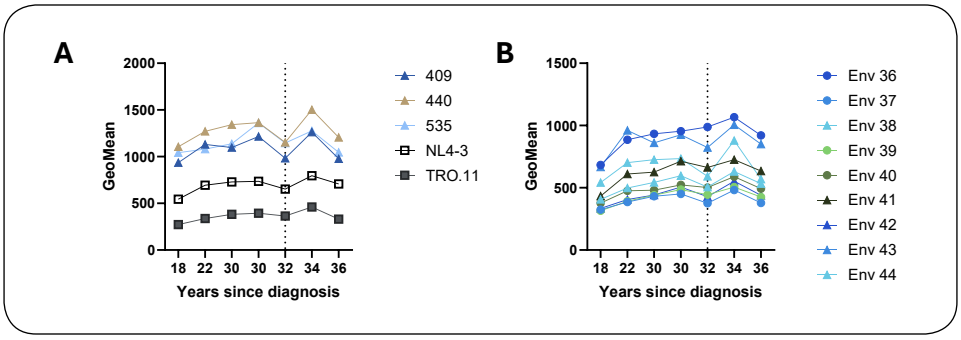

Figure 52. Binding capacity of MVS-088 plasma. Values shown are the geomean of fluorescence. Vertical line marks the start of LoC period. A) Binding against reference (NL4-3, TRO.11) and MRCA (409,440,535) HIV-1 pseudoviruses. B) Binding against autologous pseudoviruses. Envs isolated during the control period are shown as circles, and during LoC as triangles.LoC: loss of control.

In summary, loss of exceptional control 32 years after diagnosis was preceded by dynamic changes in viral sequences which translated in an increased Env diversity and functionality, reduced neutralization of contemporaneous viruses.

Persistent virological control is not necessarily associated with a steady-state scenario but may be highly dynamic and involve both virological and immunological changes that will define the outcome of exceptional control.

5. Exploring the potential of EC Envs as antigens in a VLP vaccine platform

Several strategies have been used in the past to try to develop an immunogenic antigen covering global HIV-1 sequence diversity such as the Mosaic, Consensus M vaccine and using Elite neutralizers Envs (Sliepen et al. 2019; Schorcht et al. 2020b; Barouch et al. 2010).

EC Envs, also present interesting characteristics that might make them good immunogen candidates, such as low CD4 binding, and a high exposure of bNAb epitopes (Casado et al. 2018; Lian et al. 2021). Our main hypothesis was that Env molecules isolated from HIV-1 EC, which can control viral levels even in absence of treatment, would present specific functional and antigenic properties that could be beneficial for the elicitation of broadly neutralizing antibody responses and control of infection. Therefore, immunogens derived from EC Envs could elicit better protective responses.

As seen in previous sections, we engaged in the systematic characterization of individual EC env isolates from the ECRIS EC Cohort and the definition of MRCA sequences. We first characterized the expression and antigenicity of a preliminary selection of Env isolates and MRCA by flow cytometry and fusogenicity. Both parameters were relevant for the selection of an optimal immunogen candidate.

Then, we incorporated a candidate Env into a platform of high antigenic density VLPs by fusing the antigen of interest to the structural HIV protein Gag. This strategy has been shown to be highly immunogenic (Tarrés-Freixas et al. 2023) and able to accommodate large molecules (Trinité et al. 2024).

5.1. VLP Vaccine Design

5.1.1. Design and Generation of Immunogen Candidates

To design the optimal immunogen candidates, in collaboration with the Instituto Carlos III (ISCIII), we analyzed phylogenetic trees containing EC Env sequences and identified three hypothetical ancestral EC Env sequences (MRCA Nodes): 409, 440 and 535 (Figure 36). These sequences recapitulate the functional properties of individual EC clones in terms of infectivity and sensitivity to neutralization (Figure 38, Figure 39). To have a full picture of their antigenic features, these MRCA sequences were characterized in terms of expression and antigenicity by flow-cytometry (Figure 53).

First, MRCA Node sequences were aligned. An analysis of changes in SP, TM and CT of the different candidates was performed. For the SP region, only differences were observed in 409 sequence (Figure 37). No differences were found between the TM domains of 409,440 and 535, while CT sequences showed 2 mismatches between 535 and the 2 other nodes (G737D and C837Y). As the relevant antigenic sequence

is the extracellular domain of Env, and changes in SP or CT may impact expression, we designed hybrid sequences containing identical SP, TM and CT domains. Being the node 535 the one containing 409 and 440 as well as a bigger number of sequences, we decided to use 535CT as a reference. Final sequences were created keeping the SP peptide, TM and CD of node 535. Extracellular domains, characteristic for each node were substituted in each construct and generated with GeneArt as codon optimized constructs (Figure 19).

Maintenance of the SP and TM domains of node 535 was meant to retain the same ER trafficking and Env exposure signals while analyzing the individual immunogenic role of the ED.

5.1.2. Antigenicity analysis

Once produced, antigenicity from MRCA and individual isolates was analyzed via flow cytometry against a panel of anti-Env antibodies. Initial individual EC Env isolate and MRCA characterization showed differential antigenicity detected by several bNAbs (b12,2G12,PGT145,2F5 and 10E8) (Table 9).

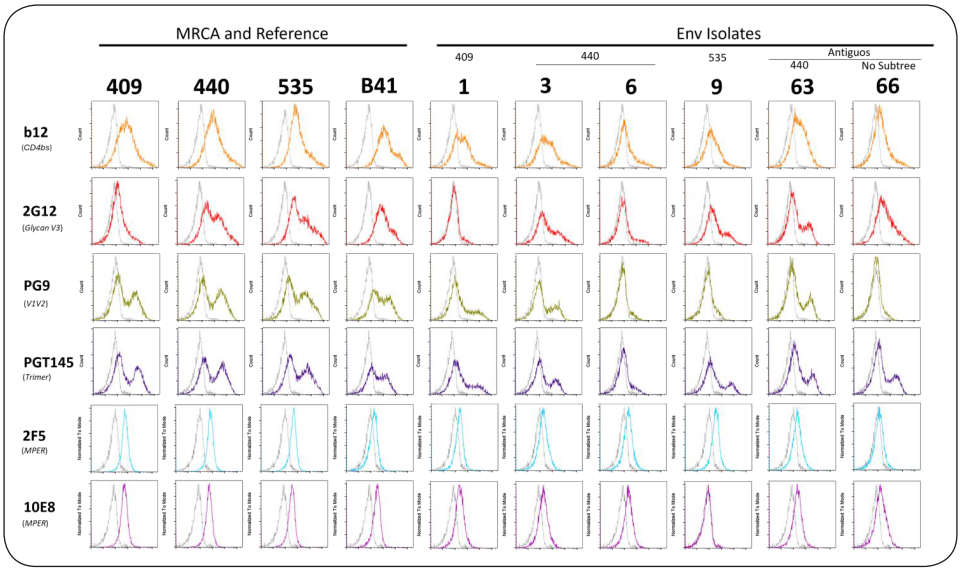

Figure 53. Antigenicity of the different codon optimized MRCA sequences (409,440,535 nodes) and individual Env isolates. Node group belonging of individual envelopes is shown on top. The Env isolate B41 was used as a reference. Control staining (grey) corresponds to untransfected cells. The panel of broadly neutralizing antibodies (bNAbs) included: b12: CD4 binding site epitope; 2G12: V3 loop; PG9, PGT145: V1/V2 trimer, 2F5 and 10E8: MPER.

Consistent with the glycosylation differences identified in node 409 and its resistance to 2G12 neutralization, a decreased 2G12 recognition of this node was identified (also visible in 409 related Env clones such as env1) (Figure 53). The lower glycosylation level and the higher sensitivity to MPER neutralization led us to select the ED of 409 as a first working candidate for the development of VLPs as immunogens.

5.1.3. VLP Construct Generation

The generation strategy of a VLP expressing high density of the 409 Env candidate consisted in the direct fusion of HIV Gag and Env which has been successfully employed in previous works from our group (Tarrés-Freixas et al. 2023; Ortiz et al. 2023; Barajas et al. 2024; Trinité et al. 2024). Construct was generated via gene synthesis in the GeneArt platform by substituting 409 CT domain by the full functional Gag sequence, without the initial methionine residue (Figure 20).

5.2. Production and Antigen Characterization

5.2.1. Antigens

To be able to express 409-Gag protein, 409-Gag plasmid was transfected into Expi293 cells and VLP production was analyzed by TEM microscopy, flow cytometry and WB. The fusion protein is a VLP-generating construct formed by a signal peptide followed by the 409 ED domain and the HIV-1 transmembrane domain fused to Gag (Figure 20). First, we analyzed culture conditions to optimize VLP production. To this end we compared antigen expression in the presence or the absence of production enhancers. Theoretically, standard VLP formation occurs in the plasma membrane; however, the fusion protein production that take place in the ER induces premature intracellular VLP formation and antigen can be detected both on the cell surface and intracellularly.

Protein production and Env expression was first analyzed by flow cytometry. In general, Env showed a better expression in presence of enhancers, as seen by the detection by several bNAbs in intracellular and extracellular stainings (Figure 54). Notably, the intracellular signal of 2G12 was exceptionally high, suggesting potential modification in glycosylation processes.

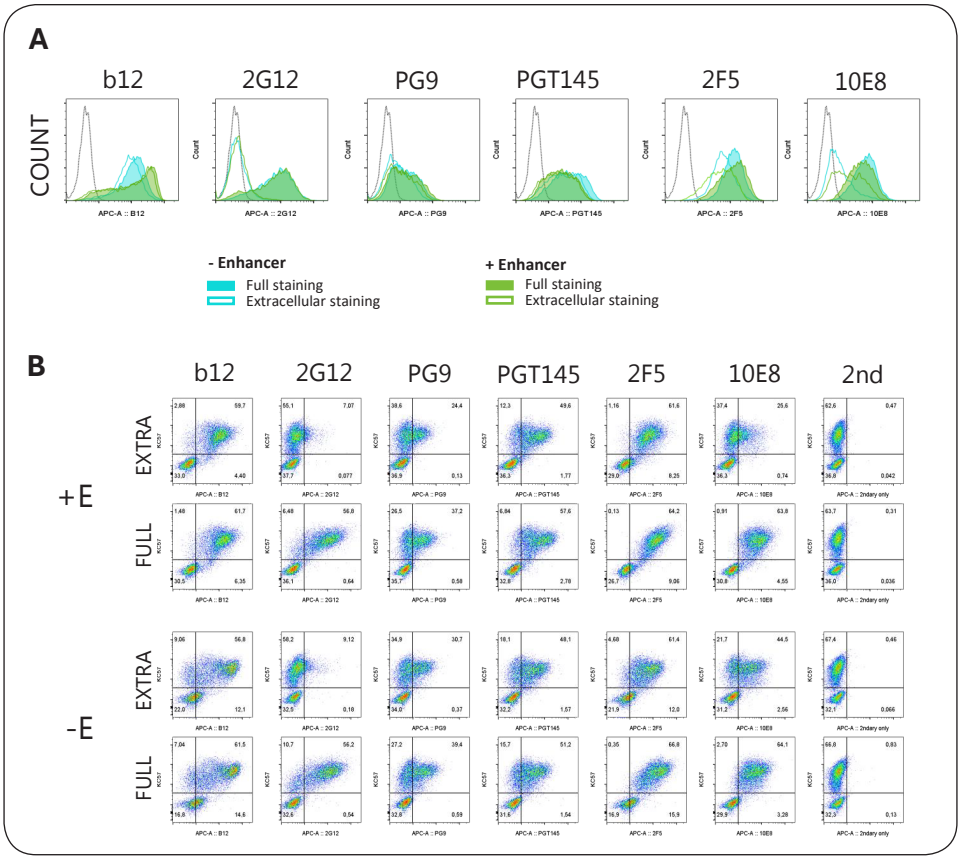

Figure 54. Flow cytometry staining of 409-Gag in presence or absence of transfection enhancers. Expression was analyzed against a bNAb panel (Table 9) and contained extracellular and full staining (extracellular + intracellular).A) Histogram plot. No enhancer condition (blue), Enhancers (green), complete staining (full area), extracellular staining (empty area). B) Density plots of expression at D2 post transfection in presence or absence of enhancers (+E/-E). 2nd: Secondary antibody only.

Protein production was also analyzed by WB both in the SN and the cell pellet (after extraction of the VLP purified fraction (XAD-4) as described in Methods. Protein was detected over a 4-day transfection course, both with and without enhancers (Figure 55). The differential detection in supernatants and cellular associated antigens suggested the expected retention of particles inside the cell. In SN, Gag levels were found to be lower in the Env-Gag fusion protein compared to the cotransfection strategy, but showed a better Env to Gag ratio as observed by p55 and 2F5 stainings with or without enhancers over a 4-day period. (Figure 55, left). In XAD-4 SN we observed a change in protein production kinetics, which was high until day 2 and progressively decreased to its lowest levels in day 4 (Figure 55, right). VLP production in days 3 and 4 showed differences in presence or absence of enhancers.

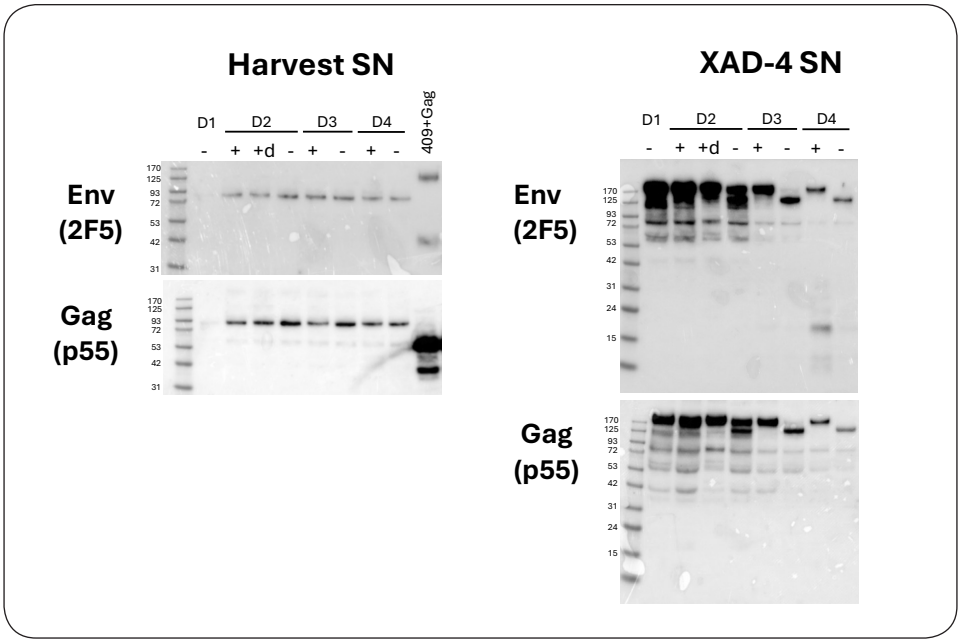

Figure 55. Kinetic VLP production of 409Gag in harvest and extracted SN analysis by WB. Supernatant was collected from transfected Expi293F cells with or without enhancers over a 4-day period. +: with enhancers, -: without enhancers. +d: enhancers and disruption. D: Day, SN: supernatant.

To confirm if VLP production and intracellular retention was taking place, TEM microscopy was performed on transfected cells to localize VLP assembly and budding. TEM imaging confirmed that 409Gag transfection did not lead to extracellular VLP release. Unfortunately, the produced proteins that were retained inside the cell formed some dense structures but no intracellular VLPs could be detected either (Figure 56). Lack of VLP formation could be due to several factors: protein size, which could cause steric hindrance or misfolding, possibly disrupting VLP assembly and budding; mutations or modification in either SP or TM sequences, that are involved in the antigen translocation.

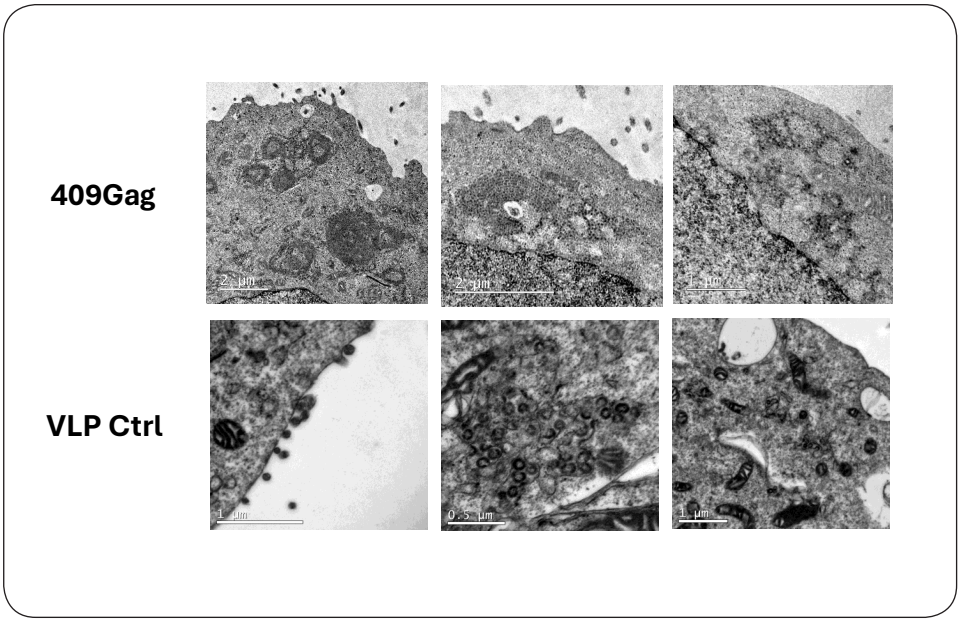

Figure 56. TEM imaging of 409Gag construct and a VLP Ctrl construct. High dense structures budding at the surface and inside the cell can be observed in the VLP producing Ctrl construct.

Several modifications were investigated to restore VLP intracellular budding, focusing on the SP and TM domains (Figure 57). The 535SP of the sequence was substituted by H5 SP from the heavy chain from human IgG which is efficient at directing proteins into the secretory pathway, which could have an impact on expression. Regarding the TM domain, the arginine in position 696 was substituted by an alanine (R696A, R>A). This modification could impact antigen display as mediates conformational changes during the fusion between HIV-1 and the host producing cell (Kim et al. 2009). Both have proved to enhance Env exposure and incorporation (Tarrés-Freixas et al. 2023; Upadhyay et al. 2024). As further characterization of these molecular modifications is necessary to fully elucidate their structural and functional implications, the corresponding results have not been included in the present work. These data are currently under investigation and will be reported in detail in future studies to ensure accuracy and completeness.

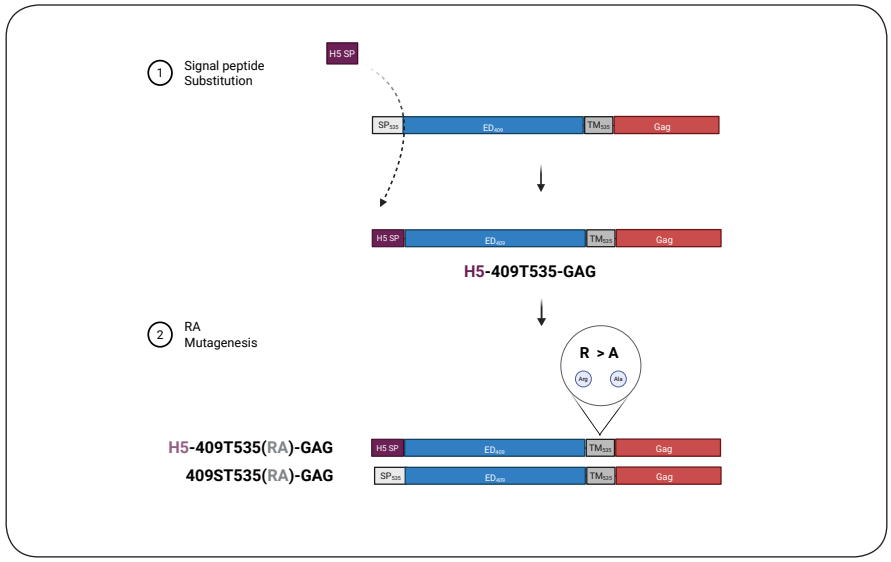

Figure 57. Representation of construct modifications to reduce antigen retention. The first was based on the substitution of the SP from 535 for H5. Additionally, a point mutation was introduced in the TM region of both the original 409-Gag and H5-409Gag.

In consequence, and parallel to the design and optimization of these modifications, we tested a classical VLP-generation approach by expressing Env and Gag as separate proteins (co-transfection). In this strategy, an Env molecule with a truncated CT was generated. The truncation of the cytoplasmic region of the Env has been widely used to increase Env exposure (P. Zhang et al. 2021).

The effect of Env CT truncation was tested by flow cytometry analysis of both full length 409 and its truncated version against a defined bNAb panel (Table 9). 409 trunc showed an improved detection by all bNAbs used, suggesting a better expression on the cell surface as predicted (Figure 58).

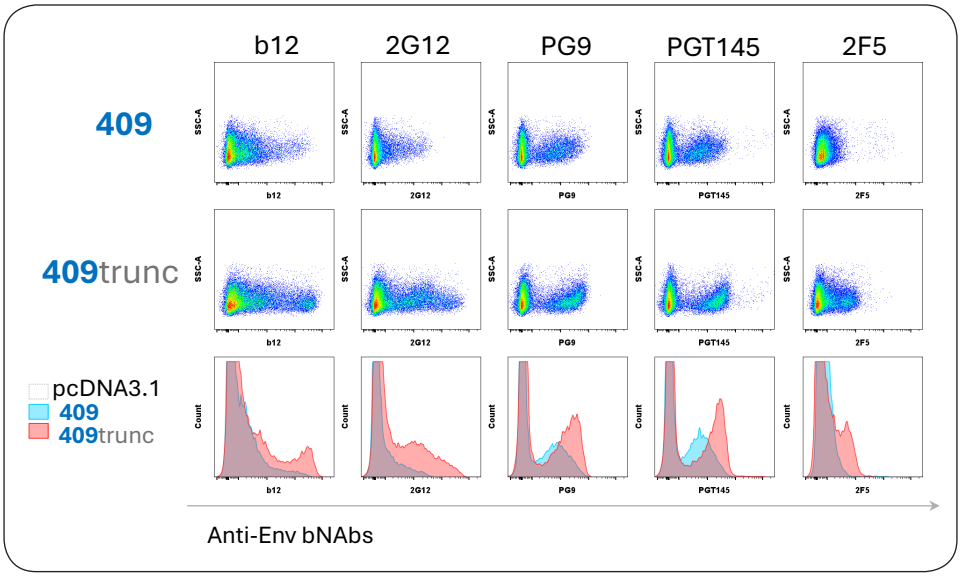

Figure 58. Flow cytometry analysis of candidate constructs by bNAb detection. Individual density plots are shown on top. Both constructs are displayed as histograms on the bottom.

5.2.2. Platform

The next step was to assess whether the improved Env cell surface expression and antigenicity observed would translate into an enhanced Env incorporation in Gag VLPs. To do so, candidate Envs were cotransfected alongside Gag-GFP allowing the evaluation of VLP Env surface expression density via STED microscopy. Gag-GFP was used to identify particle-specific Env expression. Flow cytometry on the transfected cells was first performed to verify that Gag-GFP itself was not compromising Env expression.

a. Flow cytometry

As expected, Env and Gag-GFP expression was colocalized in the same cells and as previously observed with Gag, Env expression on the cells surface was increased when using 409trunc. (Figure 59).

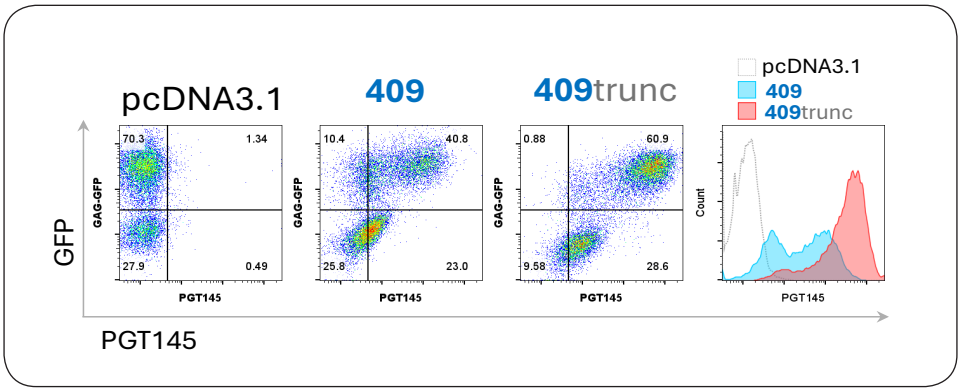

Figure 59. Flow cytometry staining of Env/Gag-GFP co-transfected constructs as density plot and histogram. 409 and its truncated version were stained with PGT145 or secondary antibody only. Cells transfected with pcDNA3.1 vector only were used as a control.

b. STED Microscopy

VLPs produced by cotransfection of Gag-GFP and 409 Env constructs were harvested, adhered on poly-Lysine coated coverslips and stained with the anti-Env bNAb b12 to be able to visualize Env and Gag-GFP expression and colocalization (Figure 60A). As a first approach, VLP particles and Env incorporation were analyzed in three independent images from each construct with ImageJ (U. S. National Institutes of Health) (Figure 60B,C). While Env intensity varied across images as expected, 409trunc showed an increased Env-associated intensity compared to 409 (Figure 60C). Moreover, we observed the presence of Env staining in GFP negative area suggesting the presence of soluble Env proteins or Env associated with extracellular vesicles. This microscopy quantification approach has evaluated the feasibility and potential use of STED microscopy for Env density characterization. While initial results have provided encouraging results, further replicates and optimized imaging parameters are needed to strengthen these conclusions.

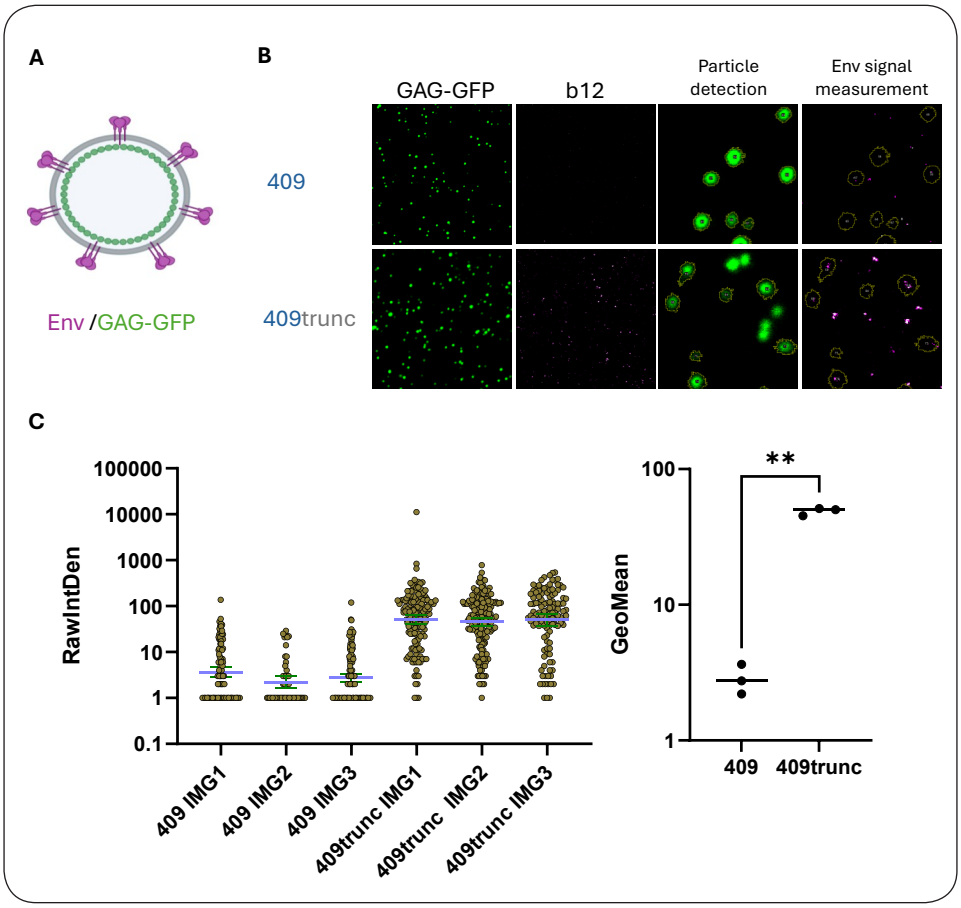

Figure 60. Candidate VLP construct analysis of Env surface expression and distribution via STED microscopy. Purified VLP particles containing Gag-GFP (green) were stained for Env (b12, pink) with a Fab AB STAR RED secondary antibody. Standard confocal mode and Gag-GFP signal were used to define particle localization. Images were acquired using the STED setup. A) Schematic illustration of the HIV-1 VLP particle structure with Env and Gag-GFP. B) STED Microscopy Images of Gag and Env channels along with the particle detection analysis.GAG-GFP localization was used to define the region of interest (ROI, yellow circle) from which associated Env signal was quantified. C) Env signal associated to GAG-GFP particles was measured as raw integrated density (RawIntDen, sum of all pixel values in the ROI) in at least 3 independent pictures per construct. Purple bars show the Mean and error of all particles detected per image. GeoMean of 409 and 409trunc pictures are shown on the right. Statistical differences were identified using a Log-normal Welch t- test. **: $p<0.005$. IMG: Image.

5.3. Immunogenicity in Animal models

While VLP production was being optimized, we used BALB/c mice to perform a preliminary evaluation of in vivo humoral response against the 409 Env candidates using a simple DNA vaccine approach. Gag DNA wasn't co-administered, therefore, we only expected Env to be expressed on the surface of transfected (muscle) cells or to be released in extracellular vesicles. The goal was to compare the immunogenicity of 409 with a control B41 Env and to assess the effect of the CT truncation. To focus the analysis on the extracellular domain, as with 409, B41 was modified to include the SP, TM and CT from MRCA 535. Negative control included the B41STC535 (B41) and an empty pcDNA3.1 vector as controls (Figure 23). BALB/c mice were immunized with two doses, with a 3-week interval, of DNA via electroporation and without adjuvants. DNA vaccination was well tolerated, with no adverse effects against the candidates nor associated with anesthesia and electroporation procedures. No weight loss was observed during the duration of the experiment (Figure 61). Blood samples were collected prior to each immunization and at endpoint, 3 weeks after the second dose, for the characterization of the humoral response. Although splenocytes were also collected at endpoint for the characterization of cellular responses, their analysis was not yet performed due to time constraints.

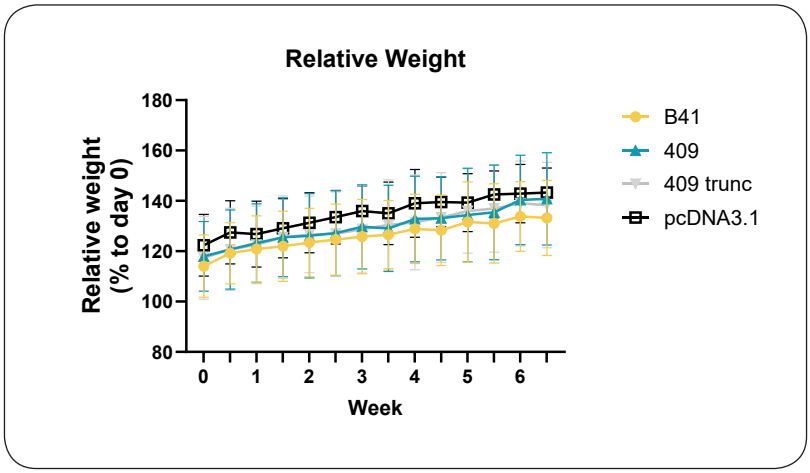

Figure 61. Relative weight follow-up during the experimental period. Values shown are the Mean+SD of 8 animals per construct, distributed in sex-balanced groups.

5.3.1. Characterization of the elicited immune response

Humoral response elicited via two DNA immunizations of the vaccine candidates was characterized in all mice via a neutralization and a binding assay as a surrogate for ADCC.

a. Evaluation of the neutralization capacity

HIV-Env specific neutralizing antibodies were analyzed in mouse sera via a pseudovirus-based neutralization assay as described previously. Analysis of sera neutralizing capacity showed no neutralization by the candidate constructs (Figure 62). Data within each group was disaggregated by sex to establish comparisons, but no differences were found between males and females for a same construct (not shown).

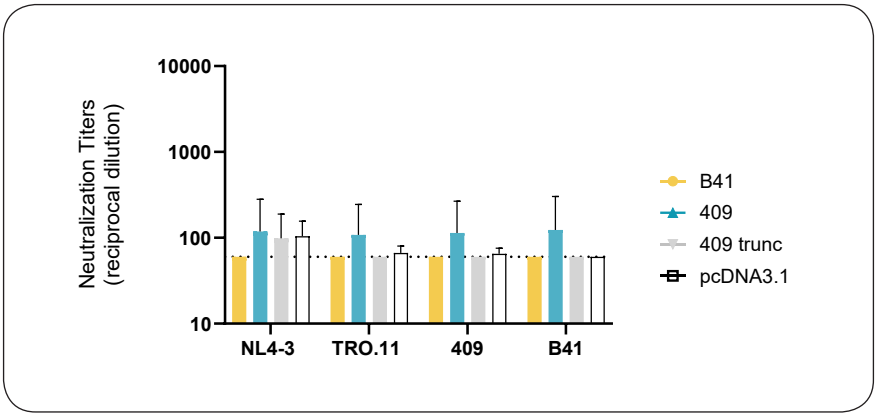

Figure 62. Neutralization capacity of the candidate constructs in a BALB/c mice model. Two DNA immunizations were delivered by electroporation. Horizontal dotted line marks the limit of detection (<60). Values are shown in LogScale.

b. Binding assay

The goal of most vaccine strategies is the elicitation of neutralizing antibodies, yet, in the case of HIV-1 it is hard to achieve. Nevertheless, antibodies can play other roles besides neutralization through their Fc domain which can be recognized notably by NK and mediate ADCC. As technical and logistical constraints limited the immediate use of ADCC assays, we used a binding assay as a faster proxy to predict antibody-mediated functionality. Even though binding capacity is not proof of the direct capacity of an antibody to promote ADCC functions, this assay focused on evaluating the antibody-antigen affinity and specificity that will later influence their development.

For this, Expi293F cells were transfected with a plasmid co-expressing Env 409 and GFP. Cells were then stained with the different endpoint mouse sera and a secondary

AF647 labeled anti-mouse IgG antibody. Staining was very heterogenous within each vaccination groups with only a few animals having developed good antibody response in each case. Due to the high variability and overall low response, no statistically significant differences were measured between vaccination groups (p=0.1351, Kruskal-Wallis). Specifically, the comparison between 409 and pcDNA3.1 presented a corrected p-value of 0.1633. However, a Mann-Whitney comparation of this two constructs revealed statistical significance (p=0.0485). Coming from a preliminary experiment, we acknowledge that this significance requires further validation through additional studies. These findings suggest that the immunization protocol might have been not optimal and protentially requires of additional doses and/or better immunogen delivery strategies to elicit a more robust immune response.

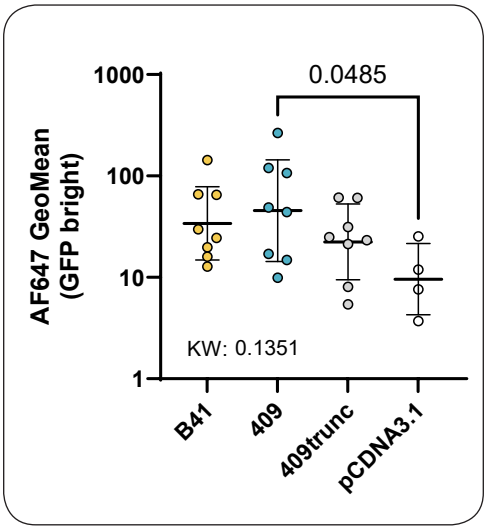

Figure 63. Binding capacity measured as GeoMean of fluorescence within the GFP bright cells (corresponding to cells with the highest surface expression of 409 Env) by flow cytometry. Horizontal lines show Geomean with geometric SD. No significant statistical differences were found between groups (p=0.1351, Kruskal-Wallis). However, specific pairwise comparison between 409 and pcDNA3.1 found significant differences (p=0.0485, Mann-Whitney) that would need futher validation.

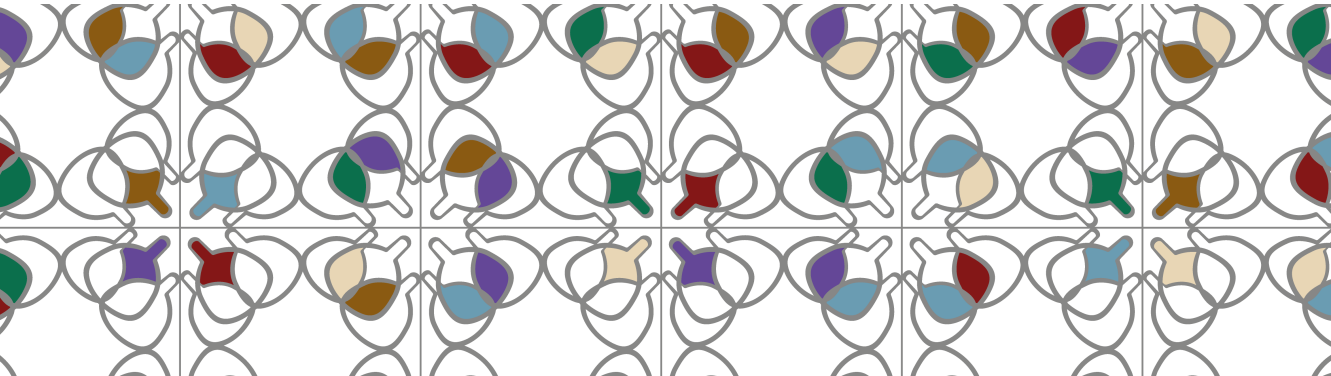

DISCUSSION

Plenty of knowledge and advances have been made over the last 40 years, benefiting not only the HIV-1 field but so many others, yet no practical cure is in sight and vaccine strategies fail to induce effective protective responses. Elite Controllers are a rare phenotype of PLWH that can maintain virological control in absence of ART for long periods of time. Consequently, the chase for an HIV-1 cure has investigated EC potential control mechanisms to translate them into therapeutic strategies, including vaccines.

The ideal HIV-1 vaccine should induce a stable, broad and potent neutralization through the induction of bNAbs along with a strong cellular response. To do so, research focuses on the optimization of antigens, by targeting germline precursors using engineered immunogens, and the use of the proper delivery mechanism to enhance its effect. In this sense, the study of EC might help design new immunogens. So far, mechanisms of viral control are still not well understood, and differ between non-progressor phenotypes (Thèze et al. 2010; Salgado et al. 2018; Climent et al. 2022; Bayón-Gil et al. 2025). In most cases, it is the interplay between genetic, immunological and viral factors that will determine progression rates in PLWH.

In the EC phenotype, although the presence of HLA protective alleles, polymorphisms in CCR5 and strong CTL responses have been shown to be prevalent, less is known for virological mechanisms. Cohort studies have found that a proportion of EC present defective Env (Lassen et al. 2009; Casado et al. 2013; 2018). Similarly defects in nef function have also been associated with the EC phenotype (Zaunders, Dyer, and Churchill 2011). These defects can potentially translate into a lower functionality, which impacts the initial events of the virus life cycle. Env essential role in this process restricts the virus from infecting and replicating, hampering its transmission. Specifically, decreased functionality might allow an easier tackling by the immune system, therefore generating lower immune damage and potentially better immune responses, including neutralizing ones.

An example of the implications of viral factors in the development of a controller phenotype, is the case of a group of five individuals who acquired HIV via injecting drug use (IDU) in the 1980s yet remained asymptomatic and controlled the virus

without antiretroviral therapy (Casado et al. 2013). The discovery of this cluster infected by low replicating viruses confirmed the heritability of this phenotype, as host control could not be explained due to their differences in genetic and immunological background (Casado et al. 2018). While this specific IDU case enabled the transmission of an otherwise not really viable virus, the decreased functionality of EC Envs has been confirmed in broader cohort studies (Pérez-Yanes et al. 2022; Lassen et al. 2009; Cabrera-Rodríguez et al. 2022). In these, several HIV phenotypes have been compared, including non-progressor subjects who are not associated with a cluster of infection (Cabrera-Rodríguez et al. 2022; Pérez-Yanes et al. 2022). It was observed that Envs from ECs are less functional compared to viremic individuals and standard progressors, both from contemporary and modern periods (old and modern progressors). The comparison with contemporary LTNPs proved that EC Env properties were not due to their ancestral origin. More specifically they presented a low binding to CD4 and a higher exposure of broadly neutralizing epitopes (Lian et al. 2021).

As a result, we hypothesized that the use of Env sequences isolated from HIV ECs as immunogens, could be beneficial for the elicitation of bNAb responses. Their lower affinity for CD4 and lower fusogenicity could help address the vaccine challenge of eliciting protective responses. To further improve antigen delivery and presentation, the candidate antigen was incorporated into VLP platforms to display higher Env density at the surface.

In this work, we took two separate yet related efforts: the characterization of an extended EC cohort in terms of Env and humoral response, and the selection and incorporation of a potential immunogen candidate in a VLP vaccine platform to deliver it while enhancing its immunogenicity.

First, to expand our comprehension of Env contribution to the development of the EC phenotype, this work characterized 70 new samples from the largest EC Spanish cohort (ECRIS). Due to the laborious work this phenotypic analysis entails, and the limited availability of EC samples, previous studies faced limitation on sample size (Pérez-Yanes et al. 2022; Casado et al. 2018; 2013). EC Envs isolated during viremic periods, even if they maintain control, are expected to have an increased functionality, as observed for viremic non-progressors. Consequently, to account for the phenotypical differences during non-viremic periods, nine Envs were excluded to truly establish functional differences during control. As a result, 59 of the 70 samples were compared in terms of expression and fusogenicity. All excluded Envs belonged to the same individual, MVS-088, and were analyzed separately in the study of this specific case.

In summary, EC Envs presented a lower fusogenicity compared to contemporary progressors but were not significantly different from VC. In terms of expression, no differences were observed between groups, supporting previous observations (Pérez-Yanes et al. 2022). While it could be argued that a lower Env expression would lead to lower fusogenic values, we observed several Env showing low expression but high fusogenicity, and, on the opposite, Envs showing high expression but weak fusogenicity. Globally, however, lower expression correlated with a lower fusogenicity (Casado et al. 2018). Fully functional Envs were identified in some EC individuals, supporting

previous findings in other non-progressors (Cabrera-Rodríguez et al. 2019; Curriu et al. 2012). Apart from fully functional Envs, fully replicative competent viruses have been isolated from some EC (Blankson et al. 2007) . This suggests that additional factors, such as a differential integration site in the host genome (Lian et al. 2021), or a strong antiviral response (Pernas et al. 2012) might be involved in the natural control of infection, beyond poor Env function.

To further validate these conclusions with a larger cohort, Env data presented was pooled with the Env characterization of our previous works. This new analysis contributes, along with the previous ones (Pérez-Yanes et al. 2022; Casado et al. 2018; 2013), to the characterization of more than a 100 Envs accounting for EC, VC and Old progressors. For consistency with our presented analysis, samples during EC viremic periods were excluded from this comparison, with a final group of 98 Envs. In contrast with previous works, both the higher sample number and clinical characterizations from the participants allowed us to analyze EC data disaggregated into the persistent (PC) and transient (TC) EC phenotypes. A proportion of EC has been described to eventually lose viral control. In contrast to the PCs, which maintain control, TCs lose it eventually (Pernas et al. 2018; Gasca-Capote and Ruiz-Mateos 2024; Leon et al. 2016b). While specific mechanisms are still not understood, studies observed differences at a metabolomic and proteomic level as well as in immunity and reservoir. Historically, most studies have analyzed EC in a cross-sectional manner, therefore grouping PC and TC over time, which could have overlooked differences between phenotypes.

Once we confirmed the feasibility of a pooled analysis, we observed that EC Envs still presented a significative lower fusogenicity compared to contemporary progressors, which correlated with a lower genetic distance to the ancestor. However, no fusogenic differences were observed in terms of sex, protective alleles, or maintenance of control (PC/TC) in the EC phenotype, suggesting other factors beyond sex and HLAs can impact the control of highly fusogenic Envs. Previous works tried to elucidate which changes in Env drive this reduced functionality both with the study of N-linked glycosylation sites in these Envs and an analysis on their variable sequence lengths (Pérez-Yanes et al. 2022; Sterjovski et al. 2007). Unfortunately, while it was outside of the scope of this work, its further study might strengthen our understanding of the role of Env glycosylation, its effect in viral progression and control mechanisms (Pérez-Yanes et al. 2022; Sterjovski et al. 2007). In summary, we corroborated in the largest Spanish EC cohort, that EC Envs present a lower functionality which associated with a reduced genetic distance to the subtype B ancestor compared to VC and progressor Envs. While their use as potential immunogens in the vaccine field has been explored later in this work, further research on their antigenic and immunogenic potential might be needed to fully unravel their potential.

As discussed, Env might be one of the causes of the establishment of a controller phenotype. There are however other mechanisms that are involved in the maintenance of this control such as the CTL response, the development of a humoral response with neutralizing antibodies or innate immune control (Climent et al. 2022). Despite their ability to control, ECs tend to show low neutralization responses, probably due

to low antigen levels. Nevertheless, the ADCC activity and polyfunctionality of their antibodies might account for their enhanced control (Ackerman et al. 2016). In this work we wanted to evaluate the neutralization capacity of a cohort of EC, containing both PC and TC. Neutralizing capacities proved to be heterogenous, and although the longitudinal analysis is only representative of some periods, it could be a good tool to observe underlying changes at immunological and virological level, that could help predict LoC and provide therapeutic strategies if needed.

Actual guidelines recommend the treatment of EC, as ART benefits in other aspects such as lowering underlying inflammation, cardiovascular risk and cognitive decline. This can differ between cases and is always decided by the medical team in the context of each individual. For this reason, the study of available ART-naive EC cases, and specially of the LoC, are of great value to decipher the mechanisms and better understand the viral control continuum as well as markers to predict the loss of control (Rosás-Umbert et al. 2019). In-depth studies will help characterize these unique potential HIV-1 remission cases (Gasca-Capote and Ruiz-Mateos 2024; Casado et al. 2020b; Salgado et al. 2024).

In this study, we also characterized the case of a loss of exceptional control 32 years after diagnosis in collaboration with research groups at ISCIII and Instituto de Biomedicina de Sevilla (IBiS) (Frances et al. 2025). The availability of longitudinal samples for a period of more than 20 years, brought invaluable data to understand the establishment of viral control and the mechanisms that might have led to its loss. This EEC presented undetectable VL for 31 years since diagnosis, except for four transient episodes ≤150 copies/mL, which correlated with dynamic changes in viral reservoir both in proviral and intact proviral DNA percentages. The LoC in this case was not abrupt but extended through a 5-year period from 2016, when the first repeatedly detectable VL was observed, until 2021 when the decrease in CD4+T cells below 500 cells/μL marked the LoC and the start of ART.

Several factors could have initially contributed to this EEC case. In terms of host factors, this case presented no protective HLA-B factors (HLA: B39:01/B44:02) but had CCR5/Δ32 heterozygosis and an HLA-C (rs9264942) polymorphism, which have been associated with slower progression (Rodríguez-Da Silva et al. 2017; Stewart et al. 1997). To further understand the possible viral and immunological factors, we analyzed the evolution and dynamics of viral sequences; infectivity and fusogenicity of isolated Env clones as well as the autologous neutralizing capacity over time. Strikingly, the Env sequence diversity of isolated clones started increasing 10 years prior LoC and was associated with an increased functionality in terms of infectivity and fusogenicity. This viral evolution, which is a sign of viral replication despite undetectable VL, might have allowed for the rise of escape mutations as well as changes in tropism.

In terms of humoral response, autologous neutralization against a dominant ancestral Env clone was observed across all analyzed samples, both prior to and after LoC, which paralleled alongside a consistent HIV-1-specific Gag T-cell immune response (Frances et al. 2025). Neutralization breadth, however, was restricted to ancestral Envs, as more evolved clones progressively escaped antibody-mediated

inhibition. These findings suggest that viral evolution might have allowed for the escape from autologous antibody, thus contributing to the LoC.

In addition, Gag-specific T-cell memory responses were observed to fluctuate during the control period, and decay prior loss of control (data not shown, Frances et al. 2025), as observed in other cases (Collins et al. 2021; Chereau, Madec, Sabin, Obel, Ruiz-Mateos, Chrysos, et al. 2017). Interestingly, an abrupt descent three years after loss was also observed as has been similarly described (Pernas et al. 2018; Gasca-Capote and Ruiz-Mateos 2024), which could be related to T-cell exhaustion.

In summary, although elite controllers (EC) typically exhibit low neutralizing antibody levels due to limited antigenic stimulation, extensive longitudinal sampling during the control period revealed dynamic fluctuations in the reservoir's size and composition, as well as quasispecies evolution inferred from Env divergence and sequence diversity. These shifts were accompanied by variations in both humoral and cellular immune responses

There are so far several hypotheses regarding the reactivation of viral replication. While there has been a perfect balance between host, genetic and immunological factors that allowed for control for 32 years, there has been one or multiple factors that have tilted the weight. Deciphering which one or several in this case might be difficult and might need more research. It is however important to investigate the factors associated with risk of viral control loss which are multifactorial and can involve coinfections, change of tropism and superinfections (Rosás-Umbert et al. 2019; Pernas et al. 2018). These factors might be different from individual to individual, as the later have been widely described in LTNPs (Casado et al. 2007) and considered to not be directly associated with loss of control by some studies (Pernas et al. 2013). The possible impact of these factors was analyzed in this case.

Superinfection in HIV occurs when a PLWH acquires a second strain of the virus. This one can be often from a different subtype and can lead or not to faster disease progression (Rosás-Umbert et al. 2019; Casado et al. 2007). Because a second infection takes place in an already weakened immune system, the focus on fighting this new strain might lead to loss of control of the first strain in some EC cases (Caetano et al. 2019). In this case, HIV superinfection was discarded by phylogenetic analysis as all isolated sequences clustered together and the virus that evolved had its origin in a sequence already present during control. As a result, viral evolution in this case seemed to be the reason for enhanced functionality and escape.

Coinfection with Hepatitis C virus (HCV) is common in HIV+ individuals due to shared transmission routes. Interestingly, while HCV/HIV coinfection is the main factor associated with non-AIDS defining events in HIV controllers (Dominguez-Molina et al. 2016), later HIV-controller cohort studies have attributed the capacity to clear other chronic viral infections to persistent controllers (Dominguez-Molina et al. 2020). This case showed coinfection with HCV and was treated (Casado et al. 2007; Pernas et al. 2018; Rosás-Umbert et al. 2019) before LoC. The potential causal relationship of both events remains undefined.

While a change of tropism to X4 virus has been predicted from isolated sequences

appearing after LoC, it will need to be tested functionally. This possible change in tropism would overcome the 'protective' effect of the CCR5Δ32 mutation in this participant, making it for the virus more possible to escape and rebound. It was however interesting to see that even X4 sequences were present from 2018, it was not until 2021 that it finally lost virological control, suggesting that other mechanisms were maintaining it. Finally, the involvement of aging and menopause should be also evaluated. These two unique processes with overlapping aspects and sex-specific features that can alter reservoir dynamics (Scully et al. 2019) and immune responses, affecting latency and possible reactivations (Das et al. 2018) need further research.

PLWH experience accelerated aging related to immune system dysregulation, chronic inflammation and immune senescence leading to a reduced T-cell function. This factors contribute to differences between chronological age and biological age, accelerated in PLWH, that can be additionally affected by different factors, such as sex-specific features in biological age (Reicher et al. 2024). While aging has been more studied and could affect the ability to control the virus , less is known on the implications of menopause for the immune system and HIV reservoir.

Menopausal transition is linked to shifts in immune and inflammatory profiles, and changes in HIV reservoir dynamics (Das et al. 2018; Leskov et al. 2025). Perimenopause might be a period of increased inflammation and immune activation, as hormones such estrogen can impact T-cell function. CD4+ T cells show upregulated inflammation during perimenopause (Leskov et al. 2025; Scully et al. 2019). However, if this change in CD4+ T cells is a cause or a consequence of changes in the reservoir is still not clear. Different studies have observed both an increase in inducible HIV RNA through reproductive aging (Gianella et al. 2022), and a sex-differential reservoir decay and accumulation of proviruses (Gandhi et al. 2023).

While studies in aging and menopause have focused on PLWH on long term ART, it is expected these changes would equally affect controllers, on which viral control relies on several cellular and humoral factors. However , additional analyses on not only estrogen levels and proinflammatory cytokines would be needed to specifically decipher the role of aging and menopause on the LoC and changes in viral reservoir in long-term controlling individuals. With an aging HIV population and all its implications, it would be of great interest to evaluate the impact it can have on controller individuals with an already aged immune system compared to the HIV- population, with a specific interest on women.

As a result, we can conclude that persistent virological control is not necessarily associated with a steady-state scenario but may be highly dynamic and involve both virological and immunological changes that will define the outcome of exceptional control.

In the last part of this work, we proceeded with the selection and incorporation of a candidate immunogen into a VLP vaccine platform to enhance its immunogenicity. For vaccine development, the antigen choice is equally important as the delivery pathway and the choice of adjuvants. They will all contribute and define the observed response. As described, the use of EC sequences, with lower CD4 binding affinity,

lower glycosylation sites among other characteristics, could be useful as priming immunogens in germline targeting strategies. Their use as immunogens would allow the targeting of rare B-cell precursors, which should be further shepherded and polished by sequential immunization of more complex envelopes to reach the desired bNAb profile. To do so, we performed the phylogenetical analysis of sequences from the ECRIS cohort, which allowed the identification of three MRCA that recapitulated individual EC characteristics. Interestingly, the reduced glycosylation profile of one of them, MRCA 409, along with its particular sensitivity to anti-MPER antibodies, highlighted it as an interesting candidate. Interestingly, this MRCA contained the cluster of EC individuals infected with the initially identified low-replicating viruses (Casado et al. 2013).

The incorporation of the candidate to a VLP platform was first intended via a fusion protein strategy. The 409 Env implementation as a fusion protein along with HIV-1 Gag was promising but failed to support VLP production. It was hypothesized to be due to the size and complexity of the Env immunogen. Indeed, this fusion protein approach, although complex, has been used successfully in our group and applied to several immunogens such as HIV-1 MPER, FeLV gp85, cancer targeted neoantigens and RSV-F (Tarrés-Freixas et al. 2023; Ortiz et al. 2023; Barajas et al. 2024; Trinité et al. 2024). That said, the full HIV Env extracellular domain represented a big step up in term of molecular weight and it is possible that Env trimerization interfered with the proper Gag oligomerization and budding. We designed several modifications, including modifications of the signal peptide and the transmembrane domain, that are still under analysis. Therefore, we decided to employ a more traditional approach consisting in the co-transfection of Env and Gag expressing plasmids allowing for a more natural HIV-like VLP formation.

As with HIV virions, Env incorporation into classic Gag VLP is characterized by a low surface incorporation. To solve this problem, we modified the 409 Env protein to include a truncated cytoplasmic tail. This approach has been previously described to increase cell surface Env expression and subsequently to enhance Env incorporation in budding viral particles and VLPs. We validated the strategy by flow cytometry, showing increased cell surface expression of truncated 409 Env, and by STED microscopy, showing higher truncated 409 Env fluorescence on individual Gag particles. In the microscopy analysis, we also noticed an increase of non-Gag associated Env in the supernatants, probably corresponding to Env protein incorporated into extracellular vesicles. This could provide alternative approach for the generation of particulate Env antigen in absence of Gag. Recently, it has been described a new strategy consisting in the insertion of ESCRT and ALIX binding regions in the cytoplasmic domain of transmembrane immunogens which leads to the recruitment of the ESCRT proteins and the "self-budding" of the immunogen into extracellular vesicles (Hoffmann et al. 2023).

As our VLP strategy was not ready in time, we decided to perform an exploratory *in vivo* experiment to test 409 Env immunogenicity. To save time, we opted for a DNA based vaccine approach which we had previously optimized and used successfully

for previous vaccine studies. This approach is particularly useful in mice as it focuses the response on the specific immunogen and avoids non-specific immunization with human protein present in vaccines produced with human based expression system (Tarrés-Freixas et al. 2023). However, in our experience, this approach works best in heterologous regimen alternating DNA vaccine and purified adjuvanted protein or VLPs and with multiple immunization schedule. However, we could only perform 2 DNA based immunizations. Total IgG antibody response was very heterogeneous and only a few animals showed an acceptable level of responsivity. Neutralization assay confirmed these underwhelming results, and no difference was detected in any experimental group. These results attest more of the mode of immunization performed (DNA vaccine) rather than immunogen itself. Additional experiments using purified VLPs or mRNA lipid nanoparticles will be necessary to properly test our immunogen strategy.

While the current candidates derived from consensus sequences from the first established phylogenetic tree, future immunogen development and studies may benefit from the use of the extended tree characterized in this work. The expansion with additional sequences might capture a more representative genetic landscape and provide better immunogens. Regarding the VLP platform, HIV-1*gag* may not form VLPs optimally in murine cells (Mariani et al. 2000). As a result, some studies questioned the relevance and accuracy of immunogenicity assessment in mice while proposing feasible solutions like modifications of the construct (Wong and Siliciano 2005), the experimental assays (Tarrés-Freixas, 2021), or the viral Gag used. In fact, while the replacement of HIV-1*gag* for VLP production with FeLV*gag* is feasible and under study (Ortiz et al. 2023), delivery of the construct via mRNA or DNA might be more useful. *In vivo* production of the antigen might avoid common problematics with VLP platforms involving but not restricted to, response against host proteins, purity, and potential analytical seroconversion in the case of HIV-1*gag*.

Overall, the study of control mechanisms in extreme phenotypes, as well as the role of Env, proves of high potential and interest to inform the development of new therapeutic strategies that could contribute to HIV cure and vaccine development.

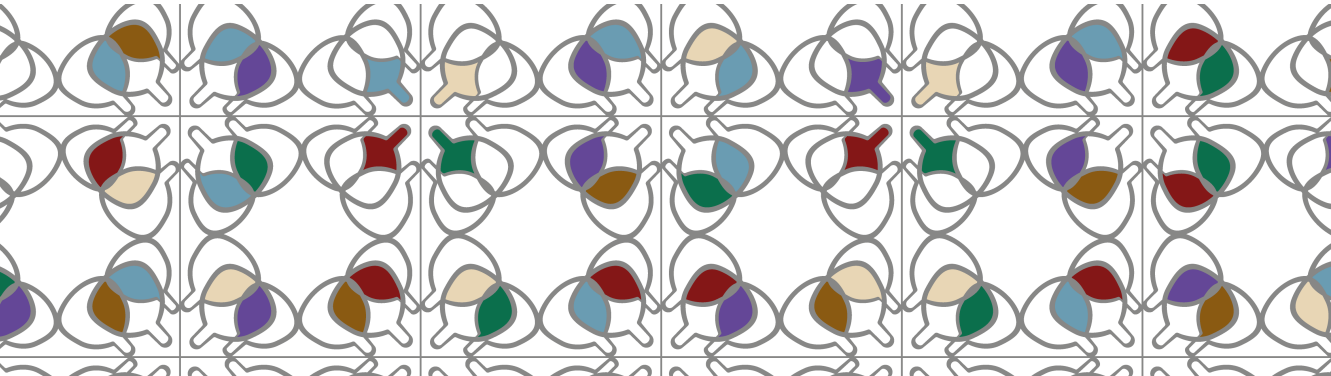

CONCLUSIONS

1. Related to the functional characterization of the Env glycoprotein (Objective 1.1)

1.1. Env sequences isolated from ECs showed lower fusogenicity compared to progressors; however, some ECs showed fully functional Envs, suggesting additional factors beyond poor Env function, are involved in the natural control of infection.

1.2. Increased functionality in EC Envs was correlated with sequence evolution as seen by genetic distance.

2. Related to the characterization of neutralizing responses and their contribution to natural control (Objective 1.2)

2.1. A subset of ECs showed neutralization activity against NL4-3 and MRCA sequences, a surrogate measure of autologous neutralization.

2.2. In some participants, this neutralization capacity increased overtime, indicating a dynamic behavior of the humoral responses.

2.2. In the case of EEC MVS-088, neutralizing activity against NL4-3 and autologous viruses was detected. Changes in Env function and neutralization sensitivity were associated with the loss of virological control.

3. Related to the antigenicity and immunogenicity analysis of EC Envs (Objective 2.1)

3.1. The selection of representative Envs from the EC cohort through the identification of MRCA sequences seems to be a good strategy, as functional and antigenicity data recapitulated individual clone characteristics.

3.2. The production of high density Env–expressing VLPs by fusing Env to Gag of HIV-1 was challenging. Modifications in both the immunogen and the fusion strategy will be required.

3.3. Preliminary analysis of MRCA Env immunogenicity in BALB/c mice showed comparable results to standard Env immunogens.

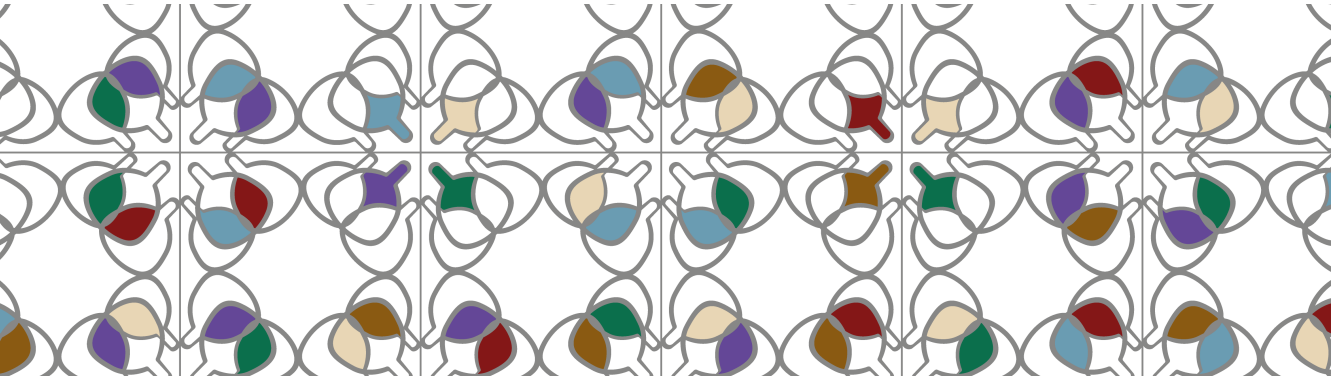

DISSEMINATION

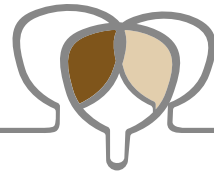

Publications related to this thesis project

- **Pons-Grífols, A.**, Guinot, F.J., Marfil, S., Rovirosa, C., Valenzuela, A., Muñoz, M.Á., Ruiz-Mateos, E., Trinité, B., Pernas, M., Casado, C., Blanco, J. Functional characterization of HIV-1 Envelope glycoproteins isolated from the Elite Controller ECRIS cohort. [In preparation, Title subject to change].

- **Pons-Grífols, A.**, Pradenas, E., Aparicio, E., Frances, S., Guinot, F.J., Vera, M., del Romero, J., Ruiz-Mateos, E., Trinité, B., Pernas, M., Casado, C., Blanco, J. Longitudinal characterization of the humoral response of an HIV-1 Exceptional Elite Controller losing control 32 years after diagnosis. [In preparation. Title subject to change].

- **Tarrés-Freixas, F.**, Aguilar-Gurrieri, C., Rodríguez de la Concepción, M. L., Urrea, V., Trinité, B., Ortiz, R., Pradenas, E., Blanco, P., Marfil, S., Molinos-Albert, L. M., Barajas, A., Pons-Grífols, A., Ávila-Nieto, C., Varela, I., Cervera, L., Gutiérrez-Granados, S., Segura, M. M., Gòdia, F., Clotet, B., Carrillo, J., Blanco, J. (2023). An engineered HIV-1 Gag-based VLP displaying high antigen density induces strong antibody-dependent functional immune responses. Npj Vaccines, 8(1), 51. https://doi.org/10.1038/s41541-023-00648-4

Publications related to other projects

- **Pons-Grífols, A.**, Tarrés-Freixas, F., Pérez, M., Riveira-Muñoz, E., Raïch-Regué, D., Perez-Zsolt, D., Muñoz-Basagoiti, J., Tondelli, B., Pradenas, E., Izquierdo-Useros, N., Capdevila, S., Vergara-Alert, J., Urrea, V., Carrillo, J., Ballana, E., Forrow, S., Clotet, B., Segalés, J., Trinité, B., & Blanco, J. (2025). A human-ACE2 knock-in mouse model for SARS-CoV-2 infection recapitulates respiratory disorders but avoids neurological disease associated with the transgenic K18-hACE2 model. MBio, 16(5), e00720-25. https://doi.org/10.1128/MBIO.00720-25

- Barajas, A., Amengual-Rigo, P., **Pons-Grífols, A.**, Ortiz, R., Gracia Carmona, O., Urrea, V., de la Iglesia, N., Blanco-Heredia, J., Anjos-Souza, C., Varela, I., Trinité, B., Tarrés-Freixas, F., Rovirosa, C., Lepore, R., Vázquez, M., de Mattos-Arruda, L., Valencia, A., Clotet, B., Aguilar-Gurrieri, C., Guallar, V., Carrillo, J., Blanco, J. (2024). Virus-like particle-mediated delivery of structure-selected neoantigens demonstrates immunogenicity and antitumoral activity in mice. Journal of Translational Medicine, 22(1), 1–14. https://doi.org/10.1186/s12967-023-04843-8

- Trinité, B., Durr, E., **Pons-Grífols, A.**, O'Donnell, G., Aguilar-Gurrieri, C., Rodriguez, S., Urrea, V., Tarrés, F., Mane, J., Ortiz, R., Rovirosa, C., Carrillo, J., Clotet, B., Zhang, L., & Blanco, J. (2024). VLPs generated by the fusion of RSV-F or hMPV-F glycoprotein to HIV-Gag show improved immunogenicity and neutralizing response in mice. Vaccine, 42(15), 3474–3485. https://doi.org/10.1016/J.VACCINE.2024.04.048

- de Campos-Mata, L., Trinité, B., Modrego, A., Tejedor Vaquero, S., Pradenas, E., **Pons-Grífols, A.**, Rodrigo Melero, N., Carlero, D., Marfil, S., Santiago, C., Raïch-Regué, D., Bueno-Carrasco, M. T., Tarrés-Freixas, F., Abancó, F., Urrea, V., Izquierdo-Useros, N., Riveira-Muñoz, E., Ballana, E., Pérez, M., Vergara/Alert, J., Segalés, J., Carolis, C., Arranz, R., Blanco, J., Magri, G. (2024). A monoclonal antibody targeting a large surface of the receptor binding motif shows pan-neutralizing SARS-CoV-2 activity. Nature Communications 2024 15:1, 15(1), 1–13. https://doi.org/10.1038/s41467-024-45171-9

- Ortiz, R., Barajas, A., **Pons-Grífols, A.**, Trinité, B., Tarrés-Freixas, F., Rovirosa, C., Urrea, V., Barreiro, A., Gonzalez-Tendero, A., Rovira-Rigau, M., Cardona, M., Ferrer, L., Clotet, B., Carrillo, J., Aguilar-Gurrieri, C., Blanco, J. (2024). Production and Immunogenicity of FeLV Gag-Based VLPs Exposing a Stabilized FeLV Envelope Glycoprotein. Viruses, 16(6). https://doi.org/10.3390/V16060987

- Ávila-Nieto, C., Vergara-Alert, J., Amengual-Rigo, P., Ainsua-Enrich, E., Brustolin, M., Rodríguez de la Concepción, M. L., Pedreño-Lopez, N., Rodon, J., Urrea, V., Pradenas, E., Marfil, S., Ballana, E., Riveira-Muñoz, E., Pérez, M., Roca, N., Tarrés-Freixas, F., Carabelli, J., Cantero, G., **Pons-Grífols, A.**, Rovirosa, C., Aguilar-Gurrieri, C., Ortiz, R., Barajas, A., Trinité, B., Lepore, R., Muñoz-Basagoiti, J., Perez-Zsolt, D., Izquierdo-Useros, N., Valencia, A., Blanco, J., Clotet, B., Guallar, V., Segalés, J., Carrillo, J. (2023). Novel Spike-stabilized trimers with improved production protect K18-hACE2 mice and golden Syrian hamsters from the highly pathogenic SARS-CoV-2 Beta variant. Frontiers in Immunology,14,1291972. https://doi.org/10.3389/FIMMU.2023.1291972/BIBTEX

- Carrillo, J., Ávila-Nieto, C., Vergara-Alert, J., Amengual-Rigo, P., Ainsua-Enrich, E., Brustolin, M., Concepción, M. L. R. de la, Pedreño-Lopez, N., Rodon, J., Urrea, V., Pradenas, E., Marfil, S., Ballana, E., Riveira-Muñoz, E., Pérez, M., Roca, N., Tarrés-Freixas, F., Cantero, G., **Pons-Grífols, A.**, Rovirosa, C., Aguilar-Gurrieri, C., Ortiz, R., Barajas, A., Trinité, B., Lepore, R., Muñoz-Basagoiti, J., Perez-Zsolt, D., Izquierdo-Useros, N., Valencia, A., Blanco, J., Clotet, B., Guallar, V., Segalés, J., Carrillo, J. (2023). Immunization with V987H-stabilized Spike glycoprotein protects K18-hACE2 and golden Syrian hamster upon SARS-CoV-2 infection. https://doi.org/10.21203/RS.3.RS-2846684/V1

- Ortiz, R., Barajas, A., **Pons-Grífols, A.**, Trinité, B., Tarrés-Freixas, F., Rovirosa, C., Urrea, V., Barreiro, A., Gonzalez-Tendero, A., Cardona, M., Ferrer, L., Clotet, B., Carrillo, J., Aguilar-Gurrieri, C., & Blanco, J. (2023). Exploring FeLV-Gag-Based VLPs as a New Vaccine Platform—Analysis of Production and Immunogenicity. International Journal of Molecular Sciences, 24(10), 9025. https://doi.org/10.3390/ijms24109025

- Pradenas, E., Marfil, S., Urrea, V., Trigueros, M., Pidkova, T., **Pons-Grífols, A.**, Ortiz, R., Rovirosa, C., Tarrés-Freixas, F., Aguilar-Gurrieri, C., Toledo, R., Chamorro, A., Noguera-Julian, M., Mateu, L., Blanco, I., Grau, E., Massanella, M., Carrillo, J., Clotet, B., Trinité, B., Blanco, J. (2023). Impact of hybrid immunity booster vaccination and Omicron breakthrough infection on SARS-CoV-2 VOCs cross-neutralization. IScience, 26(4). https://doi.org/10.1016/j.isci.2023.106457

- Tarrés-Freixas, F., Trinité, B., **Pons-Grífols, A.**, Romero-Durana, M., Riveira-Muñoz, E., Ávila-Nieto, C., Pérez, M., Garcia-Vidal, E., Perez-Zsolt, D., Muñoz-Basagoiti, J., Raïch-Regué, D., Izquierdo-Useros, N., Andrés, C., Antón, A., Pumarola, T., Blanco, I., Noguera-Julián, M., Guallar, V., Lepore, R., Valencia, A., Urrea, V., Vergara-Alert, J., Clotet, B., Ballana, E., Carrillo, J., Segalés, J., Blanco, J. (2022). Heterogeneous Infectivity and Pathogenesis of SARS-CoV-2 Variants Beta, Delta and Omicron in Transgenic K18-hACE2 and Wildtype Mice. Frontiers in Microbiology, 13(May). https://doi.org/10.3389/fmicb.2022.840757

Oral Communications

- 2022 Development and characterization of a new human ACE2 knock-in mouse model for SARS-CoV-2 infection and pathogenesis. **XXI Jornada de Virologia. Societat Catalana de Biologia - Secció de Virologia**, Barcelona. Oral Presentation.

- 2024 Longitudinal characterization of the humoral response of an HIV-1 Exceptional Elite Controller losing control 32 years after diagnosis. **XIV Congreso Nacional de GeSIDA**, A Coruña. Poster and Oral Communication.

- 2025 Loss of Virological Control 32 Years After HIV-1 Diagnosis in an Exceptional Elite Controller. **Conference on Retroviruses and Opportunistic Infections (CROI), 32nd Edition**. IAS-USA, San Francisco, California, USA. Theme Discussion and Poster.

Poster presentations

As presenter

2023

- Ancestral Envelope Glycoproteins from Elite Controllers show decreased infectivity and higher exposure of bNAb epitopes. **XIV Congreso Nacional de GeSIDA**, A Coruña, Spain. Oral Poster.

2024

- Longitudinal characterization of the humoral response of an HIV-1 Exceptional Elite Controller losing control 32 years after diagnosis. **XV Congreso Nacional de GeSIDA**, A Coruña, Spain. Poster and Oral Communication.

- Functional characterization of HIV-1 Envelope glycoproteins isolated from the Elite Controller ECRIS cohort. **XV Congreso Nacional de GeSIDA**, A Coruña. Thematic Poster.

- Longitudinal characterization of the humoral response of an HIV-1 Exceptional Elite Controller losing control 32 years after diagnosis. **IGTP Retreat,** Badalona, Spain. Poster.

2025

- Loss of Virological Control 32 Years After HIV-1 Diagnosis in an Exceptional Elite Controller. **Conference on Retroviruses and Opportunistic Infections (CROI), 32nd Edition.** IAS-USA, San Francisco, California, USA. Theme Discussion and Poster.

As collaborator

2021

- High immunogenic VLP-based vaccines elicit new T cell specificities against melanoma neoantigens in mice. Poster. Journal for ImmunoTherapy of Cancer 9 (Suppl 1):A13.1-A13. **8th Immunotherapy of Cancer Conference (ITOC8).** Online.

2023

- Impact of hybrid immunity, booster vaccination and Omicron breakthrough infection on cross-neutralization against Delta, BA.1, BA.2 and BA.4/5 SARS-CoV-2 variants. **44 Congreso de la Sociedad Española de Inmunología (SEI).** Bilbao, Spain.Oral Poster.

- Novel SARS-CoV-2-stabilized spike proteins with improved production and protective activity against SARS-CoV-2-induced disease in animal models. **44 Congreso de la Sociedad Española de Inmunología (SEI). Bilbao, Spain**. Oral Poster.

- A new and flexible vaccine platform for personalized cancer immunotherapy. **Alicante Winter Immunology Symposium in Health.** Alicante, Spain. Poster.

2024

- Immune Profile During ATI in AELIX-002 HTI Vaccine Trial and Its Role in Post-Intervention Control. **Conference on Retroviruses and Opportunistic Infections 2024**, Denver, USA.

- Spike-V987H Vaccination Protects Animal Models From SARS-COV-2–Induced Severe Disease. **Conference on Retroviruses and Opportunistic Infections 2024**, Denver, USA.

- Neutralizing antibodies and viral rebound kinetics upon art Interruption using HTI T-cell vaccines in early-treated HIV-1 infection. **HIVR4P: 5th HIV Research for Prevention Conference.** Poster.

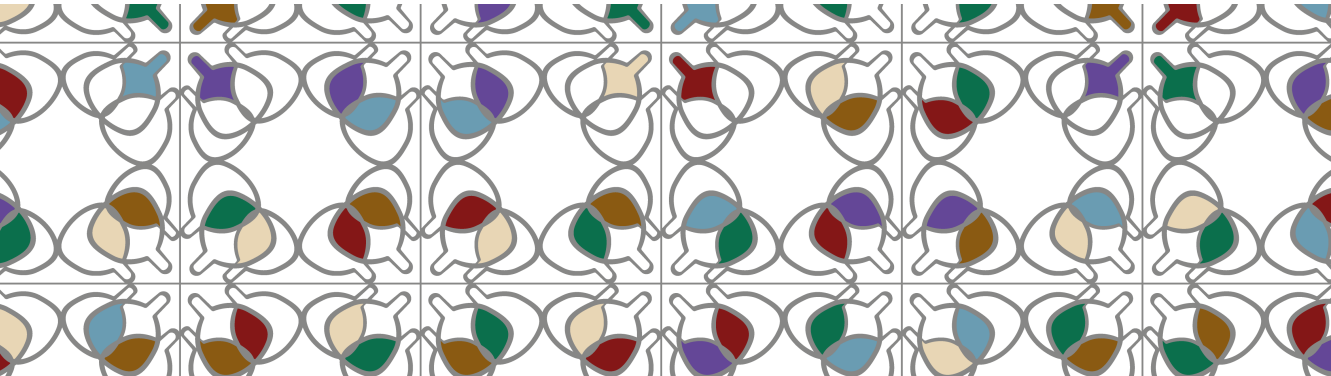

REFERENCES

Abram, Michael E., Andrea L. Ferris, Wei Shao, W. Gregory Alvord, and Stephen H. Hughes. 2010. "Nature, Position, and Frequency of Mutations Made in a Single Cycle of HIV-1 Replication." Journal of Virology 84 (19): 9864–78. https://doi.org/10.1128/JVI.00915-10.

Ackerman, Margaret E., Anastassia Mikhailova, Eric P. Brown, Karen G. Dowell, Bruce D. Walker, Chris Bailey-Kellogg, Todd J. Suscovich, and Galit Alter. 2016. "Polyfunctional HIV-Specific Antibody Responses Are Associated with Spontaneous HIV Control." PLOS Pathogens 12 (1): e1005315. https://doi.org/10.1371/JOURNAL.PPAT.1005315.

Alcamí, José, and Mayte Coiras. 2011. "Inmunopatogenia de La Infección Por El Virus de La Inmunodeficiencia Humana." Enfermedades Infecciosas y Microbiología Clínica 29 (3): 216–26. https://doi.org/10.1016/J.EIMC.2011.01.006.

Alsahafi, Nirmin, Nordine Bakouche, Mohsen Kazemi, Jonathan Richard, Shilei Ding, Sudipta Bhattacharyya, Durba Das, et al. 2019. "An Asymmetric Opening of HIV-1 Envelope Mediates Antibody-Dependent Cellular Cytotoxicity." Cell Host & Microbe 25 (4): 578-587.e5. https://doi.org/10.1016/J.CHOM.2019.03.002.

Ananworanich, Jintanat, Nicolas Chomont, Leigh Ann Eller, Eugene Kroon, Sodsai Tovanabutra, Meera Bose, Martin Nau, et al. 2016. "HIV DNA Set Point Is Rapidly Established in Acute HIV Infection and Dramatically Reduced by Early ART." EBioMedicine 11 (September):68–72. https://doi.org/10.1016/J.EBIOM.2016.07.024.

Apps, Richard, Ying Qi, Jonathan M. Carlson, Haoyan Chen, Xiaojiang Gao, Rasmi Thomas, Yuko Yuki, et al. 2013. "Influence of HLA-C Expression Level on HIV Control." Science (New York, N.Y.) 340 (6128): 87–91. https://doi.org/10.1126/SCIENCE.1232685.

Barajas, Ana, Pep Amengual-Rigo, Anna Pons-Grífols, Raquel Ortiz, Oriol Gracia Carmona, Victor Urrea, Nuria de la Iglesia, et al. 2024. "Virus-like Particle-Mediated Delivery of Structure-Selected Neoantigens Demonstrates Immunogenicity and Antitumoral Activity in Mice." Journal of Translational Medicine 22 (1): 1–14. https://doi.org/10.1186/s12967-023-04843-8.

Barblu, Lucie, Kawthar MacHmach, Christophe Gras, Jean François Delfraissy, Faroudy Boufassa, Manuel Leal, Ezequiel Ruiz-Mateos, Olivier Lambotte, and Jean Philippe Herbeuval. 2012. "Plasmacytoid Dendritic Cells (PDCs) from HIV Controllers Produce Interferon-α and Differentiate into Functional Killer PDCs under HIV Activation." The Journal of Infectious Diseases 206 (5): 790–801. https://doi.org/10.1093/INFDIS/JIS384.

Barouch, Dan H., Kara L. O'Brien, Nathaniel L. Simmons, Sharon L. King, Peter Abbink, Lori F. Maxfield, Ying Hua Sun, et al. 2010. "Mosaic HIV-1 Vaccines Expand the Breadth and Depth of Cellular Immune Responses in Rhesus Monkeys." Nature Medicine 16 (3): 319. https://doi.org/10.1038/NM.2089.

Barré-Sinoussi, F., J. C. Chermann, F. Rey, M. T. Nugeyre, S. Chamaret, J. Gruest, C. Dauguet, et al. 1983. "Isolation of a T-Lymphotropic Retrovirus from a Patient at Risk for Acquired Immune Deficiency Syndrome (AIDS)." Science (New York, N.Y.) 220 (4599): 868–71. https://doi.org/10.1126/SCIENCE.6189183.

Bayón-Gil, Ángel. 2024. "Analysis of Distinctive Host Immune Factors in HIV+ Viremic Non-Progressors."

Bayón-Gil, Ángel, Inmaculada Hernández, Judith Dalmau, Juan C. Nieto, Víctor Urrea, Lidia Garrido-Sanz, Ginevra Caratú, et al. 2025. "Host Genetic and Immune Factors Drive Evasion of HIV-1 Pathogenesis in Viremic Non-Progressors." Med (New York, N.Y.) 6 (2). https://doi.org/10.1016/J.MEDJ.2024.09.007.

Beltran-Pavez, Carolina, Ilja Bontjer, Nuria Gonzalez, Maria Pernas, Alberto Merino-Mansilla, Alex Olvera, Jose M. Miro, et al. 2021. "Potent Induction of Envelope-Specific Antibody Responses by Virus-Like Particle (VLP) Immunogens Based on HIV-1 Envelopes from Patients with Early Broadly Neutralizing Responses." Journal of Virology, no. October (October). https://doi.org/10.1128/JVI.01343-21.

Benito, José M., Daniel Jiménez-Carretero, Clara Restrepo, José M. Ligos, Jaime Valentín-Quiroga, Ignacio Mahillo, Alfonso Cabello, et al. 2024. "T Cell Homeostasis Disturbances in a Cohort of Long-Term Elite Controllers of HIV Infection." International Journal of Molecular Sciences 25 (11): 5937. https://doi.org/10.3390/IJMS25115937/S1.

Blankson, Joel N., Justin R. Bailey, Seema Thayil, Hung-Chih Yang, Kara Lassen, Jun Lai, Shiv K. Gandhi, Janet D. Siliciano, Thomas M. Williams, and Robert F. Siliciano. 2007. "Isolation and Characterization of Replication-Competent Human Immunodeficiency Virus Type 1 from a Subset of Elite Suppressors." Journal of Virology 81 (5): 2508–18. https://doi.org/10.1128/JVI.02165-06.

Braibant, Martine, Jing Xie, Assia Samri, Henri Agut, Brigitte Autran, and Francis Barin. 2010. "Disease Progression Due to Dual Infection in an HLA-B57-Positive Asymptomatic Long-Term Nonprogressor Infected with a Nef-Defective HIV-1 Strain." Virology 405 (1): 81–92. https://doi.org/10.1016/J.VIROL.2010.05.026.

Brinkkemper, Mitch, and Kwinten Sliepen. 2019. "Nanoparticle Vaccines for Inducing HIV-1 Neutralizing Antibodies." Vaccines 7 (3). https://doi.org/10.3390/VACCINES7030076.

Burdick, Ryan C., Chenglei Li, Mohamed Husen Munshi, Jonathan M.O. Rawson, Kunio Nagashima, Wei Shau Hu, and Vinay K. Pathak. 2020. "HIV-1 Uncoats in the Nucleus near Sites of Integration." Proceedings of the National Academy of Sciences of the United States of America 117 (10): 5486–93. https://doi.org/10.1073/PNAS.1920631117.

Burton, Dennis R., and Lars Hangartner. 2016. "Broadly Neutralizing Antibodies to HIV and Their Role in Vaccine Design." Annual Review of Immunology 34 (Volume 34, 2016): 635–59. https://doi.org/10.1146/ANNUREV-IMMUNOL-041015-055515/CITE/REFWORKS.

Cabrera-Rodríguez, Romina, Veronique Hebmann, Silvia Marfil, María Pernas, Sara Marrero-Hernández, Cecilia Cabrera, Victor Urrea, et al. 2019. "HIV-1 Envelope Glycoproteins Isolated from Viremic Non-Progressor Individuals Are Fully Functional and Cytopathic." Scientific Reports 9 (1): 1–12. https://doi.org/10.1038/s41598-019-42075-3.

Cabrera-Rodríguez, Romina, Silvia Pérez-Yanes, Rafaela Montelongo, José M. Lorenzo-Salazar, Judith Estévez-Herrera, Jonay García-Luis, Antonio Íñigo-Campos, et al. 2022. "Transactive Response DNA-Binding Protein (TARDBP/TDP-43) Regulates Cell Permissivity to HIV-1 Infection by Acting on HDAC6." International Journal of Molecular Sciences 23 (11): 6180. https://doi.org/10.3390/IJMS23116180/S1.

Caetano, Diogo Gama, Fernanda Heloise Côrtes, Gonzalo Bello, Suwellen Sardinha Dias De Azevedo, Brenda Hoagland, Larissa Melo Villela, Beatriz Grinsztejn, Valdiléa Gonçalves Veloso, Monick Lindenmeyer Guimarães, and Mariza Gonçalves Morgado. 2019. "A Case Report of HIV-1 Superinfection in an HIV Controller Leading to Loss of Viremia Control: A Retrospective of 10 Years of Follow-Up." BMC Infectious Diseases 19 (1): 588. https://doi.org/10.1186/S12879-019-4229-3.

Caniels, Tom G., Madhu Prabhakaran, Gabriel Ozorowski, Kellie J. MacPhee, Weiwei Wu, Karlijn van der Straten, Sashank Agrawal, et al. 2025. "Precise Targeting of HIV Broadly Neutralizing Antibody Precursors in Humans." Science, May. https://doi.org/10.1126/SCIENCE.ADV5572.

Cao, Yunzhen, Limo Qin, Linqi Zhang, Jeffrey Safrit, and David D. Ho. 1995. "Virologic and Immunologic Characterization of Long-Term Survivors of Human Immunodeficiency Virus Type 1 Infection." New England Journal of Medicine 332 (4): 201–8. https://doi.org/10.1056/NEJM199501263320401/ASSET/7C837110-134D-4983-9FF8-972F5645CDEA/ASSETS/IMAGES/LARGE/NEJM199501263320401_F4.JPG.

Carrington, Mary, and Bruce D. Walker. 2012. "Immunogenetics of Spontaneous Control of HIV." Annual Review of Medicine 63: 131–145. https://doi.org/10.1146/ANNUREV-MED-062909-130018

Cartwright, Emily K., Lori Spicer, S. Abigail Smith, David Lee, Randy Fast, Sara Paganini, Benton O. Lawson, et al. 2016. "CD8(+) Lymphocytes Are Required for Maintaining Viral Suppression in SIV-Infected Macaques Treated with Short-Term

Antiretroviral Therapy." Immunity 45 (3): 656–68. https://doi.org/10.1016/J.IMMUNI.2016.08.018.

Casado, Concepción, Sara Colombo, Andri Rauch, Raquel Martínez, Huldrych F. Günthard, Soledad Garcia, Carmen Rodríguez, Jorge del Romero, Amalio Telenti, and Cecilio López-Galíndez. 2010. "Host and Viral Genetic Correlates of Clinical Definitions of HIV-1 Disease Progression." Edited by Jean-Pierre Vartanian. PLoS ONE 5 (6): e11079. https://doi.org/10.1371/journal.pone.0011079.

Casado, Concepción, Cristina Galvez, Maria Pernas, Laura Tarancon-Diez, Carmen Rodriguez, Víctor Sanchez-Merino, Mar Vera, et al. 2020. "Permanent Control of HIV-1 Pathogenesis in Exceptional Elite Controllers: A Model of Spontaneous Cure." Scientific Reports 2020 10:1 10 (1): 1–11. https://doi.org/10.1038/s41598-020-58696-y.

Casado, Concepción, Sara Marrero-Hernández, Daniel Márquez-Arce, María Pernas, Sílvia Marfil, Ferran Borràs-Grañana, Isabel Olivares, et al. 2018. "Viral Characteristics Associated with the Clinical Nonprogressor Phenotype Are Inherited by Viruses from a Cluster of HIV-1 Elite Controllers." Edited by Dimitrios Paraskevis. MBio 9 (2): 1–18. https://doi.org/10.1128/mBio.02338-17.

Casado, Concepción, Maria Pernas, Tamara Alvaro, Virginia Sandonis, Soledad García, Carmen Rodríguez, Jorge del Romero, Eulalia Grau, Lidia Ruiz, and Cecilio Lopez-Galindez. 2007. "Coinfection and Superinfection in Patients with Long-Term, Nonprogressive HIV-1 Disease." The Journal of Infectious Diseases 196 (6): 895–99. https://doi.org/10.1086/520885.

Casado, Concepción, Maria Pernas, Virginia Sandonis, Tamara Alvaro-Cifuentes, Isabel Olivares, Rosa Fuentes, Lorena Martínez-Prats, et al. 2013. "Identification of a Cluster of HIV-1 Controllers Infected with Low Replicating Viruses." Edited by Cristian Apetrei. PLoS ONE 8 (10): e77663. https://doi.org/10.1371/journal.pone.0077663.

Catalfamo, Marta, Cecile Le Saout, and H. Clifford Lane. 2012. "The Role of Cytokines in the Pathogenesis and Treatment of HIV Infection." Cytokine & Growth Factor Reviews 23 (4–5): 207–14. https://doi.org/10.1016/J.CYTOGFR.2012.05.007.

Centlivre, Mireille, Monica Sala, Simon Wain-Hobson, and Ben Berkhout. 2007. "In HIV-1 Pathogenesis the Die Is Cast during Primary Infection." AIDS (London, England) 21 (1): 1–11. https://doi.org/10.1097/QAD.0B013E3280117F7F.

Cervera, Laura, Sonia Gutiérrez-Granados, Marta Martínez, Julià Blanco, Francesc Gòdia, and María Mercedes Segura. 2013. "Generation of HIV-1 Gag VLPs by Transient Transfection of HEK 293 Suspension Cell Cultures Using an Optimized Animal-Derived Component Free Medium." Journal of Biotechnology 166 (4): 152–65. https://doi.org/10.1016/J.JBIOTEC.2013.05.001.

Chan, David C., Deborah Fass, James M. Berger, and Peter S. Kim. 1997. "Core Structure of Gp41 from the HIV Envelope Glycoprotein." Cell 89 (2): 263–73. https://doi.org/10.1016/S0092-8674(00)80205-6.

Chen, Bing. 2019. "Molecular Mechanism of HIV-1 Entry." Trends in Microbiology 27 (10): 878–91. https://doi.org/10.1016/J.TIM.2019.06.002.

Chereau, Fanny, Yoann Madec, Caroline Sabin, Niels Obel, Ezequiel Ruiz-Mateos, Georgios Chrysos, Sarah Fidler, et al. 2017. "Impact of CD4 and CD8 Dynamics and Viral Rebounds on Loss of Virological Control in HIV Controllers." Edited by Cristian Apetrei. PLOS ONE 12 (4): e0173893. https://doi.org/10.1371/journal.pone.0173893.

Clerc, Olivier, Sara Colombo, Sabine Yerly, Amalio Telenti, and Matthias Cavassini. 2010. "HIV-1 Elite Controllers: Beware of Super-Infections." Journal of Clinical Virology 47 (4): 376–78. https://doi.org/10.1016/j.jcv.2010.01.013.

Climent, N, J Ambrosioni, C Xufré, M Plana, J Grau-Expósito, J Mallolas, J Alcamí, et al. 2022. "Immunological and Virological Findings in a Patient with Exceptional Post-Treatment Control: A Case Report." https://doi.org/10.1016/S2352-3018(22)00302-2.

Coffin, John, Jonas Blomberg, Hung Fan, Robert Gifford, Theodora Hatziioannou, Dirk Lindemann, Jens Mayer, Jonathan Stoye, Michael Tristem, and Welkin Johnson. 2021. "ICTV Virus Taxonomy Profile: Retroviridae 2021." Journal of General Virology 102 (12): 001712. https://doi.org/10.1099/JGV.0.001712/CITE/REFWORKS.

Cohen, George B., Rajesh T. Gandhi, Daniel M. Davis, Ofer Mandelboim, Benjamin K. Chen, Jack L. Strominger, and David Baltimore. 1999. "The Selective Downregulation of Class I Major Histocompatibility Complex Proteins by HIV-1 Protects HIV-Infected Cells from NK Cells." Immunity 10 (6): 661–71. https://doi.org/10.1016/S1074-7613(00)80065-5.

Cohen, Yehuda Z., Christy L. Lavine, Caroline A. Miller, Jetta Garrity, Brittany R. Carey, and Michael S. Seaman. 2015. "Glycan-Dependent Neutralizing Antibodies Are Frequently Elicited in Individuals Chronically Infected with HIV-1 Clade B or C." AIDS Research and Human Retroviruses 31 (11): 1192. https://doi.org/10.1089/AID.2015.0135.

Collins, David R., Jonathan M. Urbach, Zachary J. Racenet, Umar Arshad, Karen A. Power, Ruchi M. Newman, Geetha H. Mylvaganam, et al. 2021. "Functional Impairment of HIV-Specific CD8+ T Cells Precedes Aborted Spontaneous Control of Viremia." Immunity 54 (10): 2372-2384.e7. https://doi.org/10.1016/J.IMMUNI.2021.08.007.

Connor, Ruth I., Kristine E. Sheridan, Daniel Ceradini, Sunny Choe, and Nathaniel R. Landau. 1997. "Change in Coreceptor Use Correlates with Disease Progression in HIV-1–Infected Individuals." Journal of Experimental Medicine 185 (4): 621–28. https://doi.org/10.1084/JEM.185.4.621.

Corey, Lawrence, Peter B. Gilbert, Michal Juraska, David C. Montefiori, Lynn Morris, Shelly T. Karuna, Srilatha Edupuganti, et al. 2021. "Two Randomized Trials of Neutralizing Antibodies to Prevent HIV-1 Acquisition." New England Journal of Medicine 384 (11): 1003–14. https://doi.org/10.1056/NEJMOA2031738/SUPPL_FILE/NEJMOA2031738_DATA-SHARING.PDF.

Curlin, Marcel E., Rafael Zioni, Stephen E. Hawes, Yi Liu, Wenjie Deng, Geoffrey S. Gottlieb, Tuofu Zhu, and James I. Mullins. 2010. "HIV-1 Envelope Subregion

Length Variation during Disease Progression." PLOS Pathogens 6 (12): e1001228. https://doi.org/10.1371/JOURNAL.PPAT.1001228.

Curriu, Marta, Hughes Fausther-Bovendo, María Pernas, Marta Massanella, Jorge Carrillo, Cecilia Cabrera, Cecilio López-Galíndez, et al. 2012. "Viremic HIV Infected Individuals with High CD4 T Cells and Functional Envelope Proteins Show Anti-Gp41 Antibodies with Unique Specificity and Function." Edited by Yuntao Wu. PLoS ONE 7 (2): e30330. https://doi.org/10.1371/journal.pone.0030330.

Dalgleish, Angus G., Peter C.L. Beverley, Paul R. Clapham, Dorothy H. Crawford, Melvyn F. Greaves, and Robin A. Weiss. 1984. "The CD4 (T4) Antigen Is an Essential Component of the Receptor for the AIDS Retrovirus." Nature 1984 312:5996 312 (5996): 763–67. https://doi.org/10.1038/312763a0.

Das, Biswajit, Curtis Dobrowolski, Benjamin Luttge, Saba Valadkhan, Nicolas Chomont, Rowena Johnston, Peter Bacchetti, et al. 2018. "Estrogen Receptor-1 Is a Key Regulator of HIV-1 Latency That Imparts Gender-Specific Restrictions on the Latent Reservoir." Proceedings of the National Academy of Sciences of the United States of America 115 (33): E7795–7804. https://doi.org/10.1073/PNAS.1803468115/SUPPL_FILE/PNAS.1803468115.SAPP.PDF.

Dean, Michael, Mary Carrington, Cheryl Winkler, Gavin A. Huttley, Michael W. Smith, Rando Allikmets, James J. Goedert, et al. 1996. "Genetic Restriction of HIV-1 Infection and Progression to AIDS by a Deletion Allele of the CKR5 Structural Gene. Hemophilia Growth and Development Study, Multicenter AIDS Cohort Study, Multicenter Hemophilia Cohort Study, San Francisco City Cohort, ALIVE Study." Science (New York, N.Y.) 273 (5283): 1856–62. https://doi.org/10.1126/SCIENCE.273.5283.1856.

Deeks, Steven G., Julie Overbaugh, Andrew Phillips, and Susan Buchbinder. 2015. "HIV Infection." Nature Reviews Disease Primers 2015 1:1 1 (1): 1–22. https://doi.org/10.1038/nrdp.2015.35.

Doitsh, Gilad, Nicole L.K. Galloway, Xin Geng, Zhiyuan Yang, Kathryn M. Monroe, Orlando Zepeda, Peter W. Hunt, et al. 2013. "Cell Death by Pyroptosis Drives CD4 T-Cell Depletion in HIV-1 Infection." Nature 2014 505:7484 505 (7484): 509–14. https://doi.org/10.1038/nature12940.

Dominguez-Molina, Beatriz, for the Spanish AIDS Research Network HIV Controllers Cohort (ECRIS), Agathe Leon, for the Spanish AIDS Research Network HIV Controllers Cohort (ECRIS), Carmen Rodriguez, for the Spanish AIDS Research Network HIV Controllers Cohort (ECRIS), Jose M. Benito, et al. 2016. "Analysis of Non-AIDS-Defining Events in HIV Controllers." Clinical Infectious Diseases 62 (10): 1304–9. https://doi.org/10.1093/CID/CIW120.

Dominguez-Molina, Beatriz, Sara Ferrando-Martinez, Laura Tarancon-Diez, Jose Hernandez-Quero, Miguel Genebat, Francisco Vidal, Ma Angeles Muñoz-Fernandez, Manuel Leal, Richard Koup, and Ezequiel Ruiz-Mateos. 2018. "Immune Correlates of Natural HIV Elite Control and Simultaneous HCV Clearance-Supercontrollers." Frontiers in Immunology 9 (December). https://doi.

org/10.3389/FIMMU.2018.02897.

Dominguez-Molina, Beatriz, Laura Tarancon-Diez, Yusnelkis Milanés-Guisado, Miguel Genebat, Salvador Resino, Carmen Rodriguez, Juan Gonzalez-García, et al. 2020. "Persistent HIV-controllers Are More Prone to Spontaneously Clear HCV: A Retrospective Cohort Study." Journal of the International AIDS Society 23 (9): e25607. https://doi.org/10.1002/JIA2.25607.

El-Far, Mohamed, Pascale Kouassi, Mohamed Sylla, Yuwei Zhang, Ahmed Fouda, Thomas Fabre, Jean Philippe Goulet, et al. 2016. "Proinflammatory Isoforms of IL-32 as Novel and Robust Biomarkers for Control Failure in HIV-Infected Slow Progressors." Scientific Reports 2016 6:1 6 (1): 1–18. https://doi.org/10.1038/srep22902.

Escolano, Amelia, Pia Dosenovic, and Michel C. Nussenzweig. 2017. "Progress toward Active or Passive HIV-1 Vaccination." Journal of Experimental Medicine 214 (1): 3–16. https://doi.org/10.1084/JEM.20161765.

Etemad, Behzad, Xiaoming Sun, Yijia Li, Meghan Melberg, Daniela Moisi, Rachel Gottlieb, Hayat Ahmed, et al. 2023. "HIV Post-Treatment Controllers Have Distinct Immunological and Virological Features." Proceedings of the National Academy of Sciences of the United States of America 120 (11): e2218960120. https://doi.org/10.1073/PNAS.2218960120/SUPPL_FILE/PNAS.2218960120.SAPP.PDF.

Flórez-Álvarez, Lizdany, Juan C. Hernandez, and Wildeman Zapata. 2018. "NK Cells in HIV-1 Infection: From Basic Science to Vaccine Strategies." Frontiers in Immunology 9 (OCT): 409736. https://doi.org/10.3389/FIMMU.2018.02290/XML/NLM.

Forthal, Donald N., and Andres Finzi. 2018. "Antibody-Dependent Cellular Cytotoxicity (ADCC) in HIV Infection." AIDS (London, England) 32 (17): 2439. https://doi.org/10.1097/QAD.0000000000002011.

Frances, Sara, Anna Pons-Grífols, Carmen Gasca Capote, Virginia Sandonís, Edwards Pradenas, Cristina Moral-Turón, Ester Aparicio, et al. 2025. "Loss of Virological Control 32 Years After HIV-1 Diagnosis in an Exceptional Elite Controller. [CROI Abstract 494]." Top Antivir Med.In Special Issue: Abstracts From the CROI 2025 Conference on Retroviruses and Opportunistic Infections. 33 (1): 332–332.

Frankel, Alan D., and John A.T. Young. 1998. "HIV-1: Fifteen Proteins and an RNA." Annual Review of Biochemistry 67:1–25. https://doi.org/10.1146/ANNUREV.BIOCHEM.67.1.1.

Friedrich, Nikolas, Emanuel Stiegeler, Matthias Glögl, Thomas Lemmin, Simon Hansen, Claus Kadelka, Yufan Wu, et al. 2021. "Distinct Conformations of the HIV-1 V3 Loop Crown Are Targetable for Broad Neutralization." Nature Communications 12 (1): 6705. https://doi.org/10.1038/s41467-021-27075-0.

Gaik, Sui Kee, Narahari S. Pujar, and Nigel J. Titchener-Hooker. 2008. "Study of Detergent-Mediated Liberation of Hepatitis B Virus-like Particles from S. Cerevisiae Homogenate: Identifying a Framework for the Design of Future-Generation Lipoprotein Vaccine Processes." Biotechnology Progress 24 (3): 623–31. https://

doi.org/10.1021/BP070472I.

Gandhi, Rajesh T, Ronald J Bosch, Hanna Mar, Gregory M Laird, Elias K Halvas, Laura Hovind, Ann C Collier, et al. 2023. "Varied Patterns of Decay of Intact Human Immunodeficiency Virus Type 1 Proviruses Over 2 Decades of Antiretroviral Therapy." The Journal of Infectious Diseases 227 (12): 1376–80. https://doi.org/10.1093/INFDIS/JIAD039.

Gao, Yong, Chanuka Wijewardhana, and Jamie F.S. Mann. 2018. "Virus-like Particle, Liposome, and Polymeric Particle-Based Vaccines against HIV-1." Frontiers in Immunology 9 (FEB). https://doi.org/10.3389/FIMMU.2018.00345.

Garcia-Broncano, Pilar, Shivaali Maddali, Kevin B. Einkauf, Chenyang Jiang, Ce Gao, Joshua Chevalier, Fatema Z. Chowdhury, et al. 2019. "Early Antiretroviral Therapy in Neonates with HIV-1 Infection Restricts Viral Reservoir Size and Induces a Distinct Innate Immune Profile." Science Translational Medicine 11 (520). https://doi.org/10.1126/SCITRANSLMED.AAX7350.

Garrido, Carolina, Vanessa Roulet, Natalia Chueca, Eva Poveda, Antonio Aguilera, Katharina Skrabal, Natalia Zahonero, et al. 2008. "Evaluation of Eight Different Bioinformatics Tools To Predict Viral Tropism in Different Human Immunodeficiency Virus Type 1 Subtypes." Journal of Clinical Microbiology 46 (3): 887. https://doi.org/10.1128/JCM.01611-07.

Gartner, Matthew J., Michael Roche, Melissa J. Churchill, Paul R. Gorry, and Jacqueline K. Flynn. 2020. "Understanding the Mechanisms Driving the Spread of Subtype C HIV-1." EBioMedicine 53 (March). https://doi.org/10.1016/J.EBIOM.2020.102682.

Gasca-Capote, Carmen, Xiaodong Lian, Ce Gao, Isabelle C. Roseto, María Reyes Jiménez-León, Gregory Gladkov, María Inés Camacho-Sojo, et al. 2024. "The HIV-1 Reservoir Landscape in Persistent Elite Controllers and Transient Elite Controllers." Journal of Clinical Investigation 134 (8). https://doi.org/10.1172/JCI174215.

Gasca-Capote, Carmen, and Ezequiel Ruiz-Mateos. 2024. "Persistent Elite Controllers as the Key Model to Identify Permanent HIV Remission." Current Opinion in HIV and AIDS 0. https://doi.org/10.1097/COH.0000000000000907.

Gautam, Rajeev, Yoshiaki Nishimura, Amarendra Pegu, Martha C. Nason, Florian Klein, Anna Gazumyan, Jovana Golijanin, et al. 2016. "A Single Injection of Anti-HIV-1 Antibodies Protects against Repeated SHIV Challenges." Nature 2016 533:7601 533 (7601): 105–9. https://doi.org/10.1038/nature17677.

Gheysen, Dirk, Eric Jacobs, Françoise de Foresta, Clotilde Thiriart, Myriam Francotte, Denise Thines, and Michel De Wilde. 1989. "Assembly and Release of HIV-1 Precursor Pr55gag Virus-like Particles from Recombinant Baculovirus-Infected Insect Cells." Cell 59 (1): 103–12. https://doi.org/10.1016/0092-8674(89)90873-8.

Gianella, Sara, Stephen A. Rawlings, Curtis Dobrowolski, Masato Nakazawa, Antoine Chaillon, Matthew Strain, Laura Layman, et al. 2022. "Sex Differences in Human Immunodeficiency Virus Persistence and Reservoir Size During Aging." Clinical

Infectious Diseases : An Official Publication of the Infectious Diseases Society of America 75 (1): 73–80. https://doi.org/10.1093/CID/CIAB873.

Gupta, Ravindra Kumar, Dimitra Peppa, Alison L. Hill, Cristina Gálvez, Maria Salgado, Matthew Pace, Laura E. McCoy, et al. 2020. "Evidence for HIV-1 Cure after CCR5Δ32/Δ32 Allogeneic Haemopoietic Stem-Cell Transplantation 30 Months Post Analytical Treatment Interruption: A Case Report." The Lancet. HIV 7 (5): e340–47. https://doi.org/10.1016/S2352-3018(20)30069-2.

Gurdasani, Deepti, Louise Iles, David G. Dillon, Elizabeth H. Young, Ashley D. Olson, Vivek Naranbhai, Sarah Fidler, et al. 2014. "A Systematic Review of Definitions of Extreme Phenotypes of HIV Control and Progression." AIDS 28 (2): 149–62. https://doi.org/10.1097/QAD.0000000000000049.

Hallenberger, Sabine, Valerie Bosch, Herbert Angliker, Elliott Shaw, Hans Dieter Klenk, and Wolfgang Garten. 1992. "Inhibition of Furin-Mediated Cleavage Activation of HIV-1 Glycoprotein Gpl60." Nature 1992 360:6402 360 (6402): 358–61. https://doi.org/10.1038/360358a0.

Hargett, Audra A., Qing Wei, Barbora Knoppova, Stacy Hall, Zhi-Qiang Huang, Amol Prakash, Todd J. Green, et al. 2019. "Defining HIV-1 Envelope N-Glycan Microdomains through Site-Specific Heterogeneity Profiles." Journal of Virology 93 (1): 1177–95. https://doi.org/10.1128/JVI.01177-18/SUPPL_FILE/JVI.01177-18-SD002.XLSX.

Hartana, Ciputra Adijaya, Pilar Garcia-Broncano, Yelizaveta Rassadkina, Xiaodong Lian, Chenyang Jiang, Kevin B. Einkauf, Kenneth Maswabi, et al. 2022. "Immune Correlates of HIV-1 Reservoir Cell Decline in Early-Treated Infants." Cell Reports 40 (3). https://doi.org/10.1016/J.CELREP.2022.111126.

Haynes, Barton F. 2021. "SARS-CoV-2 and HIV-1 — a Tale of Two Vaccines." Nature Reviews Immunology 2021 21:9 21 (9): 543–44. https://doi.org/10.1038/s41577-021-00589-w.

Haynes, Barton F., Kevin Wiehe, Persephone Borrow, Kevin O. Saunders, Bette Korber, Kshitij Wagh, Andrew J. McMichael, et al. 2022. "Strategies for HIV-1 Vaccines That Induce Broadly Neutralizing Antibodies." Nature Reviews Immunology 2022 23:3 23 (3): 142–58. https://doi.org/10.1038/s41577-022-00753-w.

Heuvel, Yasemin van, Stefanie Schatz, Jamila Franca Rosengarten, and Jörn Stitz. 2022. "Infectious RNA: Human Immunodeficiency Virus (HIV) Biology, Therapeutic Intervention, and the Quest for a Vaccine." Toxins 14 (2). https://doi.org/10.3390/TOXINS14020138.

Hiroyuki Watanabe, Kousuke Numata, Takaaki Ito, Katsumasa Takagi, Akihiro Matsukawa. 2004. "Innate Immune Response In Th1- And Th2-Dominant Mouse Strains." Shock 22 (5): 460–66. https://doi.org/10.1097/01.shk.0000142249.08135.e9.

Ho, Joan Kha Tu, Beena Jeevan-Raj, and Hans Jürgen Netter. 2020. "Hepatitis B Virus (HBV) Subviral Particles as Protective Vaccines and Vaccine Platforms." Viruses 2020, Vol. 12, Page 126 12 (2): 126. https://doi.org/10.3390/V12020126.

Hoffmann, Magnus A.G., Zhi Yang, Kathryn E. Huey-Tubman, Alexander A.

Cohen, Priyanthi N.P. Gnanapragasam, Leesa M. Nakatomi, Kaya N. Storm, et al. 2023. "ESCRT Recruitment to SARS-CoV-2 Spike Induces Virus-like Particles That Improve MRNA Vaccines." Cell 186 (11): 2380-2391.e9. https://doi.org/10.1016/J.CELL.2023.04.024.

Horwitz, Joshua A., Yotam Bar-On, Ching Lan Lu, Daniela Fera, Ainsley A.K. Lockhart, Julio C.C. Lorenzi, Lilian Nogueira, et al. 2017. "Non-Neutralizing Antibodies Alter the Course of HIV-1 Infection in Vivo." Cell 170 (4): 637. https://doi.org/10.1016/J.CELL.2017.06.048.

Hosseinipour, Mina C., Craig Innes, Sarita Naidoo, Philipp Mann, Julia Hutter, Gita Ramjee, Modulakgotla Sebe, et al. 2021. "Phase 1 Human Immunodeficiency Virus (HIV) Vaccine Trial to Evaluate the Safety and Immunogenicity of HIV Subtype C DNA and MF59-Adjuvanted Subtype C Envelope Protein." Clinical Infectious Diseases 72 (1): 50–60. https://doi.org/10.1093/CID/CIZ1239.

Huang, Jinghe, Patrick S. Burke, Thai Duong Hong Cung, Florencia Pereyra, Ildiko Toth, Bruce D. Walker, Luis Borges, Mathias Lichterfeld, and Xu G. Yu. 2010. "Leukocyte Immunoglobulin-like Receptors Maintain Unique Antigen-Presenting Properties of Circulating Myeloid Dendritic Cells in HIV-1-Infected Elite Controllers." Journal of Virology 84 (18): 9463–71. https://doi.org/10.1128/JVI.01009-10.

Huang, Yaoxing, William A. Paxton, Steven M. Wolinsky, Avidan U. Neumann, Linqi Zhang, Tian He, Stanley Kang, et al. 1996. "The Role of a Mutant CCR5 Allele in HIV-1 Transmission and Disease Progression." Nature Medicine 2 (11): 1240–43. https://doi.org/10.1038/NM1196-1240.

Hunter, E., and R. Swanstrom. 1990. "Retrovirus Envelope Glycoproteins." Current Topics in Microbiology and Immunology 157:188–253. https://doi.org/10.1007/978-3-642-75218-6_7.

Hütter, Gero, Daniel Nowak, Maximilian Mossner, Susanne Ganepola, Arne Müßig, Kristina Allers, Thomas Schneider, et al. 2009. " Long-Term Control of HIV by CCR5 Delta32/Delta32 Stem-Cell Transplantation ." New England Journal of Medicine 360 (7): 692–98. https://doi.org/10.1056/NEJMOA0802905/ASSET/63598BEB-782B-4B58-9936-204A0A4800D9/ASSETS/IMAGES/LARGE/NEJMOA0802905_F4.JPG.

International HIV Controllers Study, Florencia Pereyra, Xiaoming Jia, Paul J. McLaren, Amalio Telenti, Paul I W de Bakker, Bruce D. Walker, et al. 2010. "The Major Genetic Determinants of HIV-1 Control Affect HLA Class I Peptide Presentation." Science (New York, N.Y.) 330 (6010): 1551–57. https://doi.org/10.1126/science.1195271.

Ioannidis, J. P.A., P. S. Rosenberg, J. J. Goedert, L. J. Ashton, T. L. Benfield, S. P. Buchbinder, R. A. Coutinho, et al. 2001. "Effects of CCR5-Delta32, CCR2-64I, and SDF-1 3'A Alleles on HIV-1 Disease Progression: An International Meta-Analysis of Individual-Patient Data." Annals of Internal Medicine 135 (9): 782–95. https://doi.org/10.7326/0003-4819-135-9-200111060-00008.

Isitman, Gamze, Irene Lisovsky, Alexandra Tremblay-Mclean, Colin Kovacs, Marianne

Harris, Jean Pierre Routy, Julie Bruneau, Mark A. Wainberg, Cécile Tremblay, and Nicole F. Bernard. 2016. "Antibody-Dependent Cellular Cytotoxicity Activity of Effector Cells from HIV-Infected Elite and Viral Controllers." AIDS Research and Human Retroviruses 32 (10–11): 1079–88. https://doi.org/10.1089/AID.2016.0157.

Jacques, David A., William A. McEwan, Laura Hilditch, Amanda J. Price, Greg J. Towers, and Leo C. James. 2016. "HIV-1 Uses Dynamic Capsid Pores to Import Nucleotides and Fuel Encapsidated DNA Synthesis." Nature 536 (7616): 349–53. https://doi.org/10.1038/NATURE19098.

Jiang, Chenyang, Xiaodong Lian, Ce Gao, Xiaoming Sun, Kevin B. Einkauf, Joshua M. Chevalier, Samantha M.Y. Chen, et al. 2020. "Distinct Viral Reservoirs in Individuals with Spontaneous Control of HIV-1." Nature 2020 585:7824 585 (7824): 261–67. https://doi.org/10.1038/s41586-020-2651-8.

Jin, Xia, Daniel E. Bauer, Sarah E. Tuttleton, Sharon Lewin, Agegnehu Gettie, James Blanchard, Craig E. Irwin, et al. 1999. "Dramatic Rise in Plasma Viremia after CD8+ T Cell Depletion in Simian Immunodeficiency Virus–Infected Macaques." Journal of Experimental Medicine 189 (6): 991–98. https://doi.org/10.1084/JEM.189.6.991.

Joint United Nations Programme on HIV/AIDS (UNAIDS). 2024. "Fact Sheet 2024 - Latest Global and Regional HIV Statistics on the Status of the AIDS Epidemic."

Kanekiyo, Masaru, M. Gordon Joyce, Rebecca A. Gillespie, John R. Gallagher, Sarah F. Andrews, Hadi M. Yassine, Adam K. Wheatley, et al. 2019. "Mosaic Nanoparticle Display of Diverse Influenza Virus Hemagglutinins Elicits Broad B Cell Responses." Nature Immunology 20 (3): 362–72. https://doi.org/10.1038/S41590-018-0305-X.

Kato, Yu, Robert K. Abbott, Brian L. Freeman, Sonya Haupt, Bettina Groschel, Murillo Silva, Sergey Menis, Darrell J. Irvine, William R. Schief, and Shane Crotty. 2020. "Multifaceted Effects of Antigen Valency on B Cell Response Composition and Differentiation In Vivo." Immunity 53 (3): 548-563.e8. https://doi.org/10.1016/j.immuni.2020.08.001.

Kee, Gaik Sui, Jing Jin, Bangaru Balasundaram, Daniel G. Bracewell, Narahari S. Pujar, and Nigel J. Titchener-Hooker. 2010. "Exploiting the Intracellular Compartmentalization Characteristics of the S. Cerevisiae Host Cell for Enhancing Primary Purification of Lipid-Envelope Virus-like Particles." Biotechnology Progress 26 (1): 26–33. https://doi.org/10.1002/BTPR.307.

Khaitan, Alka, and Derya Unutmaz. 2011. "Revisiting Immune Exhaustion During HIV Infection." Current HIV/AIDS Reports 8 (1): 4. https://doi.org/10.1007/S11904-010-0066-0.

Kilkenny, Carol, William J. Browne, Innes C. Cuthill, Michael Emerson, and Douglas G. Altman. 2010. "Improving Bioscience Research Reporting: The ARRIVE Guidelines for Reporting Animal Research." PLOS Biology 8 (6): e1000412. https://doi.org/10.1371/JOURNAL.PBIO.1000412.

Kim, Jong Hwa, Taryn L. Hartley, A. Rachael Curran, and Donald M. Engelman. 2009.

"Molecular Dynamics Studies of the Transmembrane Domain of Gp41 from HIV-1." Biochimica et Biophysica Acta 1788 (9): 1804–12. https://doi.org/10.1016/J.BBAMEM.2009.06.011.

Klasse, P J, Gabriel Ozorowski, Rogier W Sanders, and John P Moore. 2020. "Perspective Env Exceptionalism: Why Are HIV-1 Env Glycoproteins Atypical Immunogens?" Cell Host and Microbe 27:507–18. https://doi.org/10.1016/j.chom.2020.03.018.

Klatzmann, David, Francoise Barré-Sinoussi, Marie Thèrése Nugeyre, Charles Dauguet, Etienne Vilmer, Claude Griscelli, Francoise Brun-Vezinet, et al. 1984. "Selective Tropism of Lymphadenopathy Associated Virus (LAV) for Helper-Inducer T Lymphocytes." Science (New York, N.Y.) 225 (4657): 59–63. https://doi.org/10.1126/SCIENCE.6328660.

Koenig, Scott, Howard E. Gendelman, Jan M. Orenstein, Mauro C. Dal Canto, Gholam H. Pezeshkpour, Margaret Yungbluth, Frank Janotta, Allen Aksamit, Malcolm A. Martin, and Anthony S. Fauci. 1986. "Detection of AIDS Virus in Macrophages in Brain Tissue from AIDS Patients with Encephalopathy." Science 233 (4768): 1089–93. https://doi.org/10.1126/SCIENCE.3016903.

Kumar, Sudhir, Glen Stecher, Michael Li, Christina Knyaz, and Koichiro Tamura. 2018. "MEGA X: Molecular Evolutionary Genetics Analysis across Computing Platforms." Molecular Biology and Evolution 35 (6): 1547. https://doi.org/10.1093/MOLBEV/MSY096.

Kwong, Peter D., and John R. Mascola. 2012. "Human Antibodies That Neutralize HIV-1: Identification, Structures, and B Cell Ontogenies." Immunity 37 (3): 412–25. https://doi.org/10.1016/J.IMMUNI.2012.08.012.

Lambotte, Olivier, Faroudy Boufassa, Yoann Madec, Ahn Nguyen, Cécile Goujard, Laurence Meyer, Christine Rouzioux, Alain Venet, and Jean François Oelfraissy. 2005. "HIV Controllers: A Homogeneous Group of HIV-1-Infected Patients with Spontaneous Control of Viral Replication." Clinical Infectious Diseases : An Official Publication of the Infectious Diseases Society of America 41 (7): 1053–56. https://doi.org/10.1086/433188.

Lambotte, Olivier, Guido Ferrari, Christiane Moog, Nicole L. Yates, Hua Xin Liao, Robert J. Parks, Charles B. Hicks, et al. 2009. "Heterogeneous Neutralizing Antibody and Antibody-Dependent Cell Cytotoxicity Responses in HIV-1 Elite Controllers." AIDS (London, England) 23 (8): 897. https://doi.org/10.1097/QAD.0B013E328329F97D.

Lassen, Kara G., Michael A. Lobritz, Justin R. Bailey, Samantha Johnston, Sandra Nguyen, Benhur Lee, Tom Chou, Robert F. Siliciano, Martin Markowitz, and Eric J. Arts. 2009. "Elite Suppressor–Derived HIV-1 Envelope Glycoproteins Exhibit Reduced Entry Efficiency and Kinetics." PLOS Pathogens 5 (4): e1000377. https://doi.org/10.1371/JOURNAL.PPAT.1000377.

Leon, Agathe, Ignacio Perez, Ezequiel Ruiz-Mateos, Jose Miguel Benito, Manuel Leal, Cecilio Lopez-Galindez, Norma Rallon, et al. 2016a. "Rate and Predictors of Progression in Elite and Viremic HIV-1 Controllers." AIDS (London, England) 30 (8): 1209–20. https://doi.org/10.1097/QAD.0000000000001050.

Leskov, Konstantin, Anna Agaponova, Kathleen M Weber, Elizabeth Daubert, Antoine Chaillon, Magali Porrachia, Jennifer Kinslow, et al. 2025. "Immune Dynamics During Reproductive Aging and Substance Use in Women With HIV." In . CROI 2025.

Lewis, George K., Andrés Finzi, Anthony L. De Vico, and Marzena Pazgier. 2015. "Conformational Masking and Receptor-Dependent Unmasking of Highly Conserved Env Epitopes Recognized by Non-Neutralizing Antibodies That Mediate Potent ADCC against HIV-1." Viruses 7 (9): 5115. https://doi.org/10.3390/V7092856.

Li, Shuying S., Andrew Hickey, Shida Shangguan, Philip K. Ehrenberg, Aviva Geretz, Lauryn Butler, Gautam Kundu, et al. 2022. "HLA-B□46 Associates with Rapid HIV Disease Progression in Asian Cohorts and Prominent Differences in NK Cell Phenotype." Cell Host & Microbe 30 (8): 1173-1185.e8. https://doi.org/10.1016/J.CHOM.2022.06.005.

Lian, Xiaodong, Ce Gao, Xiaoming Sun, Chenyang Jiang, Kevin B. Einkauf, Kyra W. Seiger, Joshua M. Chevalier, et al. 2021. "Signatures of Immune Selection in Intact and Defective Proviruses Distinguish HIV-1 Elite Controllers." Science Translational Medicine 13 (624): eabl4097. https://doi.org/10.1126/scitranslmed.abl4097.

Lian, Xiaodong, Kyra W. Seiger, Elizabeth M. Parsons, Ce Gao, Weiwei Sun, Gregory T. Gladkov, Isabelle C. Roseto, et al. 2023. "Progressive Transformation of the HIV-1 Reservoir Cell Profile over Two Decades of Antiviral Therapy." Cell Host & Microbe 31 (1): 83-96.e5. https://doi.org/10.1016/J.CHOM.2022.12.002.

Long, Yufei, Fanxia Meng, Naoyuki Kondo, Aikichi Iwamoto, and Zene Matsuda. 2011. "Conserved Arginine Residue in the Membrane-Spanning Domain of HIV-1 Gp41 Is Required for Efficient Membrane Fusion." Protein and Cell 2 (5): 369–76. https://doi.org/10.1007/s13238-011-1051-0.

Lua, Linda H.L., Natalie K. Connors, Frank Sainsbury, Yap P. Chuan, Nani Wibowo, and Anton P.J. Middelberg. 2014. "Bioengineering Virus-like Particles as Vaccines." Biotechnology and Bioengineering 111 (3): 425–40. https://doi.org/10.1002/BIT.25159.

Luzuriaga, Katherine, Hannah Gay, Carrie Ziemniak, Keri B. Sanborn, Mohan Somasundaran, Kaitlin Rainwater-Lovett, John W. Mellors, Daniel Rosenbloom, and Deborah Persaud. 2015. "Viremic Relapse after HIV-1 Remission in a Perinatally Infected Child." The New England Journal of Medicine 372 (8): 786–88. https://doi.org/10.1056/NEJMc1413931.

Lynch, Rebecca M., Eli Boritz, Emily E. Coates, Adam DeZure, Patrick Madden, Pamela Costner, Mary E. Enama, et al. 2015. "Virologic Effects of Broadly Neutralizing Antibody VRC01 Administration during Chronic HIV-1 Infection." Science Translational Medicine 7 (319). https://doi.org/10.1126/SCITRANSLMED.AAD5752/SUPPL_FILE/7-319RA206_SM.PDF.

Madec, Yoann, Faroudy Boufassa, Kholoud Porter, Maria Prins, Caroline Sabin, Antonella D'Arminio Monforte, Pauli Amornkul, et al. 2013. "Natural History of

HIV-Control since Seroconversion." AIDS (London, England) 27 (15): 2451–60. https://doi.org/10.1097/01.AIDS.0000431945.72365.01.

Madhavi, Vijaya, Bruce D. Wines, Janaki Amin, Sean Emery, Ester Lopez, Anthony Kelleher, Rob J. Center, et al. 2017. "HIV-1 Env- and Vpu-Specific Antibody-Dependent Cellular Cytotoxicity Responses Associated with Elite Control of HIV." Journal of Virology 91 (18). https://doi.org/10.1128/JVI.00700-17/ASSET/1F7CC7FA-4379-484C-9830-1D446AAEFBC5/ASSETS/GRAPHIC/ZJV9991829070006.JPEG.

Magierowska, Magdalena, Ioannis Theodorou, Patrice Debré, Françoise Sanson, Brigitte Autran, Yves Rivière, Dominique Charron, and Dominique Costagliola. 1999. "Combined Genotypes of CCR5, CCR2, SDF1, and HLA Genes Can Predict the Long-Term Nonprogressor Status in Human Immunodeficiency Virus-1–Infected Individuals." Blood 93 (3): 936–41. https://doi.org/10.1182/BLOOD.V93.3.936.

Marcandalli, Jessica, Brooke Fiala, Sebastian Ols, Michela Perotti, Willem de van der Schueren, Joost Snijder, Edgar Hodge, et al. 2019. "Induction of Potent Neutralizing Antibody Responses by a Designed Protein Nanoparticle Vaccine for Respiratory Syncytial Virus." Cell 176 (6): 1420-1431.e17. https://doi.org/10.1016/J.CELL.2019.01.046.

Mariani, Roberto, Gabriel Rutter, Matthew E. Harris, Thomas J. Hope, Hans-Georg Kräusslich, and Nathaniel R. Landau. 2000. "A Block to Human Immunodeficiency Virus Type 1 Assembly in Murine Cells." Journal of Virology 74 (8): 3859. https://doi.org/10.1128/JVI.74.8.3859-3870.2000.

Martin, Maureen P., Xiaojiang Gao, Jeong Hee Lee, George W. Nelson, Roger Detels, James J. Goedert, Susan Buchbinder, et al. 2002. "Epistatic Interaction between KIR3DS1 and HLA-B Delays the Progression to AIDS." Nature Genetics 31 (4): 429–34. https://doi.org/10.1038/NG934.

Martin, Maureen P., Ying Qi, Xiaojiang Gao, Eriko Yamada, Jeffrey N. Martin, Florencia Pereyra, Sara Colombo, et al. 2007. "Innate Partnership of HLA-B and KIR3DL1 Subtypes against HIV-1." Nature Genetics 39 (6): 733–40. https://doi.org/10.1038/NG2035.

Mascola, John R., Gabriela Stiegler, Thomas C. Vancott, Hermann Katinger, Calvin B. Carpenter, Chris E. Hanson, Holly Beary, et al. 2000. "Protection of Macaques against Vaginal Transmission of a Pathogenic HIV-1/SIV Chimeric Virus by Passive Infusion of Neutralizing Antibodies." Nature Medicine 2000 6:2 6 (2): 207–10. https://doi.org/10.1038/72318.

Masip, Jenifer, Carmen Gasca-Capote, María Reyes Jimenez-Leon, Joaquim Peraire, Alberto Perez-Gomez, Verónica Alba, Ana-Irene Malo, et al. 2021. "Differential MiRNA Plasma Profiles Associated with the Spontaneous Loss of HIV-1 Control: MiR-199a-3p and Its Potential Role as a Biomarker for Quick Screening of Elite Controllers." Clinical and Translational Medicine 11 (7): e474. https://doi.org/10.1002/CTM2.474.

Matrajt, Laura, Patrick M. Younan, Hans-Peter Kiem, and Joshua T. Schiffer. 2014.

" The Majority of CD4 + T-Cell Depletion during Acute Simian-Human Immunodeficiency Virus SHIV89.6P Infection Occurs in Uninfected Cells ." Journal of Virology 88 (6): 3202–12. https://doi.org/10.1128/JVI.03428-13/SUPPL_FILE/ZJV999098774SO1.PDF.

McCaffrey, Ruth A., Cheryl Saunders, Mike Hensel, and Leonidas Stamatatos. 2004. "N-Linked Glycosylation of the V3 Loop and the Immunologically Silent Face of Gp120 Protects Human Immunodeficiency Virus Type 1 SF162 from Neutralization by Anti-Gp120 and Anti-Gp41 Antibodies." Journal of Virology 78 (7): 3279–95. https://doi.org/10.1128/jvi.78.7.3279-3295.2004.

McCune, J. M. 2001. "The Dynamics of CD4+ T-Cell Depletion in HIV Disease." Nature 410 (6831): 974–79. https://doi.org/10.1038/35073648.

McGuire, Andrew T. 2019. "Targeting Broadly Neutralizing Antibody Precursors: A Naïve Approach to Vaccine Design." Current Opinion in HIV and AIDS 14 (4): 294–301. https://doi.org/10.1097/COH.0000000000000548.

McLaren, Paul J., and Jacques Fellay. 2021. "HIV-1 and Human Genetic Variation." Nature Reviews Genetics 22 (10): 645–57. https://doi.org/10.1038/s41576-021-00378-0.

Mendoza, Daniel, Sarah A. Johnson, Bennett A. Peterson, Ven Natarajan, Maria Salgado, Robin L. Dewar, Peter D. Burbelo, et al. 2012. "Comprehensive Analysis of Unique Cases with Extraordinary Control over HIV Replication." Blood 119 (20): 4645. https://doi.org/10.1182/BLOOD-2011-10-381996.

Migueles, Stephen A., Christine M. Osborne, Cassandra Royce, Alex A. Compton, Rohan P. Joshi, Kristin A. Weeks, Julia E. Rood, et al. 2008. "Lytic Granule Loading of CD8+ T Cells Is Required for HIV-Infected Cell Elimination Associated with Immune Control." Immunity 29 (6): 1009–21. https://doi.org/10.1016/J.IMMUNI.2008.10.010.

Migueles, Stephen A., M. Shirin Sabbaghian, W. Lesley Shupert, Maria P. Bettinotti, Francesco M. Marincola, Lisa Martino, Clair W. Hallahan, et al. 2000. "HLA B*5701 Is Highly Associated with Restriction of Virus Replication in a Subgroup of HIV-Infected Long Term Nonprogressors." Proceedings of the National Academy of Sciences of the United States of America 97 (6): 2709–14. https://doi.org/10.1073/pnas.050567397.

Monroe, Kathryn M., Zhiyuan Yang, Jeffrey R. Johnson, Xin Geng, Gilad Doitsh, Nevan J. Krogan, and Warner C. Greene. 2014. "IFI16 DNA Sensor Is Required for Death of Lymphoid CD4 T Cells Abortively Infected with HIV." Science 343 (6169): 428–32. https://doi.org/10.1126/science.1243640.

Montefiori, David C, Mario Roederer, Lynn Morris, and Michael S Seaman. 2018. "Neutralization Tiers of HIV-1." Current Opinion in HIV and AIDS 13 (2): 128–36. https://doi.org/10.1097/COH.0000000000000442.

Muller, Thorsten G., Vojtech Zila, Barbara Muller, and Hans Georg Krausslich. 2022. "Nuclear Capsid Uncoating and Reverse Transcription of HIV-1." Annual Review of Virology 9 (1): 261–84. https://doi.org/10.1146/ANNUREV-VIROLOGY-020922-110929.

Müller, Thorsten G., Vojtech Zila, Kyra Peters, Sandra Schifferdecker, Mia Stanic, Bojana Lucic, Vibor Laketa, Marina Lusic, Barbara Müller, and Hans Georg Kräusslich. 2021. "Hiv-1 Uncoating by Release of Viral Cdna from Capsid-like Structures in the Nucleus of Infected Cells." ELife 10 (April). https://doi.org/10.7554/ELIFE.64776.

Murphy, Kenneth, and Casey Weaver. 2017. "Janeway's Immunobiology, 9th Edition." www.garlandscience.com,.

Ndhlovu, Zaza M., Philomena Kamya, Nikoshia Mewalal, Henrik N. Kløverpris, Thandeka Nkosi, Karyn Pretorius, Faatima Laher, et al. 2015. "Magnitude and Kinetics of CD8+ T Cell Activation during Hyperacute HIV Infection Impact Viral Set Point." Immunity 43 (3): 591–604. https://doi.org/10.1016/J.IMMUNI.2015.08.012.

Nei, Masatoshi, and Sudhir Kumar. 2000. Molecular Evolution and Phylogenetics. New York: Oxford University Press.

Noel, Nicolas, Nathalie Lerolle, Camille Lécuroux, Cécile Goujard, Alain Venet, Asier Saez-Cirion, Veronique Avettand-Fenoël, et al. 2015. "Immunologic and Virologic Progression in HIV Controllers: The Role of Viral 'Blips' and Immune Activation in the ANRS CO21 CODEX Study." PLOS ONE 10 (7): e0131922. https://doi.org/10.1371/JOURNAL.PONE.0131922.

O'Connell, Karen A., Justin R. Bailey, and Joel N. Blankson. 2009. "Elucidating the Elite: Mechanisms of Control in HIV-1 Infection." Trends in Pharmacological Sciences 30 (12): 631–37. https://doi.org/10.1016/J.TIPS.2009.09.005/ASSET/21783545-599E-426E-9E78-9BA0829EB0B2/MAIN.ASSETS/GR1.JPG.

Okulicz, Jason F., Vincent C. Marconi, Michael L. Landrum, Scott Wegner, Amy Weintrob, Anuradha Ganesan, Braden Hale, et al. 2009. "Clinical Outcomes of Elite Controllers, Viremic Controllers, and Long-Term Nonprogressors in the US Department of Defense HIV Natural History Study." The Journal of Infectious Diseases 200 (11): 1714–23. https://doi.org/10.1086/646609.

Olvera, Alex, Samandhy Cedeño, Anuska Llano, Beatriz Mothe, Jorge Sanchez, Gemma Arsequell, and Christian Brander. 2021. "Does Antigen Glycosylation Impact the HIV-Specific T Cell Immunity?" Frontiers in Immunology 11 (January):573928. https://doi.org/10.3389/FIMMU.2020.573928/BIBTEX.

Ortiz, Raquel, Ana Barajas, Anna Pons-Grífols, Benjamin Trinité, Ferran Tarrés-Freixas, Carla Rovirosa, Victor Urrea, et al. 2023. "Exploring FeLV-Gag-Based VLPs as a New Vaccine Platform—Analysis of Production and Immunogenicity." International Journal of Molecular Sciences 24 (10): 9025. https://doi.org/10.3390/ijms24109025.

Owji, Hajar, Navid Nezafat, Manica Negahdaripour, Ali Hajiebrahimi, and Younes Ghasemi. 2018. "A Comprehensive Review of Signal Peptides: Structure, Roles, and Applications." European Journal of Cell Biology 97 (6): 422–41. https://doi.org/10.1016/j.ejcb.2018.06.003.

Palmer, S, L Josefsson, J M Coffin, Abstract Palmer, Josefsson L Coffin, and Jm (

Karolinska. 2011. "HIV Reservoirs and the Possibility of a Cure for HIV Infection." Journal of Internal Medicine 270 (6): 550–60. https://doi.org/10.1111/J.1365-2796.2011.02457.X.

Pancera, Marie, Tongqing Zhou, Aliaksandr Druz, Ivelin S. Georgiev, Cinque Soto, Jason Gorman, Jinghe Huang, et al. 2014. "Structure and Immune Recognition of Trimeric Pre-Fusion HIV-1 Env." Nature 2014 514:7523 514 (7523): 455–61. https://doi.org/10.1038/nature13808.

Pastor, Lucia, Erica Parker, Jorge Carrillo, Victor Urrea, Laura Fuente-Soro, Durval Respeito, Chenjerai Jairoce, Inacio Mandomando, Julià Blanco, and Denise Naniche. 2017. "A Cytokine Pattern That Differentiates Preseroconversion From Postseroconversion Phases of Primary HIV Infection." Journal of Acquired Immune Deficiency Syndromes (1999) 74 (4): 459–66. https://doi.org/10.1097/QAI.0000000000001272.

Pérez-Yanes, Silvia, María Pernas, Silvia Marfil, Romina Cabrera-Rodríguez, Raquel Ortiz, Víctor Urrea, Carla Rovirosa, et al. 2022. "The Characteristics of the HIV-1 Env Glycoprotein Are Linked With Viral Pathogenesis." Frontiers in Microbiology 13 (March). https://doi.org/10.3389/fmicb.2022.763039.

Perez-Zsolt, Daniel, Jordana Muñoz-Basagoiti, Jordi Rodon, Marc Elosua-Bayes, Dàlia Raïch-Regué, Cristina Risco, Martin Sachse, et al. 2021. "SARS-CoV-2 Interaction with Siglec-1 Mediates Trans-Infection by Dendritic Cells." Cellular & Molecular Immunology 2021 18:12 18 (12): 2676–78. https://doi.org/10.1038/s41423-021-00794-6.

Pernas, María, Concepción Casado, Carolina Arcones, Anuska Llano, Víctor Sánchez-Merino, Beatriz Mothe, José L. Vicario, et al. 2012. "Low-Replicating Viruses and Strong Anti-Viral Immune Response Associated with Prolonged Disease Control in a Superinfected HIV-1 LTNP Elite Controller." Edited by Elvin Hsing Geng. PLoS ONE 7 (2): e31928. https://doi.org/10.1371/journal.pone.0031928.

Pernas, María, Concepción Casado, Virginia Sandonis, Carolina Arcones, Carmen Rodríguez, Ezequiel Ruiz-Mateos, Eva Ramírez De Arellano, et al. 2013. "Prevalence of HIV-1 Dual Infection in Long-Term Nonprogressor-Elite Controllers." Journal of Acquired Immune Deficiency Syndromes 64 (3): 225–31. https://doi.org/10.1097/QAI.0B013E31829BDC85.

Pernas, María, Laura Tarancón-Diez, Esther Rodríguez-Gallego, Josep Gómez, Julia G. Prado, Concepción Casado, Beatriz Dominguez-Molina, et al. 2018. "Factors Leading to the Loss of Natural Elite Control of HIV-1 Infection." Edited by Guido Silvestri. Journal of Virology 92 (5). https://doi.org/10.1128/JVI.01805-17.

Postler, Thomas S., and Ronald C. Desrosiers. 2013. "The Tale of the Long Tail: The Cytoplasmic Domain of HIV-1 Gp41." Journal of Virology 87 (1): 2–15. https://doi.org/10.1128/jvi.02053-12.

Poveda, Eva, Wendy Fitzgerald, Cristina Reglero, Alexandre Pérez-González, Ana Mariño, Hortensia Álvarez, Nieves Valcarce, et al. 2023. "Interleukin 18 (IL-18) and IL-3 in Extracellular Vesicles: Biomarkers for Durable Elite Control of HIV-1." The Journal of Infectious Diseases 227 (12): 1381–85. https://doi.org/10.1093/

INFDIS/JIAD042.

Pradenas, Edwards, Benjamin Trinité, Víctor Urrea, Silvia Marfil, Carlos Ávila-Nieto, María Luisa Rodríguez de la Concepción, Ferran Tarrés-Freixas, et al. 2021. "Stable Neutralizing Antibody Levels 6 Months after Mild and Severe COVID-19 Episodes." Med 2 (3): 313-320.e4. https://doi.org/10.1016/j.medj.2021.01.005.

Prugnolle, Franck, Andrea Manica, Marie Charpentier, Jean François Guégan, Vanina Guernier, and François Balloux. 2005. "Pathogen-Driven Selection and Worldwide HLA Class I Diversity." Current Biology : CB 15 (11): 1022–27. https://doi.org/10.1016/J.CUB.2005.04.050.

Pugach, Pavel, Gabriel Ozorowski, Albert Cupo, Rajesh Ringe, Anila Yasmeen, Natalia de Val, Ronald Derking, et al. 2015. "A Native-Like SOSIP.664 Trimer Based on an HIV-1 Subtype B Env Gene." Journal of Virology 89 (6): 3380–95. https://doi.org/10.1128/jvi.03473-14.

Rahman, M. A., M. Bissa, I. Silva de Castro, S. Helmold Hait, J. D. Stamos, F. Bhuyan, R. Hunegnaw, et al. 2023. "Vaccine plus Microbicide Effective in Preventing Vaginal SIV Transmission in Macaques." Nature Microbiology 2023 8:5 8 (5): 905–18. https://doi.org/10.1038/s41564-023-01353-7.

Ramsuran, Veron, Vivek Naranbhai, Amir Horowitz, Ying Qi, Maureen P. Martin, Yuko Yuki, Xiaojiang Gao, et al. 2018. "Elevated HLA-A Expression Impairs HIV Control through Inhibition of NKG2A-Expressing Cells." Science (New York, N.Y.) 359 (6371): 86–90. https://doi.org/10.1126/SCIENCE.AAM8825.

Reicher, Lee, Noam Bar, Anastasia Godneva, Yotam Reisner, Liron Zahavi, Nir Shahaf, Raja Dhir, Adina Weinberger, and Eran Segal. 2024. "Phenome-Wide Associations of Human Aging Uncover Sex-Specific Dynamics." Nature Aging 4 (11). https://doi.org/10.1038/S43587-024-00734-9.

Rhodes, David I., Lesley Ashton, Ajantha Solomon, Andrew Carr, David Cooper, John Kaldor, and Nicholas Deacon. 2000. "Characterization of Three Nef -Defective Human Immunodeficiency Virus Type 1 Strains Associated with Long-Term Nonprogression." Journal of Virology 74 (22): 10581–88. https://doi.org/10.1128/jvi.74.22.10581-10588.2000.

Richard, Jonathan, Gérémy Sannier, Li Zhu, Jérémie Prévost, Lorie Marchitto, Mehdi Benlarbi, Guillaume Beaudoin-Bussières, et al. 2024. "CD4 Downregulation Precedes Env Expression and Protects HIV-1-Infected Cells from ADCC Mediated by Non-Neutralizing Antibodies." Edited by Ronald Swanstrom and Diane L. Bolton. MBio 15 (11). https://doi.org/10.1128/MBIO.01827-24.

Robey, W. Gerard, Bijan Safai, Stephen Oroszlan, Larry O. Arthur, Matthew A. Gonda, Robert C. Gallo, and Peter J. Fischinger. 1985. "Characterization of Envelope and Core Structural Gene Products of HTLV-III with Sera from AIDS Patients." Science 228 (4699): 593–95. https://doi.org/10.1126/SCIENCE.2984774.

Rodríguez-Da Silva, Alfredo, Celia Miralles, Antonio Ocampo, and Diana Valverde. 2017. "Estudio de La Prevalencia de Marcadores Genéticos Asociados a La Lenta Progresión Del Virus de La Inmunodeficiencia Humana Tipo 1 En La Población Gallega." Enfermedades Infecciosas y Microbiologia Clinica 35 (2): 104–7. https://

doi.org/10.1016/j.eimc.2015.04.006.

Rodríguez-Gallego, Esther, Laura Tarancón-Diez, Felipe Garciá, Jorge Del Romero, Jose Miguel Benito, Verónica Alba, Pol Herrero, et al. 2019. "Proteomic Profile Associated With Loss of Spontaneous Human Immunodeficiency Virus Type 1 Elite Control." The Journal of Infectious Diseases 219 (6): 867–76. https://doi.org/10.1093/INFDIS/JIY599.

Romero Martín, Luis. 2022. "Alternative Components of the Cellular Immunity to SARS-CoV-2 and HIV Infection: Beyond the Classical CTL." http://hdl.handle.net/10803/687848.

Rosás-Umbert, Miriam, Anuska Llano, Rocío Bellido, Alex Olvera, Marta Ruiz-Riol, Muntsa Rocafort, Marco A. Fernández, et al. 2019. "Mechanisms of Abrupt Loss of Virus Control in a Cohort of Previous HIV Controllers." Journal of Virology 93 (4): e01436-18. https://doi.org/10.1128/JVI.01436-18.

Sabin, Caroline A., and Jens D. Lundgren. 2013. "The Natural History of HIV Infection." Current Opinion in HIV and AIDS 8 (4): 311–17. https://doi.org/10.1097/COH.0B013E328361FA66.

Sáez-Cirión, Asier, Anne-Claire Mamez, Véronique Avettand-Fenoel, Mitja Nabergoj, Caroline Passaes, Paul Thoueille, Laurent Decosterd, et al. 2024. "Sustained HIV Remission after Allogeneic Hematopoietic Stem Cell Transplantation with Wild-Type CCR5 Donor Cells." Nature Medicine 30 (December). https://doi.org/10.1038/s41591-024-03277-z.

Sáez-Cirión, Asier, Charline Bacchus, Laurent Hocqueloux, Véronique Avettand-Fenoel, Isabelle Girault, Camille Lecuroux, Valerie Potard, Pierre Versmisse, Adeline Melard, Thierry Prazuck, Benjamin Descours, Julien Guergnon, Jean-Paul Viard, Faroudy Boufassa, Olivier Lambotte, Cécile Goujard, Laurence Meyer, Dominique Costagliola, Alain Venet, Gianfranco Pancino, Brigitte Autran, Christine Rouzioux. 2013. "Post-Treatment HIV-1 Controllers with a Long-Term Virological Remission after the Interruption of Early Initiated Antiretroviral Therapy ANRS VISCONTI Study." PLoS Pathogens 9, (3): e1003211. https://doi.org/10.1371/JOURNAL.PPAT.1003211

Sajadi, Mohammad M., Yongjun Guan, Anthony L. Devico, Michael S. Seaman, Mian Hossain, George K. Lewis, and Robert R. Redfield. 2011. "Correlation between Circulating HIV-1 RNA and Broad HIV-1 Neutralizing Antibody Activity." Journal of Acquired Immune Deficiency Syndromes (1999) 57 (1): 9. https://doi.org/10.1097/QAI.0B013E3182100C1B.

Salgado, Maria, Albert Garcia-Minambres, Judith Dalmau, Esther Jiménez-Moyano, Pompeyo Viciana, Belén Alejos, Bonaventura Clotet, Julia G. Prado, and Javier Martinez-Picado. 2018. "Control of HIV-1 Pathogenesis in Viremic Nonprogressors Is Independent of Gag-Specific Cytotoxic T Lymphocyte Responses." Journal of Virology 92 (12): e00346-18. https://doi.org/10.1128/JVI.00346-18.

Salgado, María, Stephen A. Migueles, Xu G. Yu, and Javier Martinez-Picado. 2024. "Exceptional, Naturally Occurring HIV-1 Control: Insight into a Functional Cure." Med 5 (9): 1071–82. https://doi.org/10.1016/j.medj.2024.06.008.

Sánchez-Gaona, Nerea, Ana Gallego-Cortés, Antonio Astorga-Gamaza, Norma Rallón, José M. Benito, Ezequiel Ruiz-Mateos, Adrià Curran, Joaquin Burgos, Jordi Navarro, Paula Suanzes, Vicenç Falcó, Meritxell Genescà, and Maria J. Buzon. 2024. "NKG2C and NKG2A Coexpression Defines a Highly Functional Antiviral NK Population in Spontaneous HIV Control." JCI Insight 9, (20): e182660. https://doi.org/10.1172/jci.insight.182660

Sanders, Rogier W., Ronald Derking, Albert Cupo, Jean Philippe Julien, Anila Yasmeen, Natalia de Val, Helen J. Kim, et al. 2013. "A Next-Generation Cleaved, Soluble HIV-1 Env Trimer, BG505 SOSIP.664 Gp140, Expresses Multiple Epitopes for Broadly Neutralizing but Not Non-Neutralizing Antibodies." PLoS Pathogens 9 (9). https://doi.org/10.1371/journal.ppat.1003618.

Saunders, Kevin O., Kevin Wiehe, Ming Tian, Priyamvada Acharya, Todd Bradley, S. Munir Alam, Eden P. Go, et al. 2019. "Targeted Selection of HIV-Specific Antibody Mutations by Engineering B Cell Maturation." Science 366 (6470). https://doi.org/10.1126/SCIENCE.AAY7199/SUPPL_FILE/AAY7199_SAUNDERS_SM.PDF.

Schorcht, Anna, Tom L. G. M. van den Kerkhof, Christopher A. Cottrell, Joel D. Allen, Jonathan L. Torres, Anna-Janina Behrens, Edith E. Schermer, et al. 2020. "Neutralizing Antibody Responses Induced by HIV-1 Envelope Glycoprotein SOSIP Trimers Derived from Elite Neutralizers." Edited by Guido Silvestri. Journal of Virology 94 (24). https://doi.org/10.1128/JVI.01214-20.

Schuitemaker, Hanneke, Maarten Koot, Neeltje A Kootstra, M Wouter Dercksen, Ruud E Y De Goede, Reindert P Van Steenwijk, Joep M A Lange, Jan K M Eeftink Schattenkerk, Frank Miedema, and Matthijs Tersmette1. 1992. "Biological Phenotype of Human Immunodeficiency Virus Type 1 Clones at Different Stages of Infection: Progression of Disease Is Associated with a Shift from Monocytotropic to T-Cell-Tropic Virus Population." Journal of Virology 66 (3): 1354–60. https://doi.org/10.1128/JVI.66.3.1354-1360.1992.

Scully, Eileen P., Monica Gandhi, Rowena Johnston, Rebecca Hoh, Ainsley Lockhart, Curtis Dobrowolski, Amélie Pagliuzza, et al. 2019. "Sex-Based Differences in Human Immunodeficiency Virus Type 1 Reservoir Activity and Residual Immune Activation." The Journal of Infectious Diseases 219 (7): 1084–94. https://doi.org/10.1093/INFDIS/JIY617.

Seaman, Michael S., Holly Janes, Natalie Hawkins, Lauren E. Grandpre, Colleen Devoy, Ayush Giri, Rory T. Coffey, et al. 2010. "Tiered Categorization of a Diverse Panel of HIV-1 Env Pseudoviruses for Assessment of Neutralizing Antibodies." Journal of Virology 84 (3): 1439–52. https://doi.org/10.1128/JVI.02108-09/ASSET/DAD0BD5C-9337-4DE1-AFE0-21700BAFBD24/ASSETS/GRAPHIC/ZJV0031028310008.JPEG.

Simek, Melissa D., Wasima Rida, Frances H. Priddy, Pham Pung, Emily Carrow, Dagna S. Laufer, Jennifer K. Lehrman, et al. 2009. "Human Immunodeficiency Virus Type 1 Elite Neutralizers: Individuals with Broad and Potent Neutralizing Activity Identified by Using a High-Throughput Neutralization Assay Together

with an Analytical Selection Algorithm." Journal of Virology 83 (14): 7337–48. https://doi.org/10.1128/JVI.00110-09.

Sliepen, Kwinten, Byung Woo Han, Ilja Bontjer, Petra Mooij, Fernando Garces, Anna Janina Behrens, Kimmo Rantalainen, et al. 2019. "Structure and Immunogenicity of a Stabilized HIV-1 Envelope Trimer Based on a Group-M Consensus Sequence." Nature Communications 10 (1). https://doi.org/10.1038/s41467-019-10262-5.

Sliepen, Kwinten, Gabriel Ozorowski, Judith A. Burger, Thijs van Montfort, Melissa Stunnenberg, Celia LaBranche, David C. Montefiori, John P. Moore, Andrew B. Ward, and Rogier W. Sanders. 2015. "Presenting Native-like HIV-1 Envelope Trimers on Ferritin Nanoparticles Improves Their Immunogenicity." Retrovirology 12 (1): 82. https://doi.org/10.1186/s12977-015-0210-4.

Smalls-Mantey, Adjoa, Nicole Doria-Rose, Rachel Klein, Andy Patamawenu, Stephen A. Migueles, Sung-Youl Ko, Claire W. Hallahan, et al. 2012. " Antibody-Dependent Cellular Cytotoxicity against Primary HIV-Infected CD4 + T Cells Is Directly Associated with the Magnitude of Surface IgG Binding ." Journal of Virology 86 (16): 8672–80. https://doi.org/10.1128/JVI.00287-12/ASSET/A388E733-74B6-4F1B-A661-831F8627D840/ASSETS/GRAPHIC/ZJV9990963480007.JPEG.

Smith, Adrian J., R. Eddie Clutton, Elliot Lilley, Kristine E.Aa Hansen, and Trond Brattelid. 2017. "PREPARE: Guidelines for Planning Animal Research and Testing." Laboratory Animals 52 (2): 135. https://doi.org/10.1177/0023677217724823.

Smoleń-Dzirba, Joanna, Magdalena Rosińska, Janusz Janiec, Marek Beniowski, Mariusz Cycoń, Jolanta Bratosiewicz-Wąsik, and Tomasz J Wąsik. 2017. "HIV-1 Infection in Persons Homozygous for CCR5-Δ32 Allele: The Next Case and the Review." AIDS Reviews 19 (4): 219–30. http://www.ncbi.nlm.nih.gov/pubmed/28534889.

Sougrat, Rachid, Alberto Bartesaghi, Jeffrey D. Lifson, Adam E. Bennett, Julian W. Bess, Daniel J. Zabransky, and Sriram Subramaniam. 2007. "Electron Tomography of the Contact between T Cells and SIV/HIV-1: Implications for Viral Entry." PLOS Pathogens 3 (5): e63. https://doi.org/10.1371/JOURNAL.PPAT.0030063.

Steckbeck, Jonathan D., Anne Sophie Kuhlmann, and Ronald C. Montelaro. 2013. "C-Terminal Tail of Human Immunodeficiency Virus Gp41: Functionally Rich and Structurally Enigmatic." Journal of General Virology 94 (PART11): 1–19. https://doi.org/10.1099/VIR.0.046508-0/CITE/REFWORKS.

Sterjovski, Jasminka, Melissa J. Churchill, Anne Ellett, Lachlan R. Gray, Michael J. Roche, Rebecca L. Dunfee, Damian F.J. Purcell, et al. 2007. "Asn 362 in Gp120 Contributes to Enhanced Fusogenicity by CCR5-Restricted HIV-1 Envelope Glycoprotein Variants from Patients with AIDS." Retrovirology 4 (1): 1–21. https://doi.org/10.1186/1742-4690-4-89/FIGURES/9.

Stewart, Graeme J, Lesley J Ashton, Robyn A Biti, Rosemary A Ffrench, Bruce H Bennetts, Nicole R Newcombe, Elizabeth M Benson, Andrew Carr, David A Cooper, and John M Kaldor. 1997. "Increased Frequency of CCR-5 Δ32 Heterozygotes among Long-Term Non-Progressors with HIV-1 Infection." AIDS 11:1833–38.

Sugawara, Sho, R. Keith Reeves, and Stephanie Jost. 2022. "Learning to Be Elite:

Lessons From HIV-1 Controllers and Animal Models on Trained Innate Immunity and Virus Suppression." Frontiers in Immunology 13 (April):858383. https://doi.org/10.3389/FIMMU.2022.858383/XML/NLM.

Tarancon-Diez, Laura, Esther Rodríguez-Gallego, Anna Rull, Joaquim Peraire, Consuelo Viladés, Irene Portilla, María Reyes Jimenez-Leon, et al. 2019. "Immunometabolism Is a Key Factor for the Persistent Spontaneous Elite Control of HIV-1 Infection." EBioMedicine 42 (April):86–96. https://doi.org/10.1016/J.EBIOM.2019.03.004.

Tarrés-Freixas. 2021. "HIV-1 Virus-Like Particles Engineered to Display a High Antigen Density."

Tarrés-Freixas, Ferran, Carmen Aguilar-Gurrieri, María Luisa Rodríguez de la Concepción, Victor Urrea, Benjamin Trinité, Raquel Ortiz, Edwards Pradenas, et al. 2023. "An Engineered HIV-1 Gag-Based VLP Displaying High Antigen Density Induces Strong Antibody-Dependent Functional Immune Responses." Npj Vaccines 8 (1): 51. https://doi.org/10.1038/s41541-023-00648-4.

Tarrés-Freixas, Ferran, Bonaventura Clotet, Jorge Carrillo, and Julià Blanco. 2024. "Nucleic Acid Vaccines Encoding Proteins and Virus-like Particles for HIV Prevention." Vaccines 12 (3): 298. https://doi.org/10.3390/vaccines12030298.

Thalhauser, Stefanie, and Miriam Breunig. 2020. "Considerations for Efficient Surface Functionalization of Nanoparticles with a High Molecular Weight Protein as Targeting Ligand." European Journal of Pharmaceutical Sciences : Official Journal of the European Federation for Pharmaceutical Sciences 155 (December). https://doi.org/10.1016/J.EJPS.2020.105520.

Thèze, Jacques, Lisa A Chakrabarti, Benoît Vingert, Filippos Porichis, and Daniel E Kaufmann. 2010. "HIV Controllers: A Multifactorial Phenotype of Spontaneous Viral Suppression." https://doi.org/10.1016/j.clim.2011.07.007.

Tokatlian, Talar, Daniel W. Kulp, Andrew A. Mutafyan, Christopher A. Jones, Sergey Menis, Erik Georgeson, Mike Kubitz, et al. 2018. "Enhancing Humoral Responses Against HIV Envelope Trimers via Nanoparticle Delivery with Stabilized Synthetic Liposomes." Scientific Reports 2018 8:1 8 (1): 1–13. https://doi.org/10.1038/s41598-018-34853-2.

Tokatlian, Talar, Benjamin J. Read, Christopher A. Jones, Daniel W. Kulp, Sergey Menis, Jason Y.H. Chang, Jon M. Steichen, et al. 2019. "Innate Immune Recognition of Glycans Targets HIV Nanoparticle Immunogens to Germinal Centers." Science (New York, N.Y.) 363 (6427): 649–54. https://doi.org/10.1126/SCIENCE.AAT9120.

Trinité, Benjamin, Eberhard Durr, Anna Pons-Grífols, Gregory O'Donnell, Carmen Aguilar-Gurrieri, Silveria Rodriguez, Victor Urrea, et al. 2024. "VLPs Generated by the Fusion of RSV-F or HMPV-F Glycoprotein to HIV-Gag Show Improved Immunogenicity and Neutralizing Response in Mice." Vaccine 42 (15): 3474–85. https://doi.org/10.1016/J.VACCINE.2024.04.048.

Trinité, Benjamin, Ferran Tarrés-Freixas, Jordi Rodon, Edwards Pradenas, Víctor Urrea, Silvia Marfil, María Luisa Rodríguez de la Concepción, et al. 2021. "SARS-

CoV-2 Infection Elicits a Rapid Neutralizing Antibody Response That Correlates with Disease Severity." Scientific Reports 11 (1): 2608. https://doi.org/10.1038/s41598-021-81862-9.

Upadhyay, Chitra, Roya Feyznezhad, Liwei Cao, Kun-Wei Chan, Kevin Liu, Weiming Yang, Hui Zhang, et al. 2020. "Signal Peptide of HIV-1 Envelope Modulates Glycosylation Impacting Exposure of V1V2 and Other Epitopes." Edited by Alexandra Trkola. PLOS Pathogens 16 (12): e1009185. https://doi.org/10.1371/journal.ppat.1009185.

Upadhyay, Chitra, Priyanka Rao, Mohammad Amin Behzadi, Roya Feyznezhad, Gregory S. Lambert, Rajnish Kumar, Madhu Kumar, et al. 2024. "Signal Peptide Exchange Alters HIV-1 Envelope Antigenicity and Immunogenicity." Frontiers in Immunology 15 (September):1476924. https://doi.org/10.3389/FIMMU.2024.1476924/XML/NLM.

Utay, Netanya S., and Daniel C. Douek. 2016. "Interferons and HIV Infection: The Good, the Bad, and the Ugly." Pathogens & Immunity 1 (1): 107. https://doi.org/10.20411/PAI.V1I1.125.

Valenzuela-Fernández, Agustín, Romina Cabrera-Rodríguez, Concha Casado, Silvia Pérez-Yanes, María Pernas, Jonay García-Luis, Silvia Marfil, et al. 2022. "Contribution of the HIV-1 Envelope Glycoprotein to AIDS Pathogenesis and Clinical Progression." Biomedicines 10 (9): 2172. https://doi.org/10.3390/biomedicines10092172.

Van't Wout, Angélique B., Neeltje A. Kootstra, Greetje A. Mulder-Kampinga, Nei Albrecht-Van Lent, Henriëtte J. Scherpbier, Jan Veenstra, Kees Boer, Roel A. Coutinho, Frank Miedema, and Hanneke Schuitemaker. 1994. "Macrophage-Tropic Variants Initiate Human Immunodeficiency Virus Type 1 Infection after Sexual, Parenteral, and Vertical Transmission." The Journal of Clinical Investigation 94 (5): 2060–67. https://doi.org/10.1172/JCI117560.

Veazey, R S, and A A Lackner. 1998. "The Gastrointestinal Tract and the Pathogenesis of AIDS." AIDS (London, England) 12 Suppl A:S35-42.

Visciano, M. L., L. Diomede, M. Tagliamonte, M. L. Tornesello, V. Asti, M. Bomsel, F. M. Buonaguro, L. Lopalco, and L. Buonaguro. 2011. "Generation of HIV-1 Virus-Like Particles Expressing Different HIV-1 Glycoproteins." Vaccine 29 (31): 4903–12. https://doi.org/10.1016/J.VACCINE.2011.05.005.

Wandeler, Gilles, Leigh F. Johnson, and Matthias Egger. 2016. "Trends in Life Expectancy of HIV-Positive Adults on Antiretroviral Therapy across the Globe: Comparisons with General Population." Current Opinion in HIV and AIDS 11 (5): 492–500. https://doi.org/10.1097/COH.0000000000000298.

Wang, Hua, Cheng Cheng, James L. Dal Santo, Chen Hsiang Shen, Tatsiana Bylund, Amy R. Henry, Colin A. Howe, et al. 2024. "Potent and Broad HIV-1 Neutralization in Fusion Peptide-Primed SHIV-Infected Macaques." Cell 187 (25): 7214-7231.e23. https://doi.org/10.1016/J.CELL.2024.10.003.

Wei, Xiping, Julie M. Decker, Shuyi Wang, Huxiong Hui, John C. Kappes, Xiaoyun Wu, Jesus F. Salazar-Gonzalez, et al. 2003. "Antibody Neutralization and Escape

by HIV-1." Nature 2003 422:6929 422 (6929): 307–12. https://doi.org/10.1038/nature01470.

West, Anthony P., Louise Scharf, Johannes F. Scheid, Florian Klein, Pamela J. Bjorkman, and Michel C. Nussenzweig. 2014. "Structural Insights on the Role of Antibodies in HIV-1 Vaccine and Therapy." Cell 156 (4): 633–48. https://doi.org/10.1016/J.CELL.2014.01.052.

Wheeler, Cosette M., Susanne K. Kjaer, Kristján Sigurdsson, Ole Erik Iversen, Hernandez Avila Mauricio, Gonzalo Perez, Darron R. Brown, et al. 2009. "The Impact of Quadrivalent Human Papillomavirus (HPV; Types 6, 11, 16, and 18) L1 Virus-Like Particle Vaccine on Infection and Disease Due to Oncogenic Nonvaccine HPV Types in Sexually Active Women Aged 16–26 Years." The Journal of Infectious Diseases 199 (7): 936–44. https://doi.org/10.1086/597309.

Wong, S. B. Justin, and Robert F. Siliciano. 2005. "Contribution of Virus-Like Particles to the Immunogenicity of Human Immunodeficiency Virus Type 1 Gag-Derived Vaccines in Mice." Journal of Virology 79 (3): 1701. https://doi.org/10.1128/JVI.79.3.1701-1712.2005.

Yang, Otto O, William G Cumberland, Robert Escobar, Diana Liao, and Kara W Chew. 2017. "Demographics and Natural History of HIV-1-Infected Spontaneous Controllers of Viremia: Extremes on a Continuum HHS Public Access." AIDS 31 (8): 1091–98. https://doi.org/10.1097/QAD.0000000000001443.

Yin, Xin, Simon Langer, Zeli Zhang, Kristina M. Herbert, Sunnie Yoh, Renate König, and Sumit K. Chanda. 2020. "Sensor Sensibility—HIV-1 and the Innate Immune Response." Cells 2020, Vol. 9, Page 254 9 (1): 254. https://doi.org/10.3390/CELLS9010254.

Yuan, Tingting, Jingjing Li, and Mei Yun Zhang. 2013. "HIV-1 Envelope Glycoprotein Variable Loops Are Indispensable for Envelope Structural Integrity and Virus Entry." PLOS ONE 8 (8): e69789. https://doi.org/10.1371/JOURNAL.PONE.0069789.

Zaunders, John, Wayne B. Dyer, and Melissa Churchill. 2011. "The Sydney Blood Bank Cohort: Implications for Viral Fitness as a Cause of Elite Control." Current Opinion in HIV and AIDS 6 (3): 151–56. https://doi.org/10.1097/COH.0B013E3283454D5B.

Zhang, Chao, Jin Wen Song, Hui Huang Huang, Xing Fan, Lei Huang, Jian Ning Deng, Bo Tu, et al. 2021. "NLRP3 Inflammasome Induces CD4+ T Cell Loss in Chronically HIV-1–Infected Patients." The Journal of Clinical Investigation 131 (6). https://doi.org/10.1172/JCI138861.

Zhang, Peng, Elisabeth Narayanan, Qingbo Liu, Yaroslav Tsybovsky, Kristin Boswell, Shilei Ding, Zonghui Hu, et al. 2021. "A Multiclade Env-Gag VLP MRNA Vaccine Elicits Tier-2 HIV-1-Neutralizing Antibodies and Reduces the Risk of Heterologous SHIV Infection in Macaques." Nature Medicine. https://doi.org/10.1038/s41591-021-01574-5.

Zhao, Connie, Hongru Li, Talia H. Swartz, and Benjamin K. Chen. 2022. "The HIV Env Glycoprotein Conformational States on Cells and Viruses." Edited by Li Wu

and Vinayaka R. Prasad. MBio 13 (2). https://doi.org/10.1128/mbio.01825-21.
Zhu, Ping, Jun Liu, Julian Bess, Elena Chertova, Jeffrey D. Lifson, Henry Grisé, Gilad A. Ofek, Kenneth A. Taylor, and Kenneth H. Roux. 2006. "Distribution and Three-Dimensional Structure of AIDS Virus Envelope Spikes." Nature 2006 441:7095 441 (7095): 847–52. https://doi.org/10.1038/nature04817.
Zila, Vojtech, Erica Margiotta, Beata Turoňová, Thorsten G. Müller, Christian E. Zimmerli, Simone Mattei, Matteo Allegretti, et al. 2021. "Cone-Shaped HIV-1 Capsids Are Transported through Intact Nuclear Pores." Cell 184 (4): 1032-1046. e18. https://doi.org/10.1016/j.cell.2021.01.025.